

AD-A265 193



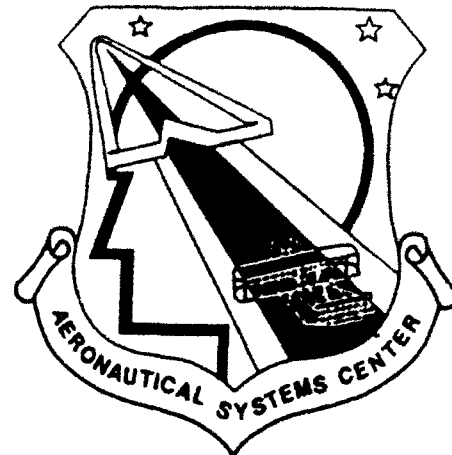
ASC-TR-93-5004

JUN 1

1993

C
E
D

1



**EVALUATION OF THE C/EC/KC-135
GROUND COLLISION AVOIDANCE
SYSTEM (GCAS) (STUDY 2)**

Justin D. Rueb, Major, USAF
Jordan R. Kriss, 1Lt, USAF
John A. Hassoun

Crew Station Evaluation Facility
Crew Station & Human Factors Section

March 1993

Final Report for the Period February 1992 through April 1992

Approved for public release; distribution is unlimited.

93 5 28 098

93-12244



15085

INTEGRATED ENGINEERING AND TECHNICAL MANAGEMENT DIRECTORATE
AERONAUTICAL SYSTEMS CENTER
AIR FORCE MATERIEL COMMAND
WRIGHT-PATTERSON AFB, OHIO 45433-7126

NOTICE


When Government drawings, specifications, or other data are used for any purpose other than in connection with a definitely Government-related procurement, the United States Government incurs no responsibility or any obligation whatsoever. The fact that the government may have formulated or in any way supplied the said drawings, specifications, or other data, is not to be regarded by implication, or otherwise in any manner construed, as licensing the holder, or any other person or corporation; or as conveying any rights or permission to manufacture, use, or sell any patented invention that may in any way be related thereto.

This report is releasable to the National Technical Information Service (NTIS). At NTIS, it will be available to the general public, including foreign nations.

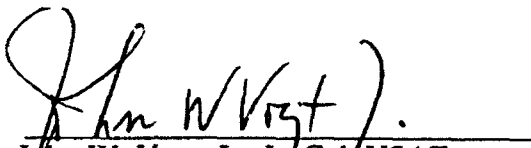
This technical report has been reviewed and is approved for publication.



John A. Hassoun
Program Manager
Crew Station Evaluation Facility



Dr. Richard J. Schiffler
Chief, Crew Station and
Human Factors Branch



John W. Vogt, Jr., Lt Col USAF
Chief, Support Systems Engineering Division
Integrated Engineering and Technical
Management Directorate

If your address has changed, if you wish to be removed from our mailing list, or if the addressee is no longer employed by your organization, please notify ASC/ENECS, Wright-Patterson AFB, Ohio 45433-7126 to help maintain a current mailing list.

Copies of this report should not be returned unless return is required by security considerations, contractual obligations, or notice on a specific document.

REPORT DOCUMENTATION PAGE			Form Approved OMB No. 0704-0188	
<small>Public reporting burden for this collection of information is estimated to average 1 hour per response, including the time for reviewing instructions, searching existing data sources, gathering and maintaining the data needed, and completing and reviewing the collection of information. Send comments regarding this burden estimate or any other aspect of this collection of information, including suggestions for reducing this burden, to Washington Headquarters Services, Directorate for Information Operations and Reports, 1215 Jefferson Davis Highway, Suite 1204, Arlington, VA 22202-4302, and to the Office of Management and Budget, Paperwork Reduction Project (0704-0188), Washington, DC 20503.</small>				
1. AGENCY USE ONLY (Leave blank)	2. REPORT DATE MAR 1993	3. REPORT TYPE AND DATES COVERED FINAL 02/01/92 - 04/30/92		
4. TITLE AND SUBTITLE EVALUATION OF THE C/EC/KC-135 GROUND COLLISION AVOIDANCE SYSTEM (GCAS) (STUDY 2)		5. FUNDING NUMBERS		
6. AUTHOR(S) Maj. Justin D. Rueb Lt Jordan R. Kriss John A. Hassoun				
7. PERFORMING ORGANIZATION NAME(S) AND ADDRESS(ES) Crew Station Evaluation Facility Crew Station & Human Factors Section Aeronautical Systems Center Wright-Patterson AFB, OH 45433-6503		8. PERFORMING ORGANIZATION REPORT NUMBER ASC-TR-93-5004		
9. SPONSORING / MONITORING AGENCY NAME(S) AND ADDRESS(ES) Crew Station Evaluation Facility Crew Station & Human Factors Section Aeronautical Systems Center Wright-Patterson AFB OH 45433-6503		10. SPONSORING / MONITORING AGENCY REPORT NUMBER		
11. SUPPLEMENTARY NOTES				
12a. DISTRIBUTION / AVAILABILITY STATEMENT APPROVED FOR PUBLIC RELEASE; DISTRIBUTION IS UNLIMITED			12b. DISTRIBUTION CODE	
13. ABSTRACT (Maximum 200 words) <p>This report represents the second of a two-study evaluation program. The first study (Rueb & Hassoun, 1991) evaluated the original Cubic GCAS algorithm in four distinct phases. Throughout the four phases, concerns and recommendations were forwarded to the System Program Office and to the Cubic Corporation. This resulted in modification of the algorithm prior to the next phase of the evaluation.</p> <p>Phase I efforts focused on the verification and validation of the algorithm. This phase simply established how well the algorithm predicted altitude loss based on current inputs. Phase II was the robot pilot model phase. During this phase, a computer pilot model tested the GCAS under different aircraft configurations and environmental conditions.</p> <p>The man-in-the-loop phase, Phase III, used a subset of the configuration in Phase II in addition to a series of Instrument Landing System (ILS) runs to determine algorithm ability to accurately predict under realistic conditions (human reaction times). In the final phase, current operational pilots flew mission scenarios based on selected CFIT mishaps. This phase permitted an evaluation of the Cubic GCAS algorithm under real-world conditions.</p> <p>Study 2 used the same four-phase approach as that used during Study 1. However, the evaluation was performed on the newly revised Cubic algorithm. The revised algorithm incorporated more extensive changes than those conducted after each of the Study 1 phases. Additionally, Study 2 evaluated Phase 1 - Phase 4 without any delay. Unlike Study 1, the algorithm was not returned to Cubic for modification prior to the next phases.</p>				
14. SUBJECT TERMS Ground Collision Avoidance System (GCAS)			15. NUMBER OF PAGES 149	
			16. PRICE CODE	
17. SECURITY CLASSIFICATION OF REPORT UNCLASSIFIED	18. SECURITY CLASSIFICATION OF THIS PAGE UNCLASSIFIED	19. SECURITY CLASSIFICATION OF ABSTRACT UNCLASSIFIED	20. LIMITATION OF ABSTRACT UL	

TABLE OF CONTENTS

Section	Page
EXECUTIVE SUMMARY	ix
INTRODUCTION	1
Background	1
GCAS System Design	1
GCAS Evaluation Procedure	2
Cubic GCAS Algorithm Changes	2
PHASE I	5
Method	5
Procedure	5
Results	5
DCAEXTRP	5
GCASDIVE	6
GCASROLL	6
Phase I Discussion	17
PHASE II	18
Method	18
Apparatus	18
Facility	18
Simulator	18
Computer Complex	18
Design	18
Procedure	19
Results	19
Phase II Discussion	24

TABLE OF CONTENTS (CONT)

Section	Page
PHASE III	25
Method	25
Subjects	25
Apparatus	25
Facility	25
Simulator	25
Computer Complex	25
Experimenter's Console	25
Voice Message Unit Mechanization	25
Visual Warning Signal	26
Part 1 - Dive Configuration	26
Design	26
Procedure	26
Part 1 Results	27
Pilot Window of Acceptability	34
Part 1 Discussion	47
Part 2 - Approach and Landing	48
Procedure	48
Part 2 Results	48
Part 2 Discussion	49
PHASE IV	50
Method	50
Subjects	50
Apparatus	50
Facility	50

TABLE OF CONTENTS (CONT)

<u>Section</u>	<u>Page</u>
Computer Complex	50
Simulator	50
Experimenter's Console	50
Voice Message Unit Mechanization	50
Visual Warning Signal	50
Procedure	50
Results	51
Phase IV Discussion	58
CONCLUSIONS and RECOMMENDATIONS	59
BIBLIOGRAPHY	60
APPENDIX A: PHASE I DCAEXTRP GRAPHS	61
APPENDIX B: PHASE I GCASDIVE GRAPHS	77
APPENDIX C: PHASE I GCASROLL GRAPHS	93
APPENDIX D: PHASE II ROBOT MODEL DIVE GRAPHS	125

DTIC QUALITY INSPECTED 2

Accession For	
NTIS CRA&I	<input checked="" type="checkbox"/>
DTIC TAB	<input checked="" type="checkbox"/>
Unannounced	<input checked="" type="checkbox"/>
Justification	
By _____	
Distribution /	
Availability Codes	
Dist	Avail and/or Special
A-1	

LIST OF FIGURES

Figure	Page
1. Flow diagram for the Cubic GCAS algorithm	3
2. DCAEXT as a function of pilot response time and g-load for a DCA of 5 degrees and true airspeed of 150	7
3. DCAEXT as a function of pilot response time and g-load for a DCA of 5 degrees and true airspeed of 300.	8
4. DCAEXT as a function of pilot response time and g-load for a DCA of 15 degrees and true airspeed of 150.	9
5. GCASDIVE predicted altitude lost as a function of gamma for: Cg=22, Slope=0, Altitude=1000, & G-load=1.25	10
6. GCASDIVE predicted altitude lost as a function of gamma for: Cg=22, Slope=21, Altitude=1000, & G-load=1.25	11
7. GCASDIVE predicted altitude lost as a function of gamma for: Cg=22, Slope=0, Altitude=1000, & G-load=2.00	12
8. GCASROLL predicted altitude lost as a function of roll and true airspeed for: Gamma=-5.0, G-load=1.50, Slope=0, & Altitude=1000	13
9. GCASROLL predicted altitude lost as a function of roll and true airspeed for: Gamma=-20.0, G-load=1.50, Slope=0, & Altitude=1000.	14
10. GCASROLL predicted altitude lost as a function of roll and true airspeed for: Gamma=-5.0, G-load=2.0, Slope=0, & Altitude=1000	15
11. GCASROLL predicted altitude lost as a function of roll and true airspeed for: Gamma=-20.0, G-load=1.50, Slope=21, & Altitude=1000	16
12. Minimum clearance as a function of gamma and roll for robot pilot model: IAS=225, Slope=0, & Elevation=1000	21
13. Minimum clearance as a function of gamma and roll for robot pilot model: IAS=325, Slope=0, & Elevation=1000	22
14. Minimum clearance as a function of gamma and roll for pilot model: IAS=225, Slope=21, & Elevation=1000	23
15. Mean minimum clearance as a function of gamma for nine pilots: IAS=225 and Slope=0.	28
16. Mean minimum clearance as a function of gamma for nine pilots: IAS=325 and Slope=0.	29
17. Mean minimum clearance as a function of gamma for nine pilots: IAS=225 and Slope=7.	30

LIST OF FIGURES (CONT)

Figure	Page
18. Mean minimum clearance as a function of gamma for nine pilots: IAS=325 and Slope=7.	31
19. Mean minimum clearance as a function of gamma for nine pilots: IAS=225 and Slope=14.	32
20. Mean minimum clearance as a function of gamma for nine pilots: IAS=325, Slope=14, & Elevation=1000.	33
21. Example of a dive configuration trial	35
22. Pilot window of acceptability for entire data set: Pilot runs.	37
23. Pilot window of acceptability for a terrain slope of 0: Pilot runs.	38
24. Pilot window of acceptability for a terrain slope of 7: Pilot runs.	39
25. Pilot window of acceptability for a terrain slope of 14: Pilot runs.	40
26. Pilot window of acceptability for entire data set: Robot runs.	41
27. Pilot window of acceptability for slopes of 0, 7, & 14: Robot runs.	42
28. Pilot window of acceptability for a terrain slope of 0: Robot runs.	43
29. Pilot window of acceptability for a terrain slope of 7: Robot runs.	44
30. Pilot window of acceptability for a terrain slope of 14: Robot runs.	45
31. Pilot window of acceptability for a terrain slope of 21: Robot runs.	46
32. Example of a "late warning-crash" data point	53
33. Example of a "terrain sloping rapidly downward false alarm" data point	54
34. Example of a "pilot error induced crash" data point.	55
35. Example of an "excessive slope/low-g recovery" data point	56
36. Example of a "rapid upward change in terrain" data point	57

LIST OF TABLES

Table	Page
1. Phase II independent variables.	19
2. Mean minimum clearance for each of the Phase II independent variables	20
3. Phase III: Pilot-in-the-loop independent variables	26
4. Rating criteria for each minimum clearance altitude.	27
5 Repeated measures analysis of variance summary table.	34

EXECUTIVE SUMMARY

This study represents the second of a two-study evaluation. The first study (Reub & Hassoun, 1991) evaluated the original Cubic Ground Collision Avoidance System (GCAS) algorithm in four distinct phases. These phases will be discussed later. Following each phase of the first study, comments and suggestions were forwarded to Cubic and the algorithm was modified. This modified algorithm was then used for the next phase. Following the completion of the first study, Cubic again modified the algorithm. This algorithm is the one evaluated in the second study. The same four phases used in the first study were again used in the second study; however, the model was not modified between phases for this study.

As mentioned earlier, each of the two studies was divided into four phases. In Phase I the algorithm was broken down into its different subroutines to determine the aircraft inputs needed by each of the subroutines to compute its predicted altitude loss. The subroutines were then subjected to a computation analysis requiring each subroutine to compute predicted altitude loss given different aircraft configurations. In Phase II a simple robot pilot model flew the aircraft in a given configuration until a warning was received. Following a delay based on the algorithm calculations for predicted pilot reaction time, the model rolled and pulled to 2 g's until the aircraft flight path would allow it to clear the terrain. Phase III was broken into two parts. In Part I, pilots flew a subset of the dive configuration runs performed during Phase II. In Part II, each pilot flew eight Instrument Landing System (ILS) approaches and the data were analyzed for the accuracy of the approach and landing subroutines of the algorithm. Finally, in Phase IV, the pilots flew a full mission using an actual terrain data base.

Results indicate that the algorithm is significantly improved over the first version. An elimination of all crashes during the dive runs and a significant reduction of crashes in the mission enhanced the reliability of the algorithm. However, as terrain slope increases, variability in minimum clearance altitude increases, and therefore, the false alarm and unsafe alarm rates increase. This demonstrates that the algorithm still does not adequately account for the effects of terrain slope. However, this may not be a limitation of the algorithm, but rather a limitation of the system, since it relies on a downward looking radar altimeter for its inputs. Finally, a false alarm "Pull-up" warning was generated during takeoff and during landing when the aircraft bounced.

Many of the limits of this system are caused by the constraint that the equipment must use a downward-looking radar altimeter. Although this evaluation discovered some problems with the algorithm, given the above improvements, the conservative nature of the algorithm, and the fact that the primary limit on the system is its reliance on downward looking radar it is an excellent candidate for flight test.

INTRODUCTION

Background

During 1976 the Federal Aviation Administration (FAA) required all commercial airliners to be equipped with Ground Proximity Warning Systems (GPWS). Such a system is designed to enhance flight safety, particularly during the takeoff and approach/landing phases of flight. Since that time, Controlled Flight into Terrain (CFIT) mishaps for commercial airliners have been near zero. The Air Force similarly became interested in GPWS systems for its potential life and cost saving benefits. Earlier focus was on the development of GPWS and Ground Collision Avoidance Systems (GCAS) for fighter-type aircraft. GPWS/GCAS systems have been incorporated or are being incorporated into the A-7, A-10, F-16, and F-111 aircraft. However, little attention has been directed toward GCAS development for cargo/transport/tanker aircraft.

From 1970-1989, United States Air Force cargo/transport/tanker aircraft have been involved in 31 Controlled Flight Into Terrain (CFIT) mishaps. A review of these mishaps (Rueb & Kinzig, 1989) revealed that over 50% of the accidents may have been prevented by an operable Ground Collision Avoidance System (GCAS). In an effort to prevent similar mishaps, the Air Force is investigating the plausibility of incorporating a GCAS system into cargo/transport/tanker type aircraft.

Air Force's Strategic Air Command (SAC Statement of Need (SON), 1987) and Military Airlift Command (MAC SON, 1987) established a user need for a large body aircraft GCAS system. Accordingly, Air Force Logistics Command (AFLC) contracted the Cubic Corporation of San Diego to develop a generic GCAS system for implementation into the cargo/transport/tanker fleet. This report is Study 2 of a two-part study conducted to evaluate the effectiveness and accuracy of the Cubic GCAS algorithm.

GCAS System Design

GCAS systems generally use software algorithms to compute the altitude for emergency warning onset based on aircraft sensor inputs such as airspeed and altitude. Two considerations are important in designing the system. First, emphasis is placed on minimizing false alarms/nuisance warnings. These occur when the pilot has not committed a ground clearance error, yet a warning is generated. The second concern requires a warning to be generated whenever a ground clearance error has been committed.

Nuisance warnings may be the result of three factors. Erroneous sensor input could cause a false alarm and is a consequence of the algorithm's level of sophistication. Another factor is the algorithm's ability to predict pilot reaction time. Pilot reaction time is the elapsed time interval between the system's recognition of a ground clearance error (warning initiation) and the pilot's initiation of the recovery maneuver. For example, reaction time differences (predicted vs. actual) of just 1 second for a steep dive (12,000 feet per minute) could add an extra 200 feet to the predicted total altitude loss. Finally, the algorithm's inability to accurately predict, calculate, or extrapolate could also cause a nuisance warning.

GCAS algorithms usually are designed using one of two approaches. The first approach used by Cubic's Ground Collision Avoidance System (Cubic, 1985) and Fairchild's Low Altitude Warning System (Shah, 1988) is based on a set of generic aerodynamic equations. These algorithms may differ in the various assumptions (e.g., G-load, roll and pitch limits, pilot reaction time) used to calculate predicted altitude loss. General Dynamic's (GD) Enhanced Ground Clobber uses the second approach. This

approach uses algorithms based on form functions (sometimes called curve-fitting) empirically derived by off-line simulation. The Cubic GCAS algorithm evaluated in this report followed the first approach.

GCAS Evaluation Procedure

This study represents the second of a two-study evaluation program. The first study (Rueb & Hassoun, 1991) evaluated the original Cubic GCAS algorithm in four distinct phases. Throughout the four phases, concerns and recommendations were forwarded to the System Program Office and to the Cubic Corporation. This resulted in modification of the algorithm prior to the next phase of the evaluation.

Phase I efforts focused on the verification and validation of the algorithm. This phase simply established how well the algorithm predicted altitude loss based on current inputs. Phase II was the robot pilot model phase. During this phase, a computer pilot model tested the GCAS under different aircraft configurations and environmental conditions.

The man-in-the-loop phase, Phase III, used a subset of the configurations in Phase II in addition to a series of Instrument Landing System (ILS) runs to determine the algorithm's ability to accurately predict under realistic conditions (human reaction times). In the final phase, current operational pilots flew mission scenarios based on selected CFIT mishaps. This phase permitted an evaluation of the Cubic GCAS algorithm under real-world conditions.

Study 2 used the same four-phase approach as that used during Study 1. However, the evaluation was performed on the newly revised Cubic algorithm. The revised algorithm incorporated more extensive changes than those conducted after each of the Study 1 phases. Additionally, Study 2 evaluated Phase 1 - Phase 4 without any delay. Unlike Study 1, the algorithm was not returned to Cubic for modification prior to the next phases.

Cubic GCAS Algorithm Changes

As before, the revised Cubic algorithm is comprised of four main subroutines labeled GCASALRT, GCASDIVE, GCASROLL, and GCASLAND and six other lower level subroutines. GCASALRT computes the predicted altitude loss due to pilot response (reaction) time. GCASDIVE computes the predicted altitude loss as a result of the Dive/Climb Angle (DCA) of the aircraft. At this point, it is important to clarify two terms: dive/climb angle and gamma. Dive/climb angle is the dive or climb angle of the aircraft as displayed on the attitude director indicator. Gamma is the actual flight path of the aircraft accounting for the angle of attack of the aircraft. However, since the angle of attack of the KC-135 aircraft rarely exceeds 2-3 degrees and the distinction between gamma and dive angle had little effect on the algorithm's evaluation, the two terms are used interchangeably throughout the report. GCASROLL computes the predicted altitude loss due to aircraft roll configuration. Exact details of the operation of the various portions of the Cubic algorithm are documented in Rueb & Hassoun (1991). In the interest of brevity, only the major changes to the algorithm are discussed below. See Figure 1 for the flow diagram of the Cubic algorithm.

The extensive changes to the Cubic algorithm affected 5 of the 10 subroutines. Specifically, DCAEXTRP previously computed the extrapolated incremental Dive Climb Angle (DCA), which was then added to the actual DCA to allow for the effects of terrain slope. For response times not greater than 1 second, the DCA was extrapolated by using vertical velocity with either change in terrain or vertical acceleration (Az) dependent on the

dive angle. The new revision eliminates this weighting scheme and uses only vertical acceleration and predicted time to roll out to extrapolate DCA forward in time. No extrapolation is calculated from the terrain. Instead, the effects of slope are figured into the individual subroutines that compute altitude loss (GCASALRT, GCASDIVE, and GCASROLL).

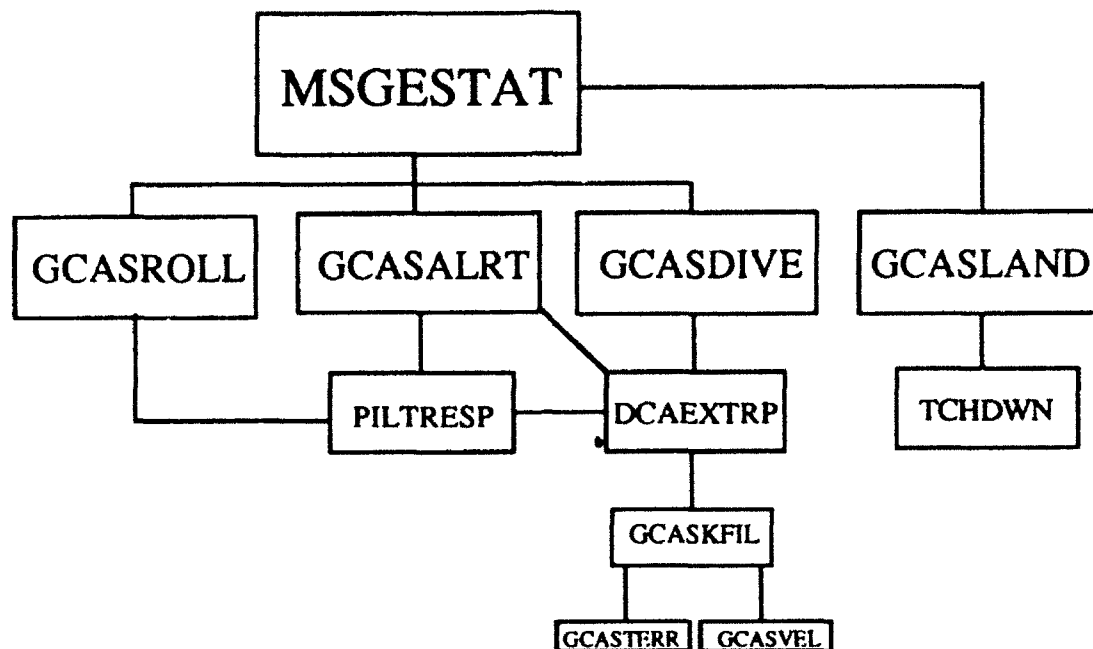


Figure 1. Flow diagram of the Cubic GCAS algorithm.

Another significant change in the algorithm was the elimination of a safety buffer. The previous version of the algorithm calculated a predicted total altitude loss and then took a percentage of this total and used it as a safety buffer. The new algorithm uses no such safety buffer. Instead, the new algorithm simply calculates the effects of each subroutine and adds them together.

The revised GCASDIVE subroutine makes adjustments in the algorithm terms associated with the expected recovery techniques. Instead of using calculations and altitude adjustments based entirely on vertical velocity, the revised algorithm uses terrain closure, which incorporates both aircraft vertical velocity and terrain slope, to calculate the predicted altitude loss due to dive climb angle of the aircraft. In order to perform its calculations, the algorithm uses integral algebra to determine terrain effects while assuming a constant horizontal velocity. In this manner, the algorithm accounts for terrain effects based on the closure rate between the aircraft and the ground.

The GCASROLL subroutine still uses aircraft bank angle, equivalent airspeed, roll rate, true airspeed, vertical acceleration, and vertical velocity inputs to compute the predicted altitude loss due to roll recovery. Using the pilot response time calculated in the subroutine PILTRESP, the GCASROLL subroutine uses a much simpler model based on a computed roll rate. This roll rate is calculated as a fraction of the roll angle determined from previous GCAS simulations. For example, if the algorithm determines that dive recovery will be completed before roll recovery, then it is possible that the algorithm will attribute no altitude loss to roll recovery. This assumption is based on the aircraft trajectory

already being in a positive (upward) direction. Additionally, it is also possible that roll recovery may occur at times well beyond dive recovery times (e.g., low dive angle/high roll angle) and actually result in a negative altitude loss calculation attributed to GCASROLL. As before, roll angles from 5° to 45° are covered by the subroutine.

The resulting altitudes from GCASALRT, GCASDIVE, and GCASROLL are then summed ($TALTLOS = GCASALRT + GCASDIVE + GCASROLL$). If the total computed altitude (TALTLOS) does not exceed the actual aircraft altitude (AGL), then the MSGESTAT algorithm will not generate a warning. When the total computed altitude exceeds that of the aircraft, then a GCAS warning will be triggered by the MSGESTAT algorithm.

The GCASLAND subroutine now activates the TCHDWN subroutine when the aircraft altitude is less than 1000 feet (AGL), and two (rather than three) of the following four conditions are met: (1) equivalent airspeed is less than 200 knots, (2) flaps are greater than 25% deployed, (3) gear are more than 50% deployed and (4) aircraft is within plus or minus 3 dots (1 dot = 0.375 degree) of glideslope. If the above conditions are not met, then the MSGESTAT subroutine will not address the GCASLAND subroutine. If the conditions above are satisfied, then the TCHDWN subroutine is activated and the aircraft is considered to be prepared for the approach and landing phase of flight. Additionally, the revised algorithm now uses a hierarchical presentation of warnings, listed below from most important to least important: "Pull-up," "glideslope" (deviation to low side), "gear," "flaps," and "glideslope" (deviation to high side).

The glideslope warning should be issued when the following three conditions are met: (1) aircraft altitude exceeds 200 feet (AGL), but is less than 1000 feet AGL, (2) equivalent airspeed is less than 200 knots, and (3) deviation from glideslope is less than 3 dots, but not less than 2 dots. If aircraft altitude is between 200-1000 feet and glideslope deviation is greater than or equal to 3 dots, then the message warning would be based on a computed altitude generated by the GCASDIVE subroutine. However, if the aircraft is between 200-1000 feet (AGL) and glideslope deviation exceeds 2 dots but is less than 3 dots, then a glideslope warning would be issued.

A gear or flap warning is generated when aircraft altitude is less than 1000 feet (AGL) and two of the following conditions exist: (1) flaps are more than 25%, (2) gear are more than 50 % deployed, (3) equivalent airspeed is less than 200 knots, and (4) glideslope deviation is less than three dots. The glideslope, flaps, and gear warnings in the TCHDWN subroutine are automatically generated when the above conditions are met. No computation of altitude loss is performed for these warnings.

PHASE I

Method

Procedure

In Study 1 (Rueb & Hassoun, 1991), the Cubic GCAS algorithm was broken down into its different subroutines to determine the aircraft inputs needed by each of the subroutines to compute its predicted altitude loss. The subroutines were then subjected to a computation analysis requiring each subroutine to compute predicted altitude loss given the different aircraft configurations. A Gould Sel 87 computer connected to a Nicolet Zeta 824/836 CS plotter generated the predicted altitude lost graphs for each of the main subroutines.

In this study the same procedure was used, but the predicted altitude lost graphs were generated through a Silicon Graphics IRIS workstation and transferred to an Apple Macintosh for printing. Only those subroutines directly affected by the changes were analyzed. Accordingly, Figures 2-11 represent examples of the resulting DCAEXTRP, GCASDIVE, and GCASROLL graphs. These altitude-lost graphs were plotted for varying levels of dive angle, pilot response time, roll, g-load, slope, and true airspeed, for each of the sub-algorithms. The actual independent variables varied from graph to graph for each of the GCASALRT, GCASDIVE, and GCASROLL subroutines dependent upon the variables used by the subroutine in calculating the predicted altitude loss. The graphs were then analyzed for any discrepancies from that logically expected to occur. For example, if gamma were increased, one would logically expect the predicted altitude loss to increase.

Results

DCAEXTRP

Predicted Dive/Climb Angle extrapolated graphs were generated for all combinations of true airspeed (150, 200, 250, and 300 knots), dive angles (5, 10, 15, and 20 degrees), and g-loads (0.25, 0.50, 0.75, 1.00, 1.25, 1.5, 1.75, and 2.0). This resulted in 16 DCAEXTRP graphs (See Appendix A for a complete set of the graphs). However, only three graphs (Figures 2 through 4) are necessary to explain the pattern of results. The y-axis of Figures 2 through 4 are the algorithm's extrapolated dive/climb angle as a function of pilot response time plus elapsed time. Each line represents the initial g-load on the aircraft at warning initiation.

Since the algorithm assumes that no dive angle adjustment is necessary for an aircraft that is maintaining a constant vertical velocity dive (i.e., $g\text{-load} = 1$), the graphs should have the line for a $g\text{-load} = 1$ at the 0-intercept with no slope as seen in Figures 2-4. Additionally, as $g\text{-load}$ deviates from the assumed $g\text{-load}$ baseline of 1, the extrapolated DCA should continue to increase over time. As evidenced in Figures 2-4, the effects of $g\text{-load}$ are similar across DCA and true airspeed indicating the algorithm is predicating DCAEXTRP in a very consistent manner. A comparison of Figures 2 and 3 indicates that as airspeed increases, the DCA extrapolated decreases. This is understandable since increased airspeed would result in an aircraft hitting the algorithm's target $g\text{-load}$ of 1.5 more rapidly. Similarly, a comparison of Figures 3 and 4 indicates that dive/climb angle had little effect on DCA extrapolated. This again is understandable as DCA at constant speed does not directly affect target $g\text{-load}$ of the recovering aircraft, whereas, airspeed does. Although comparisons for only 3 of the 16 graphs are presented, the same pattern of results was found for all graph comparisons. The consistency of the results indicates that the revised DCAEXTRP subroutine is reliable and an improvement over the earlier version.

DCA Extrapolated Example. An aircraft is in a 15 degree dive ($DCA = -15$) at 300 knots true airspeed with a positive g-configuration equal to 1.25. Based on this information, the algorithm will extrapolate ahead in time producing a positive DCA adjustment. For example, the algorithm would calculate a DCA extrapolated of 1.5 degrees for an estimated pilot response and recovery time of 3 seconds. This is then applied to its current DCA of -15 resulting in a predicted DCA of -13.5 (See Figure 4), which is then used in the GCASALRT and GCASDIVE subroutines.

GCASDIVE

The GCASDIVE subroutine was evaluated by generating various predicted altitude lost graphs based on a $C_g=22$; pressure altitude of 1,000; terrain slopes of 0, 7, 14, and 21 degrees; g-loads of 1.25, 1.5, 1.75, and 2.0 g's; airspeeds of 150, 175, 200, 225, 250, 275, 300, and 325 knots; and gammas ranging from 0° - 30° . This resulted in a total of 16 different graphs (See Appendix B for a complete set of the graphs). However, only three graphs are needed to describe the patterns of results. These predicted altitude lost due to flight path angle (GCASDIVE) graphs are shown in Figures 5-7. The x-axis is gamma, the y-axis is the predicted altitude loss due to gamma, and each line represents a given true airspeed. As seen by the true airspeed (TAS) data lines (Figure 5), higher airspeeds resulted in consistently higher values of predicted altitude loss for each condition of gamma. This was expected, because for a given gamma, downward vertical velocity increases as true airspeed increases.

By comparing Figures 5 and 6, the effects of slope can be evaluated. As anticipated, the algorithm predicts increases in predicted altitude loss as slope increases. Keep in mind that the actual altitude lost by the aircraft in this instance, is not equivalent to the predicted altitude loss due to gamma. Rather, it is a combination of altitude loss due to gamma and altitude loss due to rising terrain. This terrain change (in feet) is added to the altitude needed for dive recovery, which is equivalent to that of zero slope. Consequently, terrain slopes should and did result in larger predicted altitude losses due to gamma.

Figures 5 and 7 provide the necessary comparison to evaluate the effects of g-load. Since a higher g-load increases the rate by which the aircraft changes from a dive to climb configuration, it only follows that the higher g-loads should result in lower values of predicted altitude loss due to gamma. As expected, lower g-loads resulted in larger altitude losses. The pattern of results found above was both valid and consistent across the remaining 13 graphs. All results were as expected and no inconsistencies or anomalies for the GCASDIVE graphs were noted.

GCASROLL

The GCASROLL predicted altitude lost graphs used a pressure altitude of 1,000; gammas of -5, -10, -15, and -20 degrees; true airspeeds of 125, 150, 175, 200, 225, 250, 275, 300, and 325 knots; g-loads of 1.5 and 2.0 g's; and rolls ranging from 0 to 90 degrees. This resulted in a total of 32 GCASROLL graphs (See Appendix C for a complete set of the graphs). Again, only four graphs (Figures 8-11) are needed to explain the pattern of results. The x-axis is roll, the y-axis is predicted altitude lost, and the lines represent true airspeed.

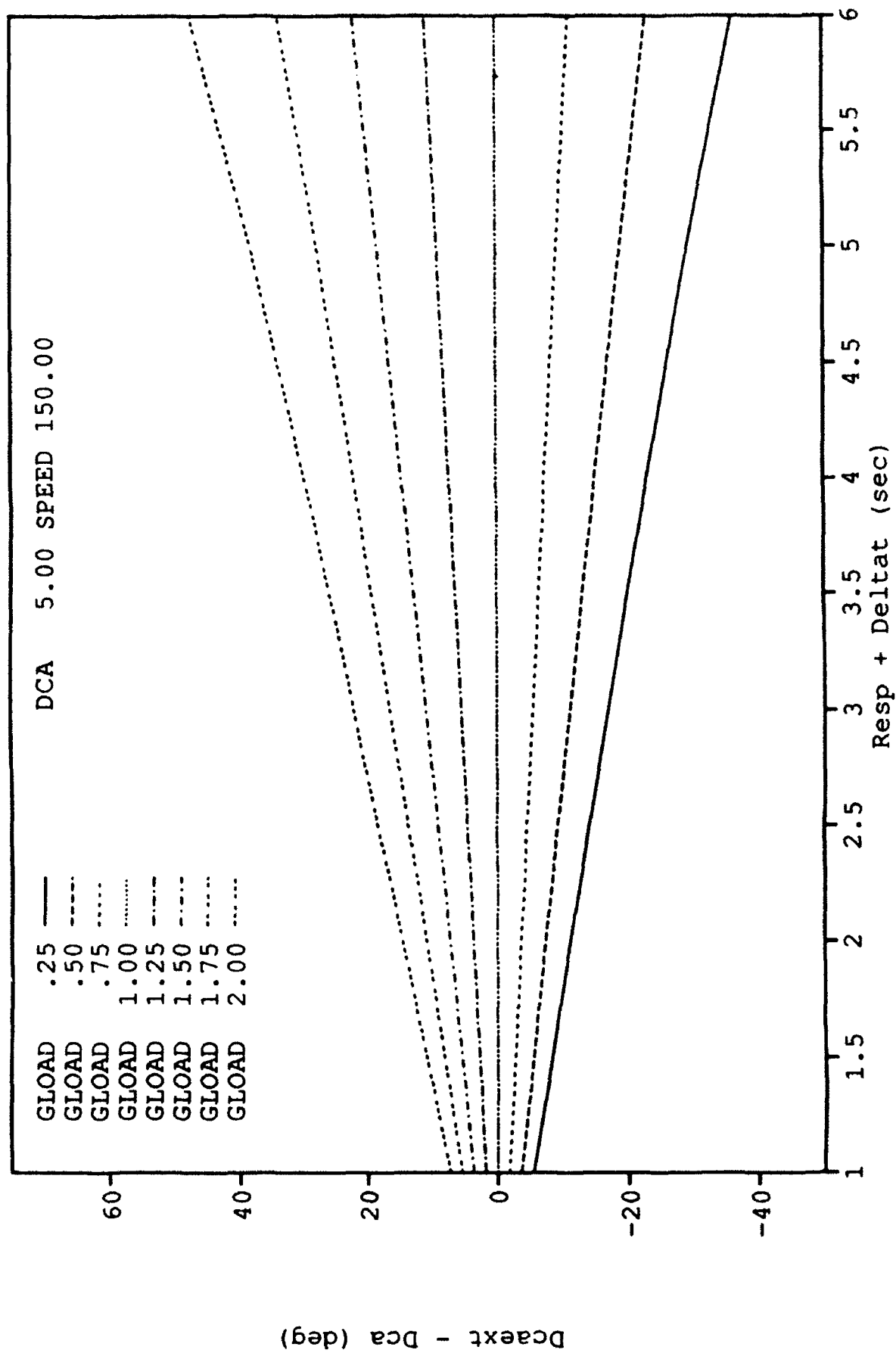


Figure 2. DCAEXT as a function of pilot response time and g-load for a DCA of 5 degrees and true airspeed of 150.

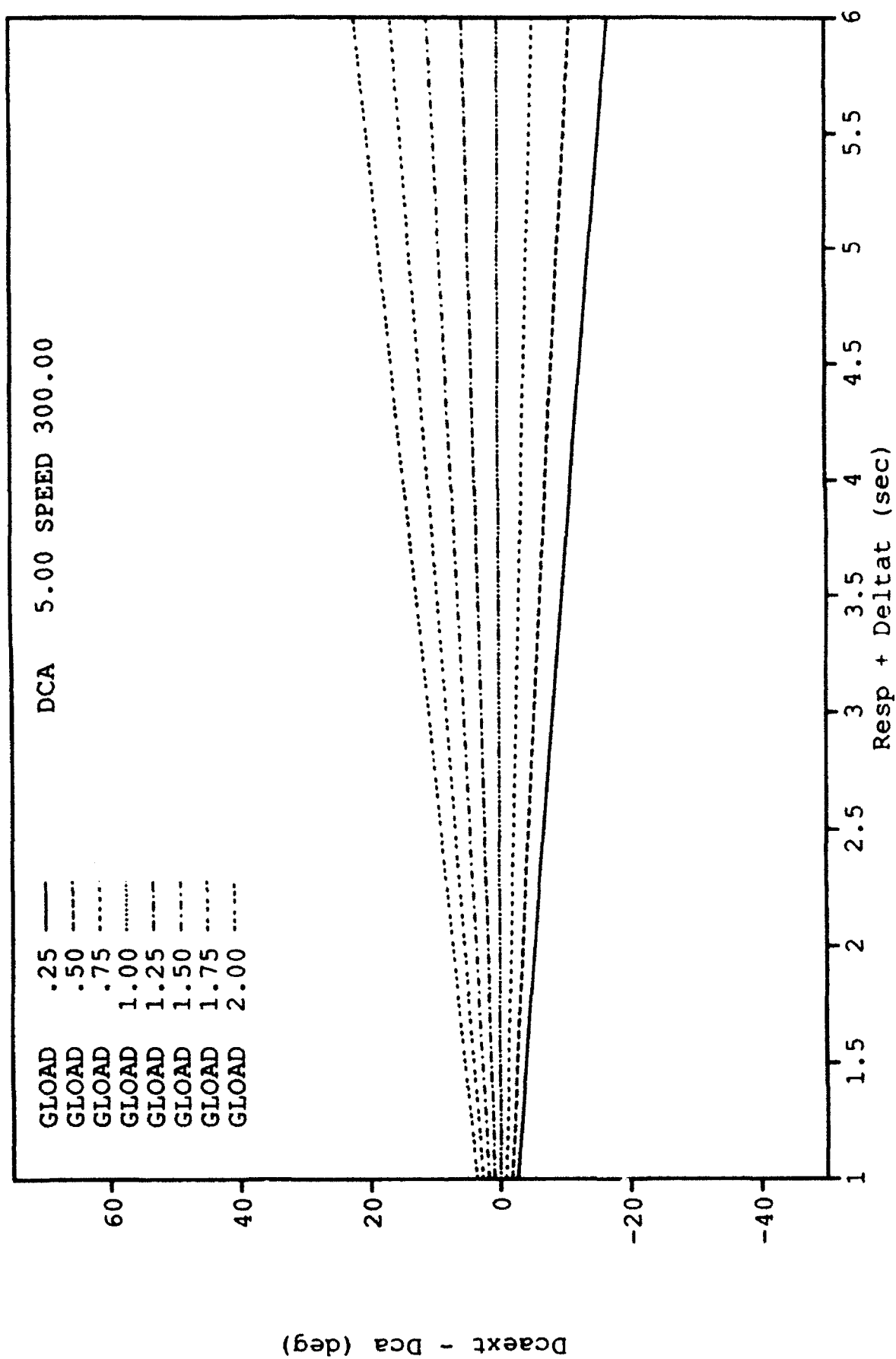


Figure 3. DCAEXT as a function of pilot response time and g-load for a DCA of 5 degrees and true airspeed of 300.

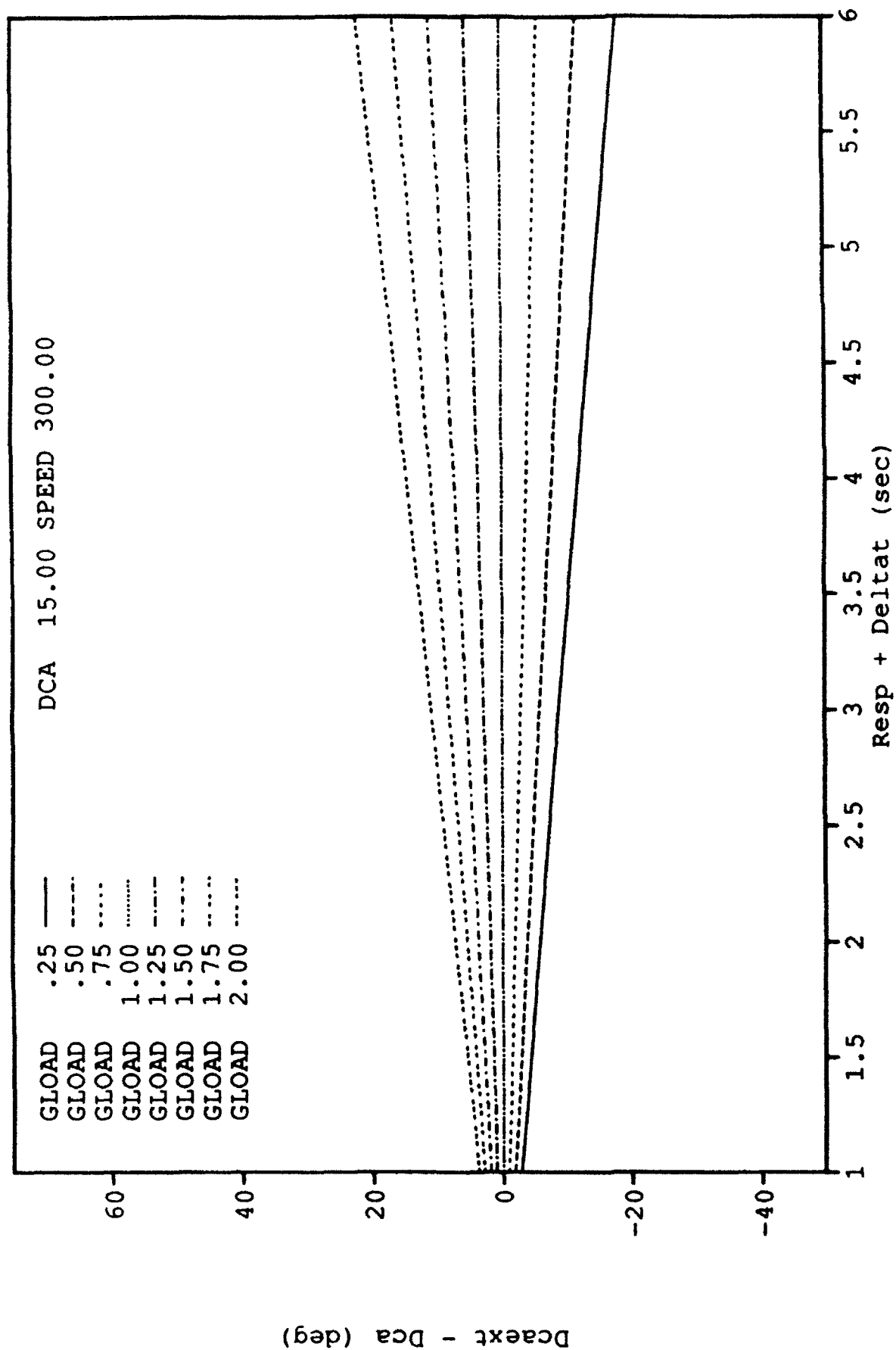


Figure 4. DCAEXT as a function of pilot response time and g-load for a DCA of 15 degrees and true airspeed of 150.

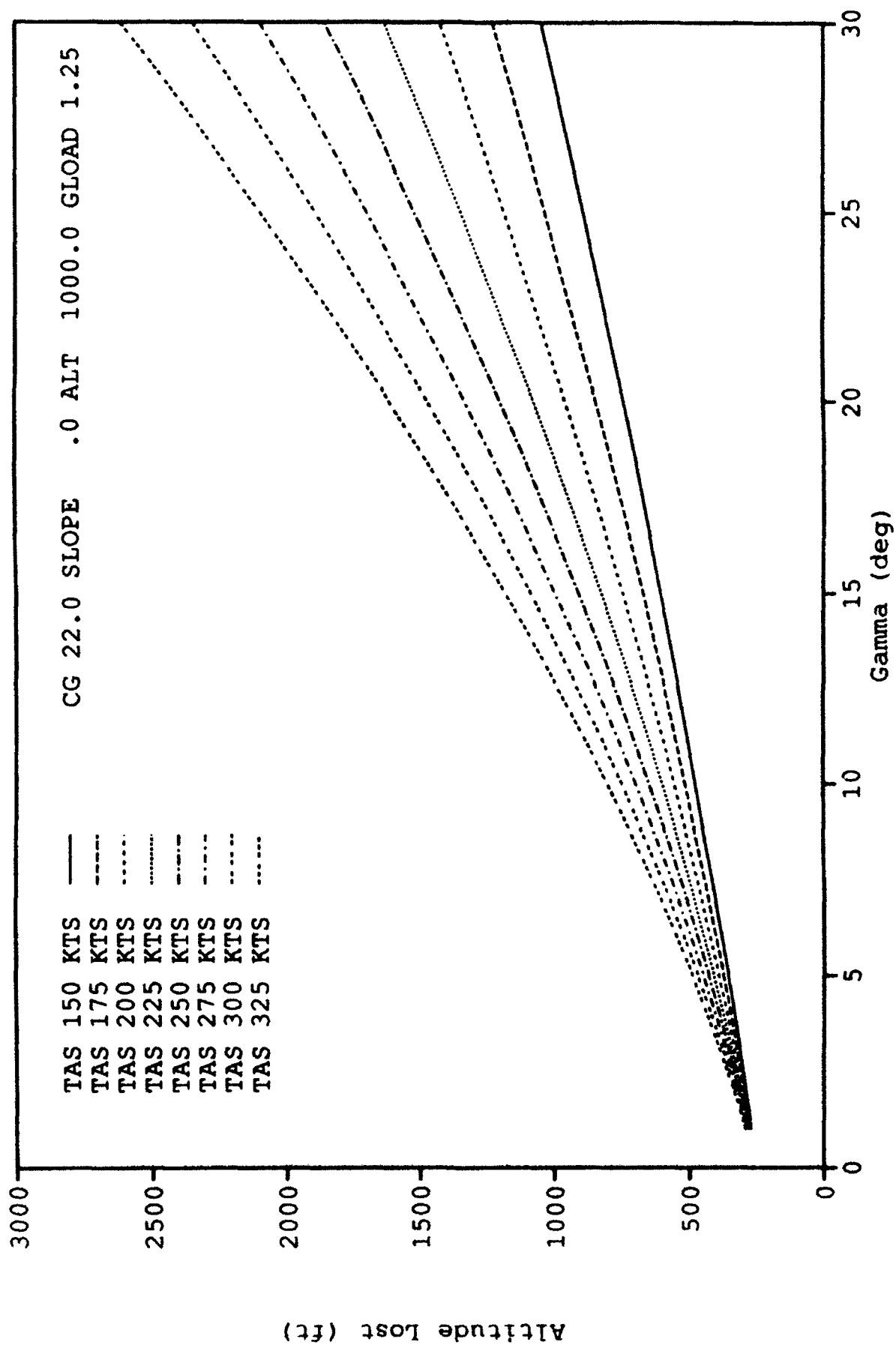


Figure 5. GCASDIVE predicted altitude lost as a function of gamma for: Cg=22, Slope=0, Altitude=1000, & G-load=1.25.

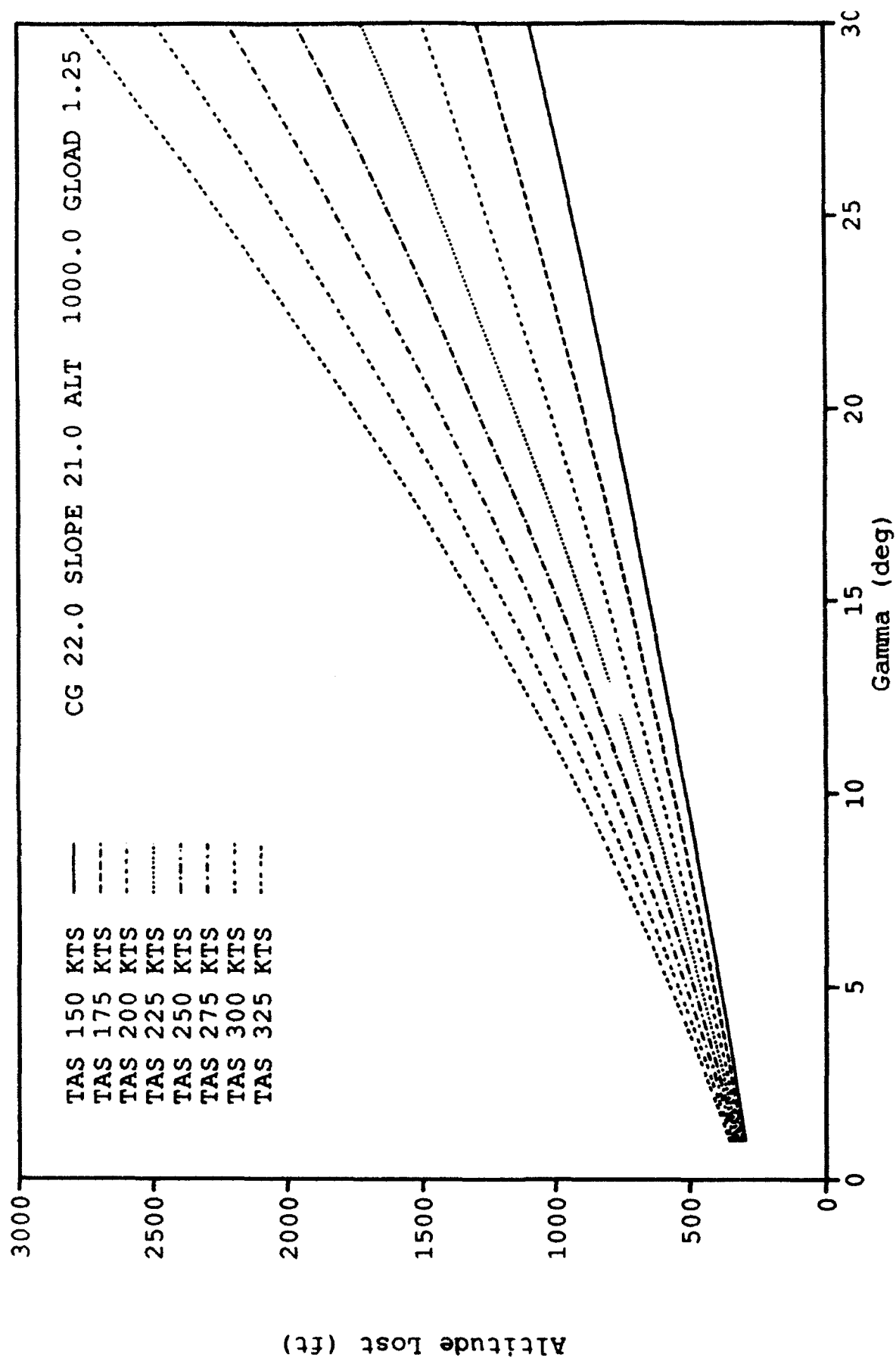


Figure 6. GCASDIVE predicted altitude lost as a function of gamma for: $C_g=22$, $Slope=21$, $Altitude=1000$, & $G-load=1.25$.

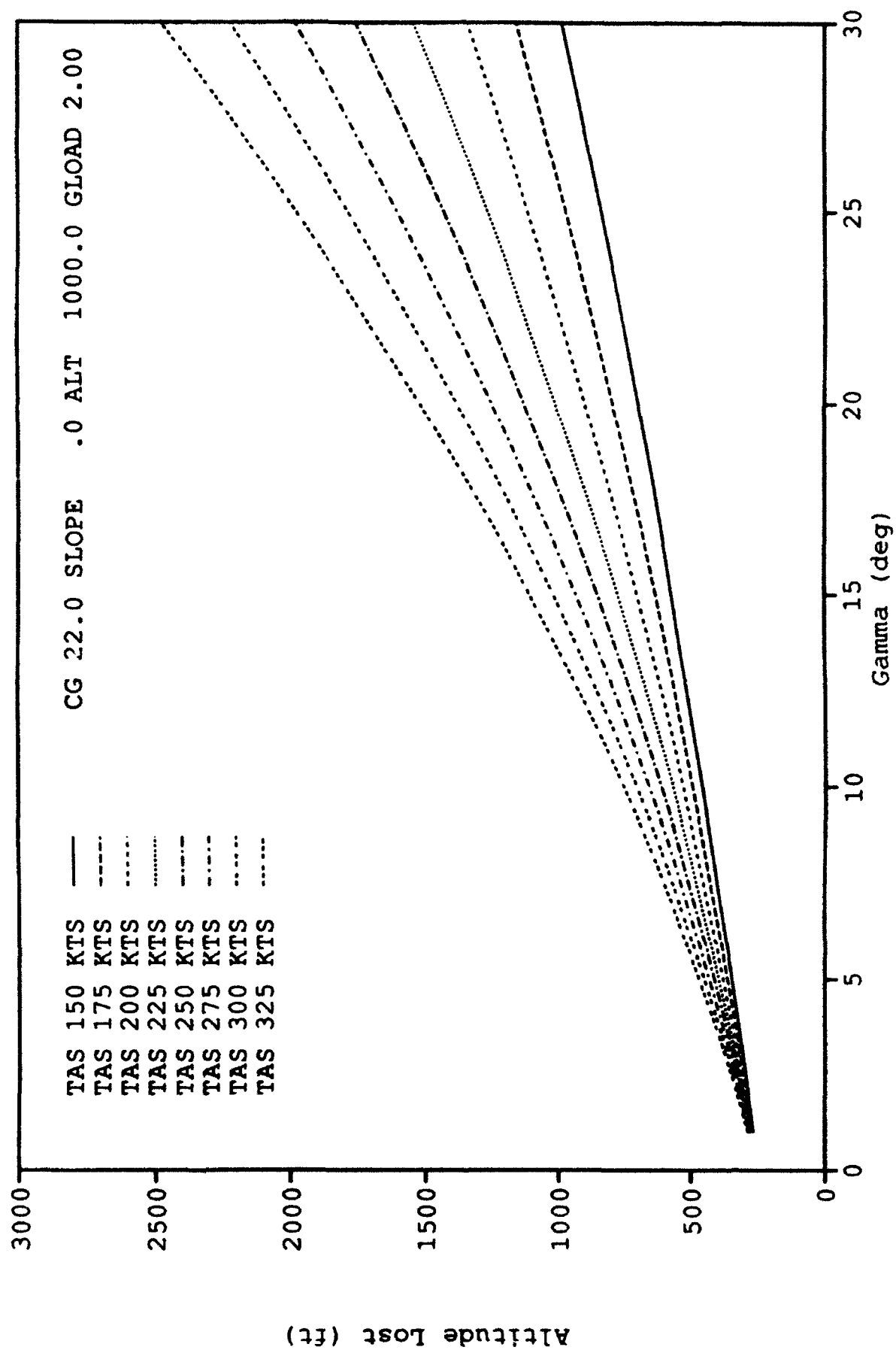


Figure 7. GCASDIVE predicted altitude lost as a function of gamma for: $C_g=22$, $Slope=0$, $Altitude=1000$, & $G-load=2.00$.

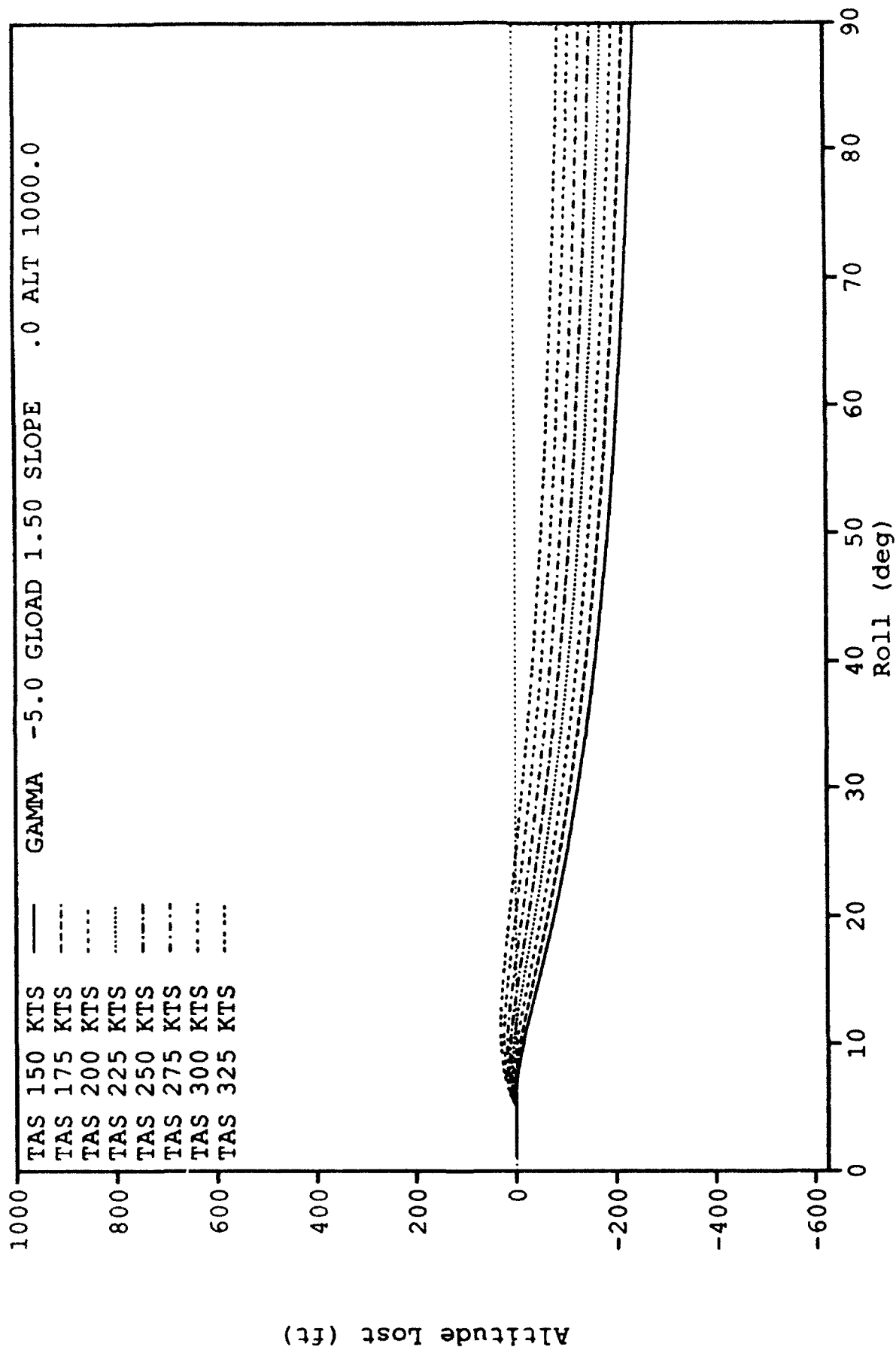


Figure 8. GCASROLL predicted altitude lost as a function of roll and true airspeed for: $\Gamma = -5.0$, $G\text{-load} = 1.50$, $\text{Slope} = 0$, & $\text{Altitude} = 1000$.

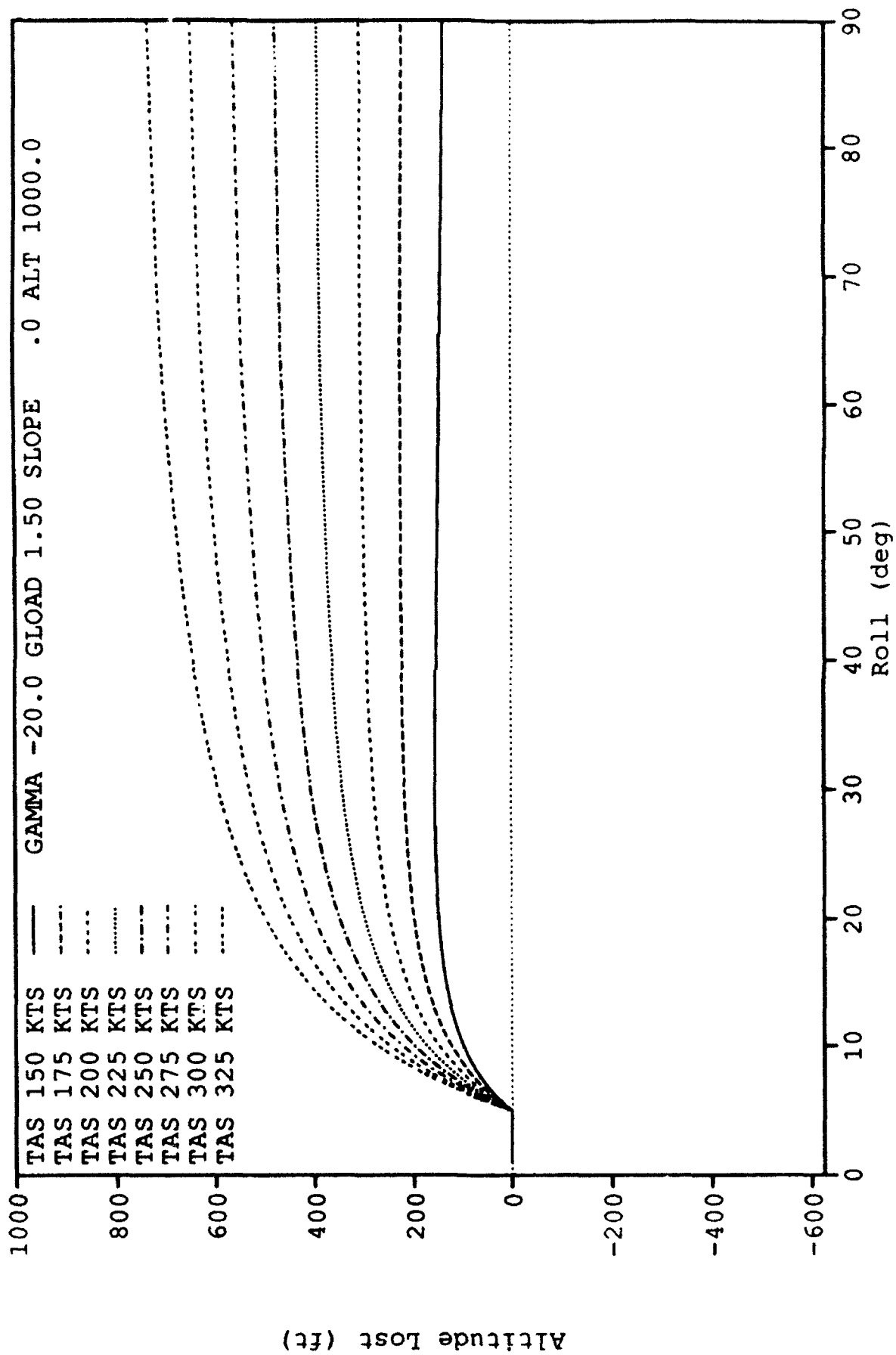


Figure 9. GCASROLL predicted altitude lost as a function of roll and true airspeed for: Gamma=-20.0, G-load=1.50, Slope=0.0, & Altitude=1000.

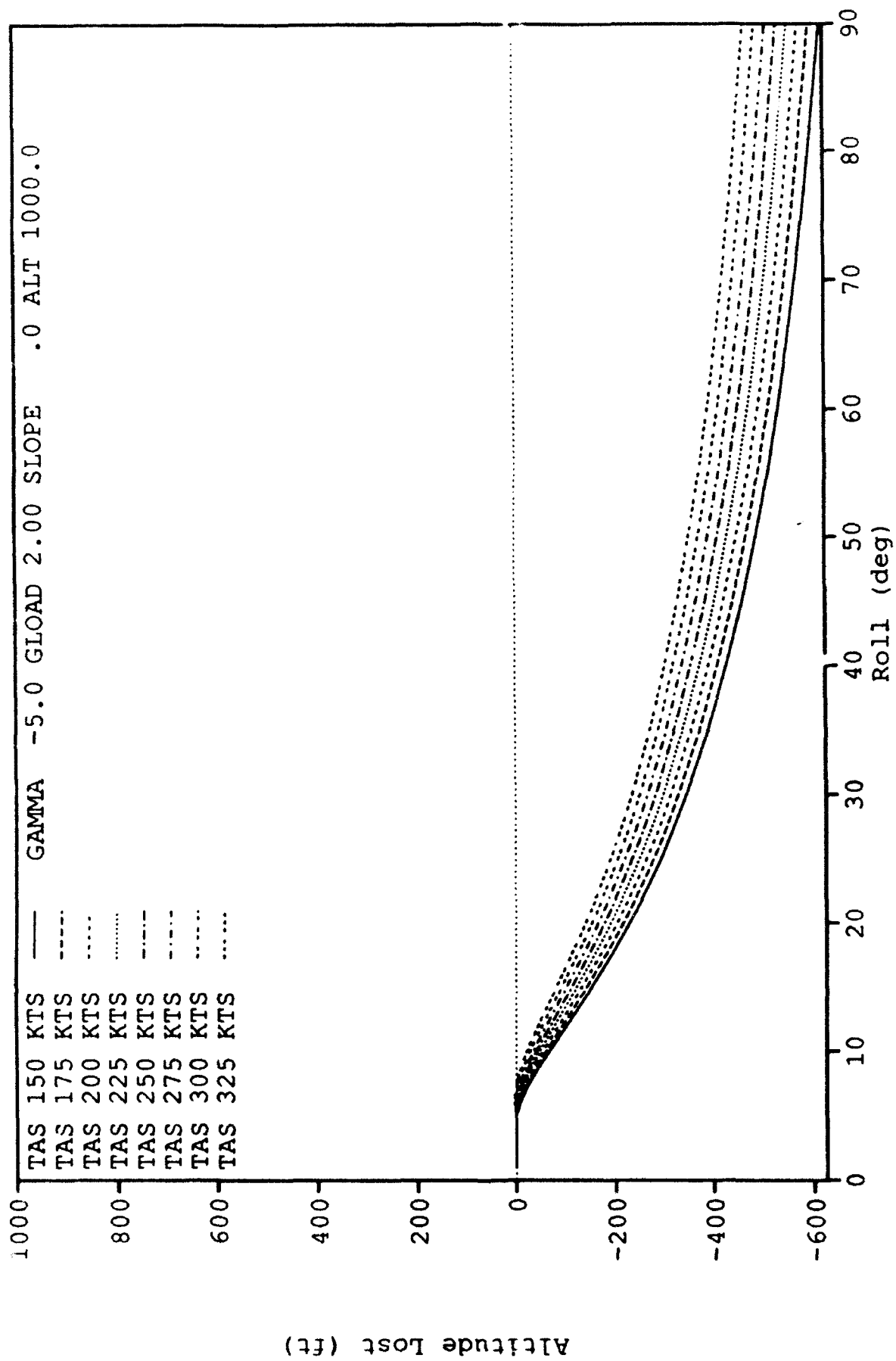


Figure 10. GCASROLL predicted altitude lost as a function of roll and true airspeed for: $\Gamma = -5.0$, $G\text{-load} = 2.0$, $\text{Slope} = 0$, & $\text{Altitude} = 1000$.

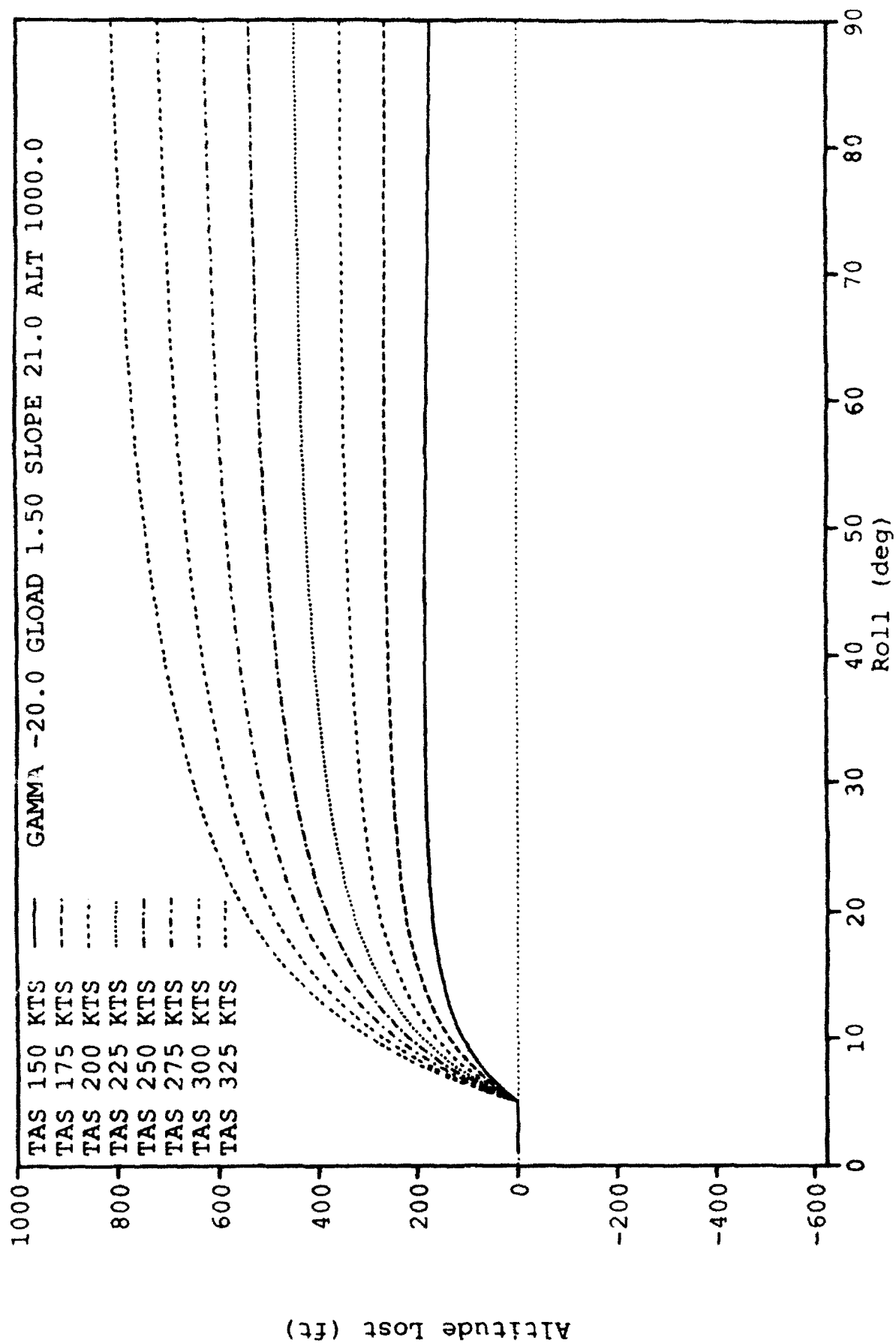


Figure 11. GCASROLL predicted altitude lost as a function of roll and true airspeed for: $\Gamma = -20.0$, $G\text{-load} = 1.50$, $\text{Slope} = 21.0$, & $\text{Altitude} = 1000$.

It is important to recall that GCASROLL computes altitude loss that results due to the effect of roll. As stated earlier, it is possible for roll to have no or actually an opposite effect on altitude loss, especially under low gamma and high g-load conditions. An inspection of Figure 8 quickly brings this point to bear. Under a relatively shallow gamma condition of -5° and a g-load of 1.5 g's, predicted altitude losses of a negative nature occur as early as 10° roll for the 150 TAS condition. This creates a potential problem. Under conditions where rollout is predicted to occur after the aircraft has already begun a climb, the algorithm would actually reduce the predicted total altitude loss (negative altitude loss due to roll). This ignores the conditions where the plane is climbing, but the terrain is actually climbing at a faster rate. Under such a condition the pilot would still be correcting for roll yet losing ground clearance. This condition is ignored by the GCASROLL portion of the algorithm.

Since increases in true airspeed also increase downward vertical velocity for a given gamma, it was predicted that increases in true airspeed would increase predicted altitude loss. A review of Figures 8-11 indicates that predicted altitude loss increases as true airspeed increases, as hypothesized. A comparison of Figures 8 and 9 shows that increases in gamma resulted in higher predicted altitude losses. Additionally, a comparison of Figures 8 and 10 demonstrates the effects of g-loads. As mentioned earlier, higher g-load conditions increase the change rate of the aircraft from dive to climb angles and, therefore, should use less altitude. Not surprisingly, increases in g-loads resulted in the expected decreases in altitude loss due to roll.

Figures 9 and 11 provide the necessary information to determine the effect of slope in the GCASROLL algorithm. In order for recovery conditions to be safe, increases in the warning altitude would be necessary as the slope of terrain increases. Accordingly, we would expect the predicted altitude loss to increase as the terrain slope increases. This is exactly the pattern of results shown in Figures 9 and 11. For example, an airspeed of 300 knots, a gamma of -20° , a g-load of 1.5 g's, a roll of 30° , and a slope of 0° yields an altitude loss of approximately 590 feet; whereas, the same conditions with a slope of 20° gives an altitude loss of approximately 650 feet. The pattern of results were consistent across all of the GCASROLL graphs.

Phase I Discussion

During Phase I, emphasis was placed on evaluating those portions of the Cubic algorithm that were influenced by the most recent changes. These resulted in a reevaluation of the DCAEXTRP, GCASDIVE, and GCASROLL subroutines. The predicted altitude loss graphs were based on varying levels of gamma, roll, true airspeed, g-load, pilot response time, and slope and were compared to detect any inconsistencies in the algorithm. None of the subroutines exhibited any inconsistency in their predictive power. Based on visual inspection of the data, only the GCASROLL subroutine was even considered to be a potential problem. The potential problem was exhibited by the subroutine actually reducing the total altitude loss by the computed GCASROLL value when a low-dive high-g-load condition existed. This assumes that roll has no detrimental effect on altitude loss if rollout occurs after aircraft pull-up. This assumption by Cubic was based on a limited sample of simulation data runs and not based on any theoretical research.

Despite the potential GCASROLL problem, initial indications from Phase I suggest the revised Cubic algorithm had corrected the errors identified in Study 1. The algorithm predicted consistently across all of the conditions tested. Yet, Phase I is designed only to identify early errors that can be attributed to the computations performed by the algorithm. To determine whether the algorithm provides an adequate ground clearance, without regard to pilot opinion, Phase II was performed.

PHASE II

The objective of the Phase II evaluation was to determine the GCAS algorithm response characteristics as a function of four independent variables: Terrain slope, true airspeed, aircraft roll angle, and flight path angle (γ). A KC-135 simulator was placed in a specific configuration based on the independent variables listed above. Upon release of the simulator, a simple robot pilot model attempted to stabilize the simulator at one "g" while maintaining the given run conditions until a pull-up warning was initiated. Following a predetermined delay, based on the algorithm calculations for predicted pilot reaction time, the pull-up maneuver was then performed by the pilot model based on the following criteria: Roll and pull simultaneously to a target g-load of 2 g's. This condition was maintained until the flight path angle of the aircraft became greater than that of the terrain.

Method

Apparatus

Facility. The study was conducted at the Crew Station Evaluation Facility (CSEF), which is a U.S. Air Force simulation facility that belongs to the Aeronautical Systems Center (ASC) of Air Force Materiel Command. CSEF government personnel are assigned by the Crew Systems Division (ASC/ENEC). The facility is used to perform human engineering experiments in support of a variety of System Program Offices.

Simulator. The KC-135 simulator included such major components as the control loading assemblies, seats, yokes, and visual windows. A Digital Equipment Corporation (DEC) PDP 11/35 computer used one of a number of databases to generate sets of lights, simulating various night visual scenes, for the Night Visual System (NVS). These visual scenes were then displayed on two wide angle collimating windows that provided a panoramic scene for the pilot. This provided the pilot with a visual capability used in Phases III and IV of our study. The KC-135 simulator contained all the instrumentation found in the actual cockpit for both the pilot and copilot positions. The software package contained all flight, engine, atmosphere, weights and balances modules; a dictionary of all KC-135 data variables; and several other specific commons and data pools for the KC-135C model aircraft. For a more detailed explanation of the simulator the reader is referred to Rueb & Hassoun (1991, Study 1) and Barnaba, Rueb, Hassoun, Ward, and Dudley (1992).

Computer Complex. The simulator was connected to a series of large and small computer systems. This computer complex included five Gould series 32/7780, one Gould concept 32/8780, and several Silicon Graphics Iris Work Stations.

Design

The objective of the Phase II evaluation was to determine the GCAS algorithm response characteristics as a function of four independent variables: Terrain slope, true airspeed, aircraft roll angle, and flight path angle (γ). The four variables were recorded at the time of warning initiation. Table 1 lists the different levels for each of the independent variables.

Table 1. Phase II independent variables.

ROLL	GAMMA	TAS	SLOPE
0	-5	225	0
15	-10	275	7
30	-15	325	14
45	-20		21

The actual configuration of the aircraft and the predicted altitude loss by each of the subroutines were recorded for each of the robot runs. Three dependent measures of interest were also recorded for subsequent data analysis. These were maximum g's, minimum clearance altitude, and total altitude lost. Maximum g's represented the highest instantaneous g-force placed on the aircraft, and acted as our criterion for accepting or rejecting a given robot run. If a run exceeded 3.0 g's, then the run was discarded and a new run performed.

The minimum clearance altitude, defined as the minimum distance between the aircraft and the ground (feet-AGL) during aircraft recovery, was the primary dependent variable of interest. This variable was used to determine if the algorithm had provided adequate ground clearance. The overall experimental design was comprised of a single run per condition for a total of 192 trials (4 Roll x 4 Gamma x 3 TAS x 4 Slope). All runs were successfully completed.

Procedure

The same procedure used in Study 1 was again used to complete these Phase II runs. A set-up control interface program developed to simplify user-computer interaction allowed the experimenter to monitor real-time characteristics of the simulator as it flew each configuration. For an example of the computer program pages the experimenter used to manipulate a number of variables related to the simulator, the terrain it flew over, and the response characteristics of the pilot model, see Rueb & Hassoun (1991).

Upon releasing the aircraft, the experimenter was presented with a new data page that allowed the monitoring of real-time simulator performance characteristics (See Rueb & Hassoun, 1991). The pilot model attempted to stabilize and maintain the simulator at 1 g, until the warning signal was initiated. The response delay of the robot pilot model was configured so that the pull-up maneuver was delayed for approximately the same amount of time as that calculated for the pilot response time by the algorithm's PILTRESP subroutine. Rolling out and pulling back were executed simultaneously with a maximum of 3 g's. The recovery procedure continued until a positive radar altitude rate of climb was established.

Results

In order to evaluate whether increases in the four independent variables resulted in the hypothesized increases in minimum clearances, means and standard deviations of the minimum clearances were calculated. As seen in Table 2, the expected pattern of mean minimum clearances resulted. Specifically, for every increase in airspeed, roll, gamma, and terrain slope, a corresponding increase in mean minimum clearance occurred. When reviewed for any potential interaction, none was evident. The results, although promising, must be viewed with caution because a full Analysis of Variance (ANOVA) was not possible because of the cell size limitation of 1. Consequently, the results may be slightly skewed by the group averages.

Table 2. Mean minimum clearance for each of the Phase II independent variables.

I.V.	Condition	Mean	S.D.
Roll Angle	0	1024	423
	15	1236	516
	30	1484	588
	45	1665	653
<hr/>			
Flight Path Angle (Dive)	5	991	486
	10	1233	560
	15	1510	616
	20	1675	498
<hr/>			
Airspeed	225	1098	415
	275	1346	556
	325	1613	687
<hr/>			
Terrain Slope	0	841	349
	7	1152	392
	14	1542	495
	21	1875	562
<hr/>			

In order to see the effects of each independent variable and to provide further understanding of the Table 2 results, the data from all 192 runs were sorted by true airspeed and terrain slope, and graphed for minimum clearance as a function of gamma for all the roll angle conditions. However, only 3 (Figures 12-14) of 12 such graphs are necessary to explain the results that occurred (See Appendix D for a complete set of the graphs). The x-axis is gamma in degrees nose down as indicated by the negative sign. The y-axis is minimum clearance altitude (how close the aircraft came to the ground). Each line represents a given roll condition. The airspeed and terrain slope for each of the graphs are listed at the top of the figure.

Figure 12 shows that increases in gamma do result in increased minimum clearances, as predicted. This is noticeable by following a given roll line from the right side of the graph (shallow dive angle) to the left side of the graph (steep dive angle). Similarly, roll increases resulted in increases in minimum clearances, as indicated by the separation of the roll lines. These trends were consistent across all of the graphs and coincide with the Table 2 findings discussed above.

The study of the effects of airspeed and terrain slope is slightly more tedious. Comparisons of Figure 12 with Figures 13 and 14 show the effects of airspeed and slope, respectively, on minimum clearance. These comparisons reveal that increases in airspeed and in slope did result in increases in the minimum clearance altitude. As before, these trends were consistent across all of the graphs and also agreed with the earlier findings presented in Table 2.

GCAS ROBOT RUNS
IAS=225 SLOPE=0 ELEVATION=1000

—■— ROLL=0 —□— ROLL=15 —◆— ROLL=30 —◇— ROLL=45

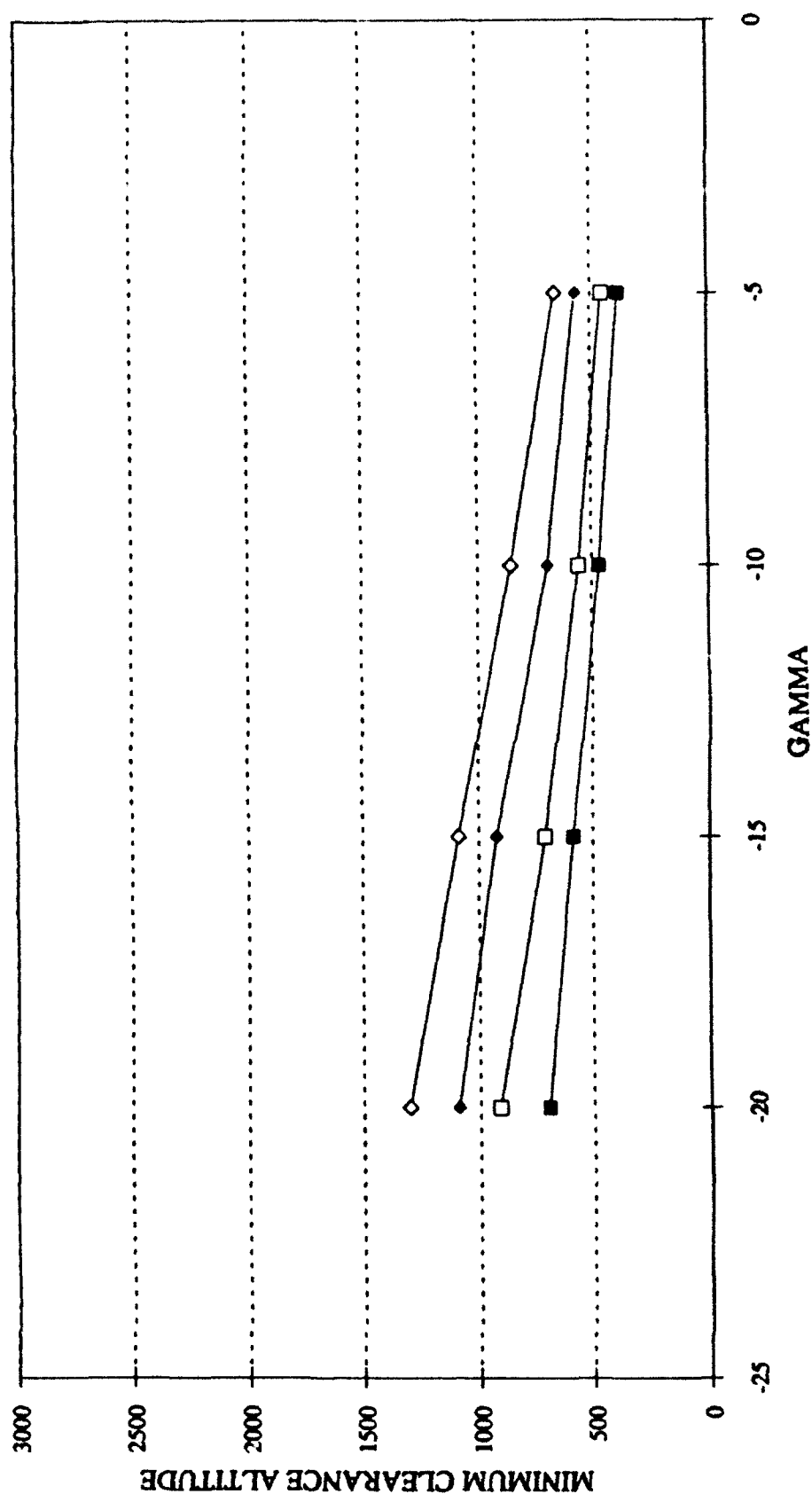


Figure 12. Minimum clearance as a function of gamma and roll for robot pilot model: IAS=225, Slope=0, & Elevation=1000.

GCAS ROBOT RUNS
IAS=325 SLOPE=0 ELEVATION=1000

—■— ROLL=0 —□— ROLL=15 —◆— ROLL=30 —◇— ROLL=45

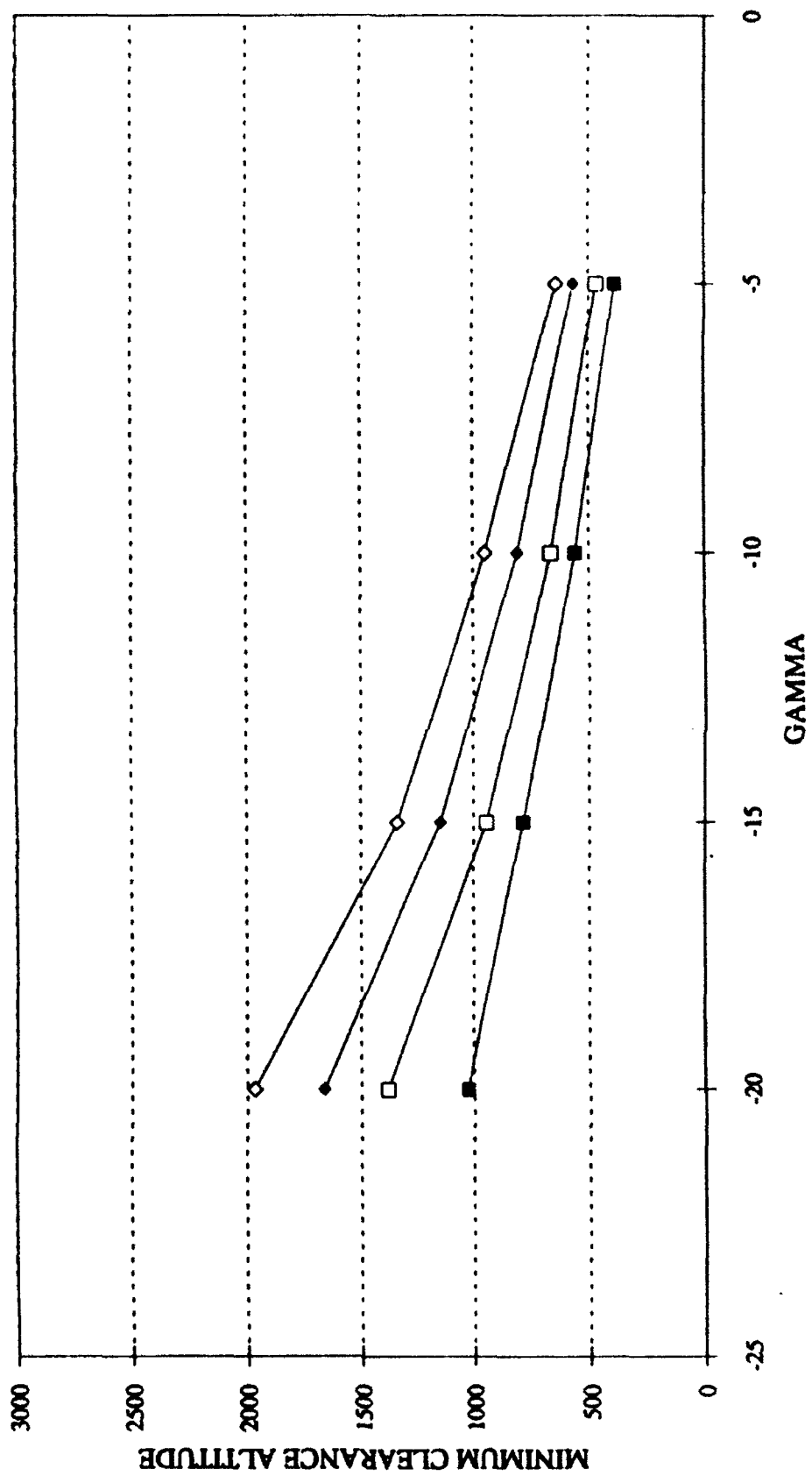


Figure 13. Minimum clearance as a function of gamma and roll for robot pilot model: IAS=325, Slope=0, & Elevation=1000.

GCAS ROBOT RUNS
IAS=225 SLOPE=21 ELEVATION=1000

ROLL=0 ROLL=15 ROLL=30 ROLL=45

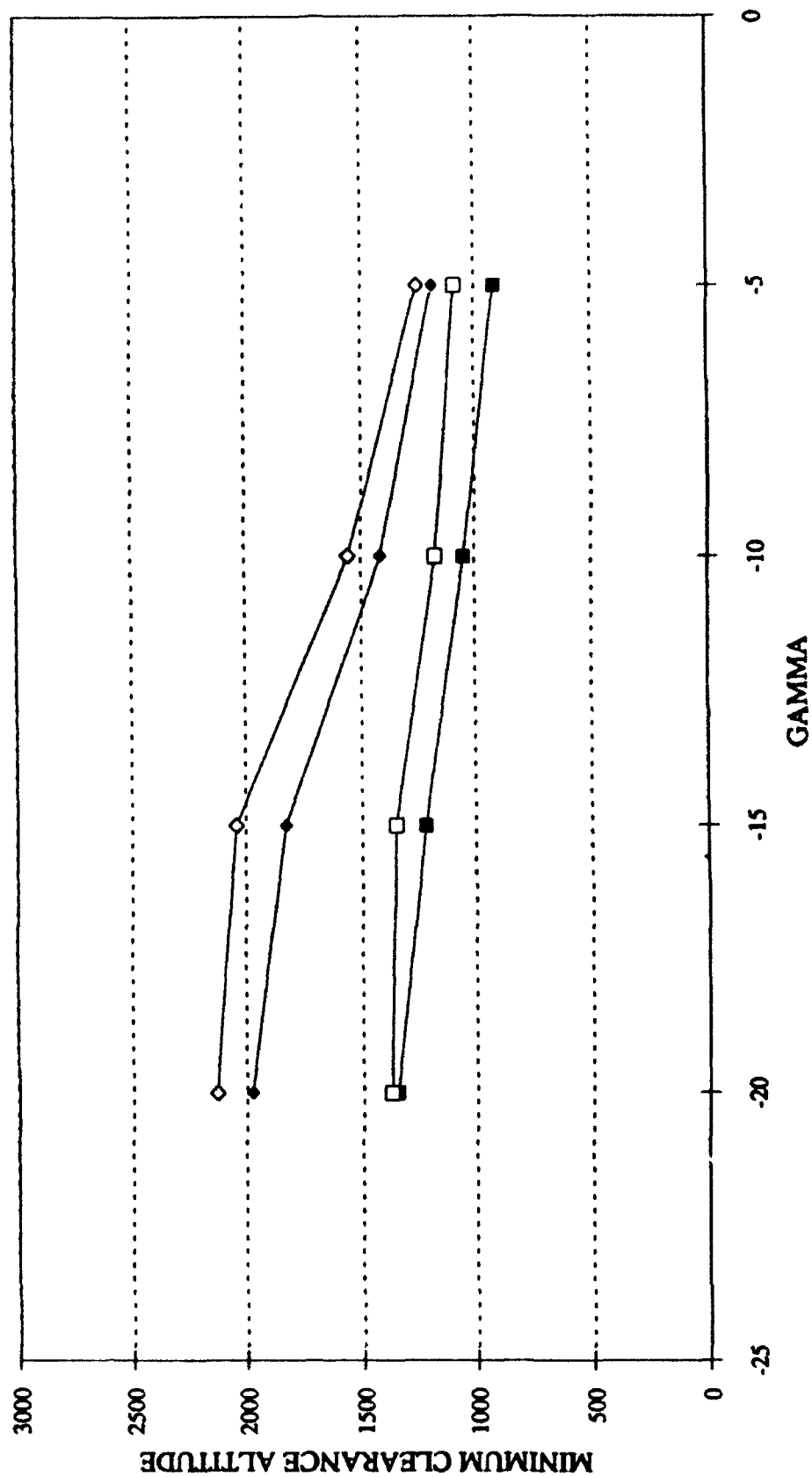


Figure 14. Minimum clearance as a function of gamma and roll for robot pilot model: IAS=225, Slope=21, & Elevation=1000.

Phase II Discussion

The results from Phase II suggest that the Cubic algorithm provides adequate minimum clearance for a wide assortment of conditions. Under all of the conditions tested, the algorithm successfully predicted altitudes that ensured no ground collision occurred. Additionally, the algorithm systematically provided increased minimum clearances for increases in each of the independent variables as hypothesized. Given the above, the Cubic algorithm does seem to provide reliable and consistent warning altitudes that provide minimum clearances above ground level. However, these minimum clearance altitudes are based on the algorithm predicted response time and a consistent recovery technique.

Increased variability is more likely as the human factor, the pilot, is brought into the loop. What now becomes critical is whether the algorithm can predict warning altitudes and minimum clearance altitudes above the ground that are considered safe, reliable, and acceptable to the user. The algorithm must be able to adapt to the variety of responses that the pilots make while flying the aircraft. Phases III and IV consider the pilot as the human factor and test whether the Cubic algorithm is acceptable to the pilot under controlled dive and real-time full mission conditions. It is only after successful completion of Phases III and IV, in conjunction with Phase I and II, that the algorithm can be deemed as completely acceptable to the pilot.

PHASE III

The objective of the third phase of the evaluation was to introduce the pilot factor and replicate a subset of the runs flown by the robot pilot model throughout Phase II, with an increased emphasis on standard flying configurations. Phase III allowed C/EC/KC-135 pilots to fly a GCAS equipped KC-135 simulator in order to evaluate and critique the most current version of the GCAS algorithm. Phase III was broken into two parts. During Part 1, pilots flew a subset of the dive configuration runs performed during Phase II. For Part 2, each pilot flew 8 ILS approaches and the resulting data were analyzed to determine the predictive accuracy of the GCASLAND and TCHDOWN subroutines.

Method

Subjects

A total of 9 pilots (8 males and 1 female) rated in the C/EC/KC-135 were used for data collection. All subjects were volunteers from the 4950th Test Wing at Wright-Patterson AFB, Ohio. The average age of the subjects was 30. The subjects averaged 2093 total flight hours with 1455 hours in the KC-135 aircraft. All of these pilots were current in their respective model of the KC-135 aircraft.

Apparatus

Facility. Refer to Phase II for a description of the facility.

Simulator. Refer to Phase II for a description of the KC-135 simulator. The analog ADI and HSI were replaced with an electronic ADI and HSI. Refer to Barnaba et al., 1992 for an in-depth description of the unique characteristics of the simulator. The decision height lights and landing gear warning horn were disabled to keep the pilot from anticipating a possible GCAS warning.

Computer Complex. Refer to Phase II for a description of the computer complex.

Experimenter's Console. The experimenter's console was located outside of the simulator. It included a complete intercom system, with communication to and from the pilot inside the simulator. The console displays provided information about what was displayed on the simulator instruments and displays, and were used to monitor the pilot and aircraft performance. The console controls also permitted the experimenter to start, stop, and reset the simulation at any time.

Voice Message Unit Mechanization. One warning ("pull-up") and three caution ("flaps," "gear," and "glideslope") voice messages were presented to the pilot's headset through the intercom channel. The pilots were allowed to adjust the volume of the interphone. The voice messages were recorded on an Amiga micro computer by a female employee of the CSEF. The employee, who had a distinctive and mature mid-western voice, presented the messages in a formal and impersonal manner. The Amiga used a high speed voice digitizer (Future Sounds), with a sampling rate of 10,000 samples per second, to convert the messages from analog to digital format. The Amiga was, thereafter, connected to the main frame computers using an RS-232 interface. This enabled the warning messages to be transmitted to the pilot's headset through the intercom channel.

Visual Warning Signal. A flashing red light placed 15 degrees right of the center field of view and just to the left of the engine and fuel instrument panels provided the visual warning stimulus. The word "Altitude" was etched in black lettering on a red background. This type of light and nomenclature was chosen based on the results of an earlier GCAS questionnaire (Rueb & Hassoun, 1990).

Part 1 - Dive Configuration

Design

Phase III of the evaluation was designed to compare C/EC/KC-135 pilot performance and subjective data as a function of four independent variables. These variables were (1) terrain slope, (2) indicated airspeed, (3) roll angle (both left and right to avoid response biases), and (4) flight path angle (gamma). Table 3 presents the levels for each of the independent variables. The zero condition was added to the slope variable for this study.

Table 3. Phase III: Pilot-in-the-loop independent variables

ROLL	GAMMA	TAS	SLOPE
15	-5	225	0
30	-10	325	7
	-15		14

The overall experiment was a repeated measures design for which each pilot was required to fly each of the 36 different run conditions (2 Roll x 3 Gamma x 2 TAS x 3 Slope). The four independent variables were recorded at the time of warning initiation. All runs were successfully completed. Refer to Rueb & Hassoun, 1991 for further details of the design.

Procedure

The procedure remained virtually unchanged from that of Study 1. The pilot was given a standardized briefing explaining the background for the study, simulator capabilities and peculiarities, and the particular flight profiles they would be required to fly. Upon completion of the briefing, the pilot was provided instructions on the simulator GCAS warning and on the various locations of the aircraft controls. The pilot was then allowed to fly the aircraft simulator until he felt comfortable with his ability to fly the simulator proficiently. In all cases, the pilot felt comfortable enough with his ability to fly the simulator proficiently within 1 hour of beginning the training period. At that time, the pilot began the Part 1 portion of the Phase III evaluation.

Part 1 required the pilot to perform a subset (See Table 3) of the dive configuration runs performed during Phase II of our evaluation. This portion of the evaluation simulated flying in the weather without an outside window visual scene. This eliminates any ground rush the pilot may sense and helps to avoid pilot anticipation of the warning. In an additional attempt to decrease pilot reaction time performance biases (i.e., possibility for the pilot accurately anticipating the warning), the simulator was initially frozen at an altitude between 1000-5000 feet above the estimated warning altitude. Prior to the release of the KC-135 simulator, the pilot was given the desired aircraft parameters (Roll angle, TAS, and Gamma) for each particular dive configuration trial. The experimenter completed this exchange with a "Ready when you are" statement. The pilot then adjusted his stab trim and responded "Ready" when he/she was prepared for simulator release.

Upon release, the pilot was required to maintain the actual roll angle and gamma of the simulator within 2.5 degrees of the desired parameters until warning initiation. Failure to be within 2.5 degrees of the desired roll angle or gamma parameter at warning initiation, or failure to keep the maximum g's of the aircraft below 2.5 (see Design section of Rueb & Hassoun, 1991) during recovery would require that trial to be rerun. No criteria were established for the indicated airspeed parameter, because pilots were limited as to what they could do to maintain airspeed in a steep (15°) dive condition, especially under the low (225 knots) airspeed condition.

At warning initiation, the pilot was required to recover the simulator as quickly as possible within the operational limitation of the aircraft. The pilot was informed to continue the recovery until a positive climb was indicated on the radar altimeter. When this occurred, the experimenter terminated the trial. Upon termination, the experimenter used the "quick-look results" display (See Rueb & Hassoun, 1991) generated on the experimenter's console to inform the pilot of the actual dive angle, roll angle, and downward vertical velocity at warning initiation, in addition to the minimum clearance altitude reached during recovery. The pilot was then required to make the following subjective rating: "In your opinion, based on your vertical velocity of (vertical velocity at initiation of warning), was the ground clearance provided by the GCAS for your last run: Too high, slightly high, about right, slightly low, or too low" (see Table 4). The pilot was then asked, "In your opinion, based on your terrain closure (terrain closure takes into account both the aircraft vertical velocity and the terrain rise or fall in relation to the aircraft) of (terrain closure at initiation of warning), was the ground clearance provided by the GCAS for your last run: Too high, slightly high, about right, slightly low, or too low." The evaluation number was entered onto the screen by the experimenter and then recorded as part of the overall data collection trial. This information was later used to develop the pilot window of acceptability (discussed later). Each pilot flew 36 dive configuration trials. The order of trial presentation was randomized to avoid task order effects.

Table 4. Rating criteria for each minimum clearance altitude.

MINIMUM CLEARANCE ALTITUDE

1. TOO HIGH
2. SLIGHTLY HIGH
3. ABOUT RIGHT
4. SLIGHTLY LOW
5. TOO LOW

Part 1 Results

The same data were collected for the present study as in Study 1. These included predicted altitude loss due to each part of the algorithm, roll, gamma, airspeed, altitude, aircraft g's, vertical velocity, and terrain slope at warning initiation; total altitude lost, maximum g's, and minimum clearance altitude during the recovery. Terrain closure at the time of warning initiation was the new variable which was also recorded.

A mean minimum clearance was computed across all nine pilots for each of the 36 configuration trials. The resulting means were sorted by indicated airspeed and terrain slope and graphed as a function of flight path angle (gamma) for all roll angle conditions. These graphs (Figures 15-20) provided the information needed to determine the algorithm's ability to provide adequate minimum clearance.

GCAS PILOT RUNS
IAS=225 SLOPE=0

ROLL

■ 15 □ 30

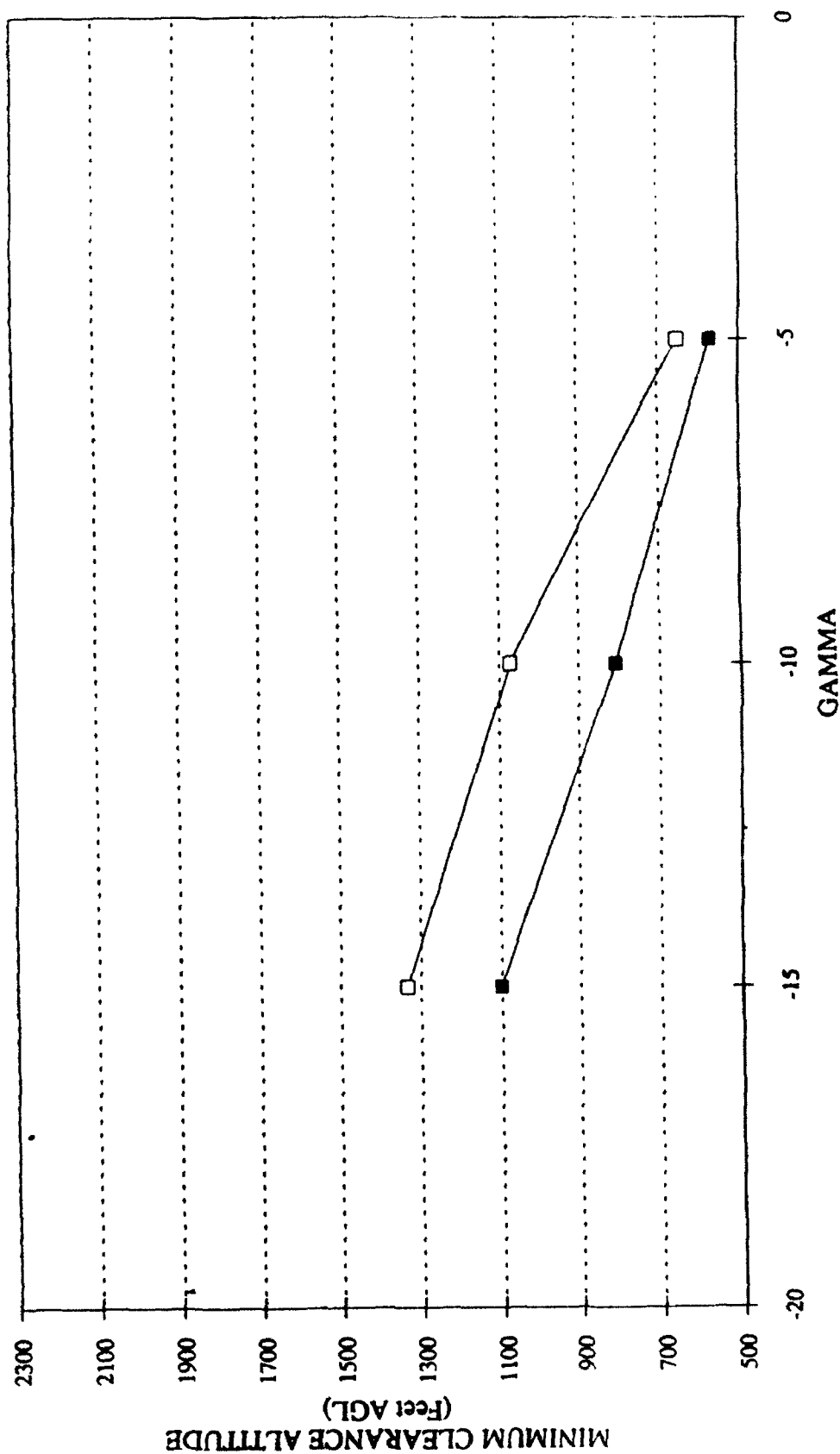


Figure 15. Mean minimum clearance as a function of gamma for nine pilots: IAS=225 and Slope=0.

GCAS PILOT RUNS
IAS=325 SLOPE=0

ROLL

—■— 15 —□— 30

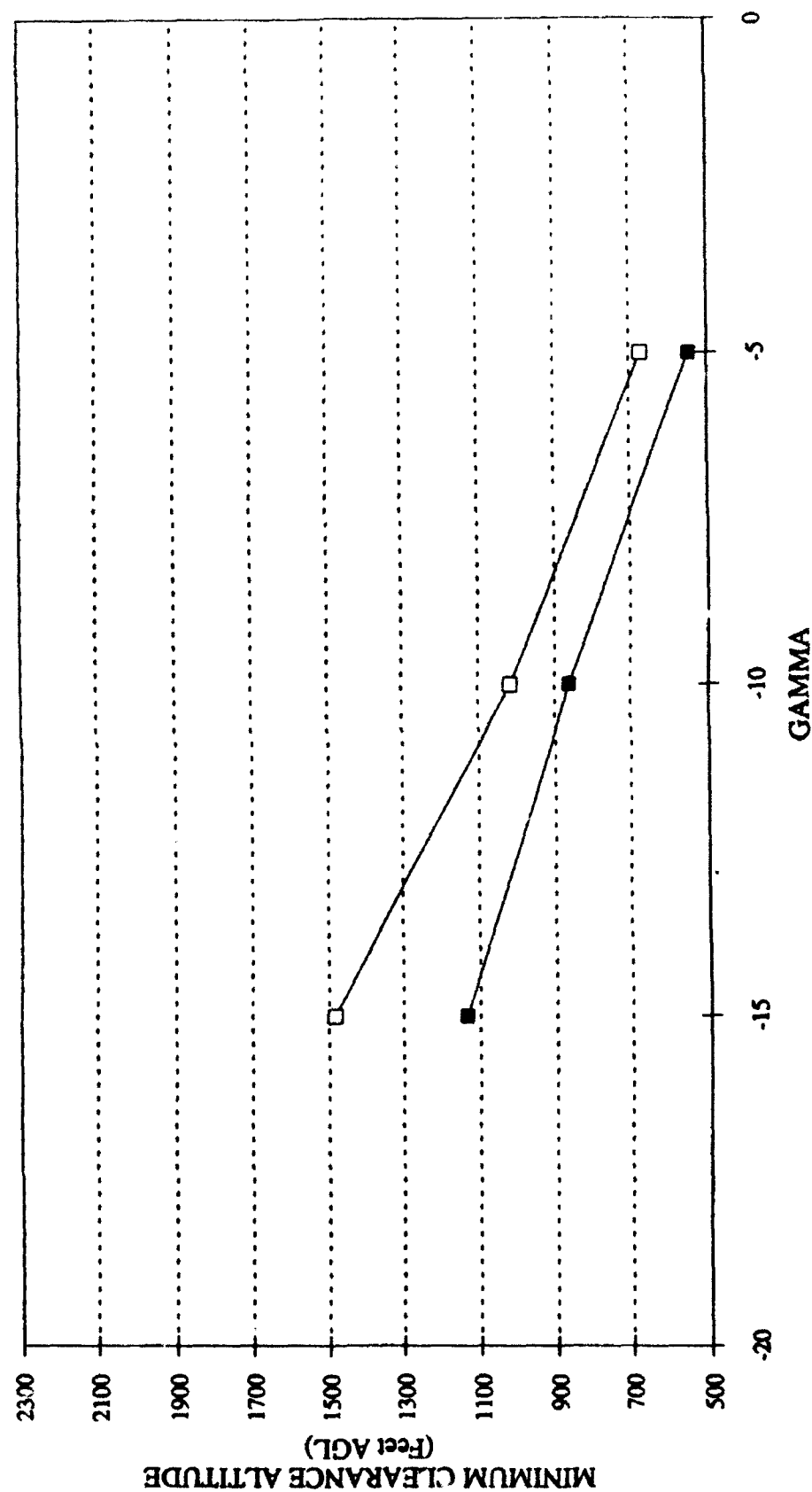


Figure 16. Mean minimum clearance as a function of gamma for nine pilots. IAS=325 and Slope=0.

GCAS PILOT RUNS
IAS=225 SLOPE=7

ROLL

■ 15 □ 30

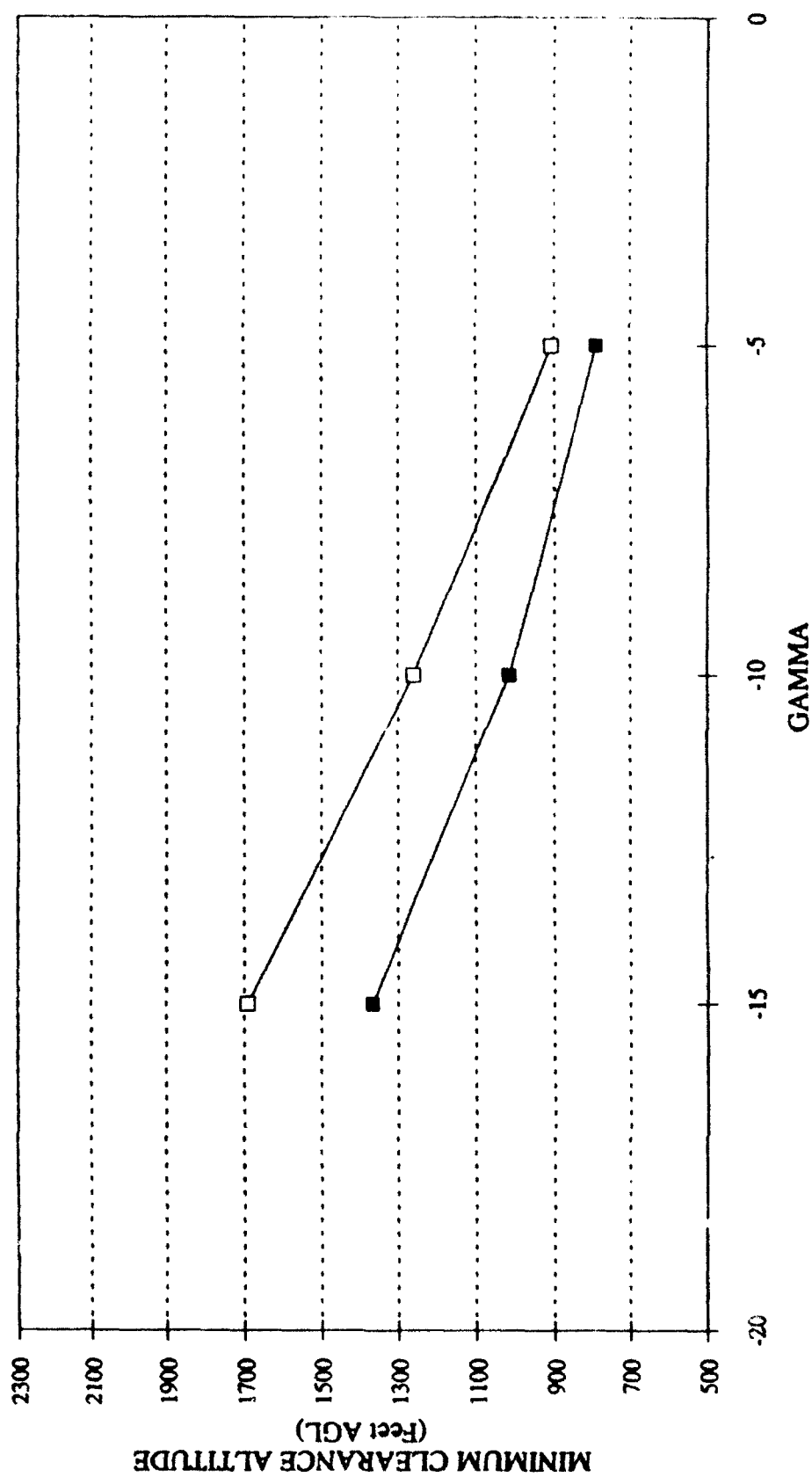


Figure 17. Mean minimum clearance as a function of gamma for nine pilots: IAS=225 and Slope=7.

GCAS PILOT RUNS
IAS=325 SLOPE=7

ROLL

■ 15 □ 30

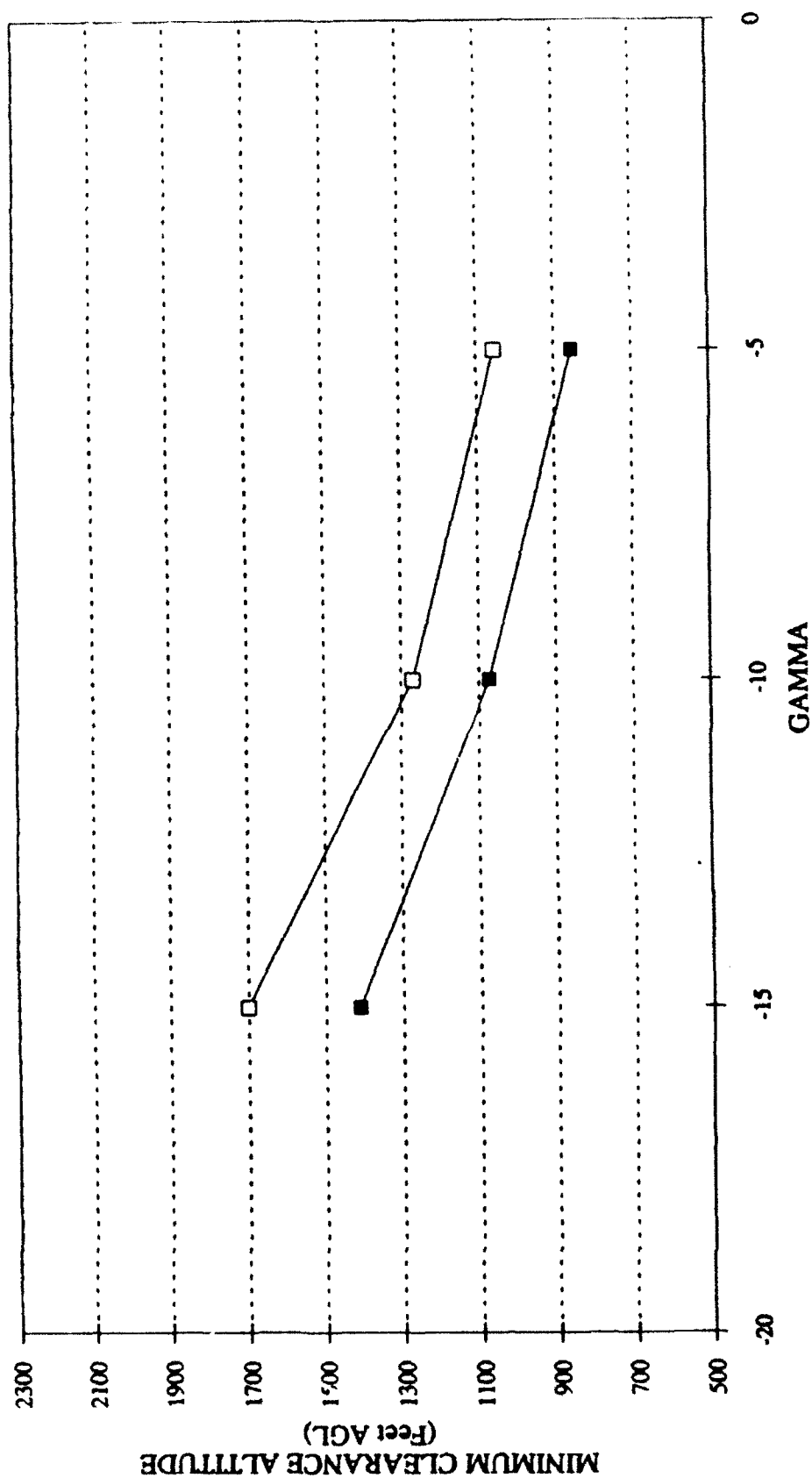


Figure 18. Mean minimum clearance as a function of gamma for nine pilots: IAS=325 and Slope=7.

GCAS PILOT RUNS
IAS=225 SLOPE=14

ROLL

■ 15 □ 30

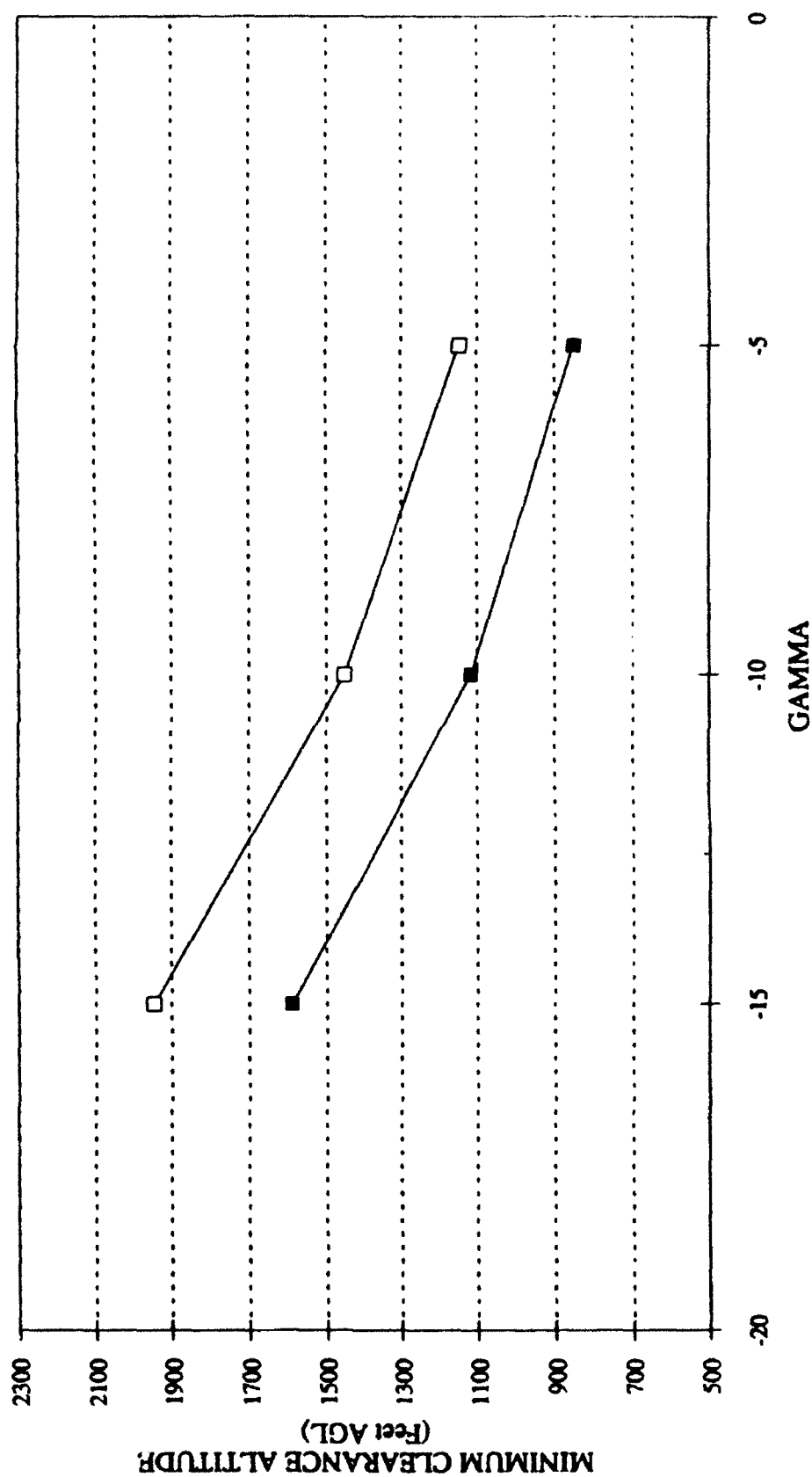


Figure 19. Mean minimum clearance as a function of gamma for nine pilots: IAS=225 and Slope=14.

GCAS PILOT RUNS
IAS=325 SLOPE=14

ROLL

■ 15 □ 30

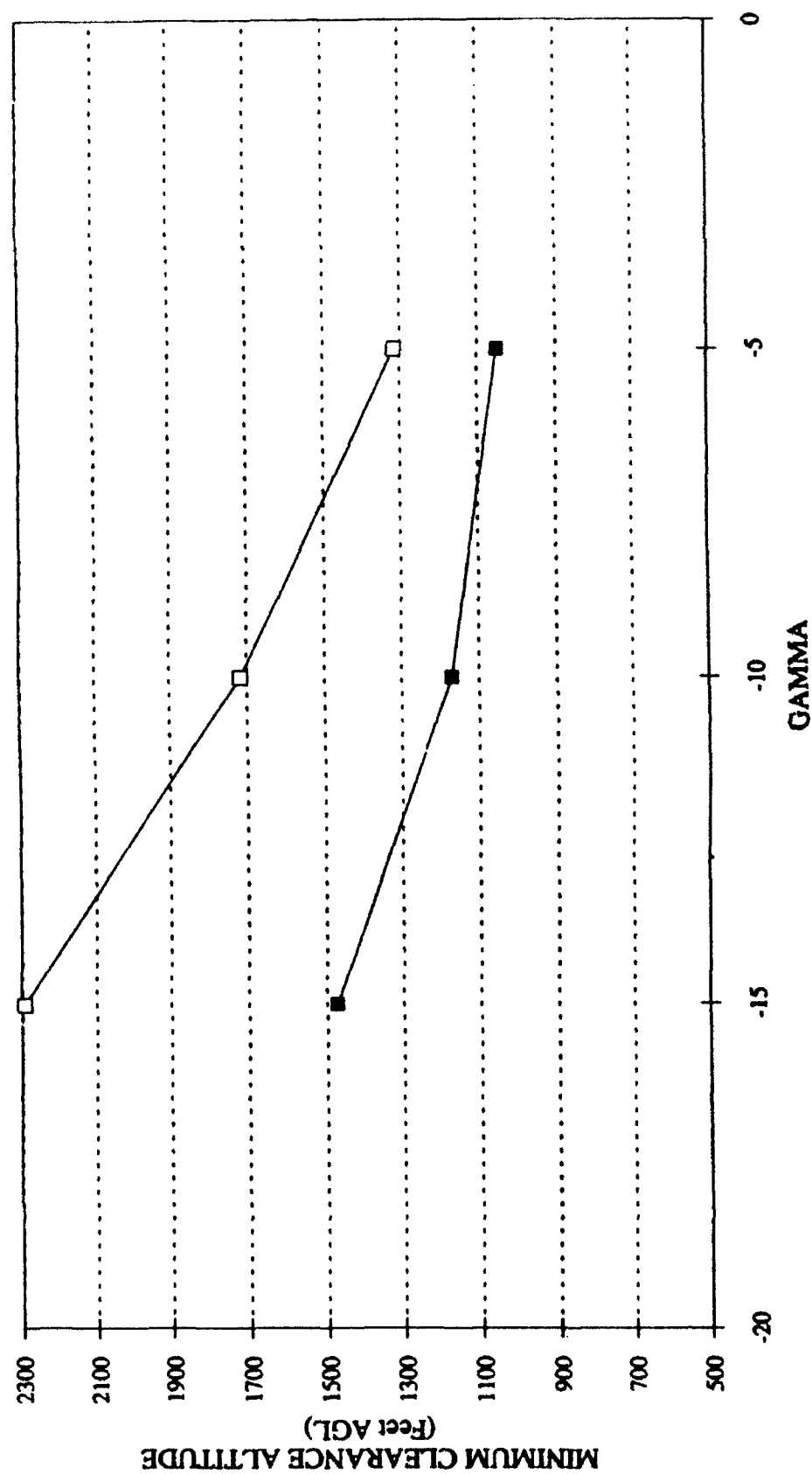


Figure 20. Mean minimum clearance as a function of gamma for nine pilots: IAS=325 and Slope=14.

Comparisons between Figures 15 and 16, Figures 17 and 18, and Figures 19 and 20 indicate that higher airspeeds generally resulted in higher minimum clearance altitudes. A repeated measures Analysis of Variance (Table 5) reveals that airspeed effects were significant ($p = 0.0230$). The effects of airspeed appear to be accounted for in the current version of the algorithm.

A review of Figures 15-20 also indicates that larger roll angles result in higher minimum clearance altitudes ($p = 0.0001$). Similar effects were noted for gamma ($p = 0.0001$) and terrain slope ($p = 0.0001$). The ANOVA also revealed that there was a significant interaction effect between roll and gamma and between roll and terrain slope ($p = 0.0023$ and $p = 0.0125$, respectively).

Table 5. Repeated measures Analysis of Variance summary table.

Source	df	SS	F	p
Gamma (G)	2	24885516	179.80	0.0001*
Roll (R)	1	6761554	114.97	0.0001*
Speed (Sp)	1	504384	7.87	0.0230*
Slope (Sl)	2	12949614	60.35	0.0001*
G*R	2	625385	9.10	0.0023*
G*Sp	2	13340	.11	0.8977
G*Sl	4	216548	1.03	0.4071
R*Sp	1	120614	2.80	0.1329
R*Sl	2	893236	5.84	0.0125*
Sl *Sp	2	228505	1.43	0.2675
G*R*Sp	2	111216	1.42	0.2700
G*R*Sl	4	63029	.37	0.8253
G*Sp*Sl	4	95497	.24	0.9150
R*Sp*Sl	2	192201	1.85	0.1895
G*R*Sp*Sl	4	246899	1.49	0.2285

Pilot Window of Acceptability

Pilots' rating data were divided into five separate data sets (one set for each possible response, see Table 4) for both terrain closure and vertical velocity, and analyzed independently using the linear regression technique. Minimum clearance altitude was considered the main dependent variable, while vertical velocity (which includes two critical factors: airspeed and flight path angle) and terrain closure (which includes airspeed, flight path angle and terrain slope) were considered the main independent variables. However, differences between the two were minimal and the fact that pilots stated they did not feel comfortable responding based on terrain closure is the reason that terrain closure results will not be directly addressed in this report.

Figure 21 is an example of an actual dive configuration run performed by a pilot. The initial run conditions are displayed across the top of the page as well as in the first six lines on the right side of the graph. The minus sign preceding the roll value indicates roll was to the left. The next four lines on the right side of the graph are the algorithm predicted altitude loss for each of the subroutines. The safety buffer (SAFT BUF) is zero because that subroutine was deleted from the algorithm. The values were summed for a total predicted altitude loss (ALT LOSS). The reaction time (REAC TIM) is that used by the algorithm. The next six variables are the actual conditions of the aircraft simulator at the time of warning initiation. Minimum clearance (MIN ALT) is the minimum distance between the aircraft and the terrain that occurred during the recovery. Maximum g's (MAX G's) and total altitude

Speed 225 Slope 14 Roll -30 Gamma -5 Subj 2

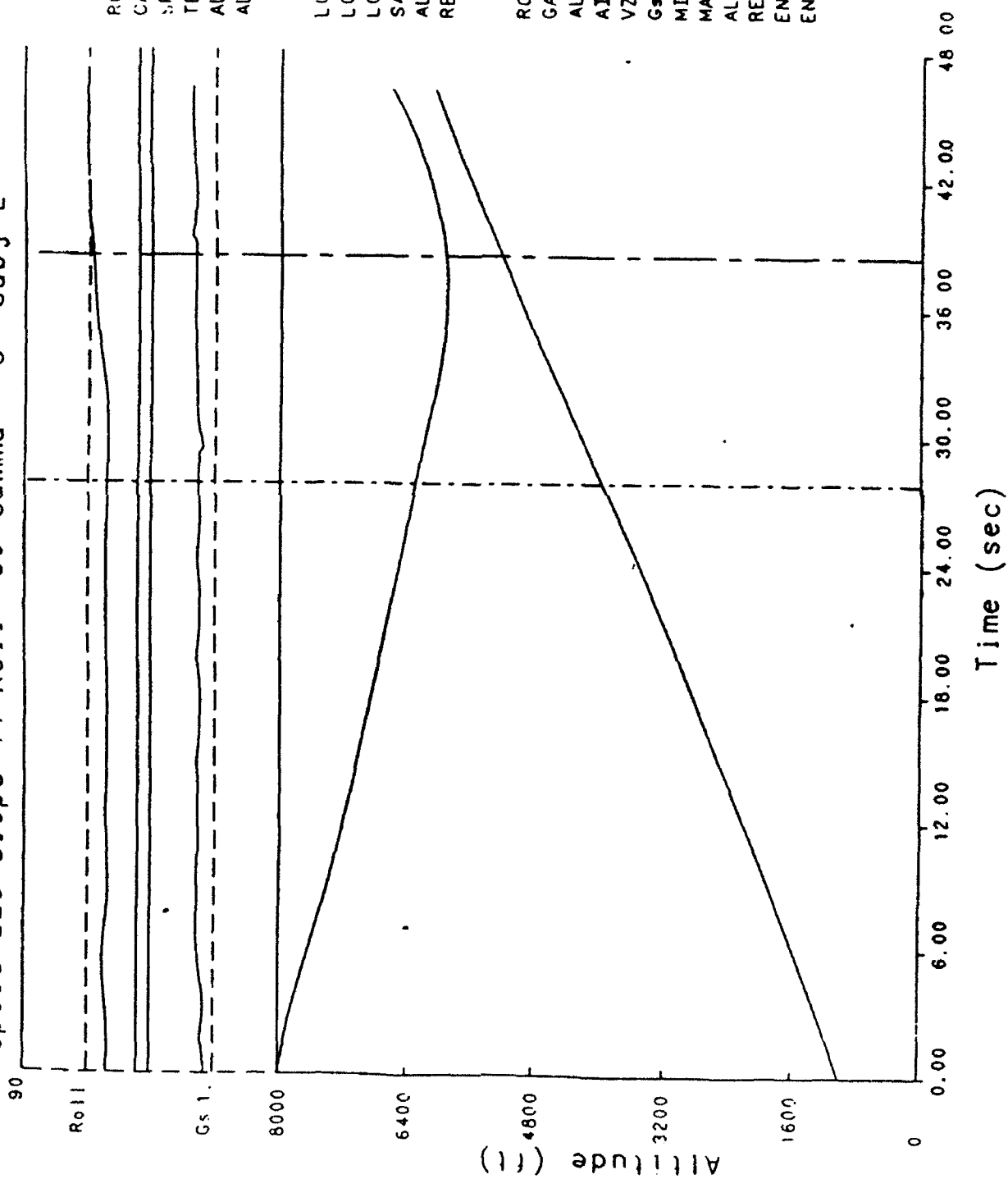


Figure 21. Example of a dive configuration trial.

loss (ALT LOSS) were the maximum values obtained during aircraft recovery. Reaction time (REAC TIM) was the actual time between warning initiation and control inputs by the pilot. The two final variables, pilot rating of minimum clearance based on vertical velocity (ENUM WOT) and pilot rating based on terrain closure (ENUM), are the values of the pilot's rating of the minimum clearance as shown in Table 4. ENUM WOT was the rating value used to formulate the pilot window of acceptability discussed below. The x-axis is the total running time from the beginning of the trial. The y-axis is the altitude of the aircraft in feet (MSL). The aircraft flight path is represented by the curved upper line. The ground level is represented by the lower straight line that begins at a terrain elevation of 1000 feet.

A composite "window of acceptability" was created by regressing the minimum clearance altitudes onto the vertical velocity for all trials given a rating of 2 (slightly high) from both Studies 1 and 2. This represents the upper limit of the window. The lower limit of the window was calculated in a similar manner for a rating of 4 (slightly low). For a more detailed description of the pilot window of acceptability, refer to Hassoun et al., (1990) and Rueb & Hassoun (1990, 1991). The window of acceptability is valid up to a vertical velocity of 11,000 feet/minute. Data from both studies were used to generate the pilot window of acceptability because the pilot subjective judgments are minimum clearance altitude based and independent of the algorithm used. This allowed for a larger, yet more stable database resulting in a more accurate window of acceptability. On the other hand, the actual data points plotted are from the present study only. By plotting only Study 2 data points, a direct evaluation of the current algorithm against the pilot window of acceptability is possible. Minimum clearances greater than the upper limit would be considered too high (false alarms). Minimum clearances less than the lower limit would be considered too low (unsafe-too close for comfort). As seen in Figure 22, of the 324 warnings, 38.6% were considered "false alarms" and 2.5% were considered to be "unsafe" warnings. A total of 58.9% fell within the pilot "window of acceptability."

The pilot window of acceptability was further broken down as a function of terrain slope. Figure 23 shows the data for a slope of 0 degrees. A total of 4% of the minimum clearances were considered "false alarms," 96% of the minimum clearances fell within the "window of acceptability." When the slope was increased to 7 degrees (Figure 24), 45% of the minimum clearances fell in the "false alarm" zone, 4% were "unsafe," and 51% fell within the "window of acceptability." The trend continues with a slope of 14 degrees (Figure 25), 65.7% of the warnings were considered "false alarms," 4% were "unsafe," and 30.3% were within the limits of the window of acceptability. As the terrain increased in slope, false alarms and unsafe warnings became more prevalent.

In a post hoc analysis, the data set from Phase II was plotted against the pilot window of acceptability developed in Phase III to determine whether the false alarms are caused by the algorithm or are an artifact of inconsistent pilot response and recovery procedure. As evidenced in Figure 26, the overall false alarm rate actually increased from 38.6% to 47.9%; whereas, only 49.0% of the data points fell within the pilot window of acceptability. This, however, includes the 21°-slope data points that are not included in the Phase III runs. In order to make an accurate comparison, the 21° slope data from Phase II were not included in Figure 27. The resulting "false alarm" rate was substantially lower at 38.9%. This number is almost unchanged from the Phase III figure of 38.6% reported earlier. The percentage of points considered as "too close for comfort" remained relatively unchanged at 3.1%. As before, the pilot window of acceptability for each slope condition was also plotted, but this time using Phase II data. As seen in Figures 28-31, the "false alarm" rates of 0%, 33.3%, 72.9%, and 91.7% continually increased as slope increased again indicating the algorithm's difficulty in accounting for the effect of slope.

PILOT WINDOW OF ACCEPTABILITY Phase III - Pilot Runs All Slopes

◆ Data point —□— Slightly high —◆— Slightly low

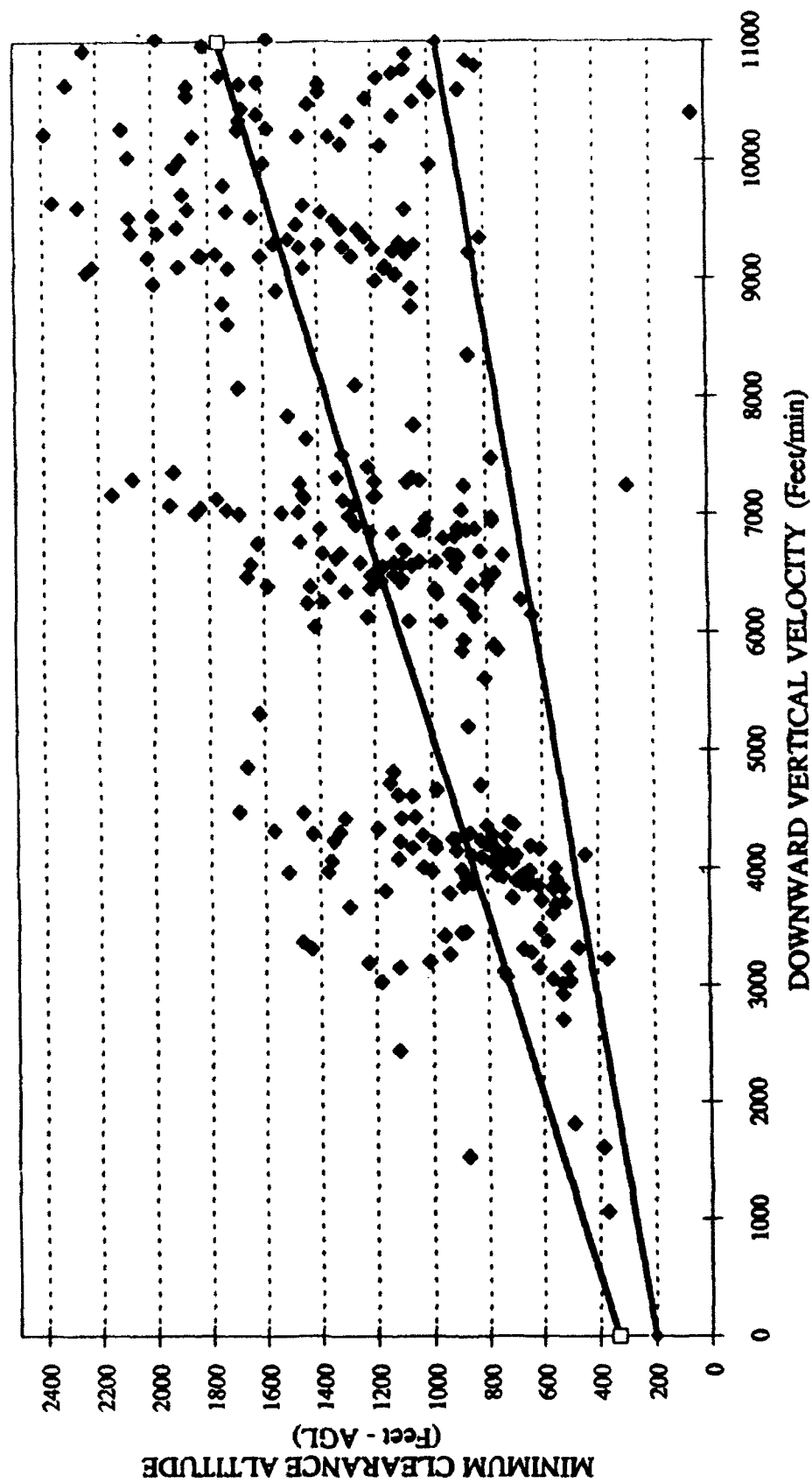


Figure 22. Pilot window of acceptability for entire data set: Pilot runs.

PILOT WINDOW OF ACCEPTABILITY Phase III - Pilot Runs Slope = 0

◆ Data point —■— Slightly high —◆— Slightly low

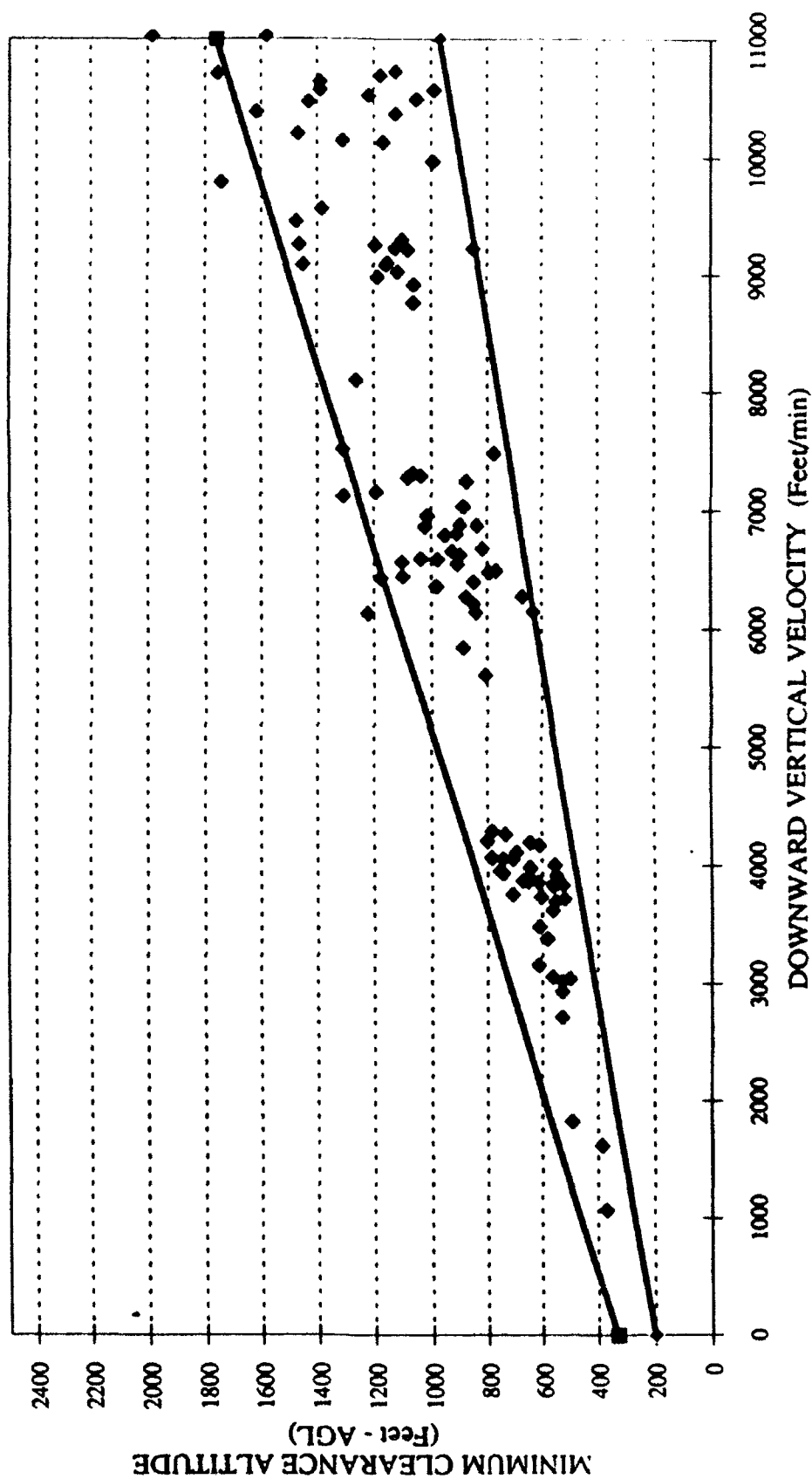


Figure 23. Pilot window of acceptability for a terrain slope of 0: Pilot runs.

PILOT WINDOW OF ACCEPTABILITY
Phase III - Pilot Runs Slope = 7

◆ Data point — □ — Slightly high — ● — Slightly low

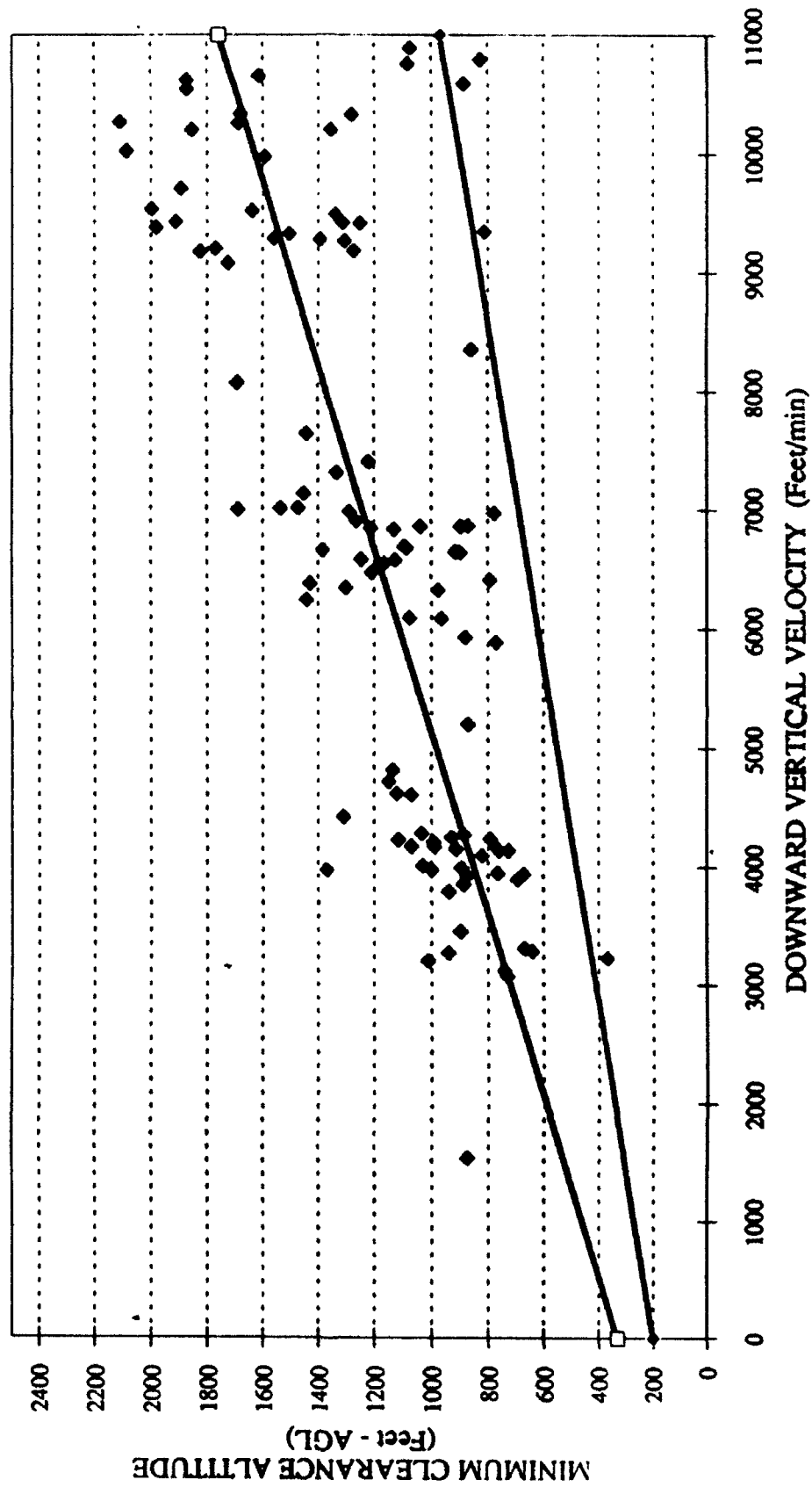


Figure 24. Pilot window of acceptability for a terrain slope of 7: Pilot runs.

PILOT WINDOW OF ACCEPTABILITY
Phase III - Pilot Runs Slope = 14

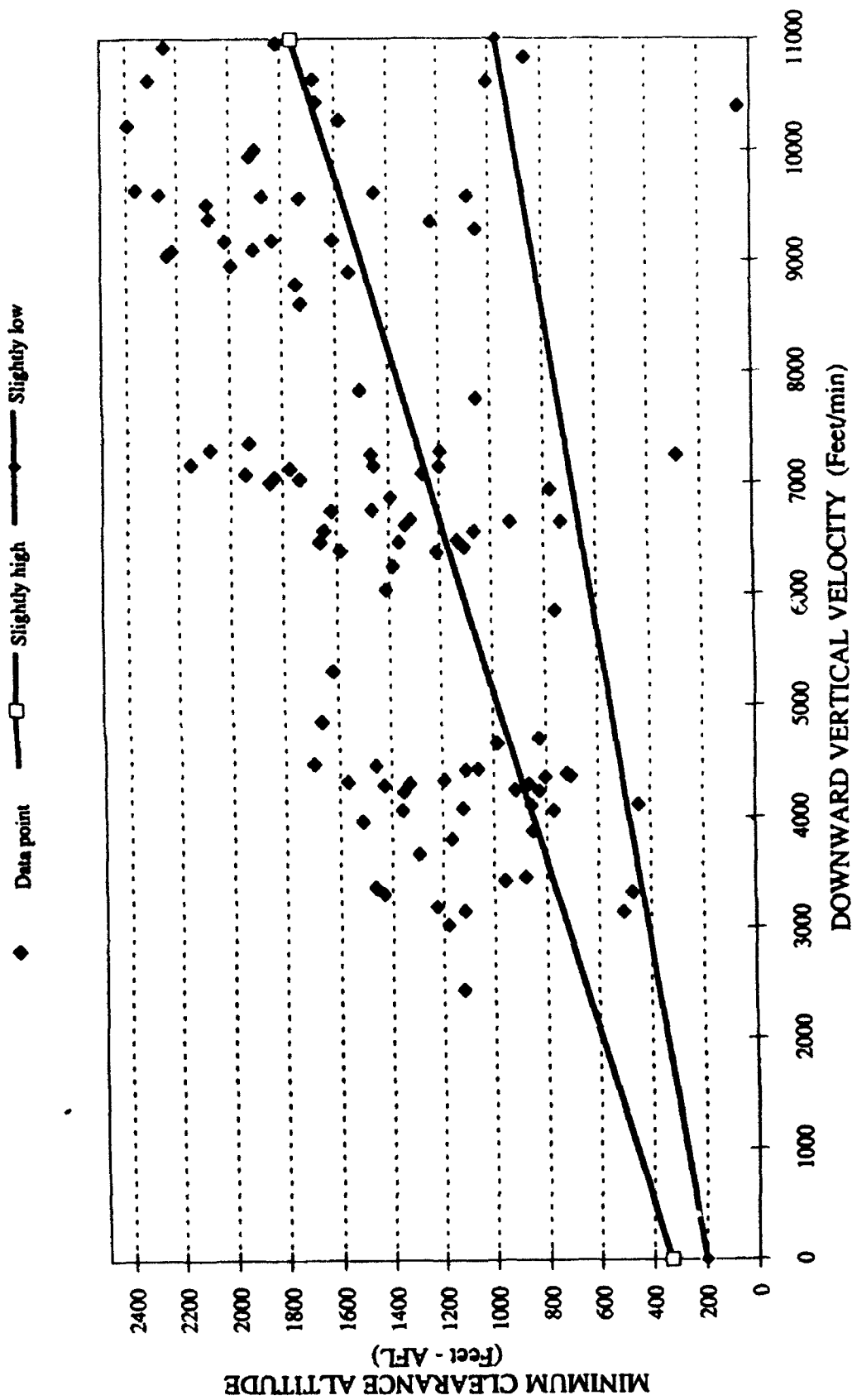


Figure 25. Pilot window of acceptability for a terrain slope of 14: Pilot runs.

PILOT WINDOW OF ACCEPTABILITY Phase II - Robot Runs All Slopes

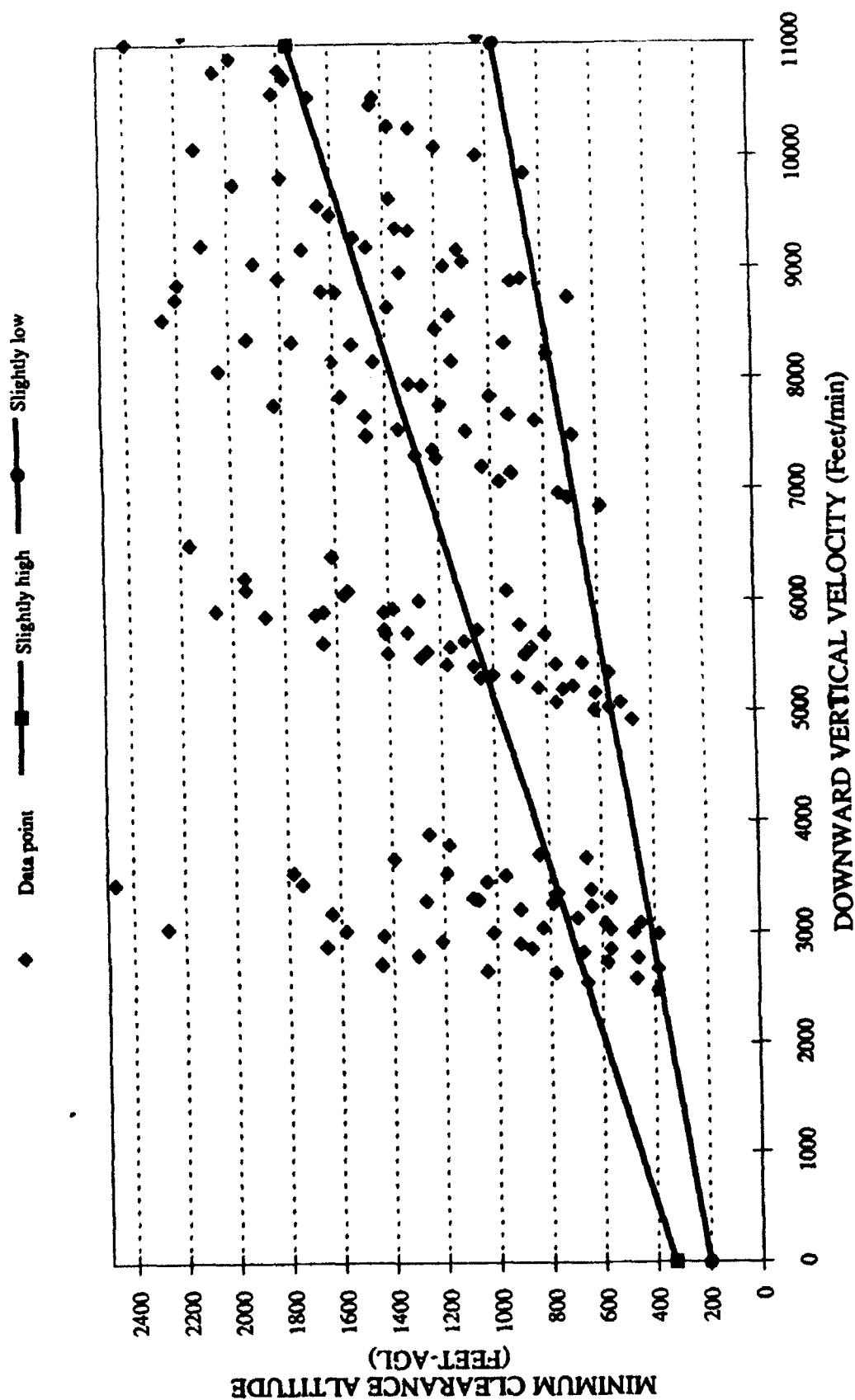


Figure 26. Pilot window of acceptability for entire data set: Robot runs.

PILOT WINDOW OF ACCEPTABILITY Phase II - Robot Runs Slopes = 0, 7 & 14

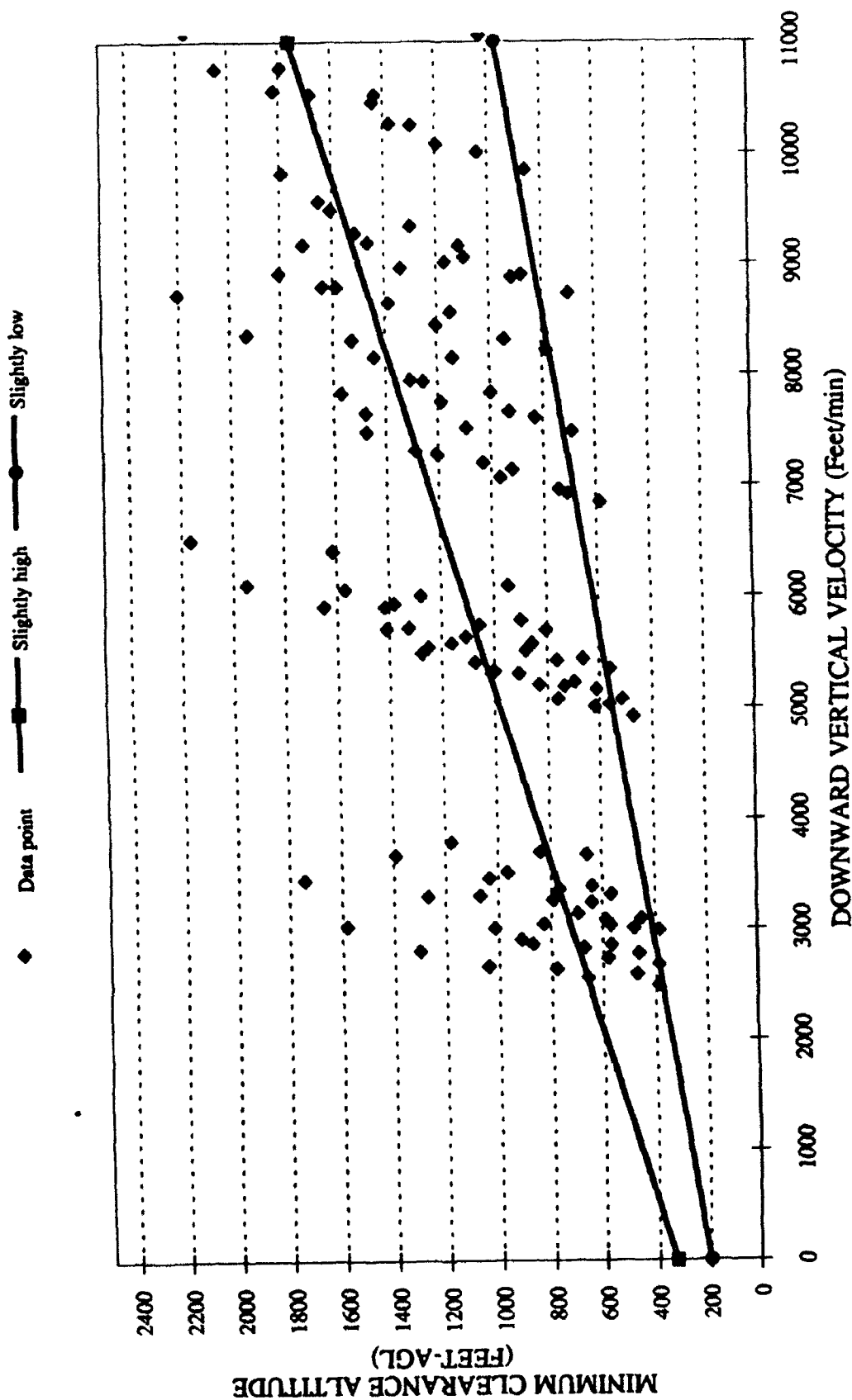


Figure 27. Pilot window of acceptability for slopes of 0, 7, & 14: Robot runs.

PILOT WINDOW OF ACCEPTABILITY Phase II - Robot Runs Slope = 0

◆ Data point — Slightly high — Slightly low

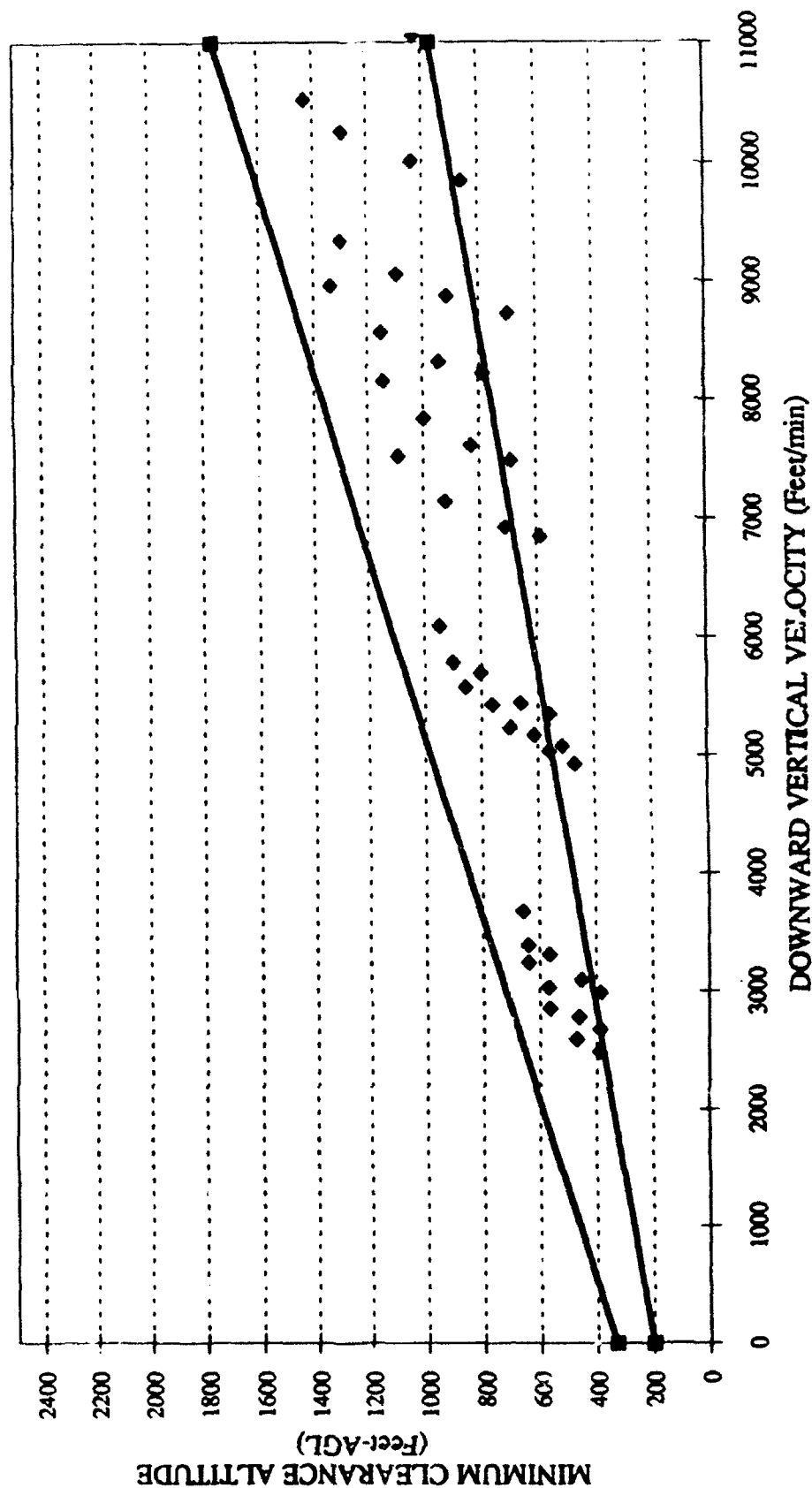


Figure 28. Pilot window of acceptability for a terrain slope of 0: Robot runs.

PILOT WINDOW OF ACCEPTABILITY Phase II - Robot Runs Slope = 7

◆ Data point — Slightly high — Slightly low

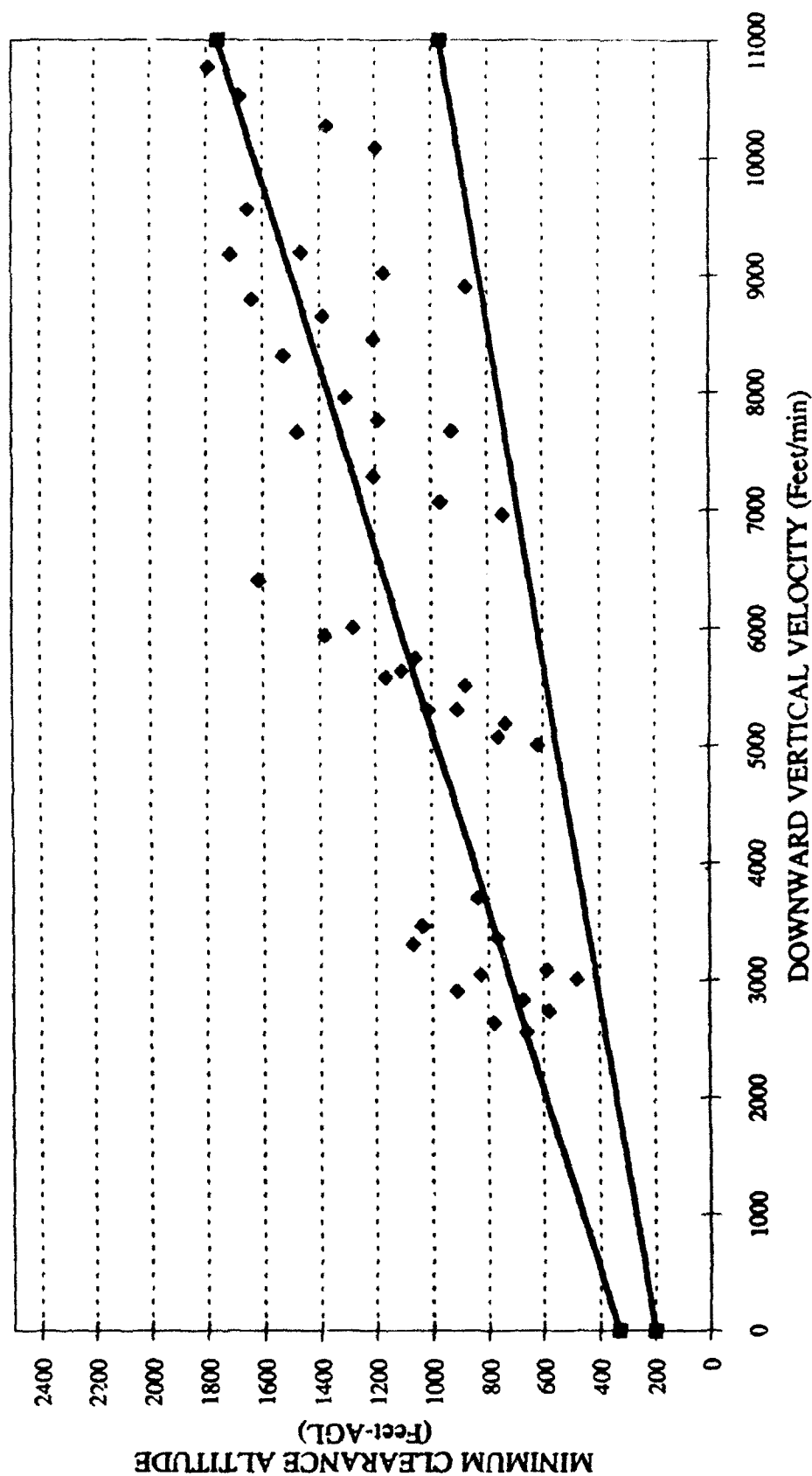


Figure 29. Pilot window of acceptability for a terrain slope of 7: Robot runs.

PILOT WINDOW OF ACCEPTABILITY Phase II - Robot Runs Slope = 14

◆ Data point — Slightly high — Slightly low

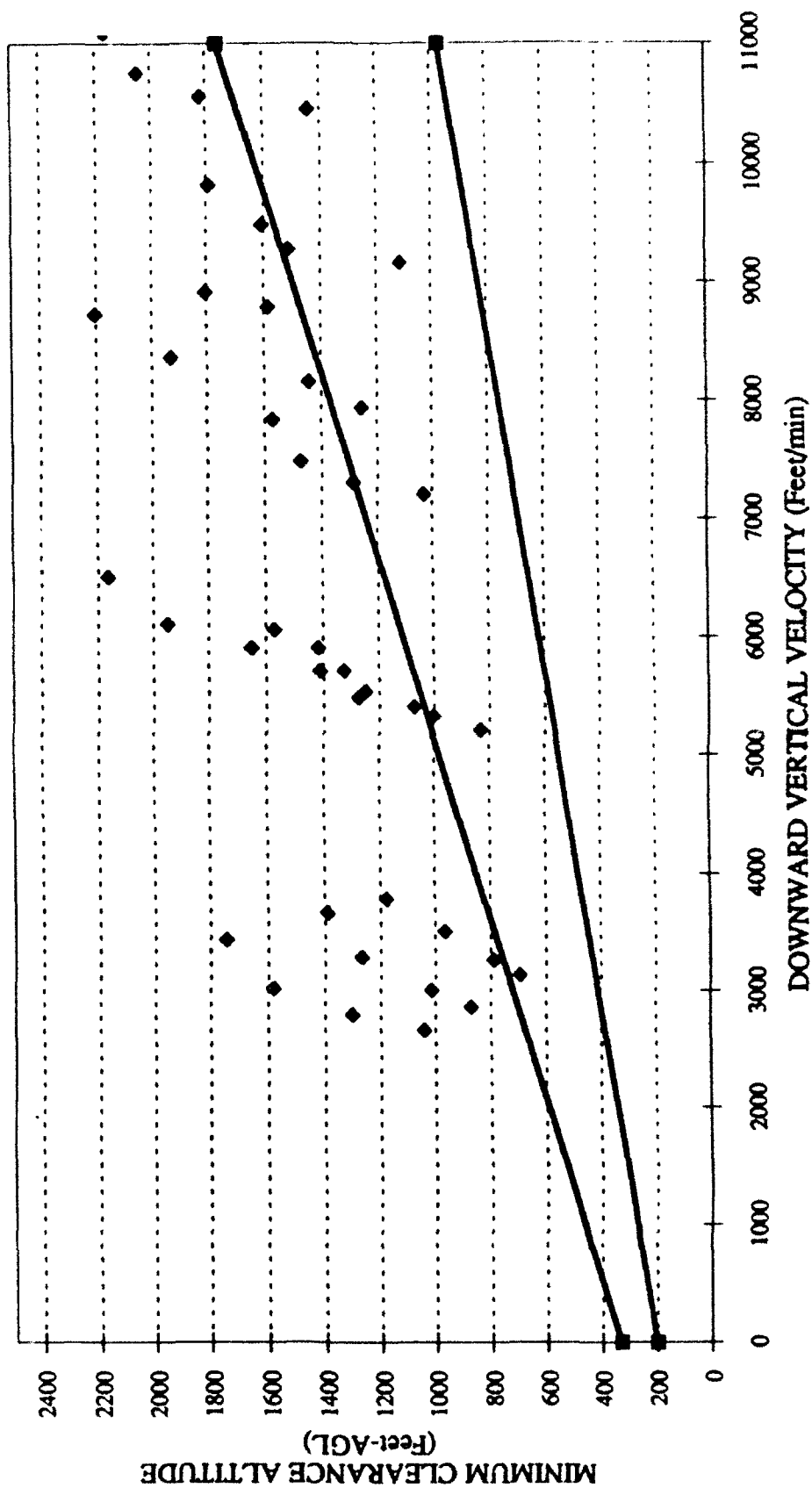


Figure 30. Pilot window of acceptability for a terrain slope of 14: Robot runs.

PILOT WINDOW OF ACCEPTABILITY Phase II - Robot Runs Slope = 21

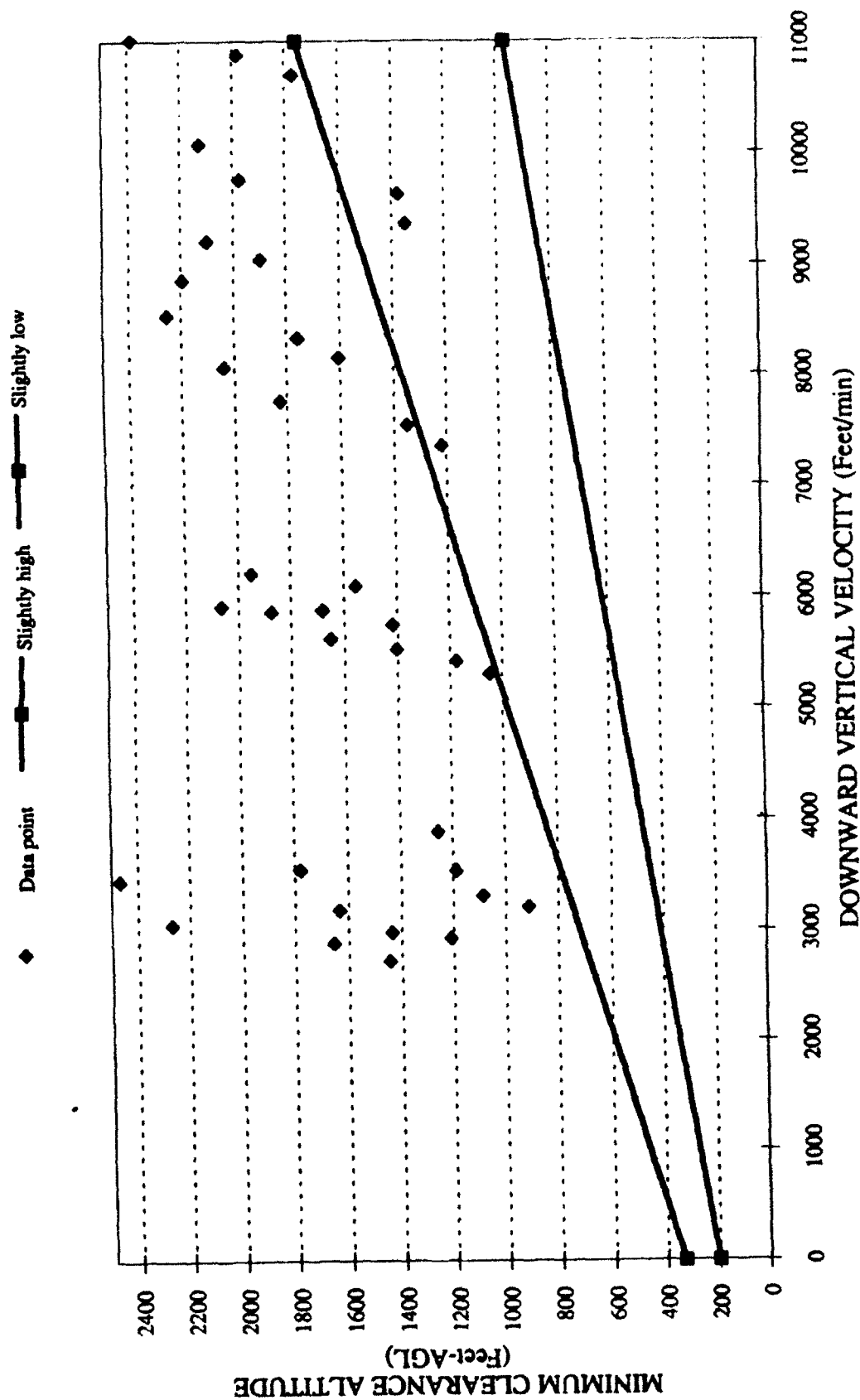


Figure 31. Pilot window of acceptability for a terrain slope of 21: Robot runs.

Part 1 Discussion

The Phase III Part I results were very straightforward and generally as expected. All of the independent variables did increase minimum clearance altitudes as they themselves increased. Two interactions (roll by gamma and roll by slope) occurred. Although not originally hypothesized, they are both easily explained. For instance, the roll by gamma interaction is a result of how altitude loss due to roll is computed. As mentioned earlier (Phase I, GCASROLL), the altitude loss due to roll can actually decrease as gamma increases. Consequently, the overall increase in minimum clearance attributed to roll is lessened and the interaction effect is produced. In a similar fashion, the roll by slope interaction effect is produced. Slope effects are used in GCASDIVE and GCASROLL to compute an overall terrain closure effect. This resulting value is then used to compute altitude loss due to gamma and roll. As previously discussed, increases in gamma act to reduce the effect of roll. Therefore, the interaction of slope by roll is created.

The general pattern of results for the dive configuration runs in Part 1 indicate the algorithm successively provided minimum clearances that cleared the ground 100% of the time (Figures 15-20). At first glance, an observer might construe this to indicate that the algorithm is very usable. However, this fails to account for the number of false alarms that a given system might have. A system plagued with numerous false alarms may actually result in user weariness and promote unsafe practices. For example, early ground collision avoidance systems were plagued with an over abundance of false alarms. To adapt to all these false warnings, pilots formulated a rather unorthodox, unacceptable, and unsafe corrective action by simply turning the system off, rendering it useless.

To avoid such a situation, the evaluator must query the user as to the acceptability of the alarm and its consequence. The pilot window of acceptability is used specifically for that reason. As seen in Figure 17, 38.6% of the minimum clearances fell in the false alarm region. In a breakdown of the pilot window of acceptability by slope (Figures 22-24), it becomes apparent that the underlying cause of the false alarm is a result of the system's inability to account for the pilot's perception of the effect of slope. As slope increases from 0- to 7- to 14-degrees slope, false alarms also increased from 4% to 45% to 66%, respectively.

In an effort to determine whether the false alarm rate was pilot induced or algorithm induced, the robot run data from Phase II were plotted against the pilot window of acceptability. If the Phase II data points result in a lower false alarm rate than that of the pilots, then it could be concluded that the pilot variability is causing the increase in false alarms. A glance at Figure 27 reveals that little change in false alarm rate occurred. A review of Figures 28-31 also indicate that the false alarm rate similarly increase from 0 to 33.3% to 72.9% for the 0, 7, and 14 degrees slopes, respectively. Based on the above results and analysis, it appears the false alarm rate is a direct result of the algorithm and not the pilot. It should be noted that the performance of the system as terrain slope increases could be attributed to the use of downward looking radar for slope prediction. The system must take radar altitude information and use it to predict future terrain. This is a drawback of the type of system, with the only way to improve performance being to use some sort of forward looking system.

A question that arises is "What percentage of false alarms is considered as acceptable?" To date, no study known to the authors has specifically addressed this question. Accordingly, setting a false alarm criteria for acceptance might seem somewhat arbitrary. However, after a discussion with various human factors engineers and based on the premise that most operational systems require a minimum reliability of at least 90%, a criteria of no more than 10% false alarm rate was established. Consequently, the system

appears to have not met the needed success rate in dive run recovery. This finding does not by itself render the algorithm useless. Several considerations, which will be discussed in the summary section, must be taken into account.

As mentioned earlier, subjective ratings for terrain closure were also used to evaluate acceptable minimum clearances for a pilot window of acceptability. Several problems arose from this data. First, terrain closure ratings were found to vary greatly between pilots and by the same pilot for similar conditions. When queried during the debriefing as to what might have caused this discrepancy, five of the nine pilots suggested that the response variance was the result of their inexperience with terrain closure as a numerical judgment of descent. The other major problem is that pilots have no way of assessing terrain closure in the cockpit. Several pilots stated that having no terrain closure readout on the aircraft made such an evaluation technique artificial and, therefore, inaccurate.

Part 2 - Approach and Landing

Procedure

After completing the dive configuration trials, the pilot was given a short break. He was then given a detailed briefing describing the ILS approach to be performed. The pilot was then allowed to practice as many ILS approaches as desired. When the pilot felt comfortable, the practice trials were terminated.

The pilots were required to fly an ILS approach to Runway 24R at Los Angeles (Refer to Rueb & Hassoun, 1991 for a diagram of the approach). All radio and navigation frequencies were set prior to simulator release. The KC-135 was positioned at a point 14 NM Northeast of the airfield at an altitude of 2000 feet. The pilot was required to intercept both the localizer course and glideslope. Simulated weather prevented the pilot from transitioning to a visual approach until 300 feet AGL. Each pilot flew a total of eight approaches with various configurations of flaps (up or down), gear (up or down), and forced glideslope deviation (yes or no, high or low).

Part 2 Results

Data collection was begun at glideslope intercept or 1000 feet AGL, whichever occurred first. It continued on a 30-Hz cycle until 100 feet AGL. The data set used for analysis was based on individual data points recorded every 15 seconds, and for every crash and warning. Refer to Rueb & Hassoun, 1991 for more details.

The data set consisted of 680 data points. These data were individually inspected for the actual airspeed, flap, gear, glideslope deviation, and altitude conditions that existed. Based on the actual conditions existing, it was determined whether a warning should have been generated, and if so, what type of warning it should have been. A comparison of what should have occurred with what actually happened was then made. This allowed the experimenters to determine the success rate of the algorithm in accurately providing a warning for the approach and landing phase of flight.

Out of 680 data points, 659 were correct identifications. These points were broken into two categories, "correct rejections" and "correct warnings." A "correct rejection" was made when no warning was provided and the conditions did not warrant a warning. This occurred 546 times for a rate of 80.3%. A "correct warning" was made when a warning

occurred and the conditions warranted a warning. This occurred 113 times for a rate of 16.6%. This represents a rate of 96.9% for correct identifications.

The algorithm failed to identify 21 data points. These points were broken into two categories, "false alarms" and "incorrect rejections" (misses). "False alarms" occur when a warning is given and conditions are such that no warning should have been given. This occurred three times for a rate of .44%. "Incorrect rejections" occur when no warning is given and conditions are such that a warning should be given. This occurred 18 times for a rate of 2.65%.

Part 2 Discussion

Two major terms of distinction, confidence and reliability, must be clarified at this point. Confidence refers to the degree of confidence that we place in the system being able to generate the appropriate response (signal/ no signal) to the given aircraft condition. If the aircraft status is such that a warning should be given, then the system should generate a warning. If the aircraft is not in a warning configuration, then no alarm should be given. Any other situation is considered a failure and detracts from our confidence in the system.

Reliability in this context refers to how well the algorithm generates a warning when a warning should indeed be generated. Since a GCAS would predominantly be in a null (non-warning) state, it would be somewhat deceiving to commute percentages based on the entire data set composed of false alarms (warning given when it should not have been), incorrect rejections (warning not given but should have been), correct rejections (No warning), and correct warnings because the correct rejections would increase the overall confidence we might have in the system. After all, an aircraft with no GCAS would generate 100% accuracy rate in generating no alarm when none was needed. Of greater importance is whether the system generates the correct alarm when indeed a warning should be given (reliability).

As shown in the results section, we have 96.9% confidence that the algorithm will accurately detect the current aircraft status and initiate a warning when necessary. However, the actual reliability with which the algorithm generates a warning is equivalent to the correct warnings (113) divided by the sum of all the false alarms (3), incorrect rejections (18), and correct warnings (113). In this case, a reliability of 84.3% resulted. Using the criteria of 90% established earlier in Part 1, this algorithm again performed below acceptable standards.

In comparison to the earlier Cubic GCAS algorithm (Rueb & Hassoun, 1991), the revised algorithm showed numerous improvements. First, the algorithm now uses a warning hierarchy reported as acceptable to the pilots. Second, the "gear" and "flap" warning initiation altitudes were increased from 500 feet to 1000 feet, thereby, providing the pilots with ample time to properly reconfigure the aircraft for landing. Third, the revised algorithm provides "glideslope" warnings for deviations to both sides of glideslope. However, the algorithm still provided a nuisance "pull-up" warning for bounces that occurred on landing. Some form of inhibit should be included to cancel this nuisance warning.

PHASE IV

The objective of the fourth phase of the evaluation was to introduce the pilot to a full mission using an actual terrain database. By doing so, the pilot was able to fly the simulator under normal flight conditions over terrain and obtain real-time radar altimeter information. This scenario allowed the GCAS algorithm to be evaluated under normal operational flight profiles, and also helped reduce possible pilot response biases that might have occurred in Phase III. Response bias would be reduced because Phase IV pilots would be uncertain of an upcoming GCAS warning; whereas, Phase III pilots were guaranteed to hear a warning on every dive configuration and ILS trial. The procedure and results of Phase IV follow.

Method

Subjects

Seven of the nine pilots from Phase III of our evaluation were again used during Phase IV. One of the two pilots not involved was used as a checkout pilot for the full mission scenario. The other pilot was unable to complete the mission phase due to scheduling constraints.

Apparatus

Facility. Refer to the Phase II Apparatus section for a description.

Computer Complex. Refer to the Phase II Apparatus section for a description.

Simulator. Refer to the Phase II and Phase III Apparatus sections for a description of the KC-135 simulator. In addition, a computer program read a Defense Mapping Agency (DMA) terrain database into memory of a Gould Sel 87 computer. The elevation of the terrain was then computed based on an extrapolation of the simulator's position in relationship to the database. The subtraction of the terrain elevation from the aircraft's barometric altitude (computer based) provided the above ground information fed back to the aircraft's radar altimeter indicator.

Experimenter's Console. Refer to the Phase III Apparatus section for a description.

Voice Message Unit Mechanization. Refer to the Phase III Apparatus section for a description.

Audio Systems. Refer to the Phase III Apparatus section for a description.

Visual Warning Signal. Refer to the Phase III Apparatus section for a description.

Procedure

This portion of the evaluation was performed on the same day as Phase III. However, the pilots flew the Phase IV full mission during the afternoon after a minimum of a 1 hour lunch break. Upon return, the pilot was given a standardized briefing concerning the requirements of the mission. No additional simulator training was given to the pilot since ample flight time had resulted from the Phase III portion of the evaluation. As in Study 1, none of the pilots considered this a problem.

The pilot was briefed to fly the planned route and altitudes (for a description of the mission, refer to Rueb & Hassoun, 1991) unless told by the navigator, LA center, or the experimenter (all roles were played by the experimenter) to deviate from that planned. Multiple interactions and interventions with the navigator and LA center occurred throughout the flight to simulate realistic flight communications. The interactions were both planned and random in nature. Pilots were informed an intervention by Center or the navigator did not necessarily indicate a warning was forthcoming. On the contrary, less than 20% of all the ground impacts or warnings occurred outside the 2 minute period following an intervention.

The pilot was normally required to fly the aircraft at altitudes under 1000 feet (AGL) in an effort to place the aircraft in an environment where GCAS warnings would occur. Although this environment is not typical for a tanker, none of the pilots felt that it represented a major difficulty, since they were only required to fly the aircraft under normal flight profiles (i.e., straight and level, standard climbs and descents). The pilot was allowed full use of his instruments with the exception that the radio altimeter bug switch had to be set to less than 100 feet, so the light would not allow the pilot to anticipate a possible GCAS warning. During flight, the experimenter continually tracked aircraft position and configuration through the experimenter's console.

In the event of a crash, the pilot would continue to fly the simulator as though the impact with the ground had not occurred. The pilot and experimenter were made aware of a crash by the zeroing of the radio altimeter with a simultaneous clicking sound as the aircraft impacted the terrain. The experimenter would reset the simulator at the point of impact, but at an altitude high enough to avoid an immediate crash with the ground. The pilot was then briefed on the aircraft position and configuration and asked to state when he was ready for release. When the pilot was ready, the simulation would continue and the pilot would again fly the simulator as briefed. The planned mission was scheduled for 2 1/2 hours. When the simulation portion of Phase IV was terminated, the pilot was given two questionnaires (Rueb & Hassoun, 1991) to gather their subjective opinions concerning the implementation of the GCAS, the reliability of this GCAS algorithm, and the quality of the simulation provided. The pilot was then debriefed and thanked for his/her participation in our evaluation.

Results

In order to make the data set manageable and to adequately evaluate the algorithm's predictive ability, only data points where an actual GCAS warning was given or when a crash occurred were placed into the database for final analysis. This resulted in a database of 103 data points. The data were sorted by minimum clearances, gamma, and terrain slope. A frequency analysis revealed the 97 data points consisted of valid warnings, 2 crashes with no warning, and 4 false alarm warnings. Of the 103 warnings, 6 resulted in ground impacts. With the 2 crashes that received no warning, the final total is 8 of 103 (8%) possible data points resulted in aircraft crashes.

To investigate the cause of the false alarms and crashes, the aircraft's actual flight path in relationship to the terrain database was also plotted for each of the data points. Figures 32-36 are some examples. They display the subject number at the top of the page. The first five lines along the side of the graph were the algorithm's predicted altitude loss for each of the subroutines, GCASALRT, GCASROLL, and GCASDIVE. These are then summed to obtain the total predicted altitude loss, ALT LOSS. SAF BUF (Safety buffer) was always zero for this revision of the algorithm. The first reaction time listed was that

used by the algorithm. The roll, gamma, altitude, airspeed, and vertical velocity (VZ), found in the second group of variables, were the actual conditions of the aircraft simulator at warning initiation (dashed vertical line). Maximum g's (MAX Gs) and actual total altitude loss (ALT LOSS) were the maximum values obtained during aircraft recovery. Minimum clearance (MIN ALT) represents the minimum distance between the aircraft and the terrain that occurred during the aircraft's recovery. The roll line and g's line, at the upper portion of the graph, represent the real-time roll and g-load values of the aircraft during its flight. The x-axis is the total running time since the mission began. The y-axis is the altitude of the aircraft in feet (MSL). The flight of the aircraft is represented by the curved upper line beginning at the higher region of the y-axis. The ground level is represented by the jagged line that begins at the lower region of the y-axis.

The reader is cautioned that the pictorial presentation of the ground is distorted since the x-axis is in seconds and not in feet. Consequently, one can not measure the slope of the terrain simply by placing a protractor directly on the figure. To obtain the slope of the terrain, one must convert the x-axis scale to feet and then adjust it to the same scaling as the y-axis. Since this technique is both cumbersome and requires substantially more graph space, the x-axis was presented in seconds. However, whenever slope is pertinent to the discussion, the exact slope value will be given.

The data were further analyzed by breaking down the crashes by most likely cause. The two crashes with no warning both occurred when two peaks were flown over within a minute of each other. The smaller first peak triggered a warning; whereas, the taller second peak generated a late warning (Figure 32). The four false alarms were caused by terrain sloping rapidly downward immediately after warning initiation. As seen in Figure 33, the terrain is rapidly rising (27° slope) and then drops downward immediately after the alarm is given. Of the six crashes with warnings, three were due to pilot error, two were due to a steep slope and low max g's combination, and one was attributed to a late algorithm warning resulting from a change in terrain slope.

Figure 34 provides an excellent example of pilot error. In this instance, slope was 17 degrees with max g's of 1.47 g's. This max g was below the target g of the algorithm (1.5 g). Consequently, the calculations the algorithm used to provide adequate ground clearance were violated. Although, the pilot was instructed and trained to recover the aircraft between 1.5 and 2.0 g's, two of the recoveries were at max g values below 1.5 g's. The third pilot error was attributed to an inordinately long pilot response time. Figure 35 displays what occurred when a higher than usual terrain slope (18.19°) was countered by the pilot with a relatively low g recovery (1.59 g's) maneuver. The combination of the two resulted in ground impact. A final cause seemed to indicate that a rapid upward change in terrain slope as indicated by point "A" in Figure 36 may result in a possible ground collision.

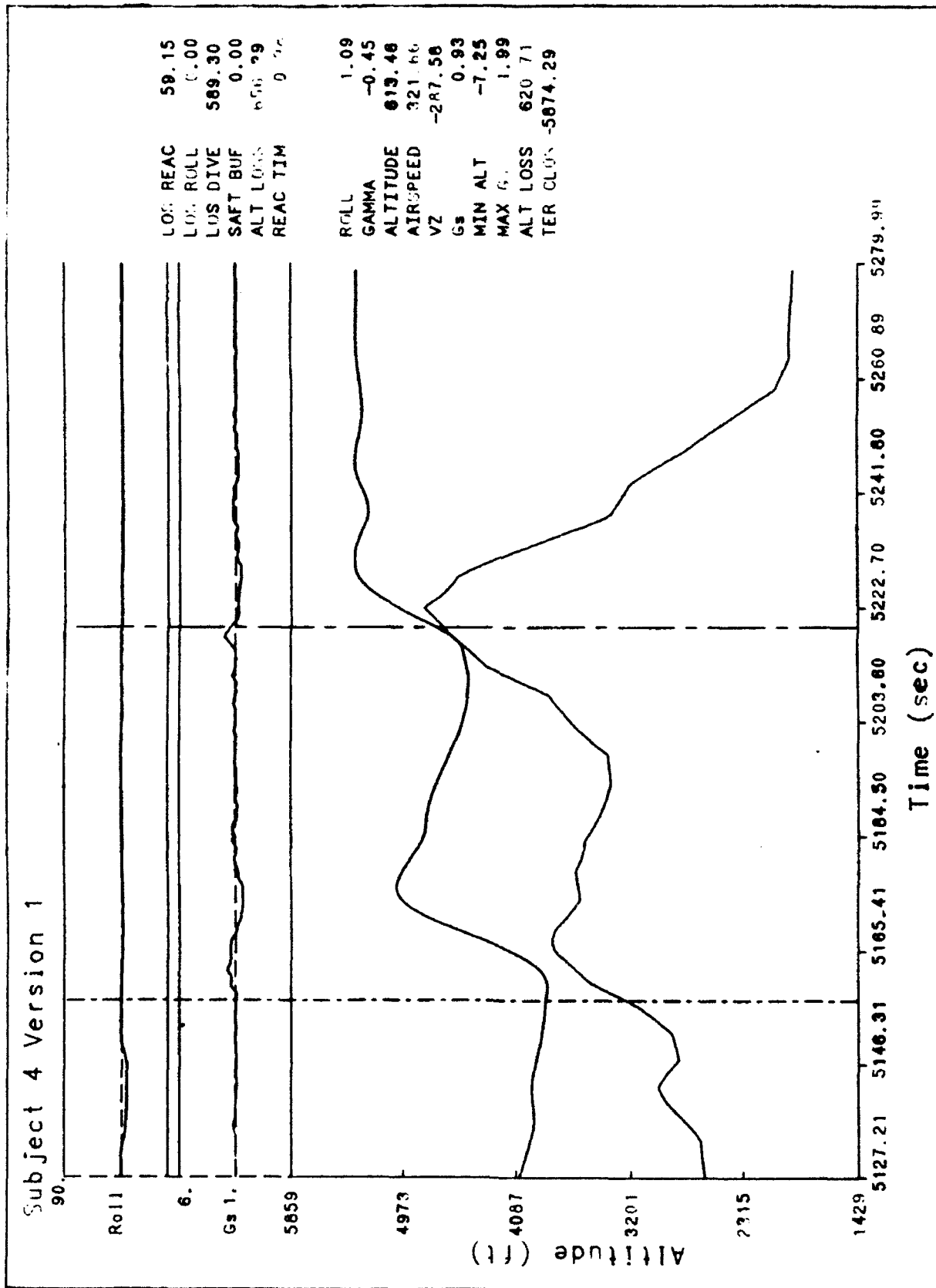


Figure 32. Example of a "late warning-crash" data point.

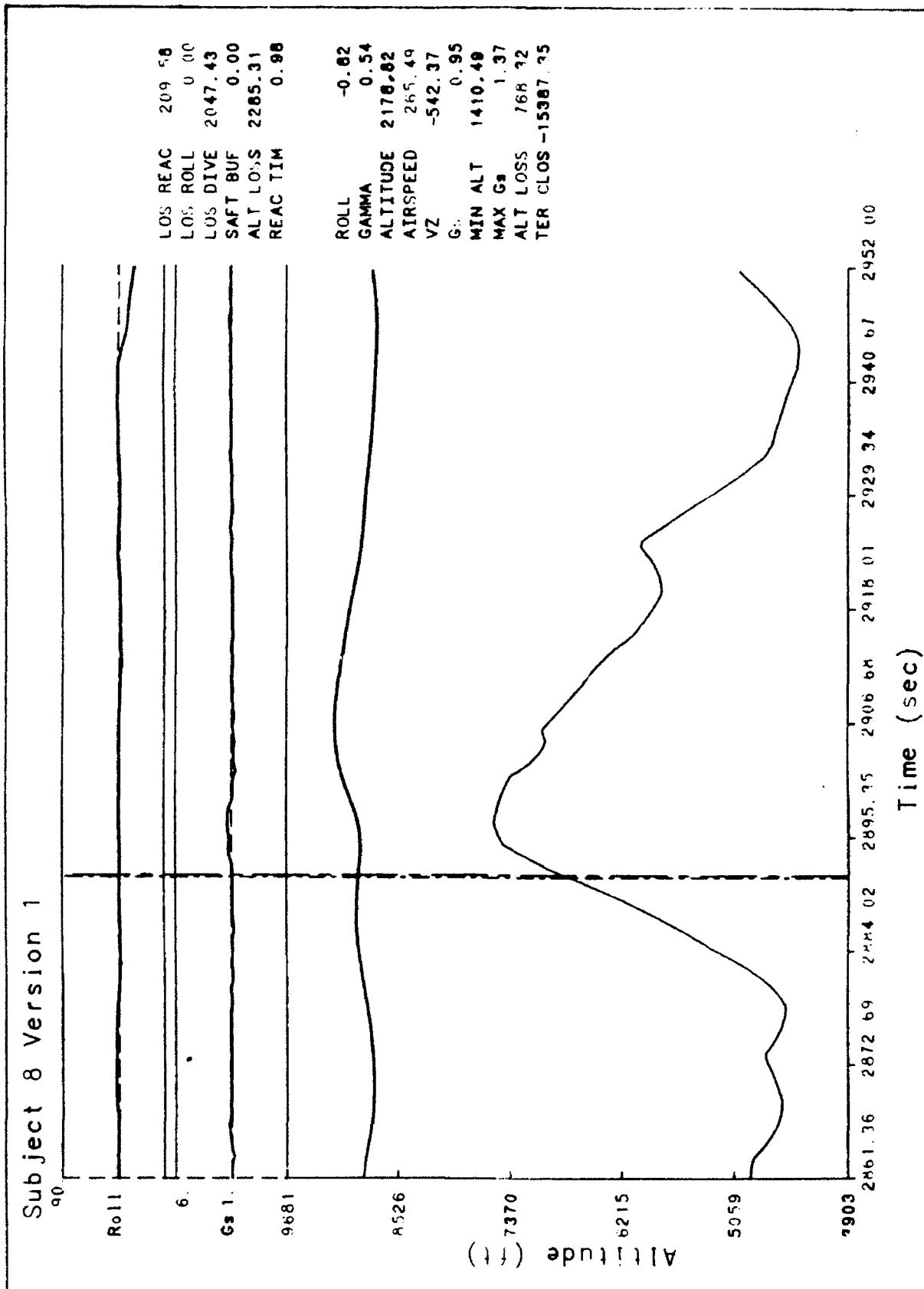


Figure 33. Example of a "terrain sloping rapidly downward false alarm" data point.

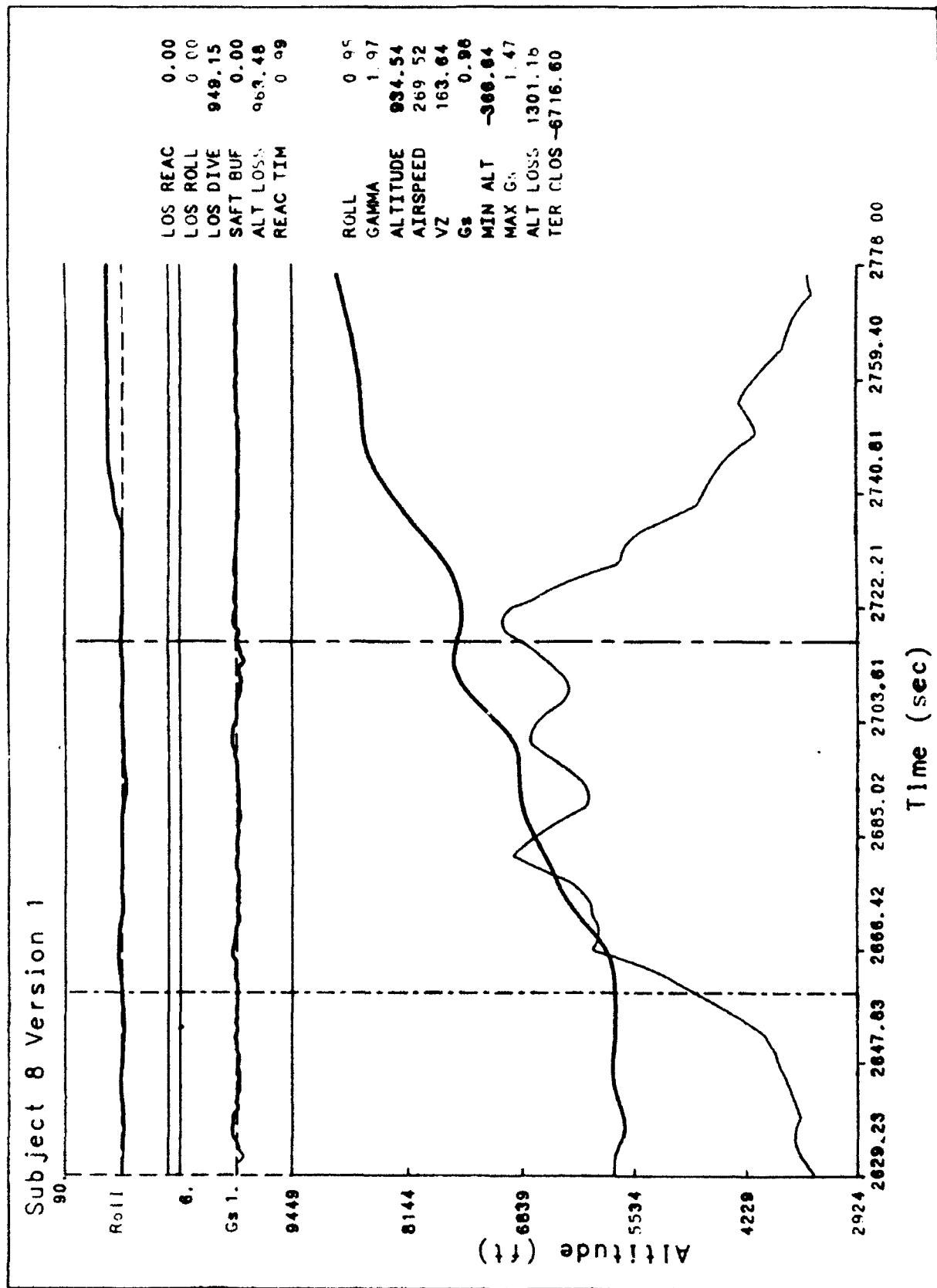


Figure 34. Example of a "pilot error induced crash" data point.

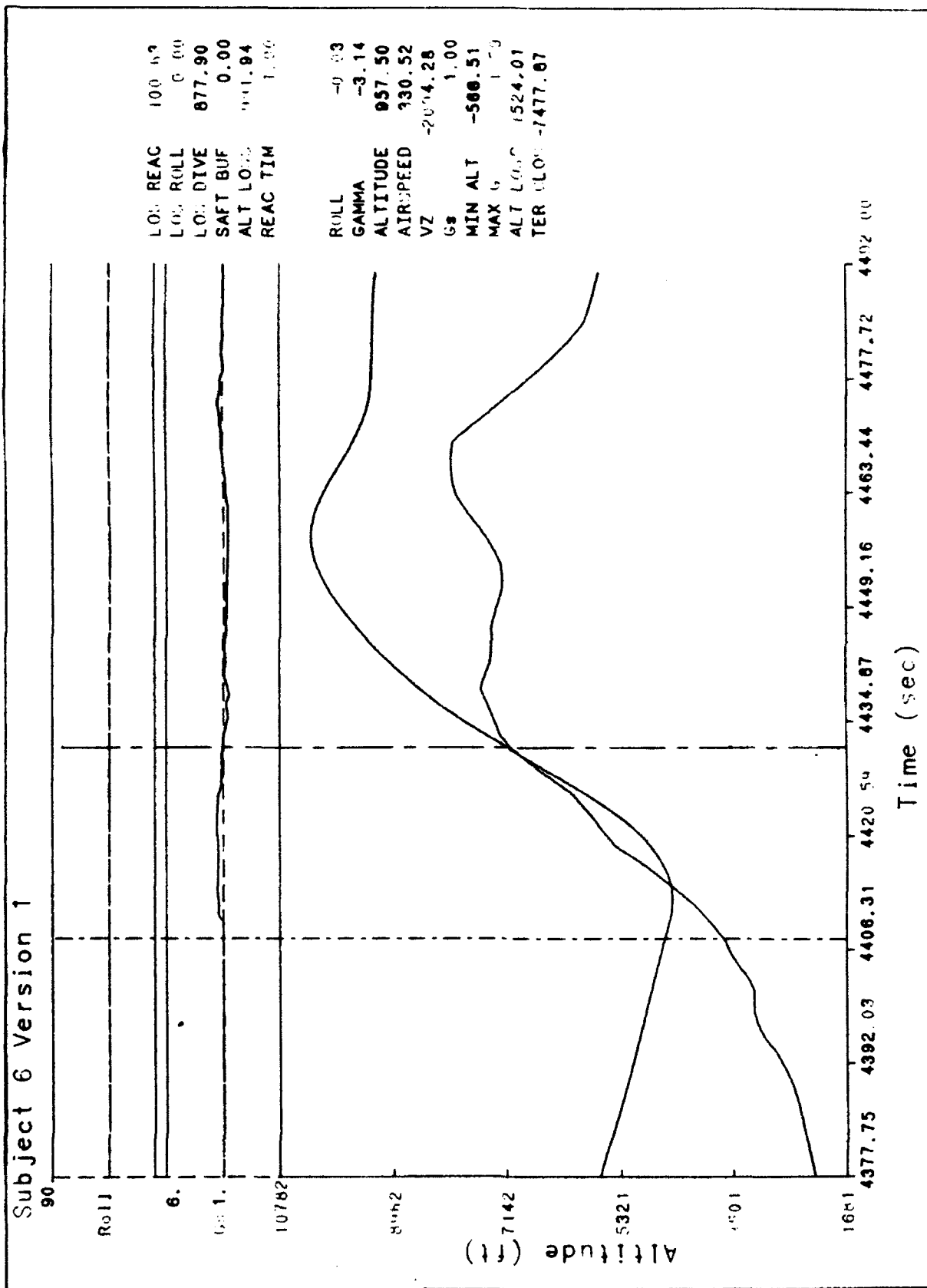


Figure 35. Example of an "excessive slope/low-g recovery" data point.

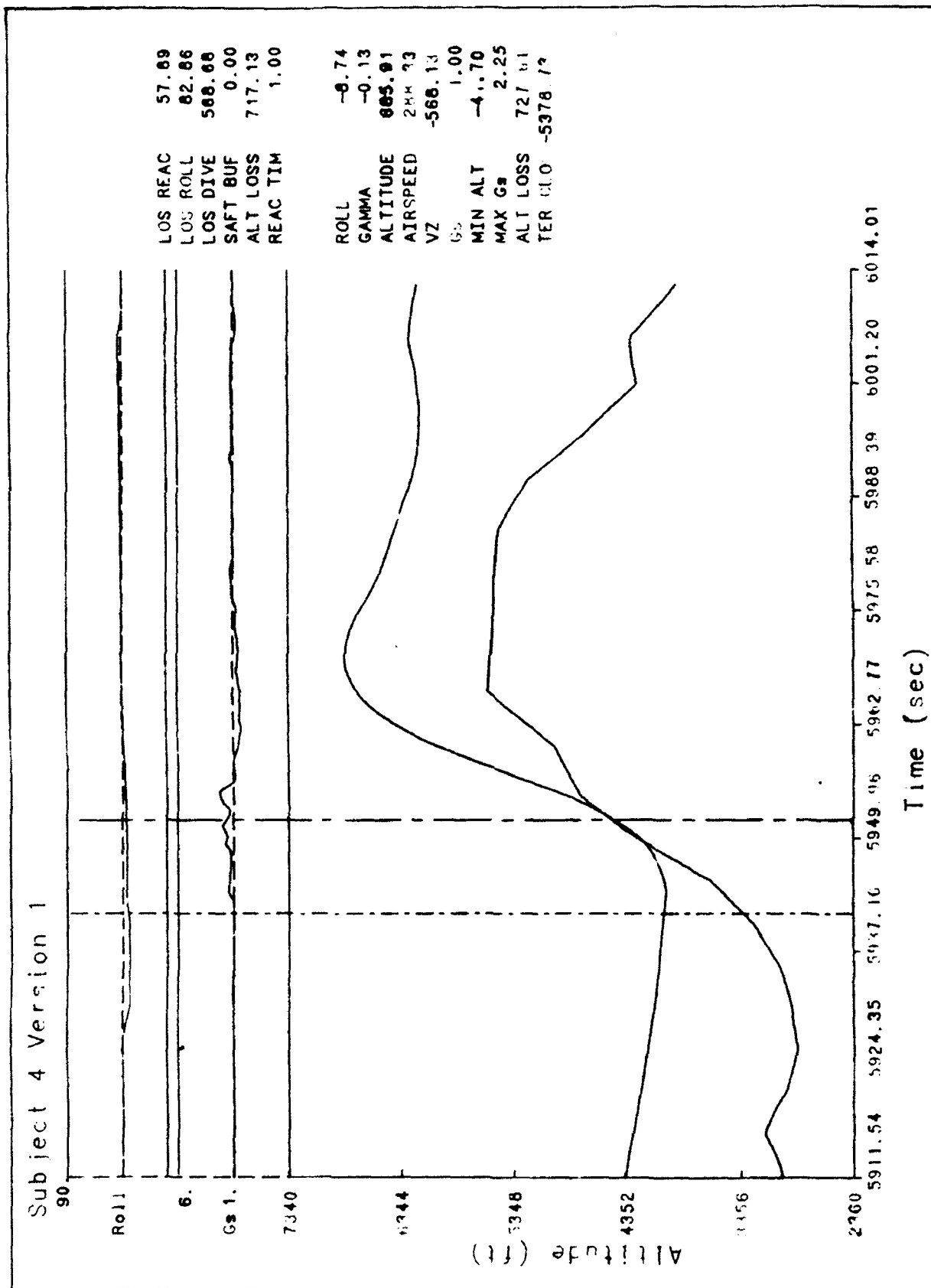


Figure 36. Example of a "rapid upward change in terrain" data point.

Phase IV Discussion

The evaluation of a ground collision avoidance system is often very subjective in nature. Objective data like minimum clearance and warning altitudes must undergo the scrutiny of the engineers evaluating it. During Phase IV the various ground collisions underwent multiple screenings by the evaluators to determine the most likely cause of the collision. In 37.5% (3 out of 8) of the collisions, pilot error was listed as the cause. Pilots either failed to exceed the minimum target g-load of the algorithm or were slow to respond to the warning. In either case the algorithm was not inaccurate. A warning should have been and was generated.

The results of Phase IV demonstrated the algorithm's inability to accurately account for some of the effects of slope. This inability was due to the algorithm not providing adequate increases in warning altitude as a result of slope effects. This might seem to contradict the findings of Phase III. However, the distinction lies in the actual effect of slope. In Phase III, it was noted that false alarms were a consequence of increased slope. Phase IV appears to supplement this information further by showing that not only does increased terrain slope cause problems for the algorithm, but also increased terrain slope rates (changes in terrain slope over time) further complicate the problem because the algorithm cannot look ahead in time and predict a terrain slope change. This could be a limitation of all GCAS systems that use downward looking radar altimeters. With this type of system, the algorithm must take past and current terrain altitude and predict future terrain.

As seen in Figures 33 and 36, rapid changes in terrain slope could result in algorithm inaccuracies. Specifically, if terrain drops off rapidly, a false alarm will ensue. If terrain slope increases rapidly, a ground collision is possible. Again, this is a limitation of any ground collision avoidance system that does not incorporate a forward looking radar. If the algorithm could use information from in front of the plane (forward looking radar), the accuracy of the warning predication would be increased. Yet, a GCAS must depend on current terrain slope information to extrapolate where the terrain would become a factor in the recovery maneuver. The question now becomes one of, "How much inaccuracy is acceptable?"

The pilot window of acceptability discussed in Phase III attempts to address this acceptability problem. As stated earlier, the algorithm provided safe clearances in every dive configuration run. However, a large percentage (40%) of the data points fell outside of the acceptability range of the pilots as represented by the pilot window of acceptability. This indicates that the algorithm, although it provides consistently safe clearance altitudes, may become a casualty of false alarms. Given too many false alarms, pilots will learn to ignore the system and the system would consequently be rendered as useless.

Another question that derives from the way a GCAS works is "What should the limit of the terrain slope extrapolation be?" In this evaluation, the Cubic algorithm was designed to account for a terrain slope of 20° . This was an arbitrary value chosen on the premise that most terrain slope is less than 20° . It is quite possible that by reducing the amount of terrain slope for which a GCAS must be accountable, a reduction of the false alarm rate would occur without any degradation in the algorithm's predictive power. For example, three of the four false alarms that occurred during Phase IV would not have occurred without degradation to the algorithm had a 10° slope limitation been imposed. The above questions concerning specifications must be addressed by the users before a definitive pass/fail decision is made.

CONCLUSIONS AND RECOMMENDATIONS

The Cubic GCAS algorithm was evaluated in a four phase simulation effort. Phase I attempted to verify and validate the sub-algorithms. In Phase II, a robot pilot model was used to test the algorithm in the KC-135 simulator. The robot pilot model performed various dive recovery maneuvers, a subset of which were used in Phase III. Phase III and Phase IV involved man-in-the-loop simulation.

Results from the four phases indicate that the revised Cubic algorithm was improved over the previous edition. First, the introduction of the hierarchy of warnings during the approach and landing phase was well liked and accepted by the pilots. Second, raising the warning initiation altitude from 500 feet to 1000 feet now enables the pilot adequate time to reconfigure his aircraft and land safely. A significant reduction in the total number of crashes for both the dive runs and the mission definitely enhanced the usability of the algorithm.

However, several flaws to the algorithm were also identified. Specifically, as shown in Figures 22-31, the algorithm is still not adequately accounting for the effects of terrain slope. As slope increases, the algorithm generates progressively larger percentages of false alarms. The current Cubic algorithm false alarm rate of about 40% is still entirely too high. Another problem that still exists is the inappropriate pull-up command that occurs when the pilot accidentally bounces the aircraft on landing and during takeoff. Activation of a false alarm during critical stages of flight as these could be catastrophic.

At first glance, the solution is obvious. The algorithm must be altered to reduce the number of false alarms. This would increase the overall confidence the user places in the system and render it more effective. Second, an inhibit of the false alarm "pull-up" during takeoff and again during approach and landing must be incorporated. Yet, this is **easier** said than done. Any change to the algorithm to correct this deficiency may have reversal effects. In other words, the change may correct the false alarm rate by increasing the crash rate. This would be unacceptable and may be a consequence of the limitations of a ground collision avoidance system. Extreme attention should be given to this potential problem.

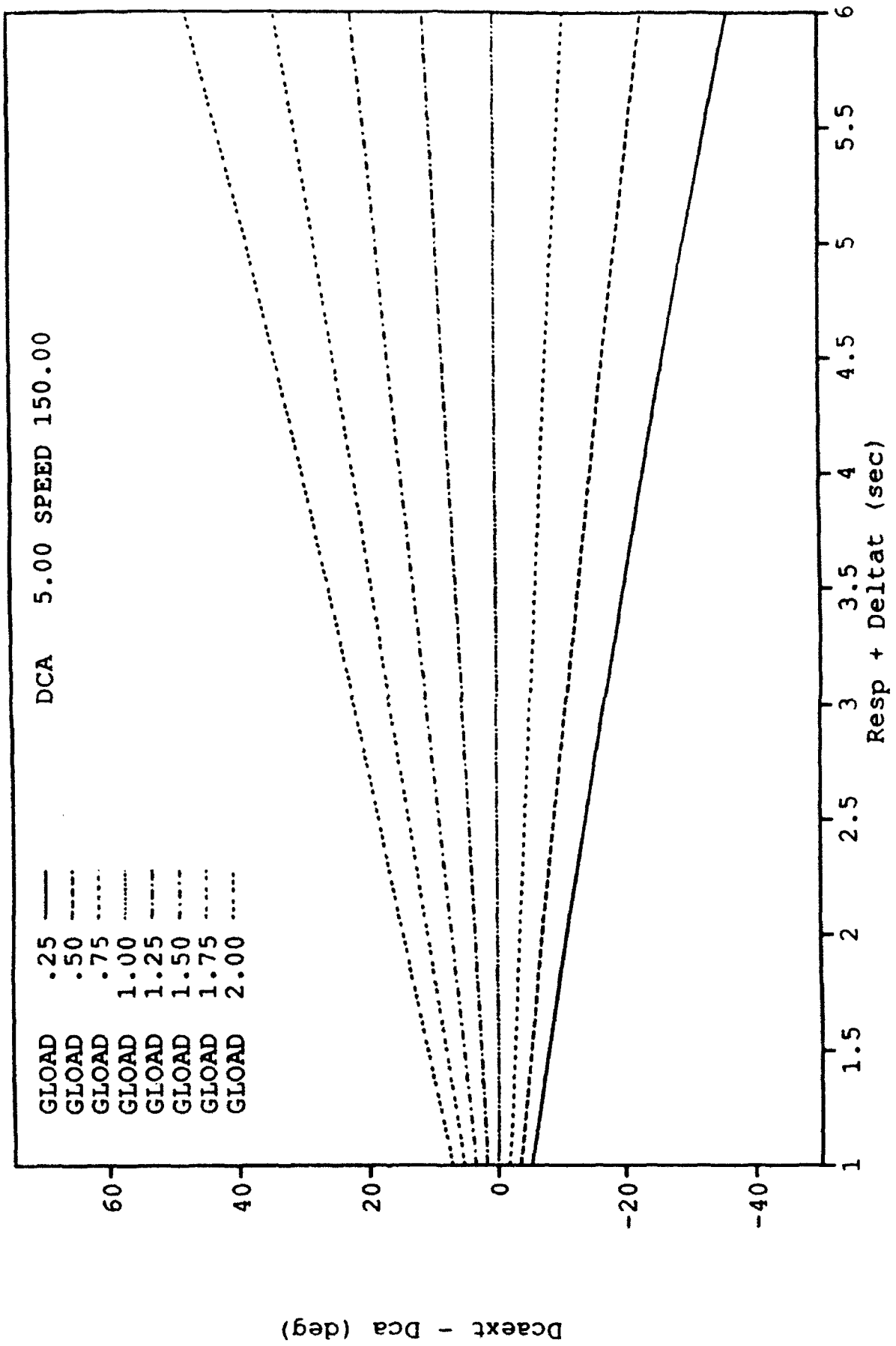
Without entering into the details discussed earlier, the lack of a forward looking sensor onboard the aircraft may indeed limit the total accuracy of any GCAS system. It is possible that a small false alarm rate, while highly desirable, may not be achievable given the limitations of the type of system. Should this be the case, the question now becomes, "What false alarm rate is acceptable?" This study used a 90% reliability figure with a maximum of a 10% false alarm rate. Future research should be directed at determining what false alarm rate is acceptable.

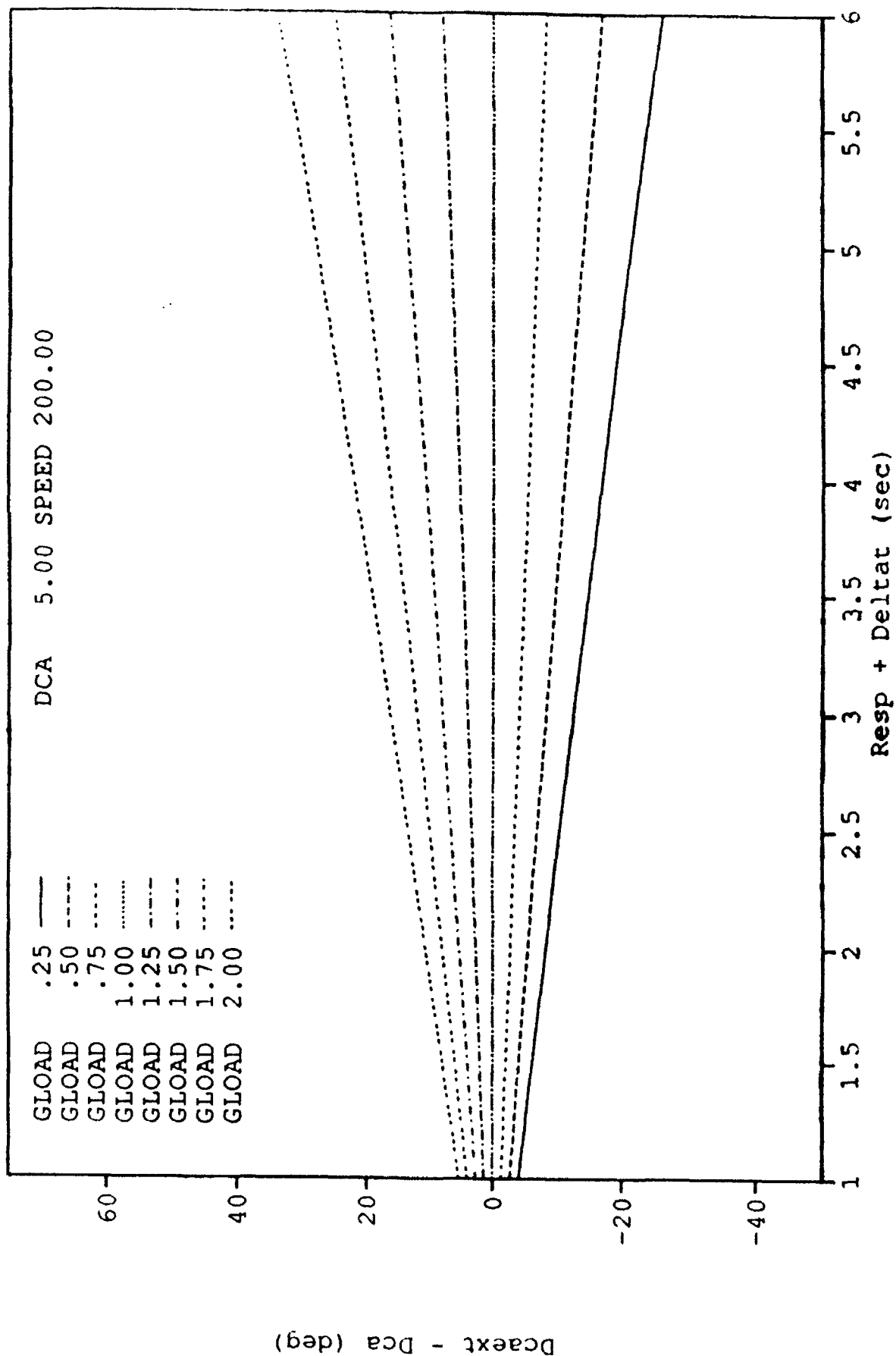
Given the above system improvements, system deficiencies, system limitations, and experimental questions, a definite "yes" or "no" to whether the system is acceptable is not possible. However, the improvements to and the conservative nature of the algorithm make it an excellent candidate for flight test.

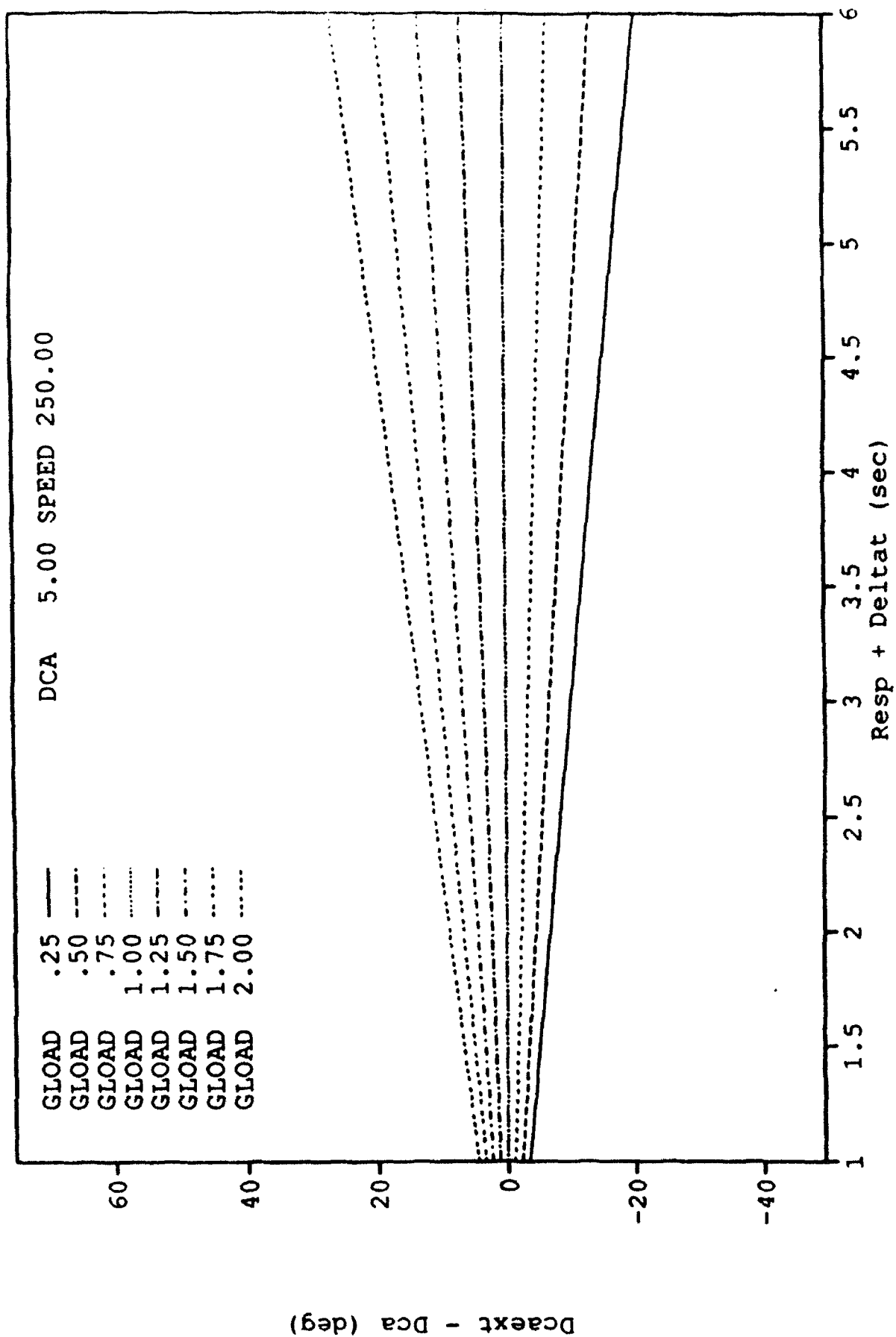
BIBLIOGRAPHY

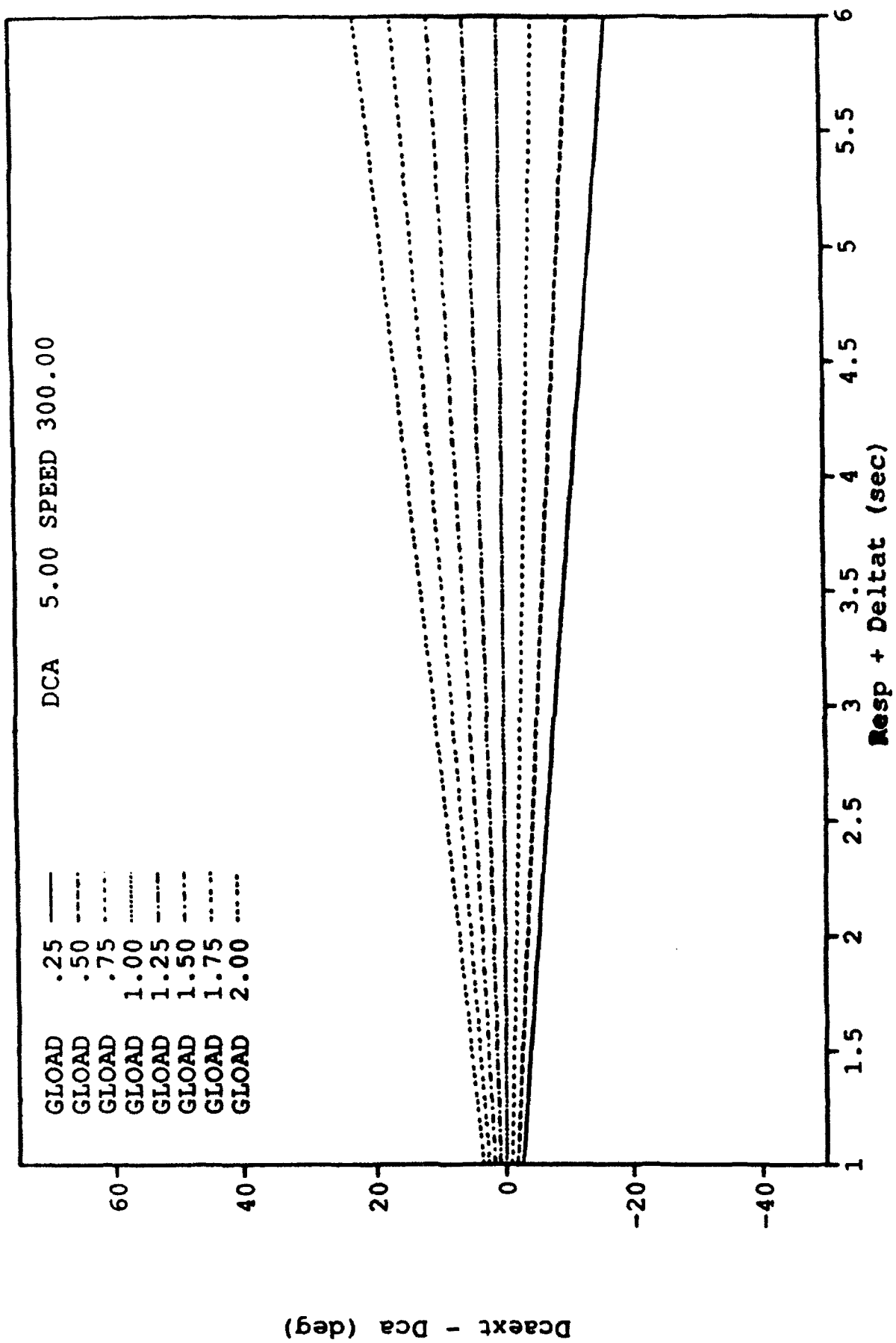
- Department of Defense (1970). Aircrew Station Signals (MIL-STD-411D). Washington, D.C.: Author.
- Department of Defense. (1981). Human Engineering Design Criteria for Military Systems, Equipment, and Facilities (MIL-STD-1472D). Washington, D.C.: Author.
- Department of Defense. (1982). Aircrew Station Passenger and Accommodations (MIL-STD-1776). Washington, D.C.: Author.
- Department of Defense (1988). Flight Manual Performance Data-Appendix 1: USAF Series KC-135R Aircraft (T.O. 1C-135(F)R-1-1). Washington, D.C.: Author.
- Hassoun, J. A., Barnaba, J. M., & Matheson, E. M. (1988). An Evaluation of the F/FB/EF-111 Crew/Voice Message System Interface (ASD-TR-88-5037). Aeronautical Systems Division. Wright-Patterson AFB, OH.
- Hassoun, J. A., Ward, G. F., Capt., Barnaba, J. M., & McCarthy, D. M., C1C. (1989). Evaluation of the F/FB/EF-111 Ground Collision Avoidance System (GCAS) (ASD-TR-90-5002). Aeronautical Systems Division. Wright-Patterson AFB, OH.
- Military Airlift Command (MAC) Statement of Operational Need, 06-84.
- Rueb, J. D., & Kinzig, J. R. (1989). Cargo/Transport/Tanker Controlled Flight into Terrain (CFIT) (1970-Present) and the Possible Impact of an Operable Ground Collision Avoidance System (GCAS) (CSEF-TR-89-135-01). Crew Station Evaluation Facility, Aeronautical Systems Division. Wright-Patterson AFB, OH.
- Rueb, J. D., & Hassoun, J. A. (1990). KC-135 Ground Collision Avoidance System Questionnaire (ASD-TR-90-5010). Wright-Patterson AFB, OH: Aeronautical Systems Division.
- Rueb, J. D., & Hassoun, J. A. (1991). Evaluation of the C/EC/KC-135 Ground Collision Avoidance System (GCAS) (Study 1) (ASD-TR-91-5004). Wright-Patterson AFB, OH: Aeronautical Systems Division.
- Strategic Air Command (SAC) Statement of Operational Need: KC-135 Avionics Modernization, 013-84, May 1987.
- Shah, D. S. (1988). Ground Collision Warning System Performance Criteria for High Maneuverability Aircraft (ASD-TR-88-5034). Aeronautical Systems Division. Wright-Patterson AFB, OH.

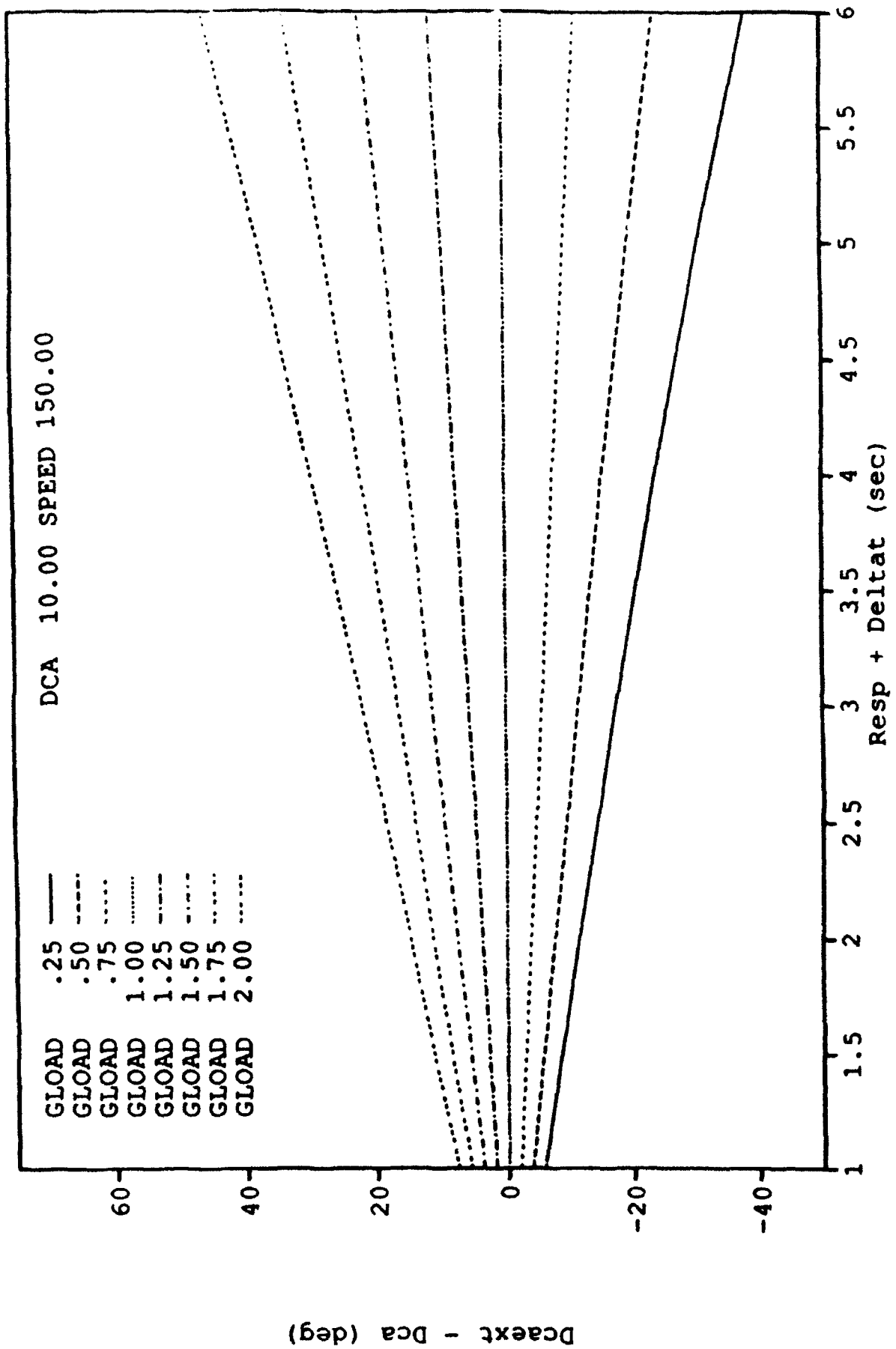
Appendix A
PHASE I
DCAEXTRP GRAPHS

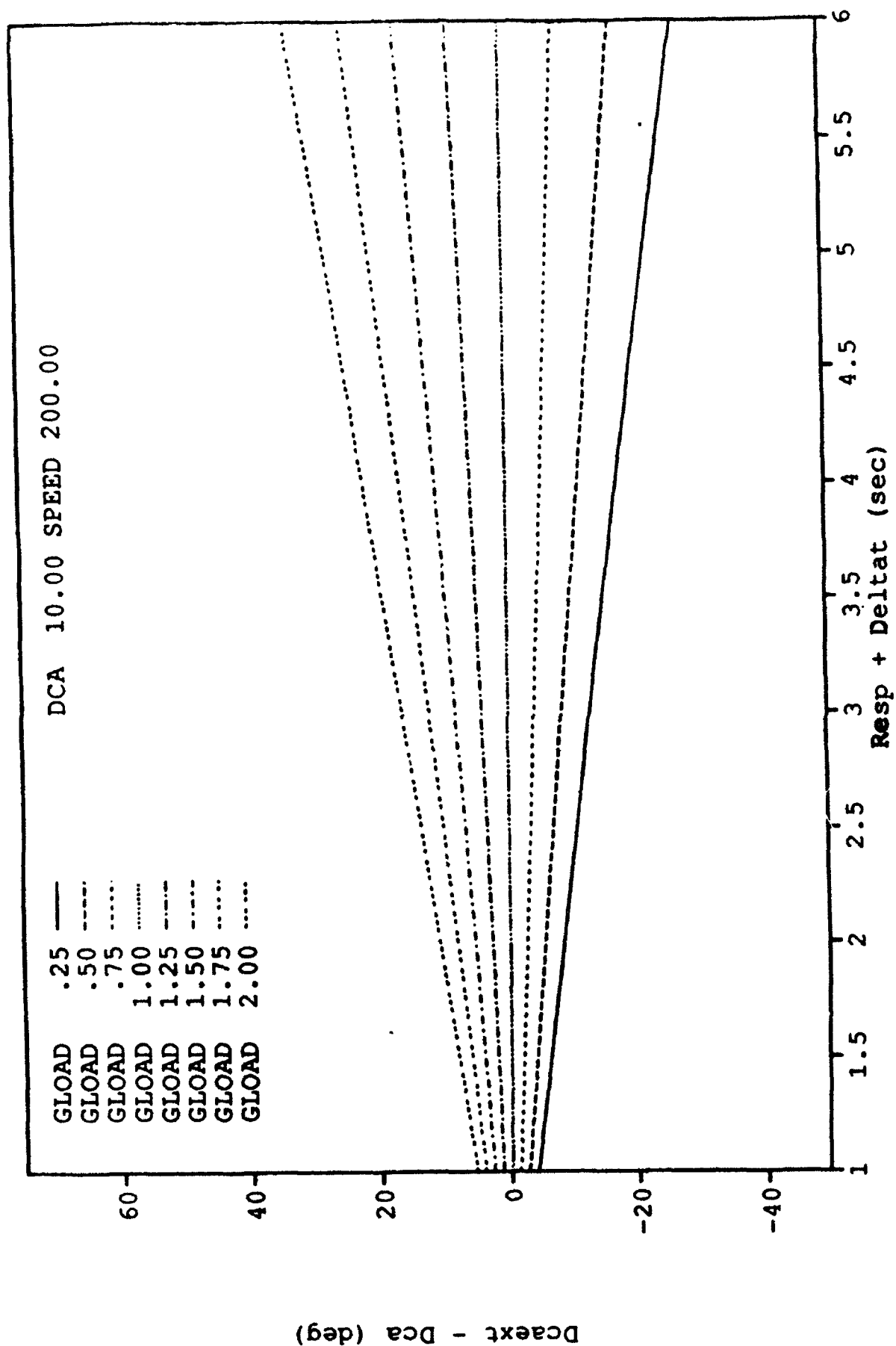


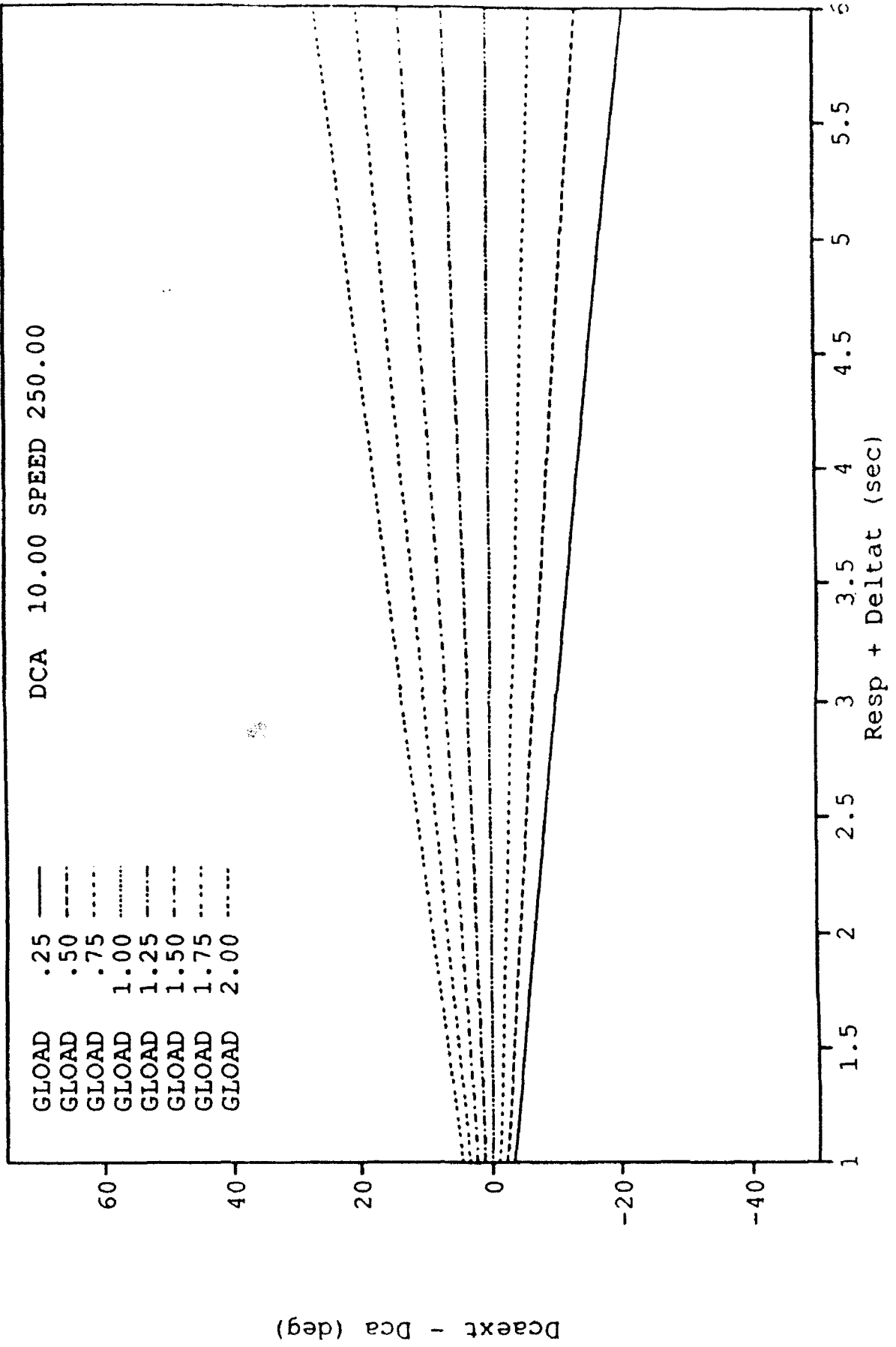


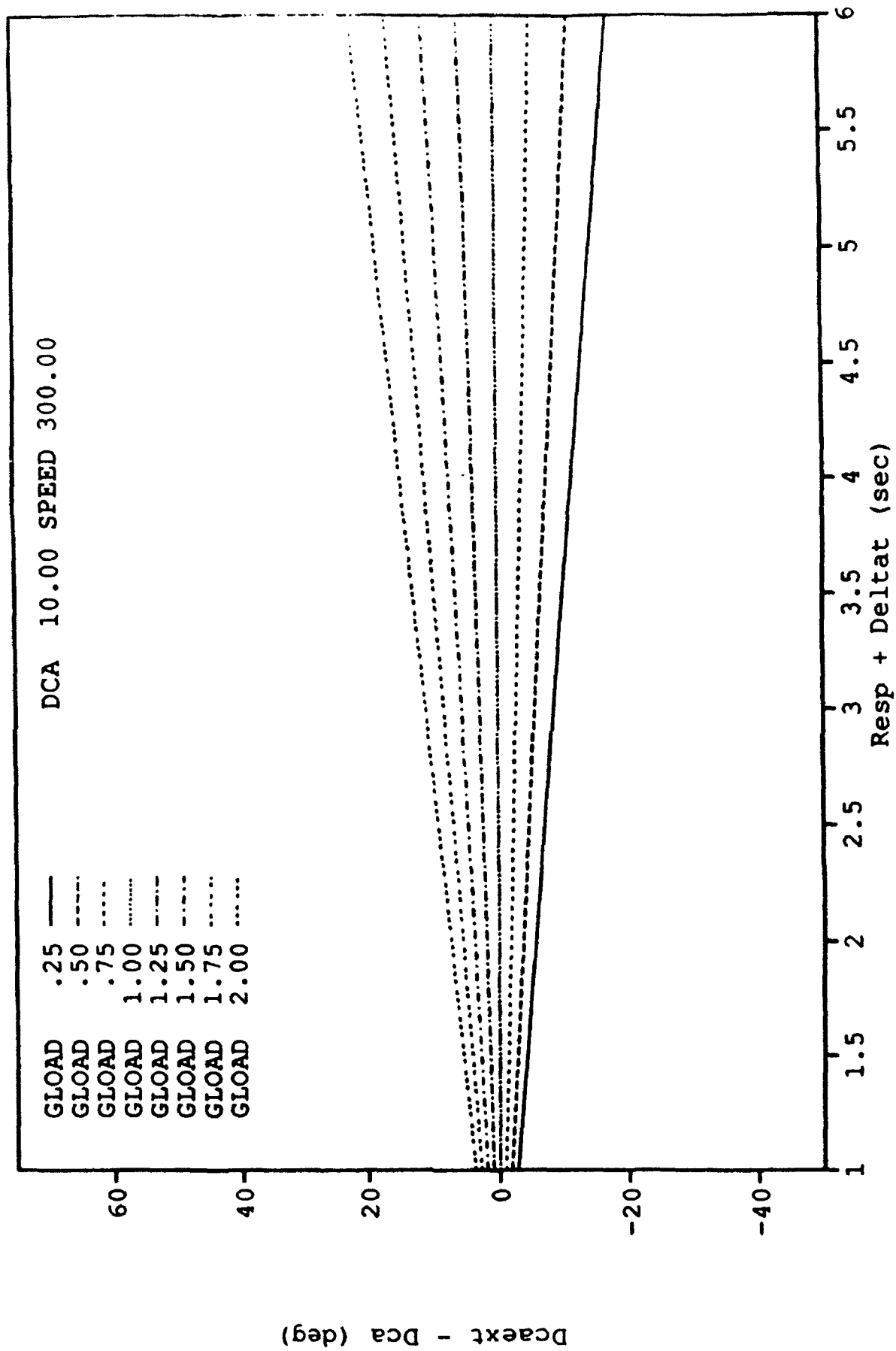


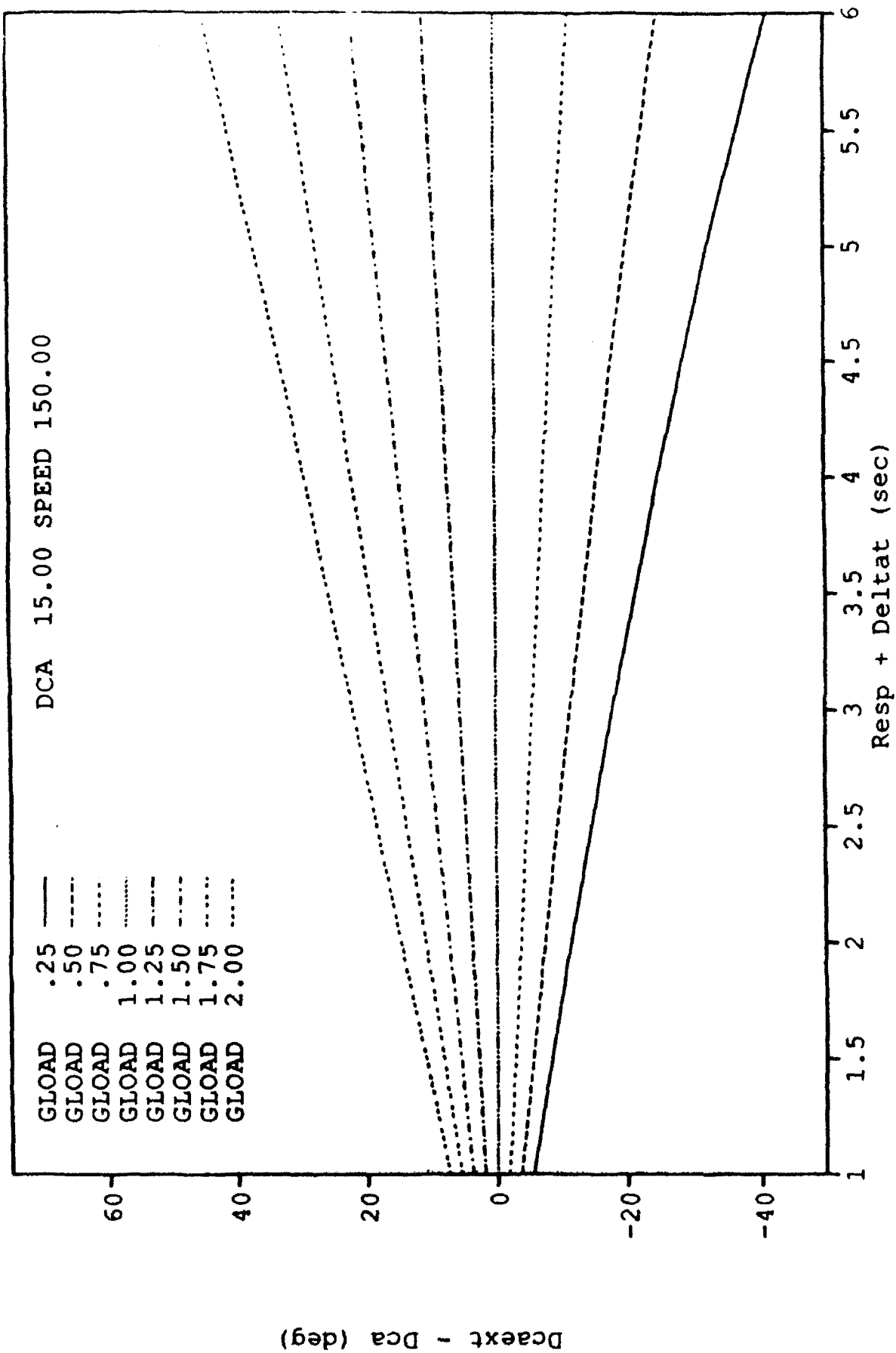


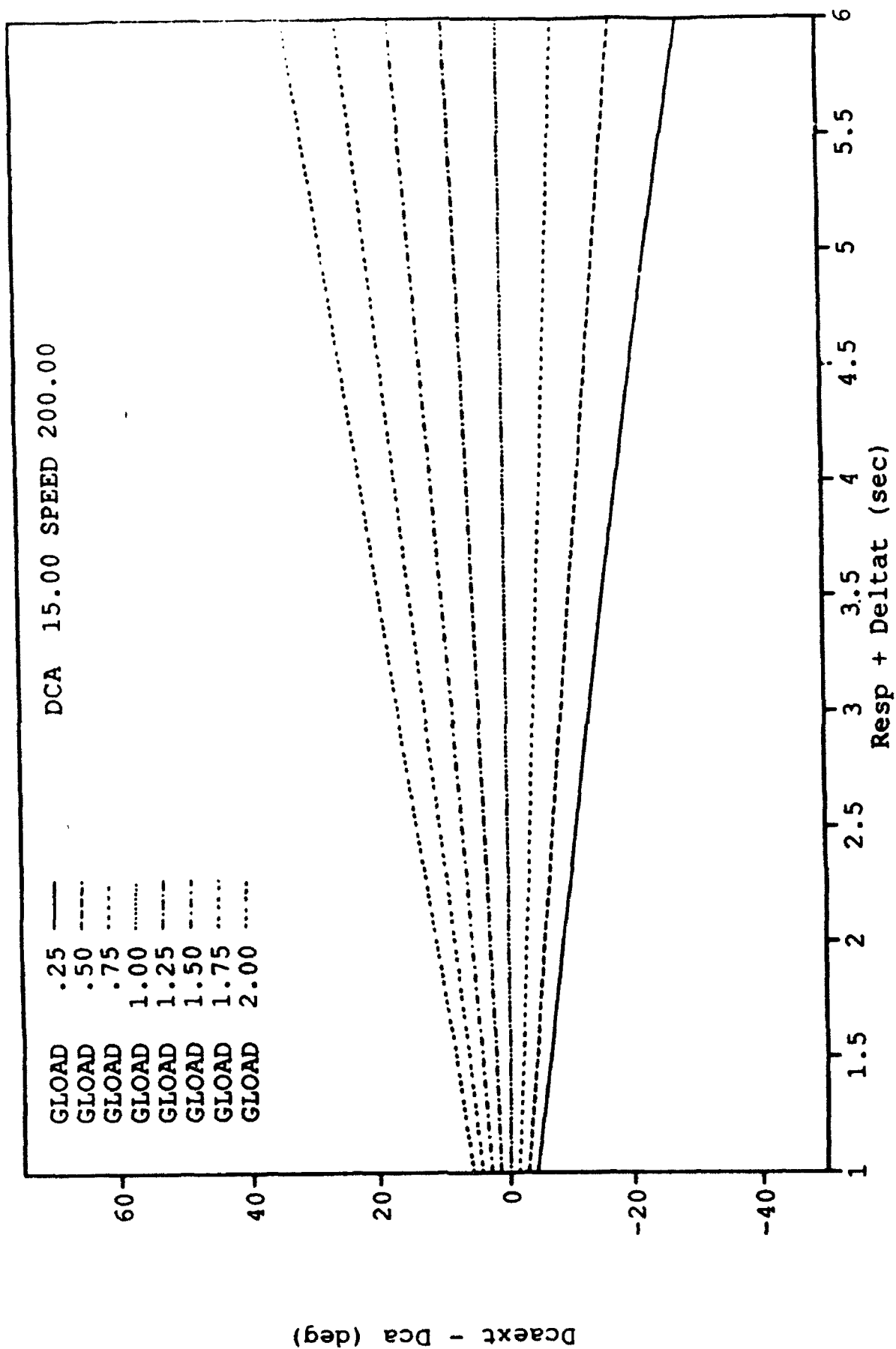


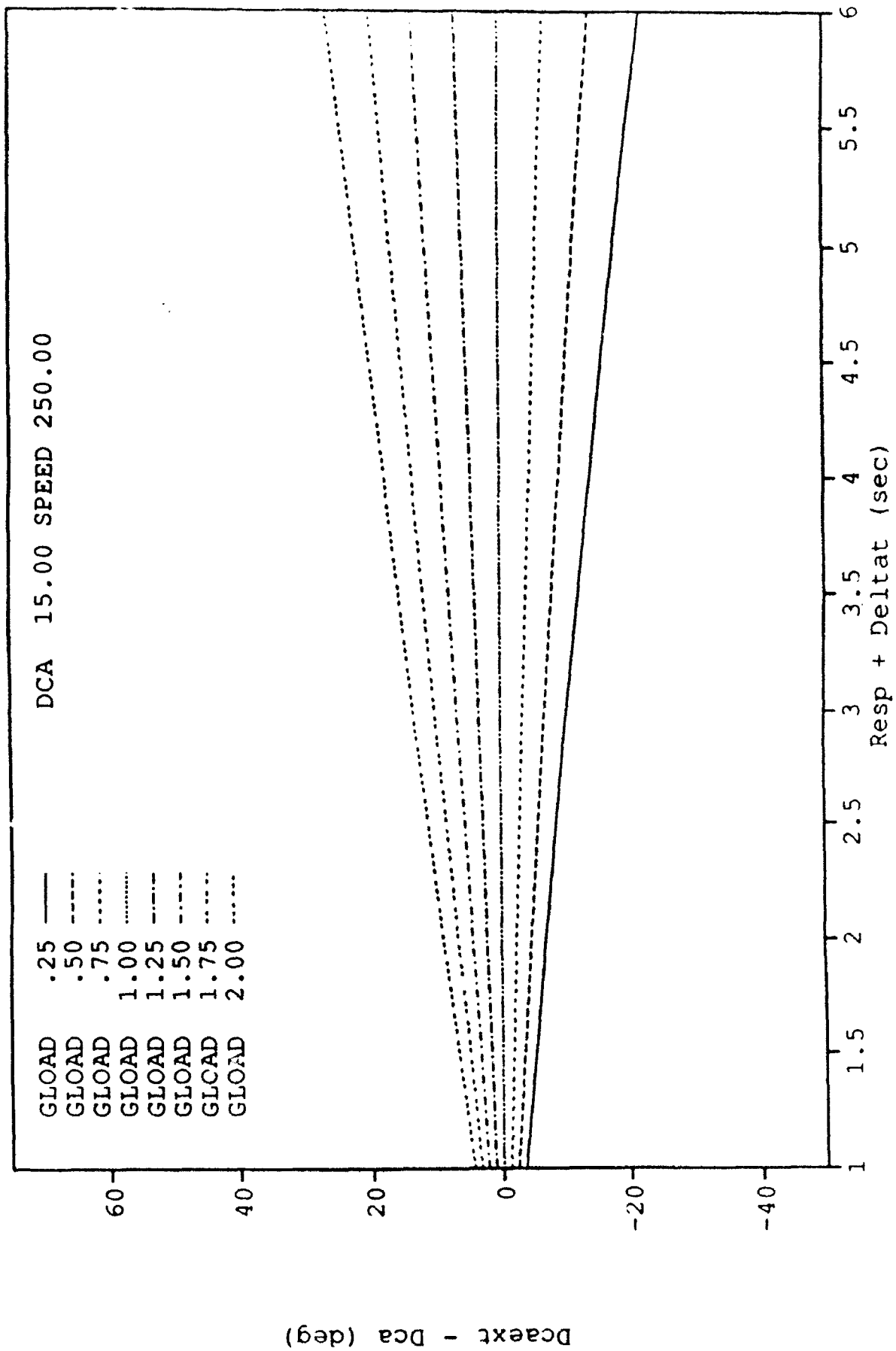


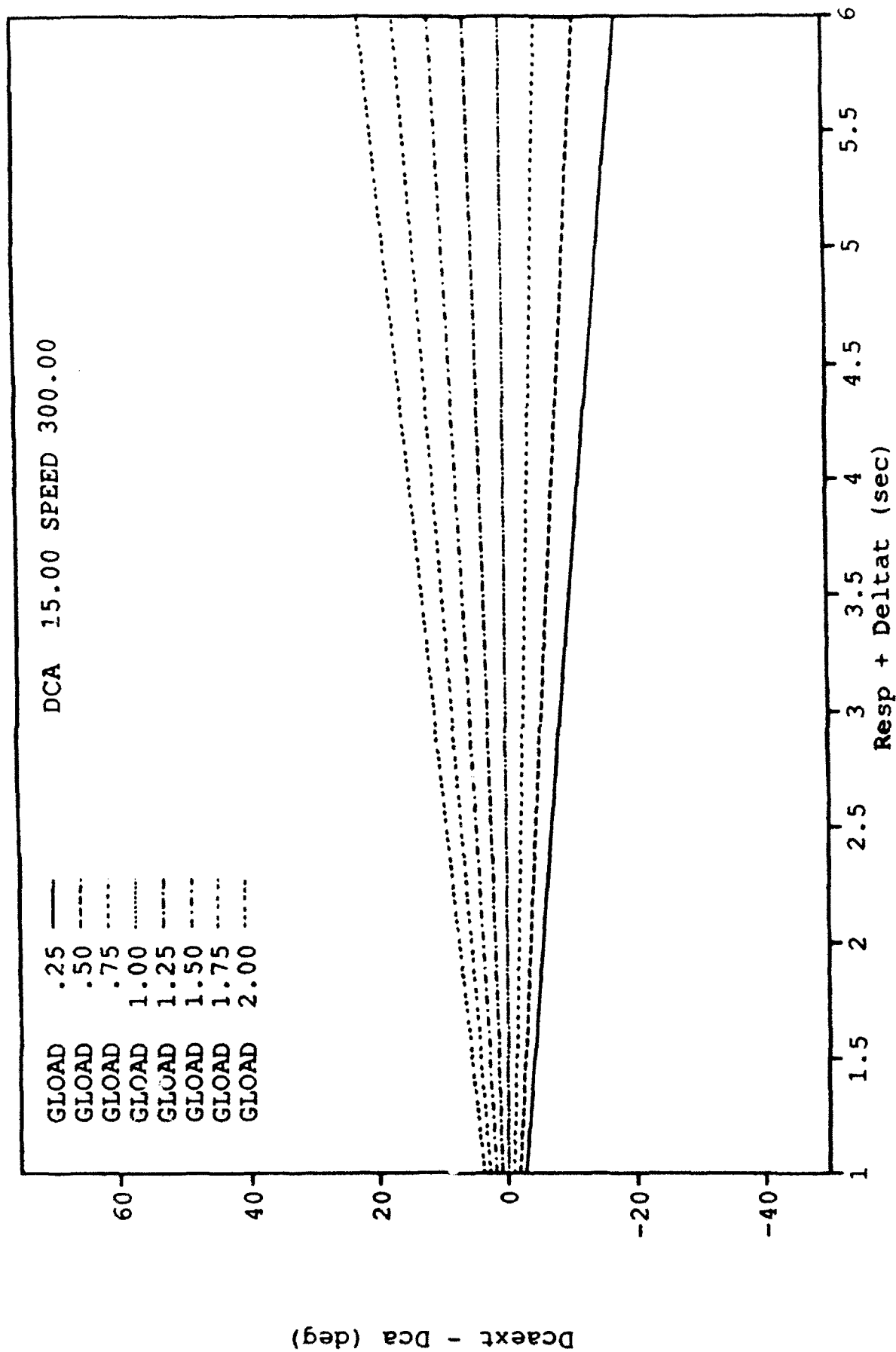


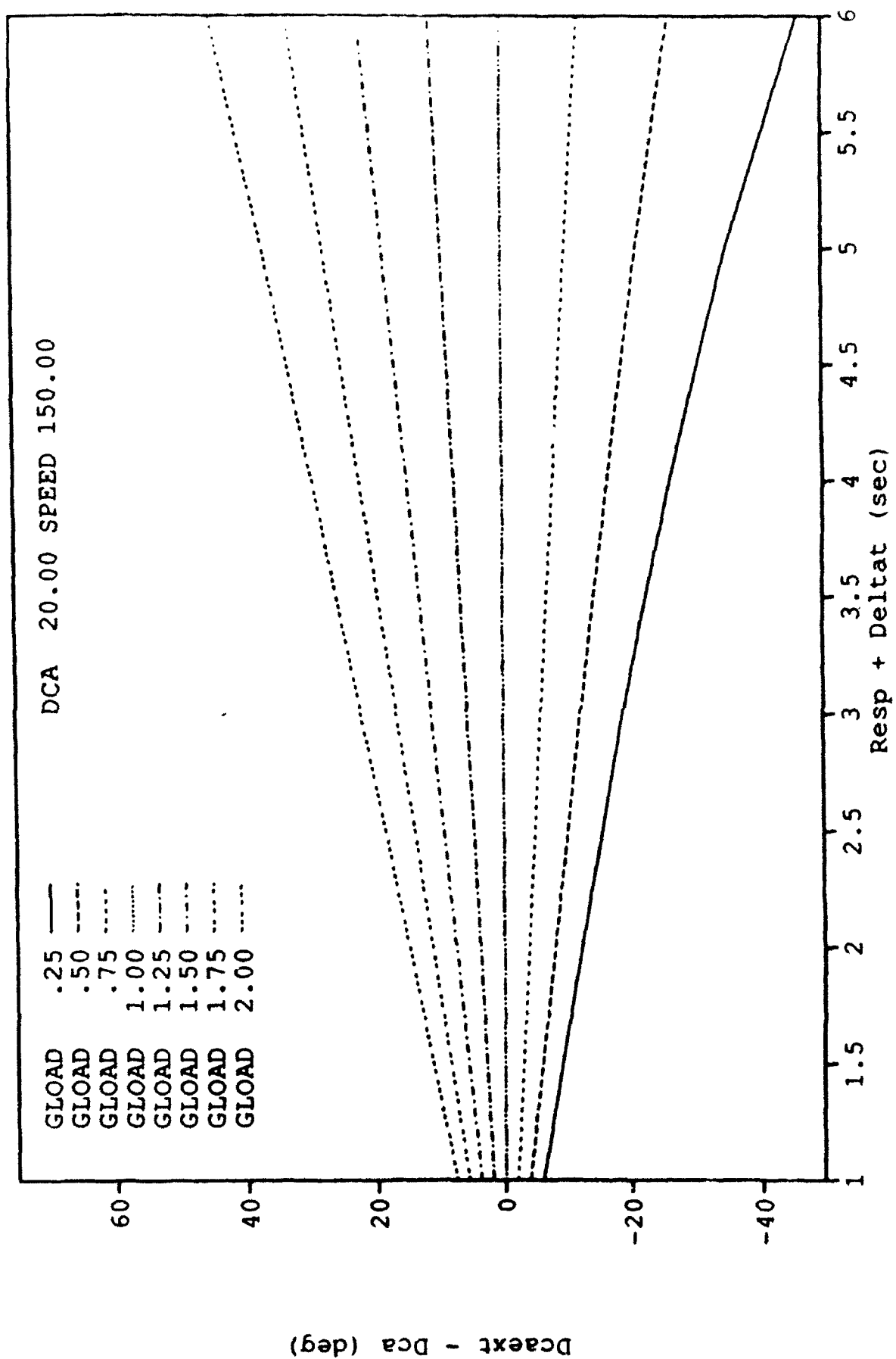


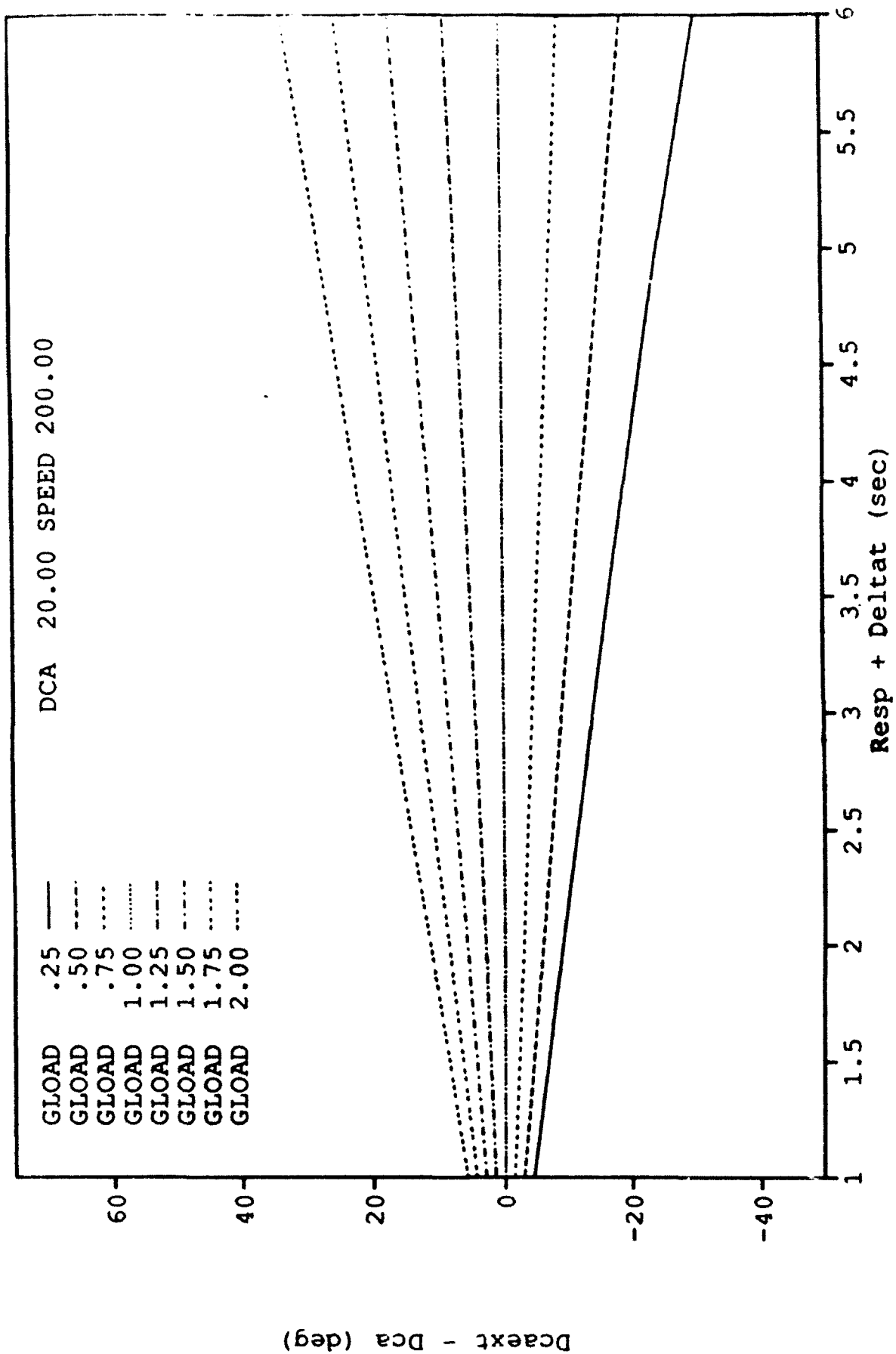


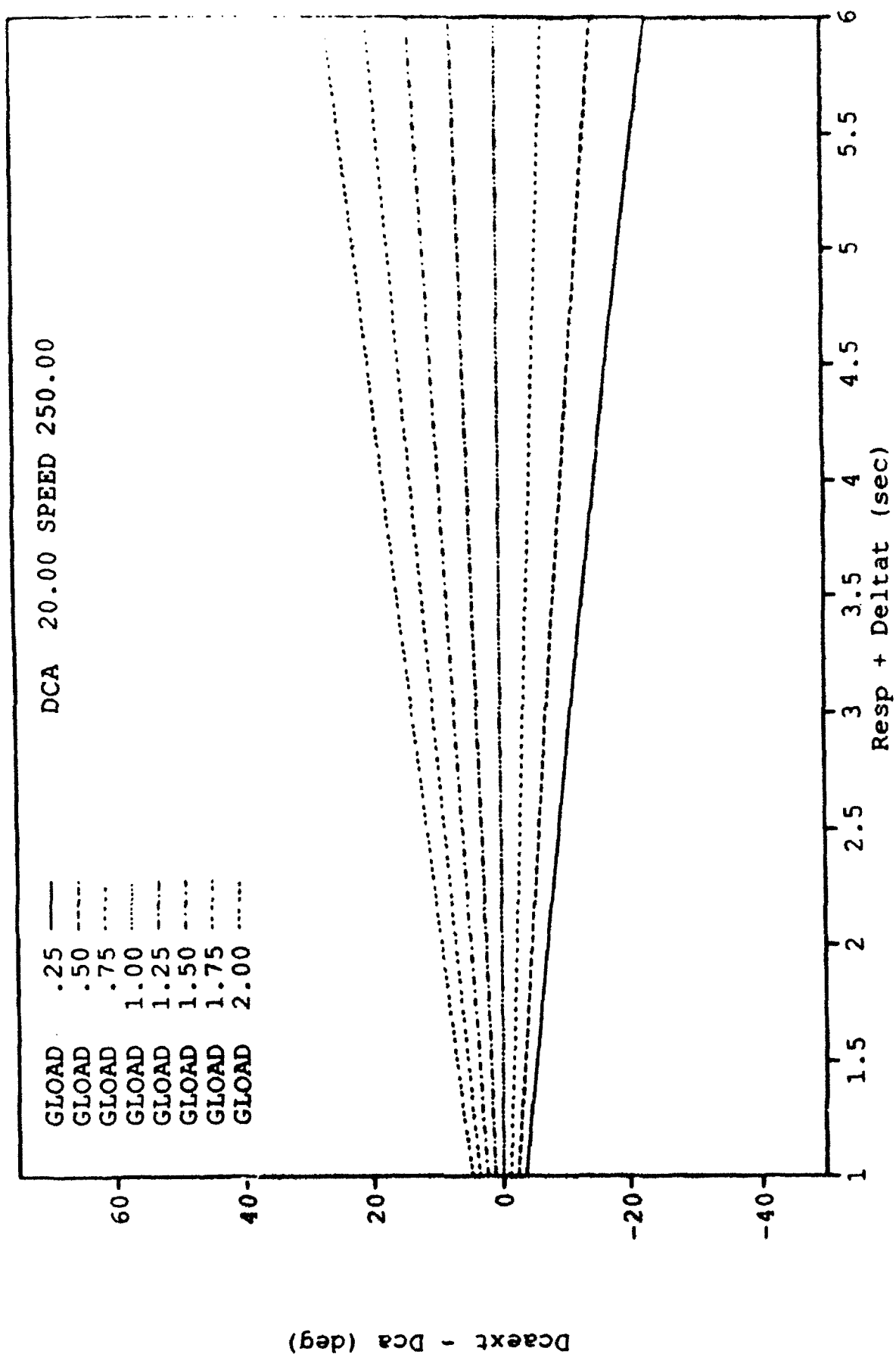


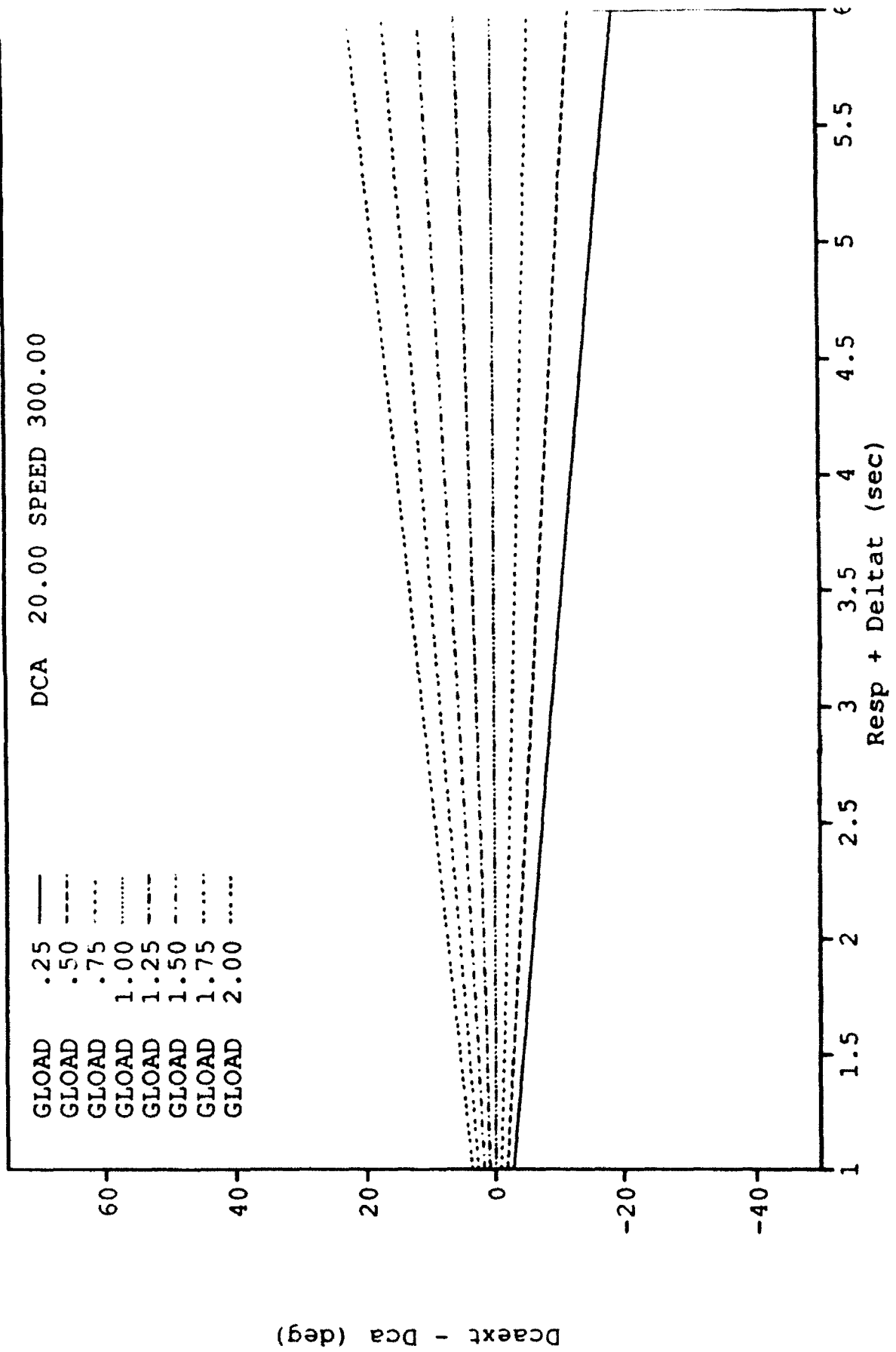




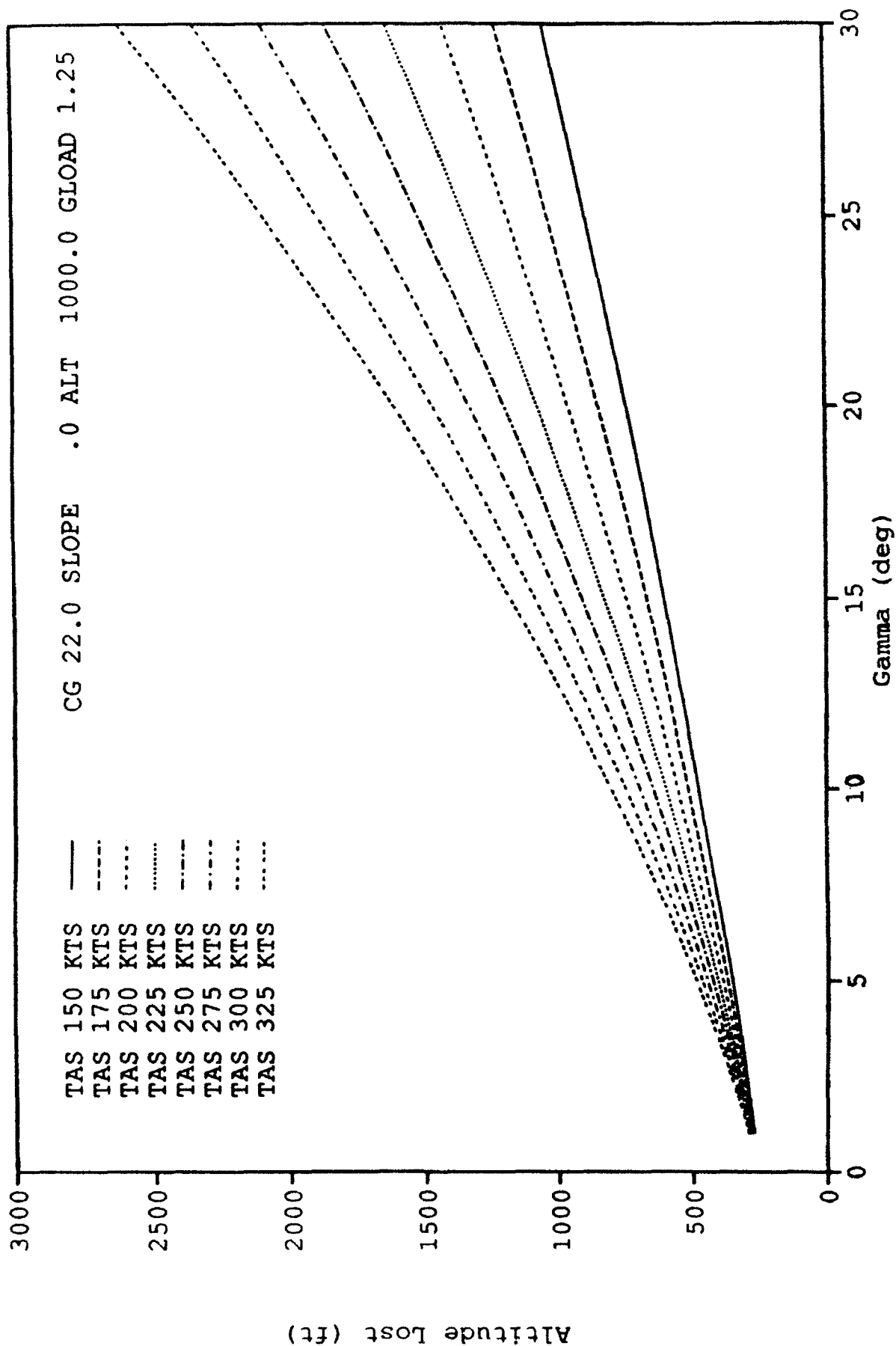


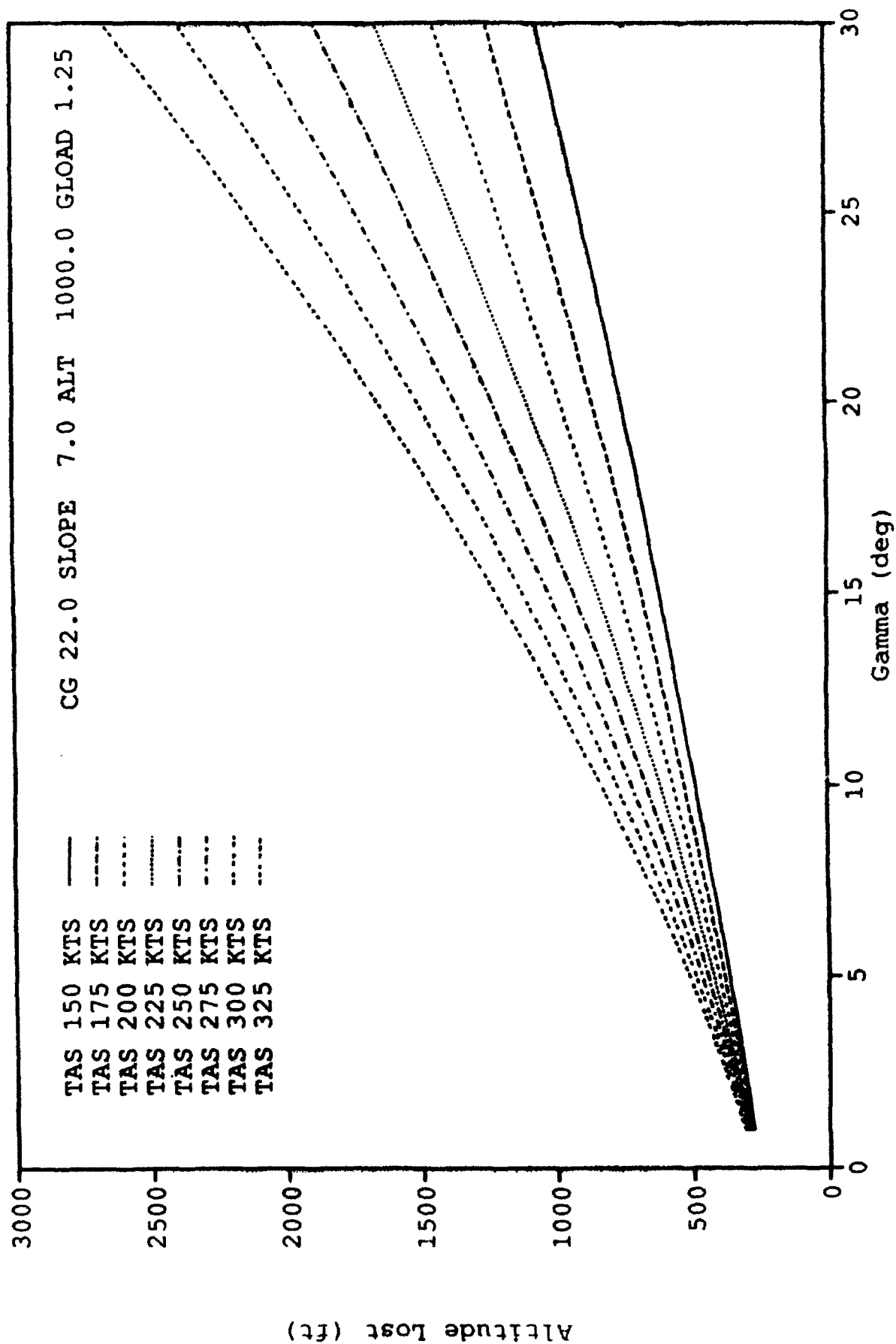


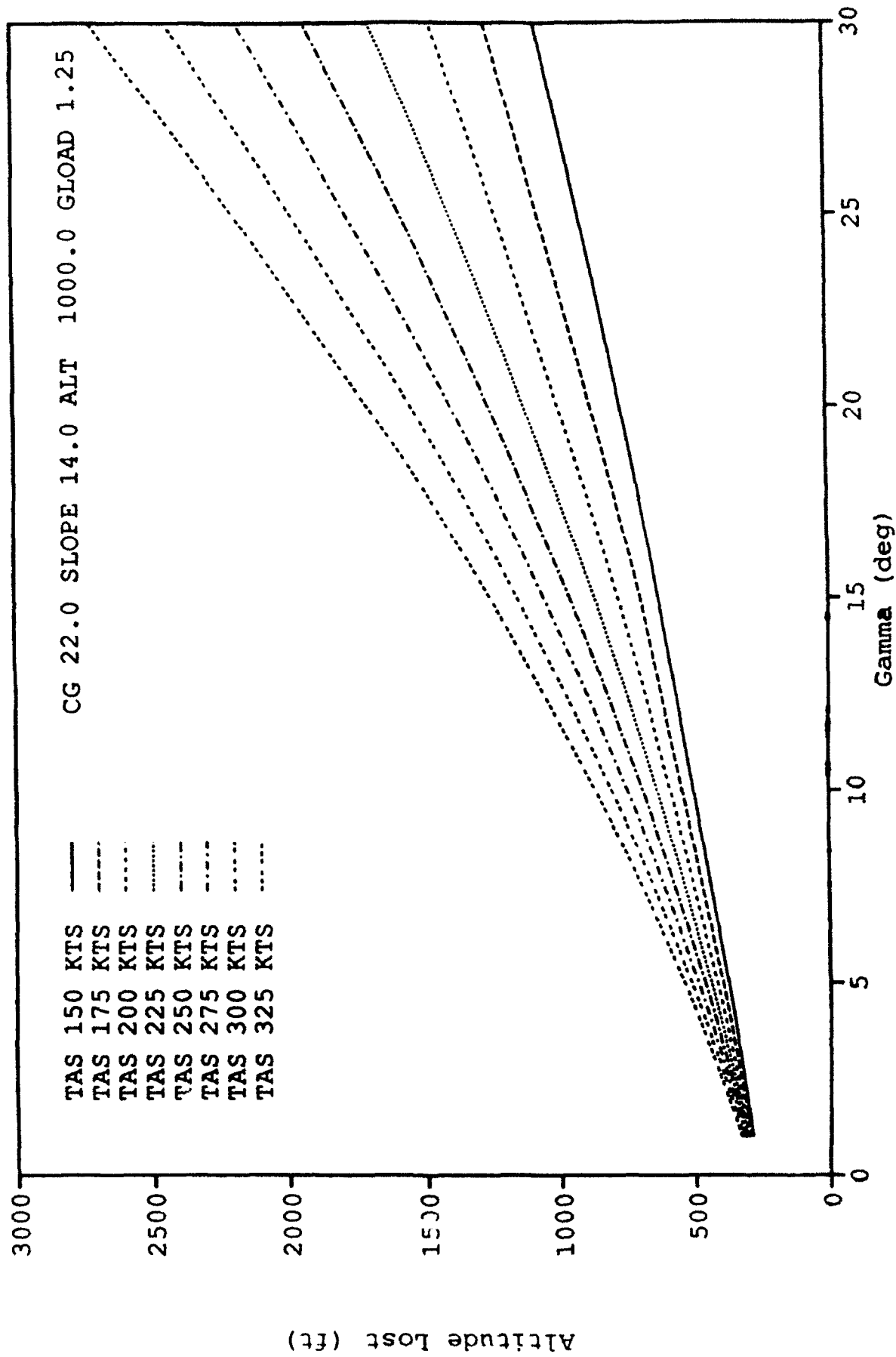




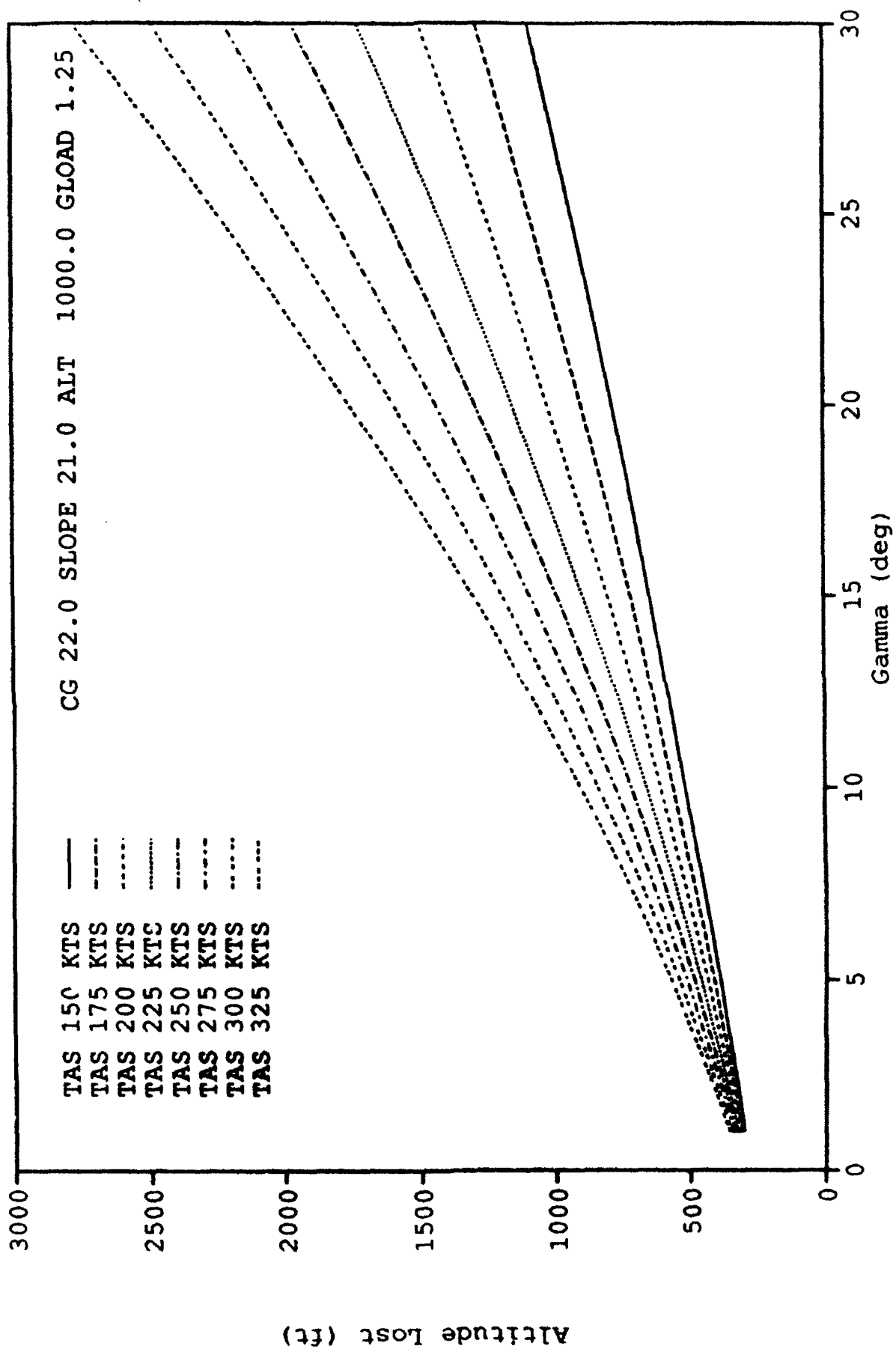
Appendix B
PHASE I
GCASDIVE GRAPHS

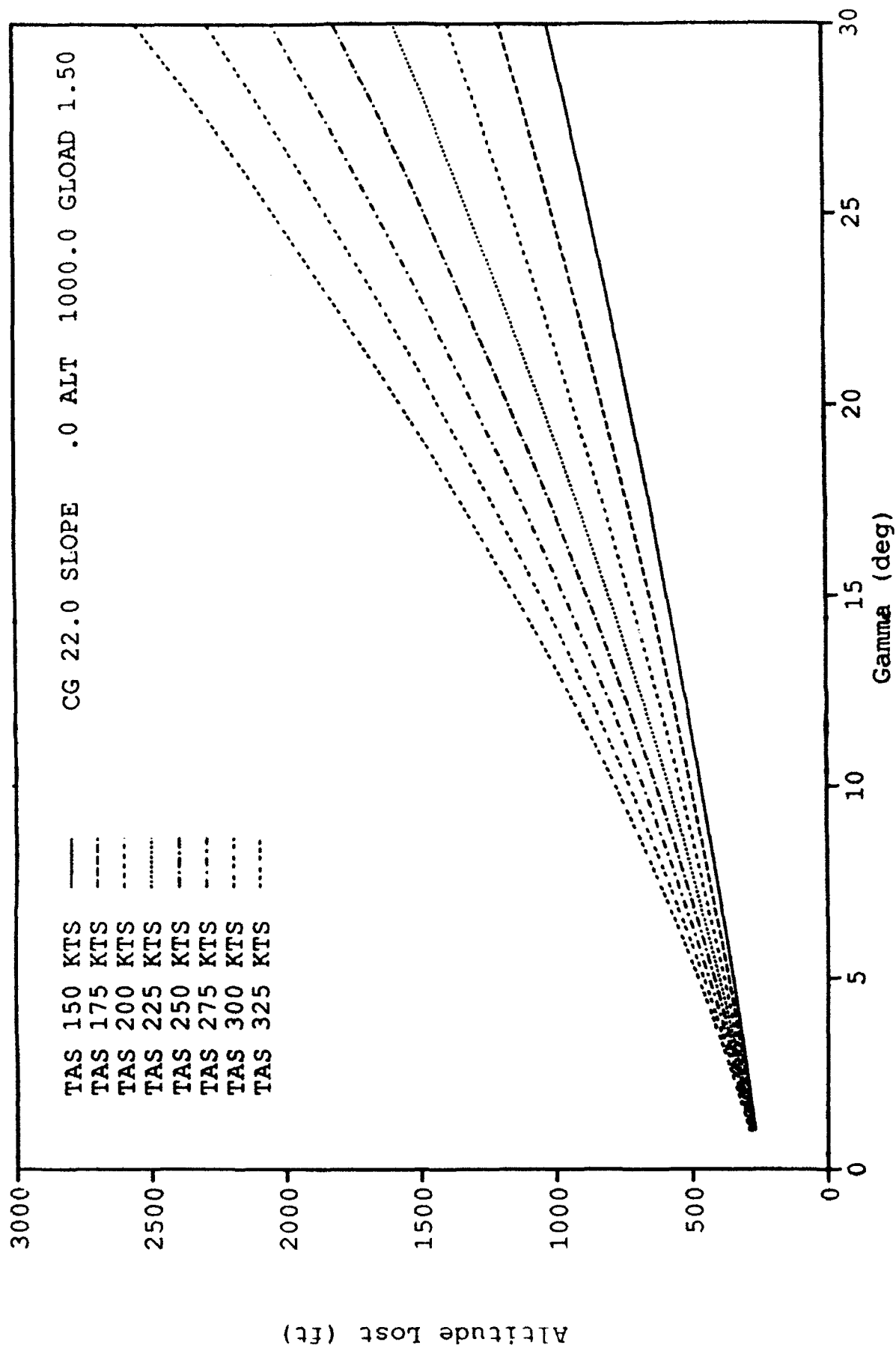


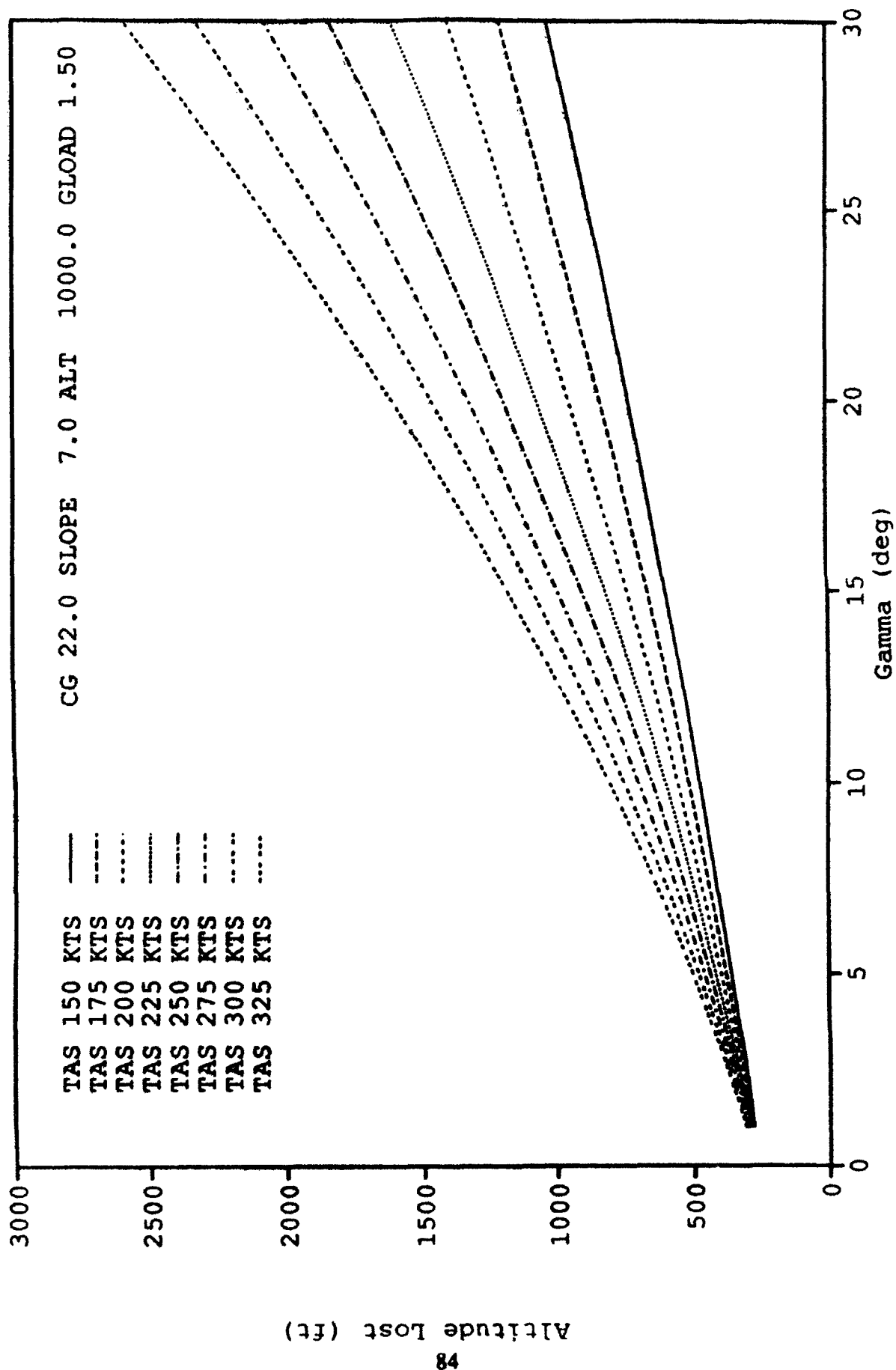


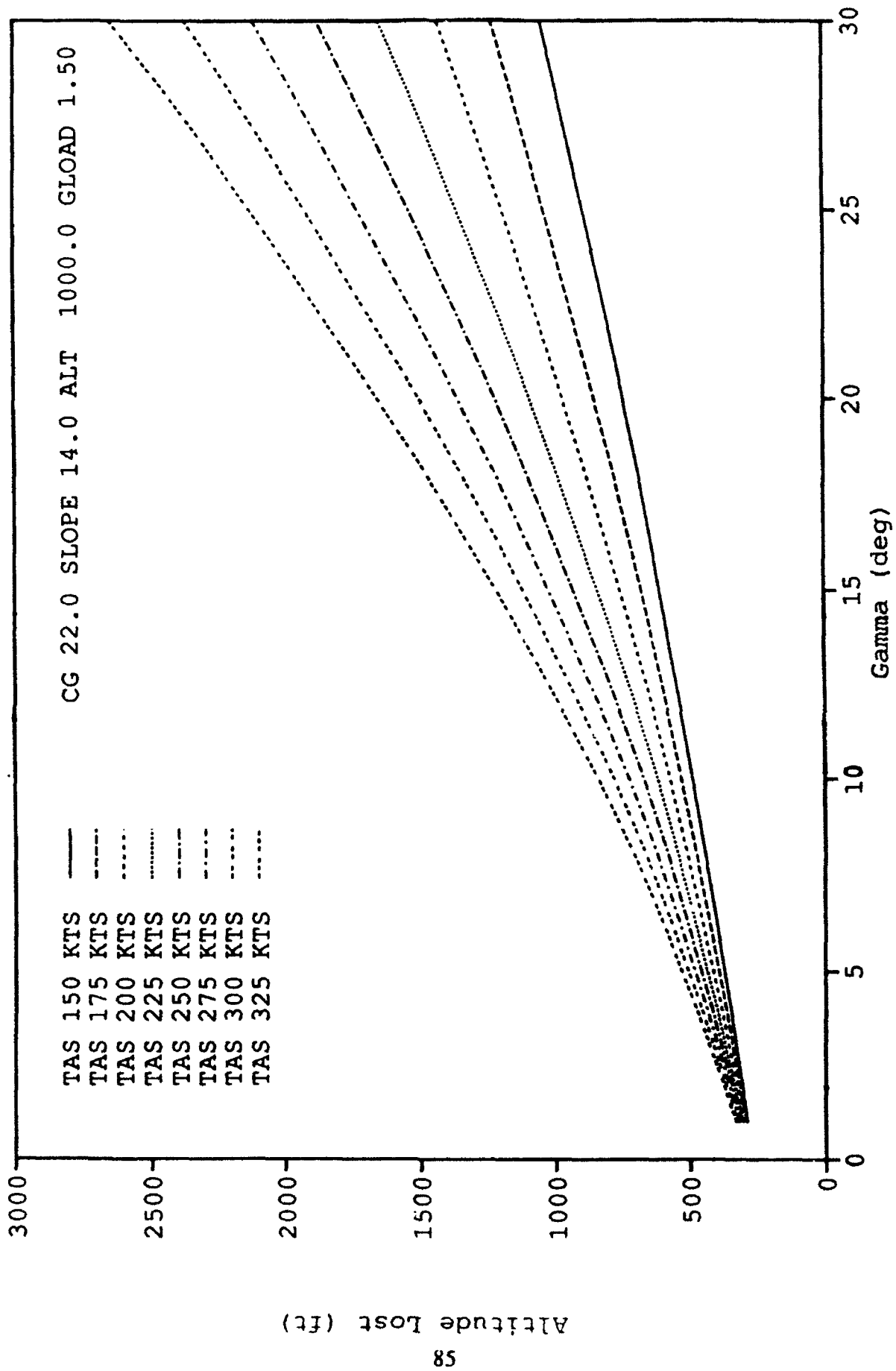


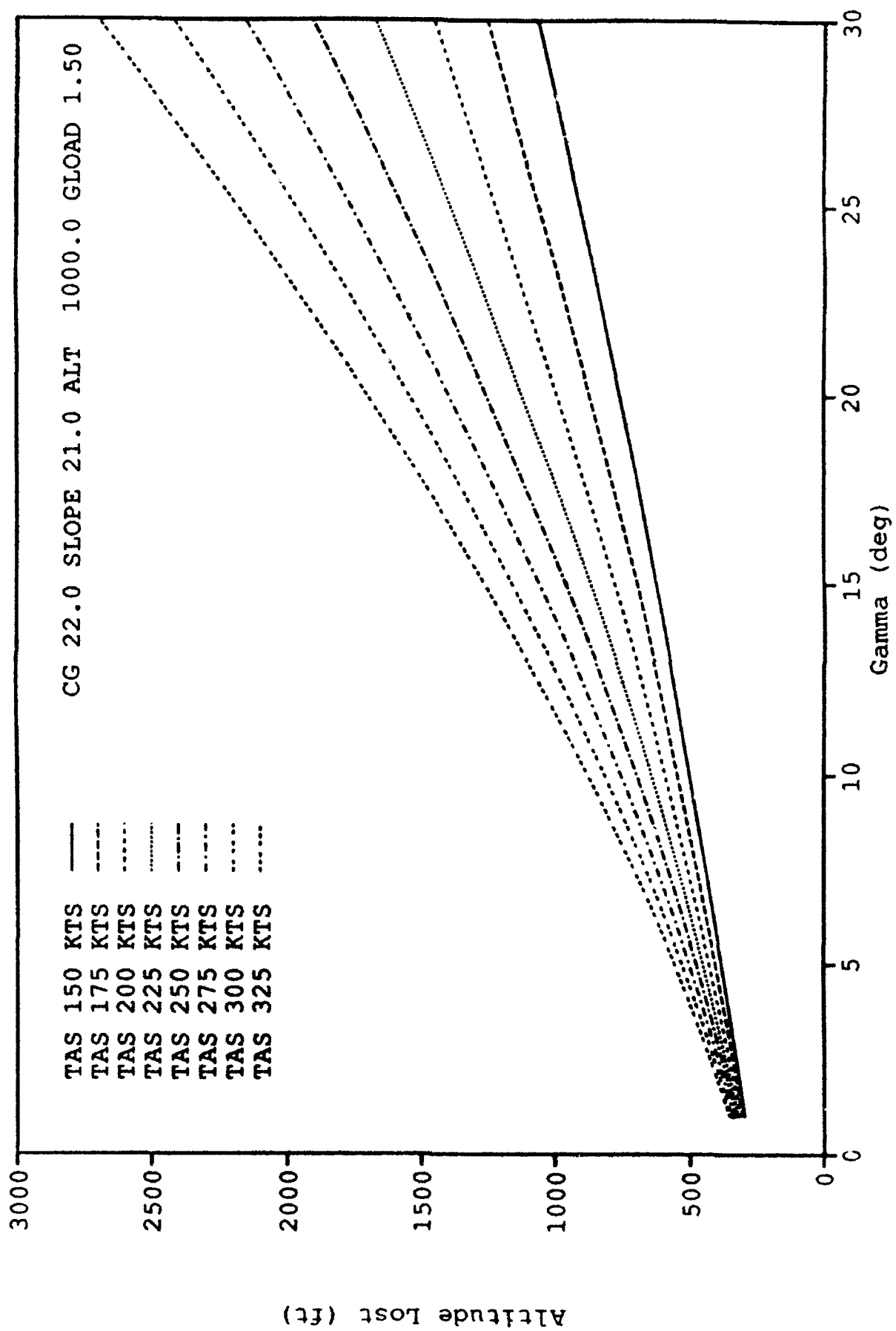
Altitude Lost (ft)

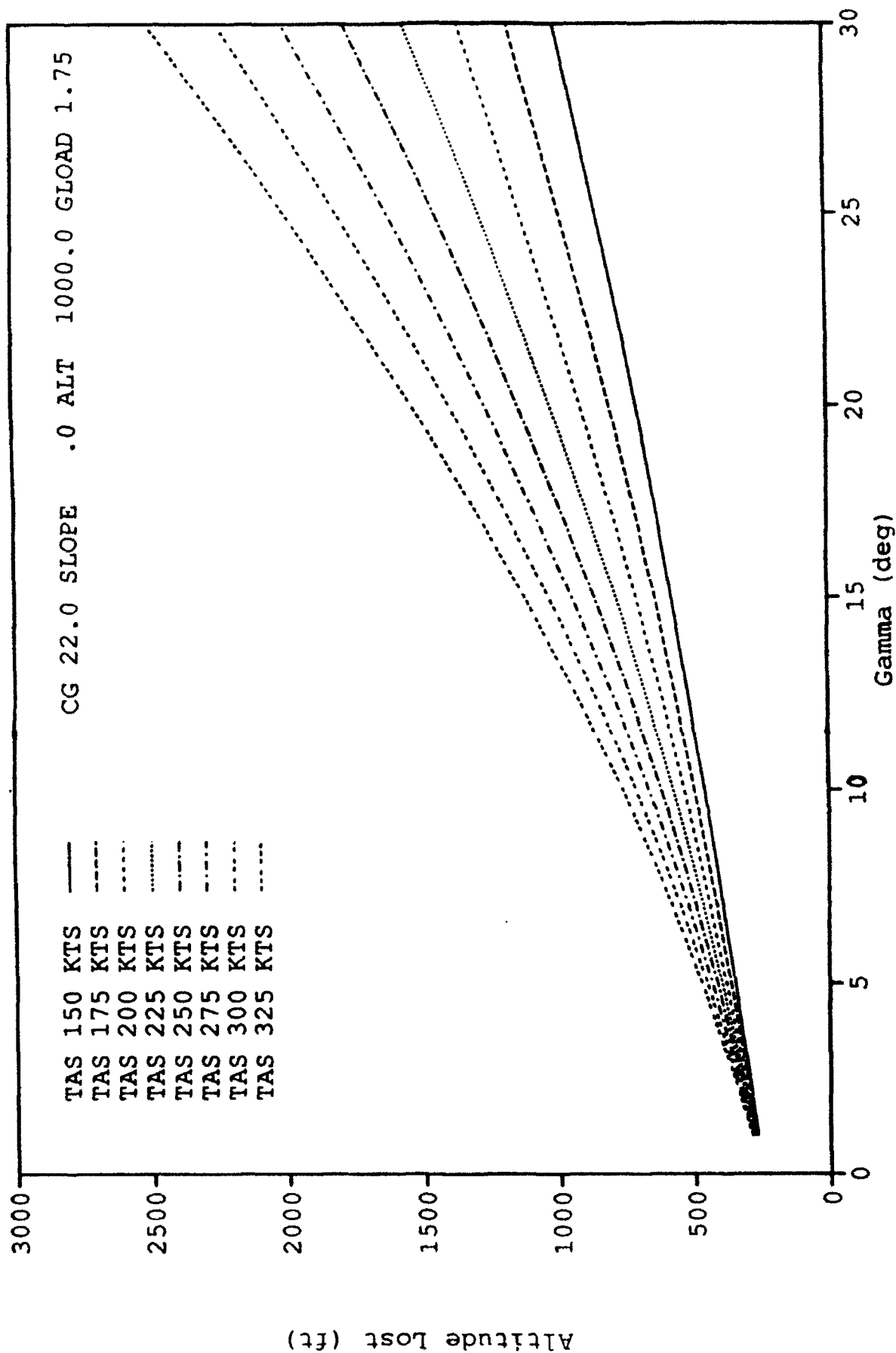


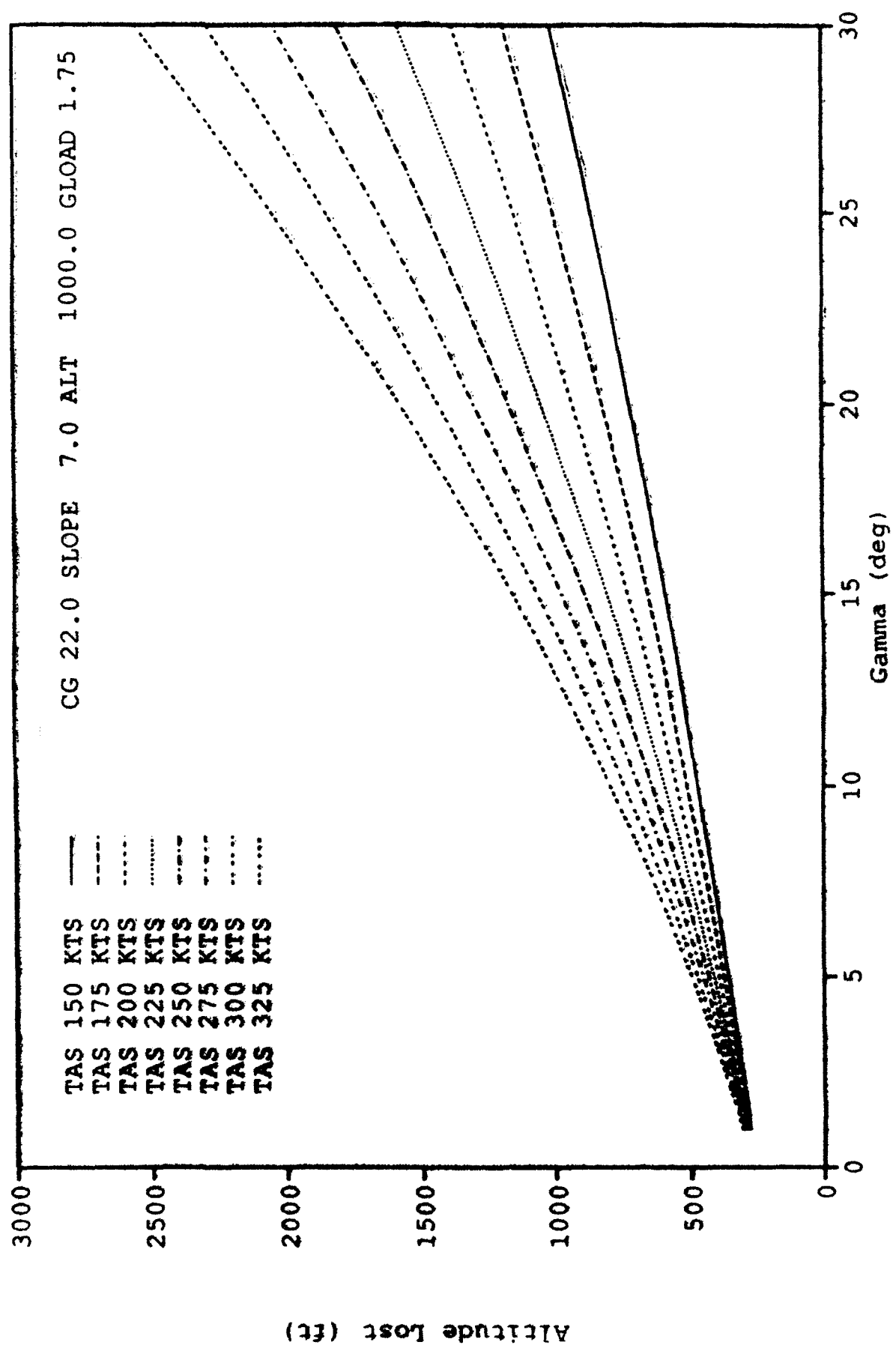


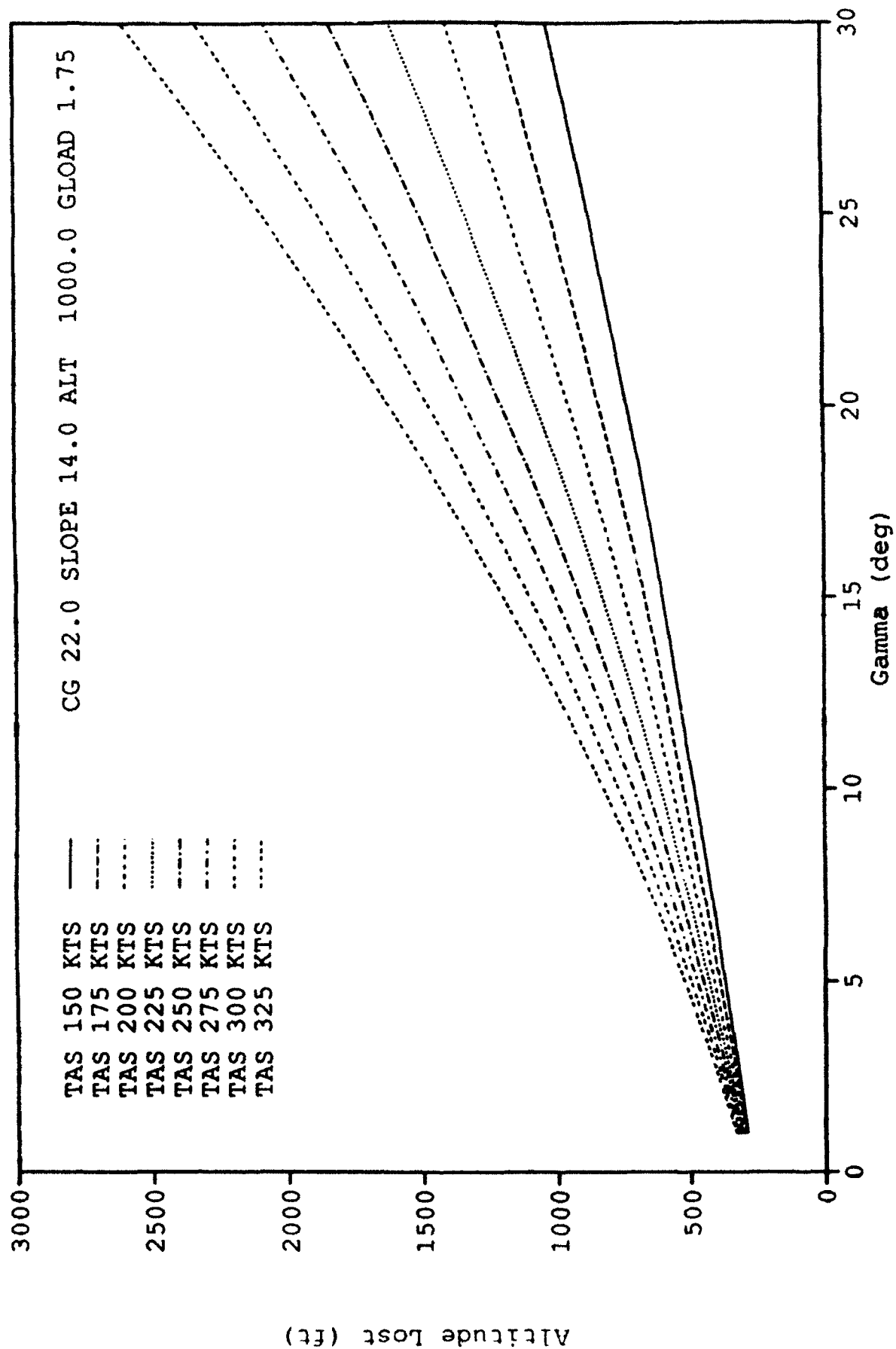


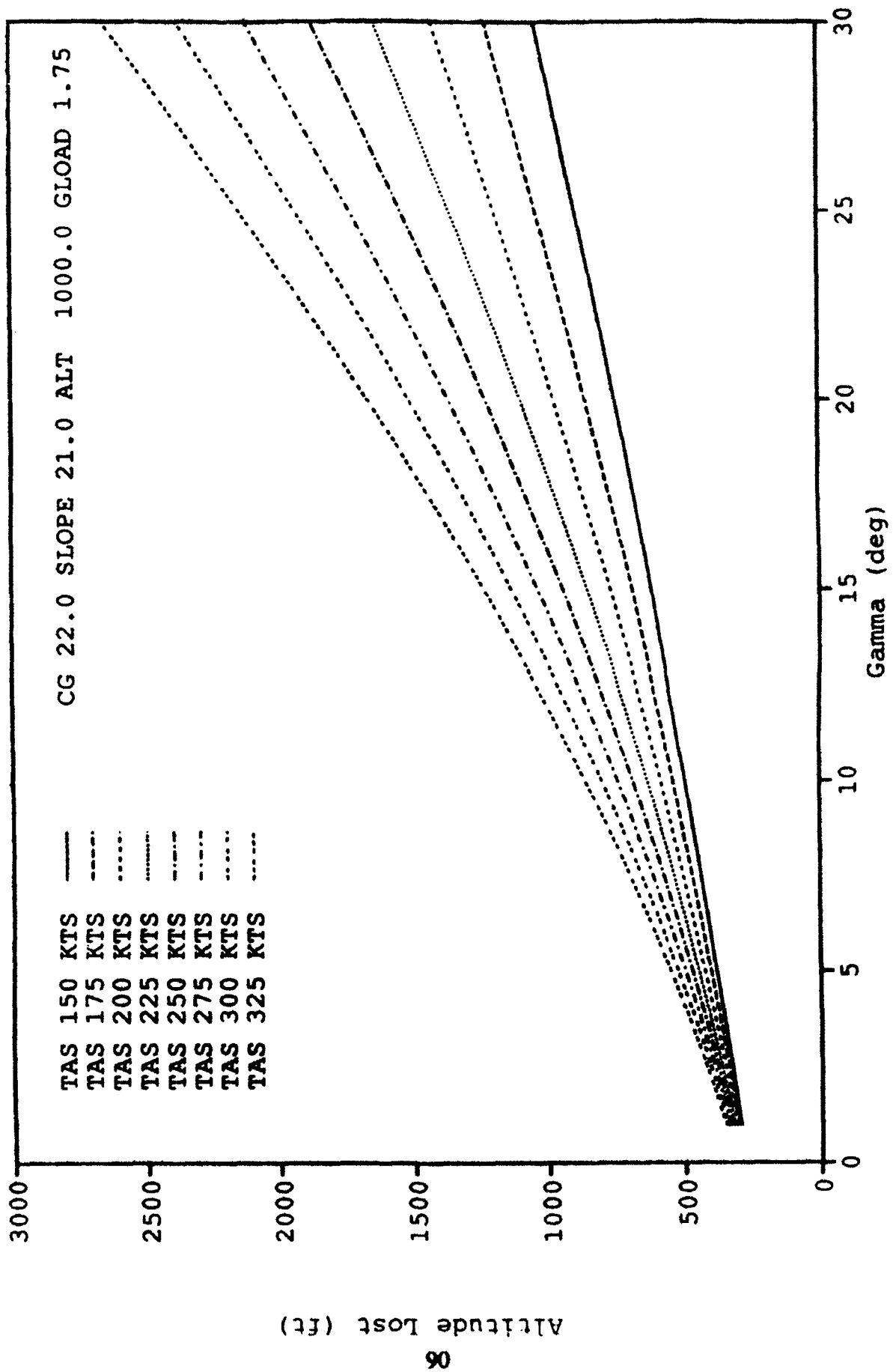


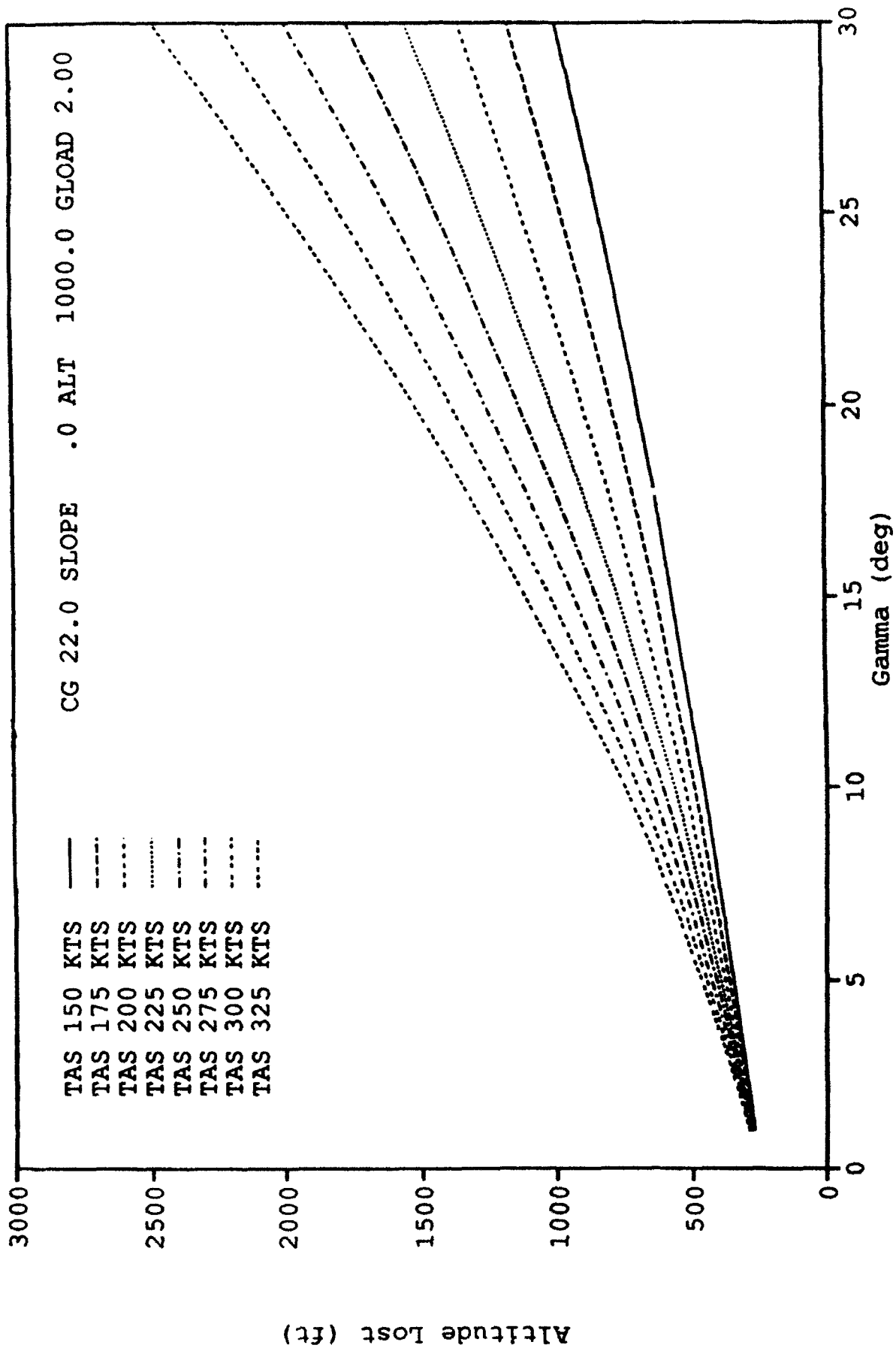


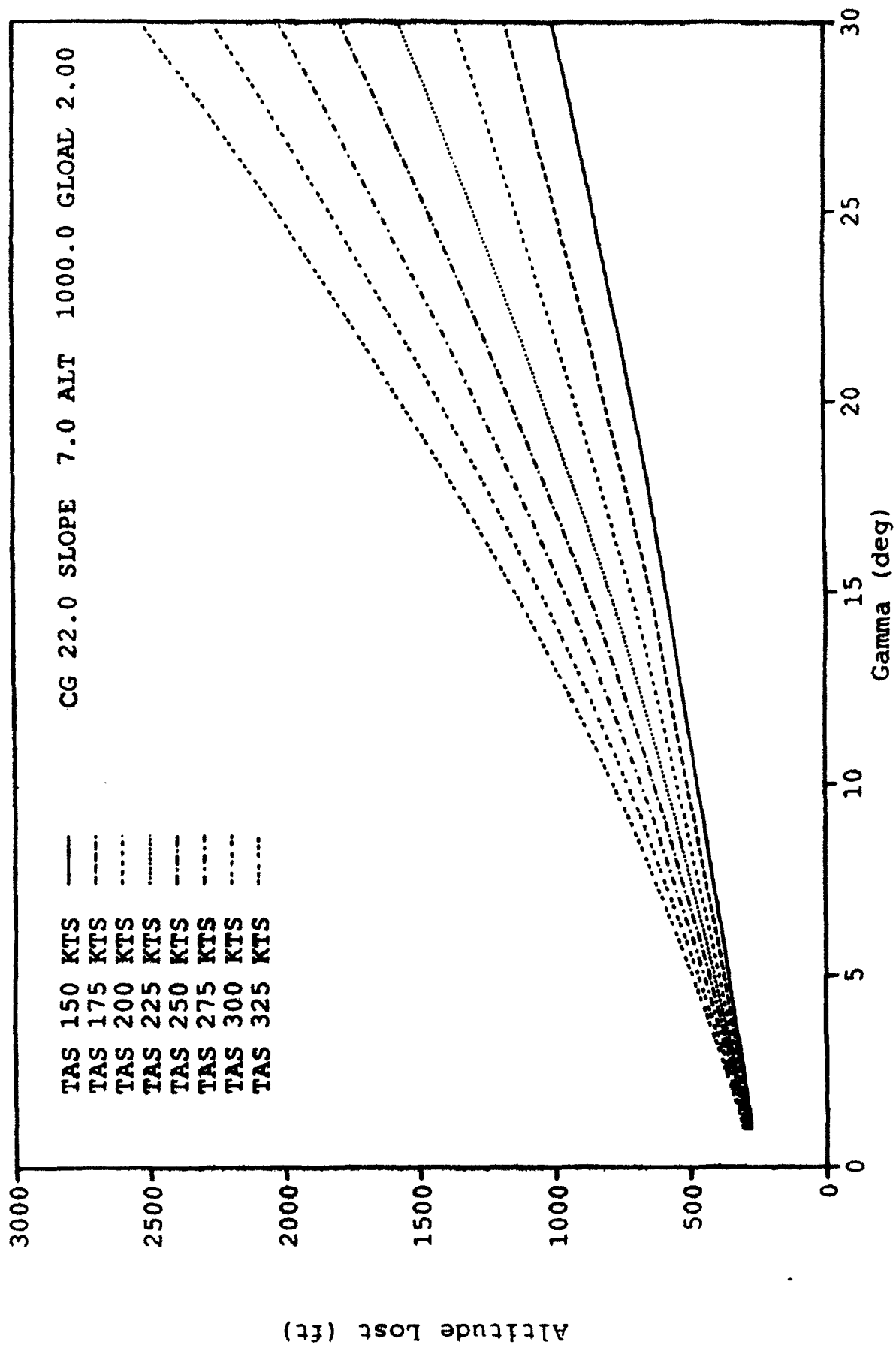


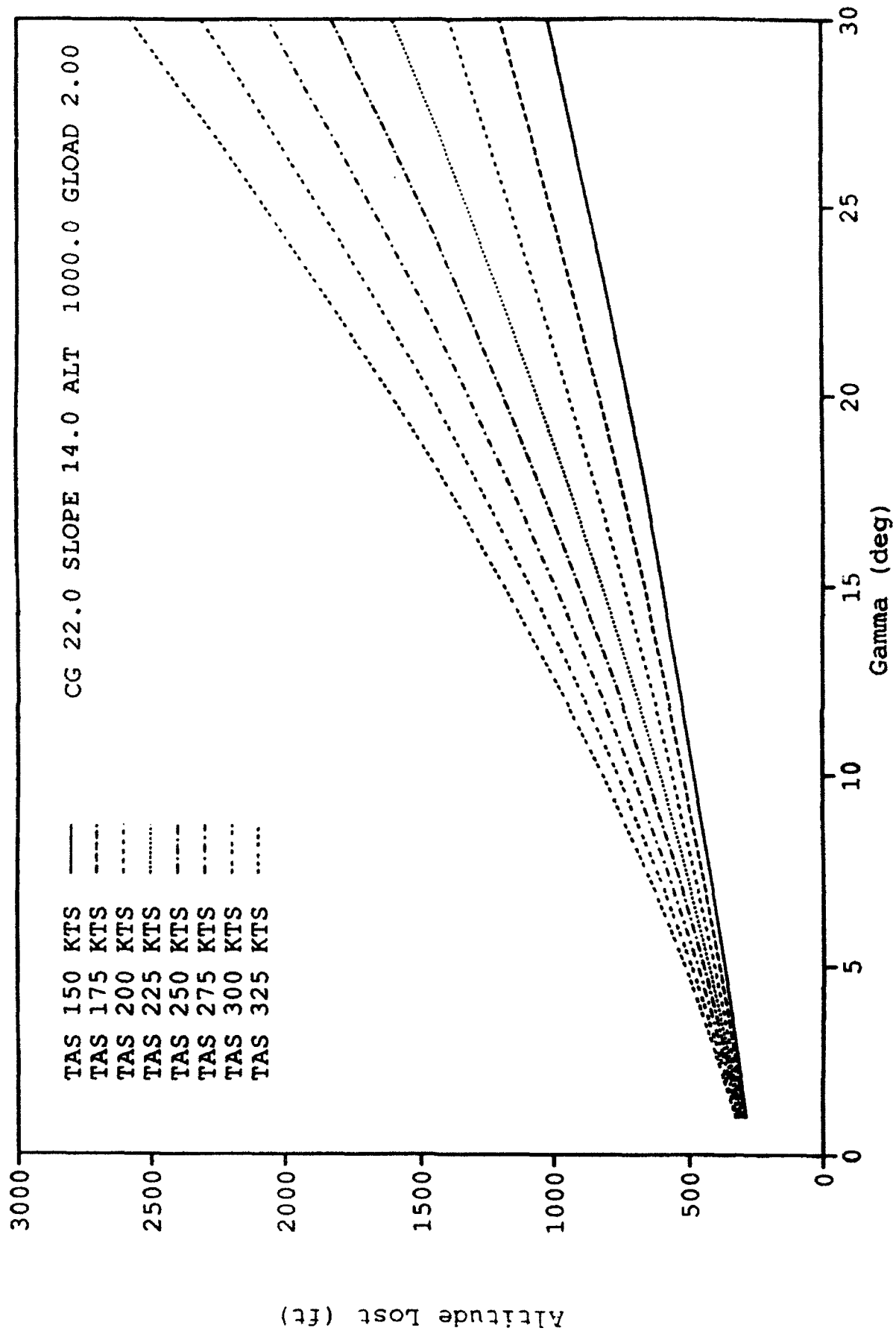


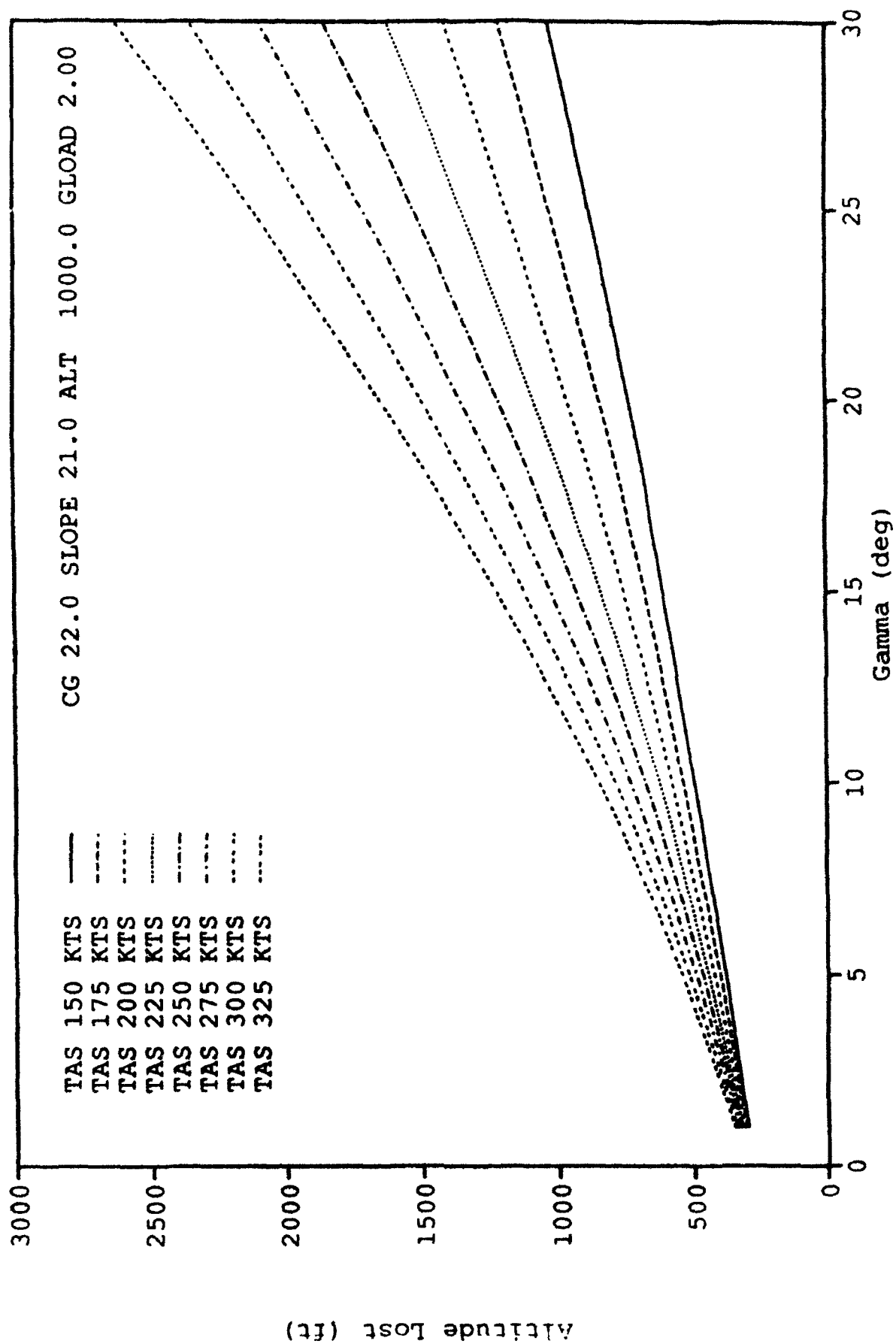




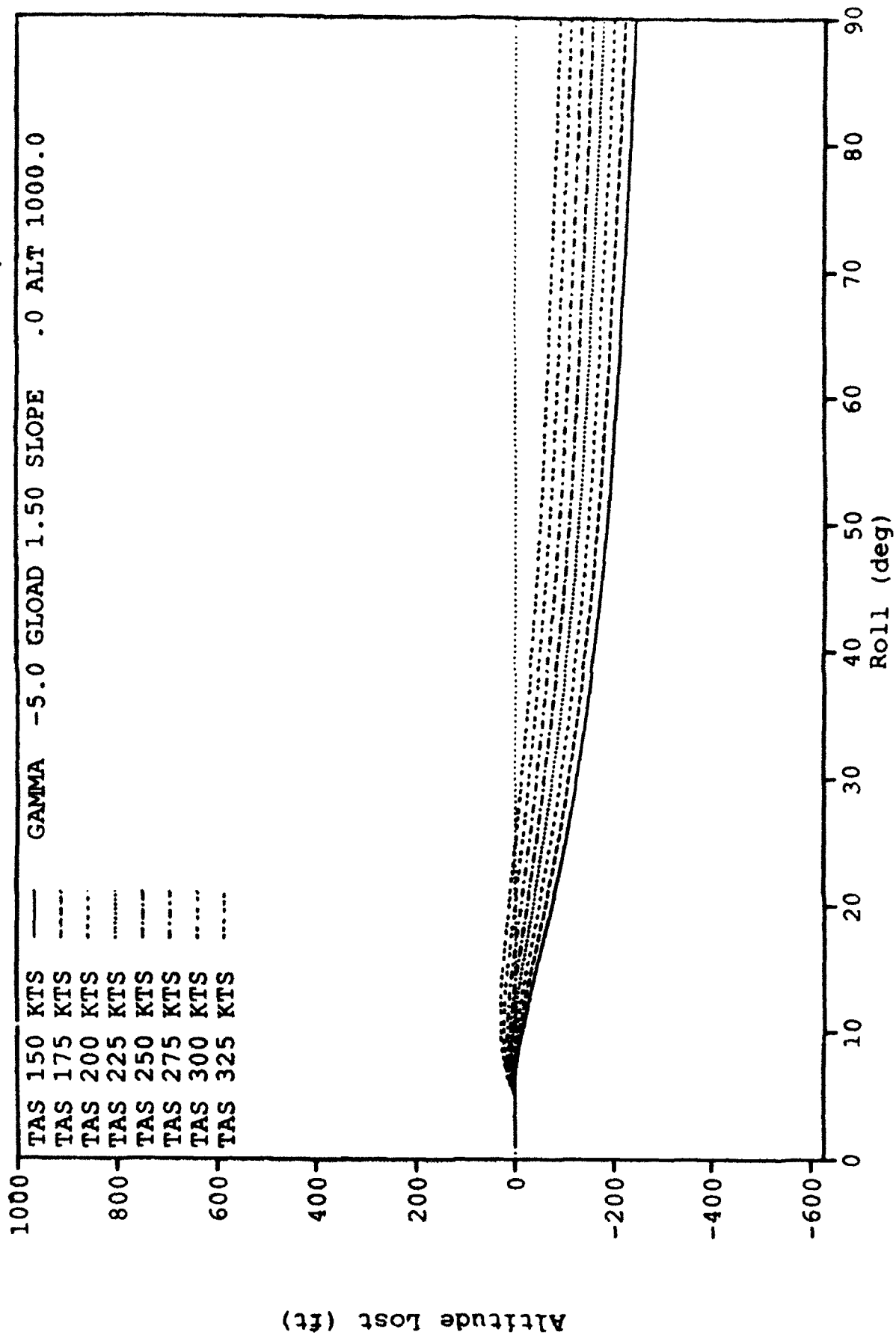


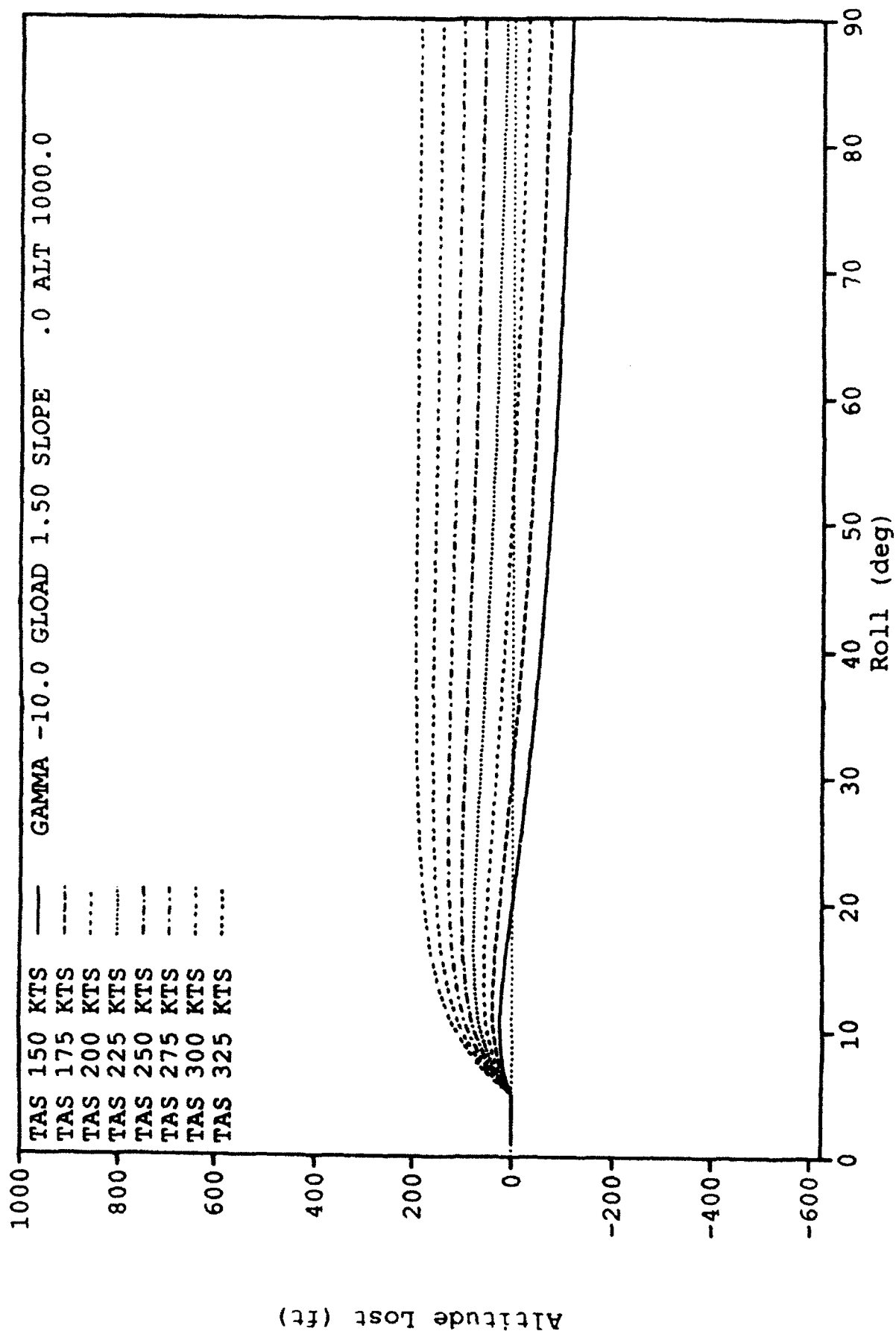


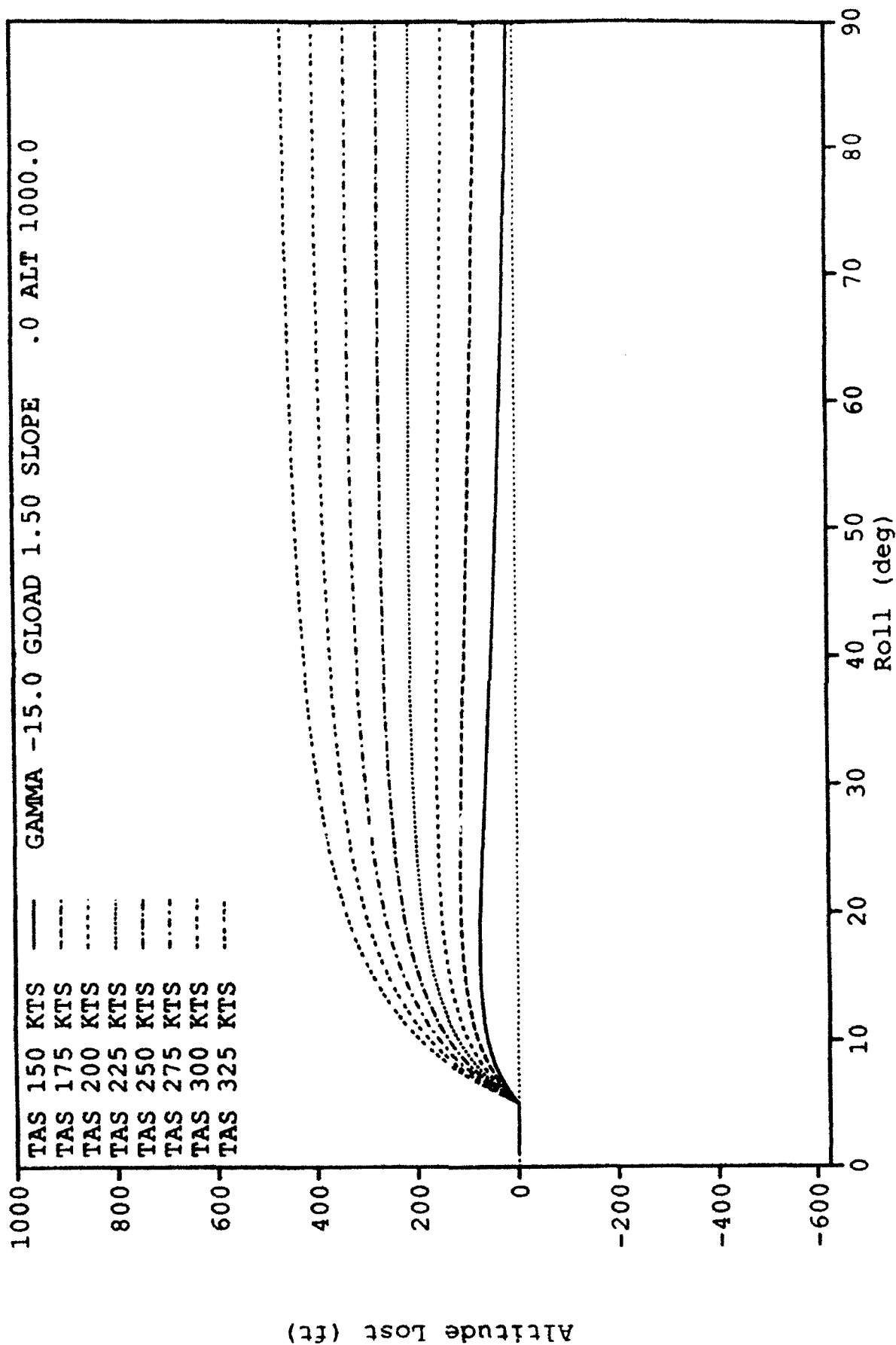


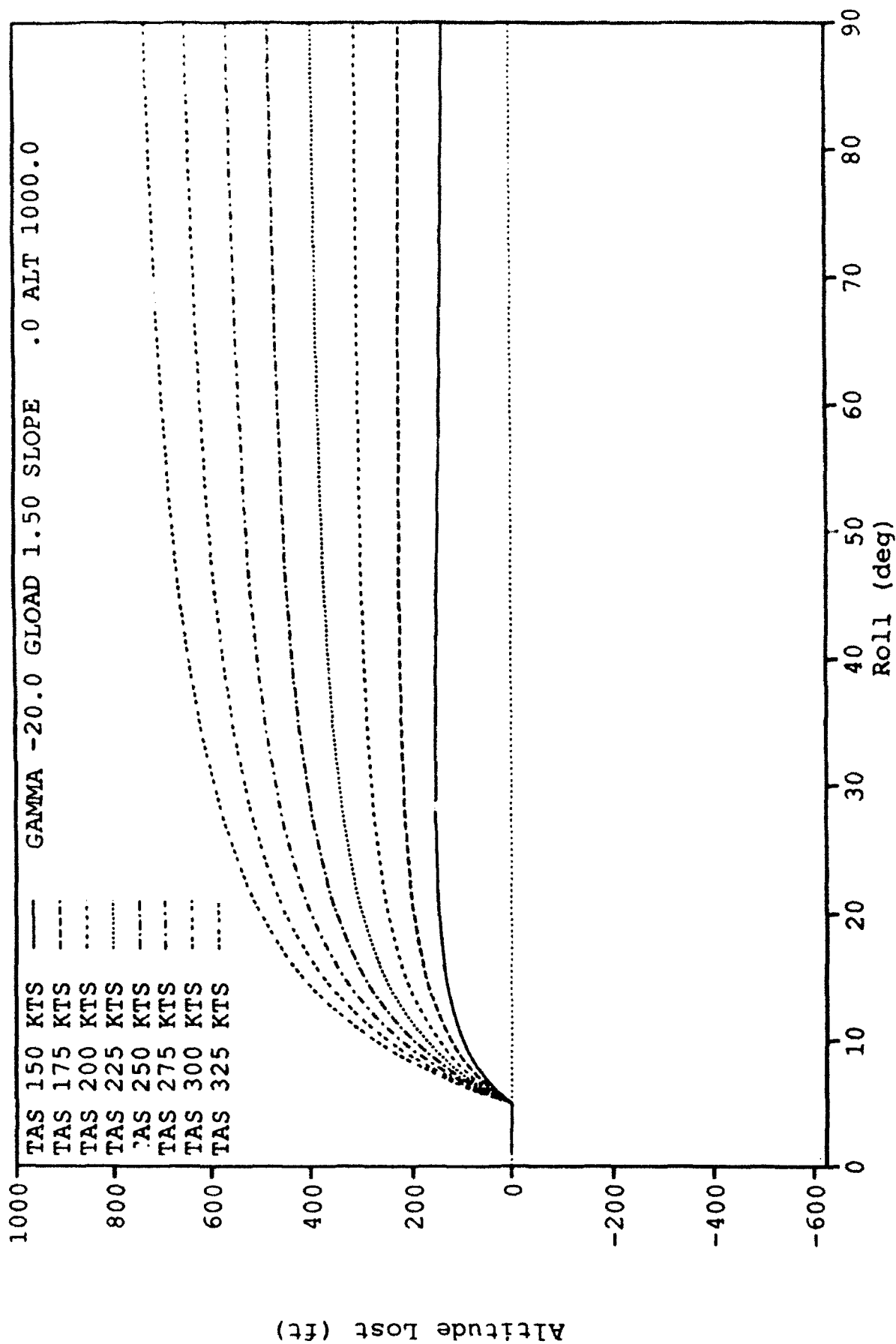


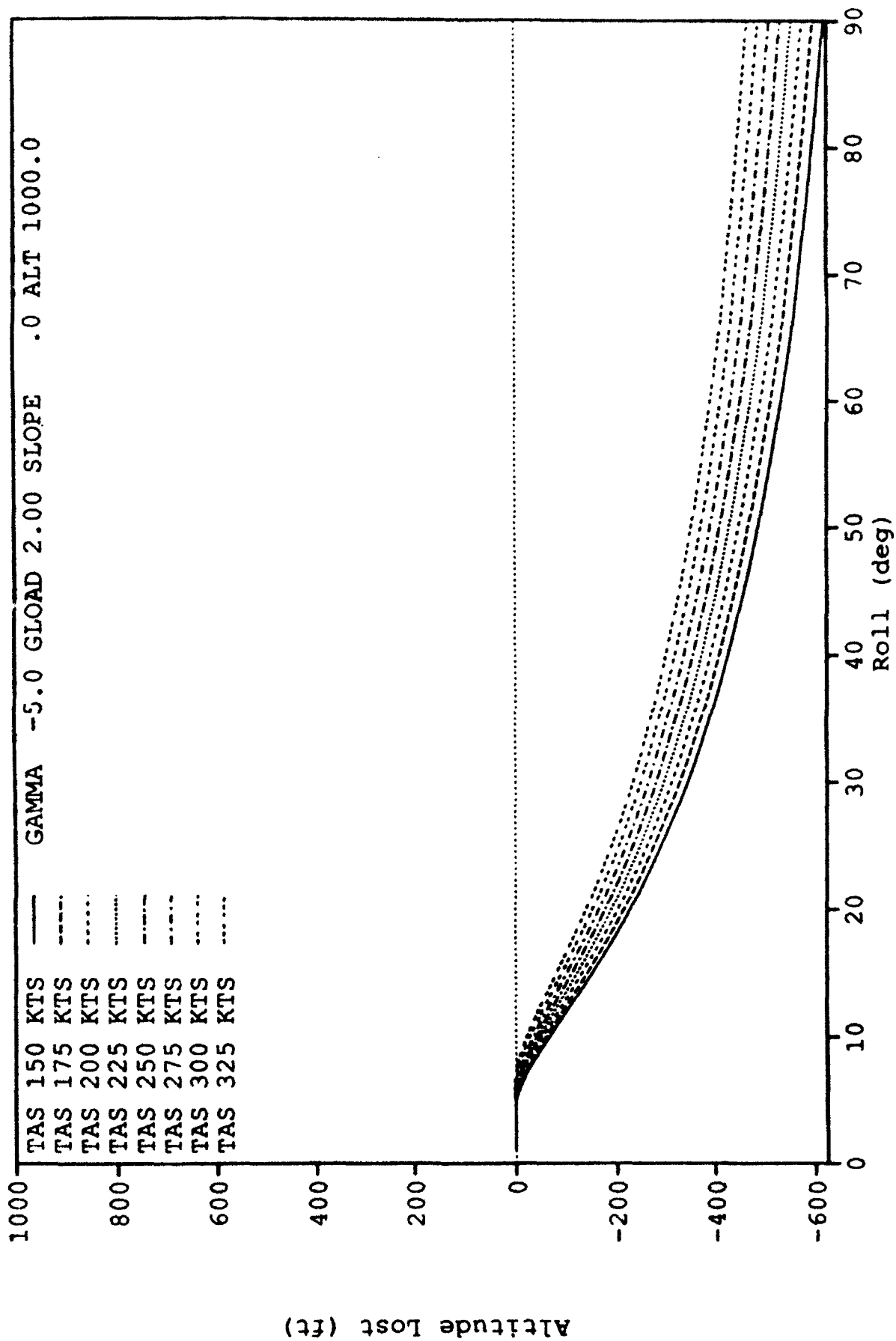
Appendix C
PHASE I
GCASROLL GRAPHS

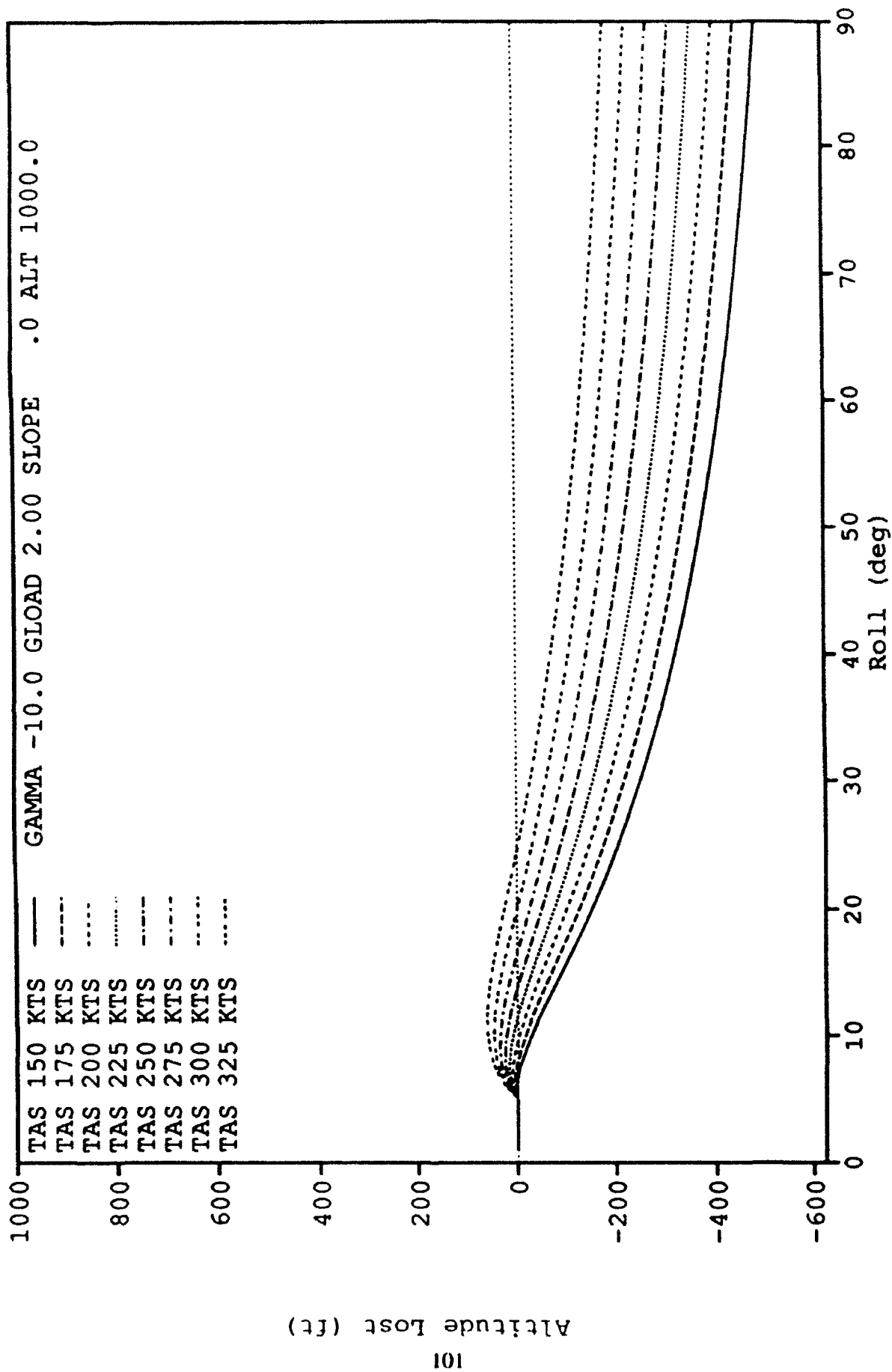


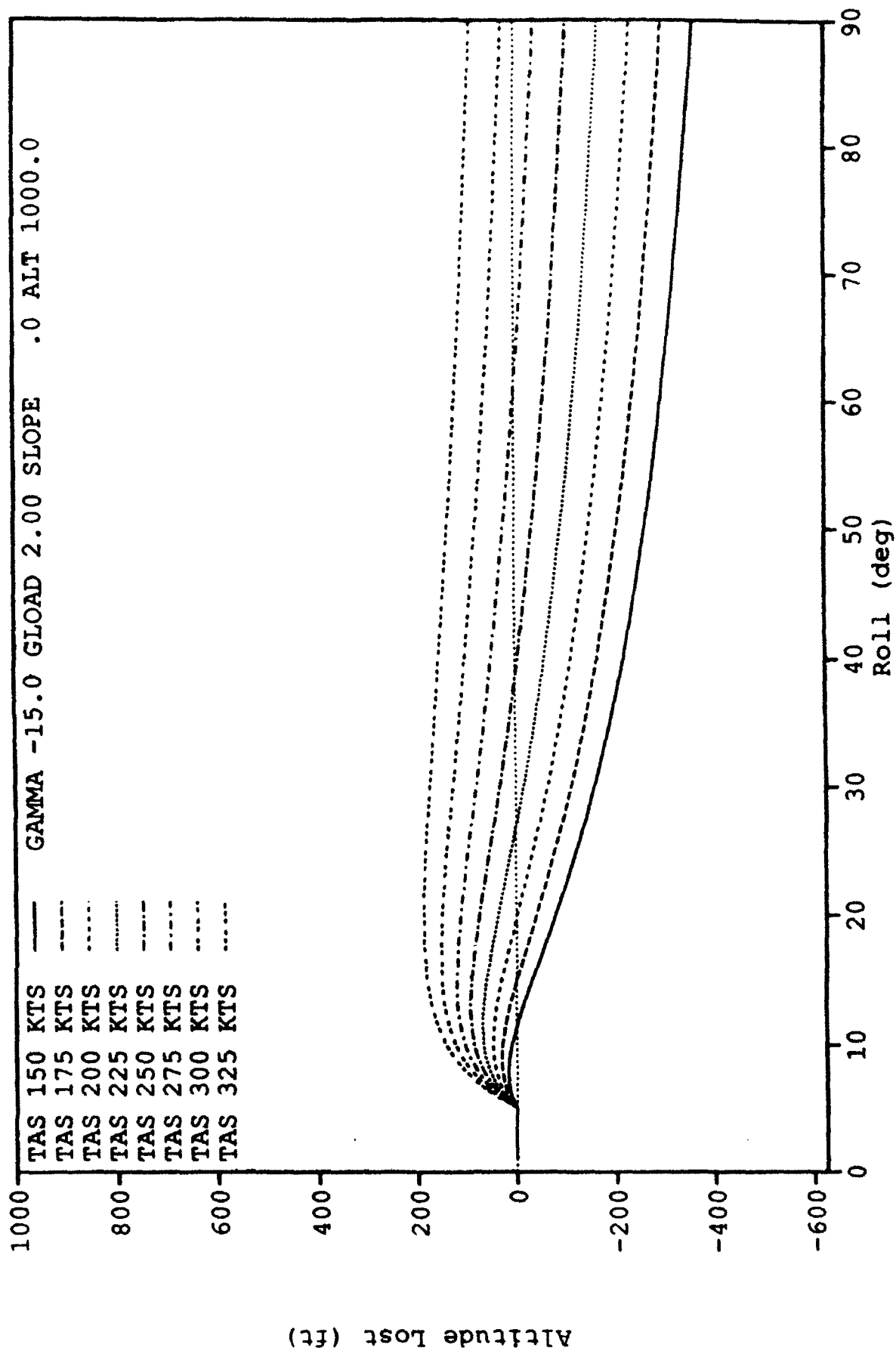


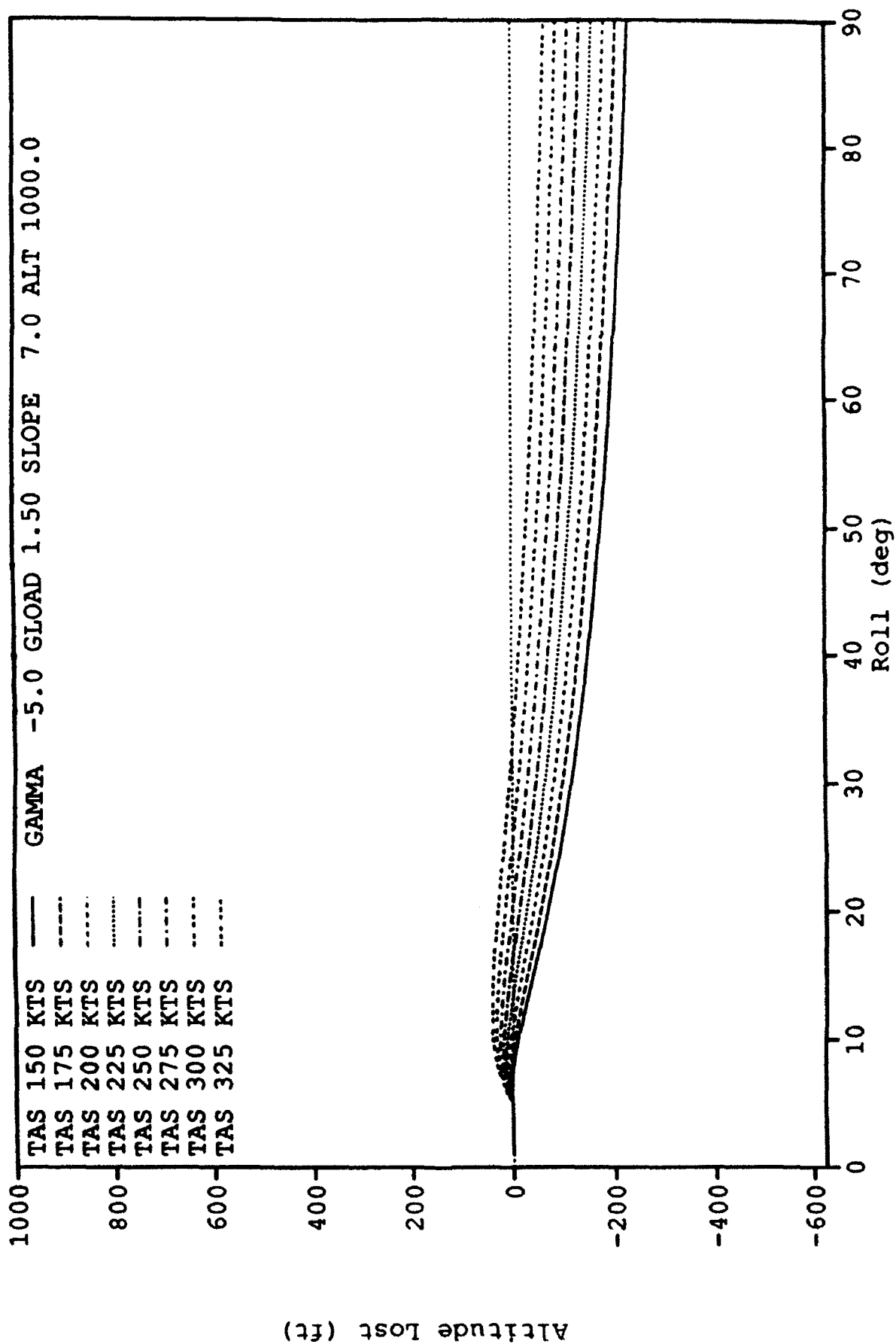


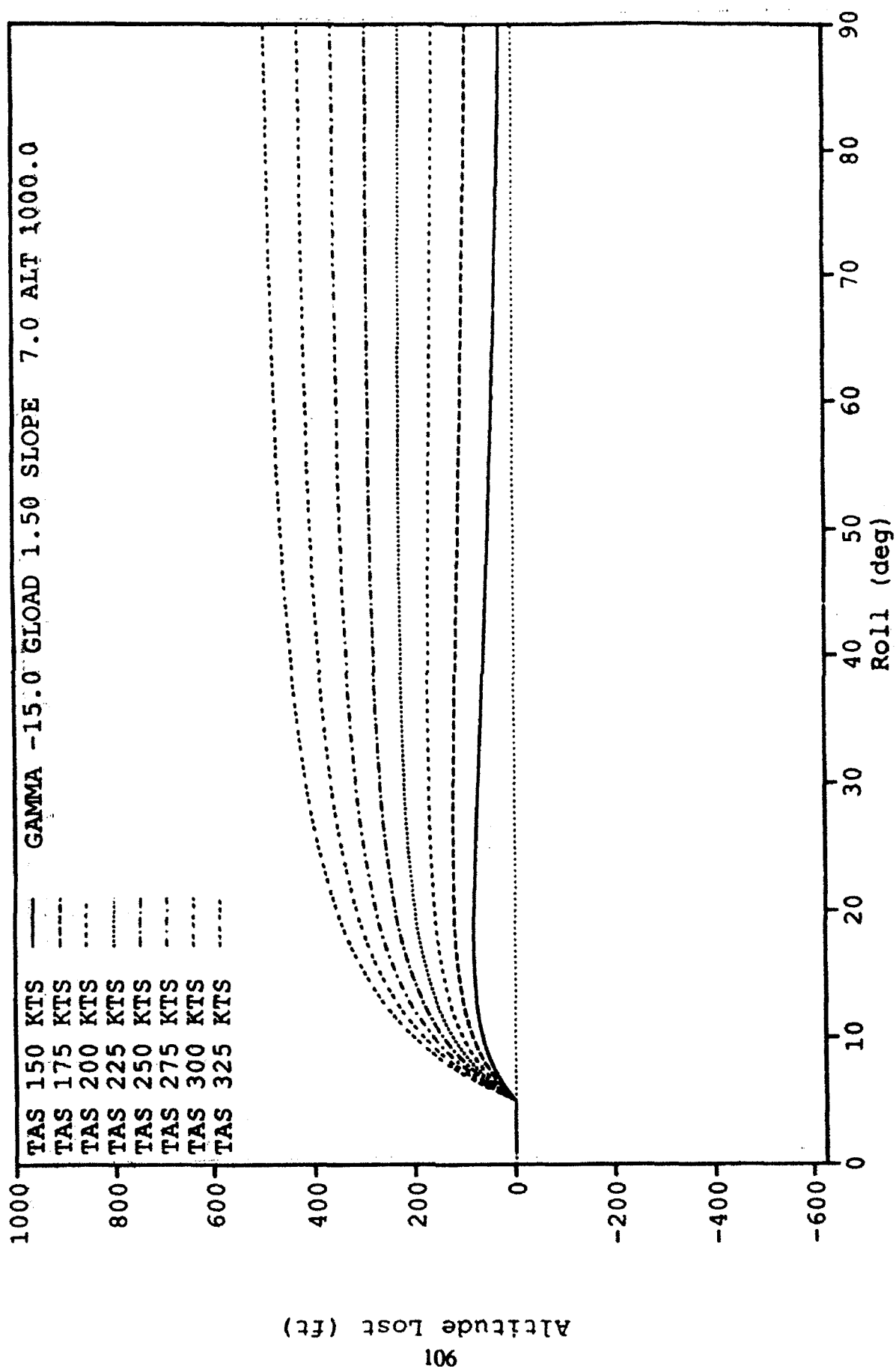


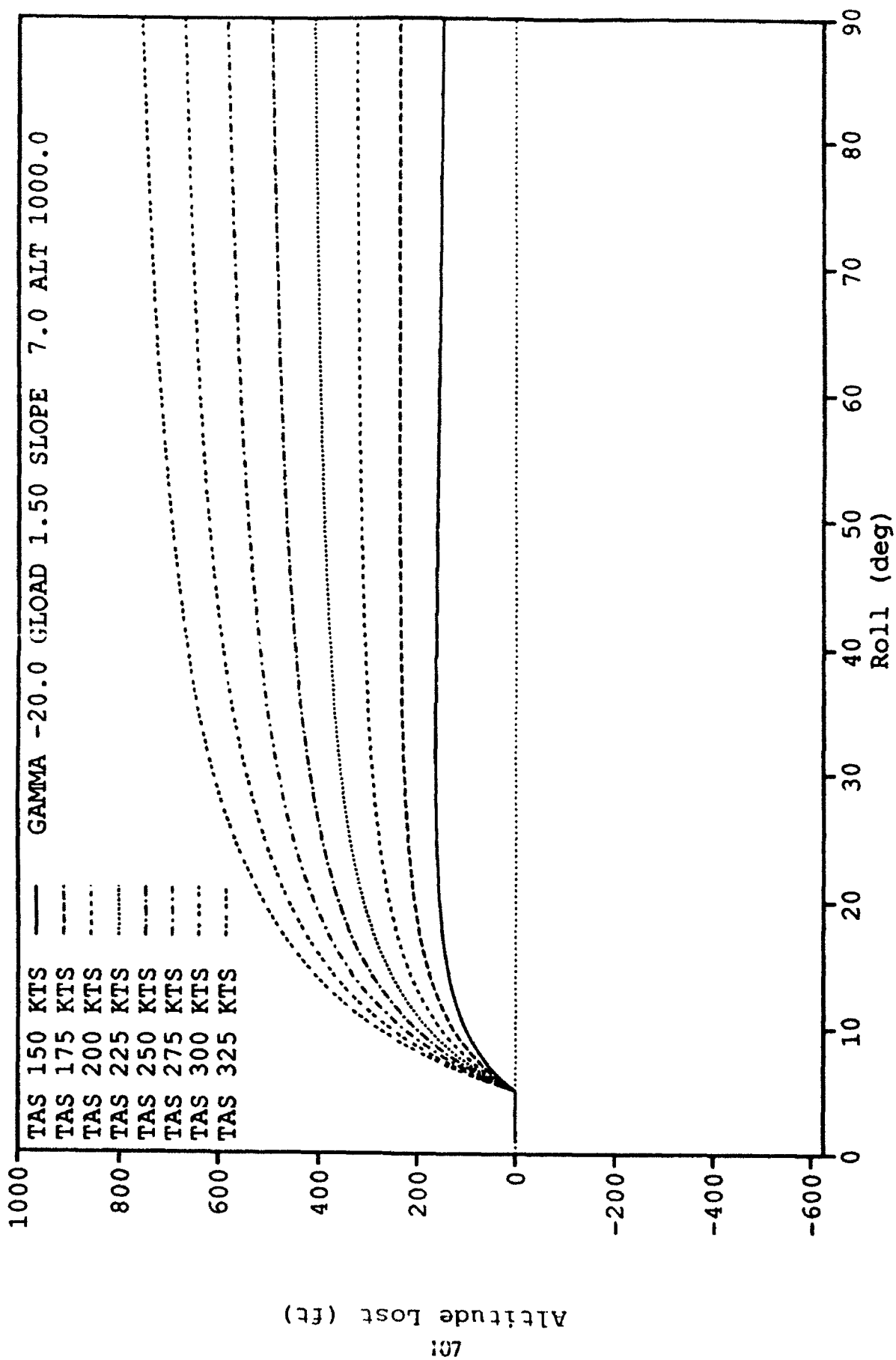


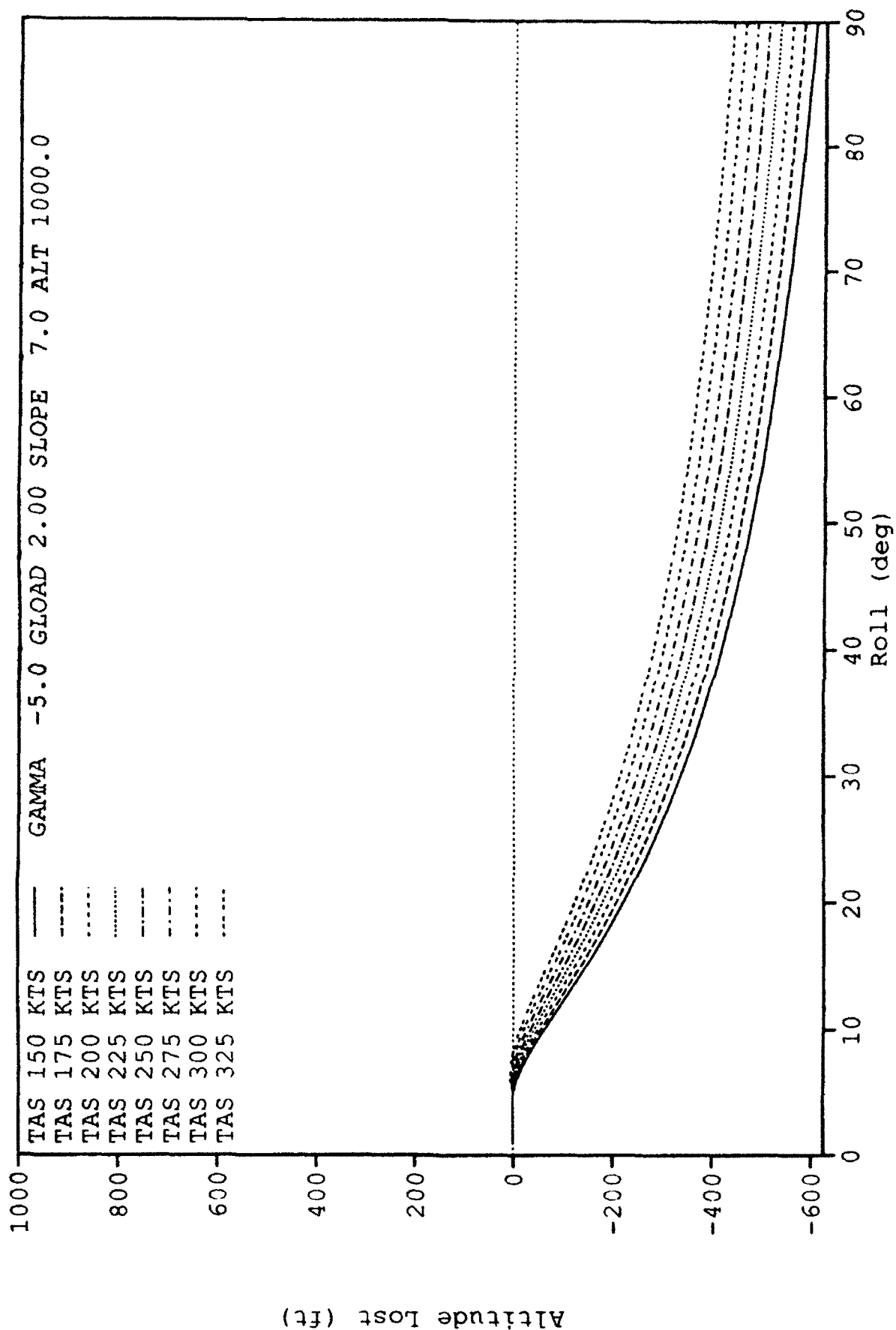


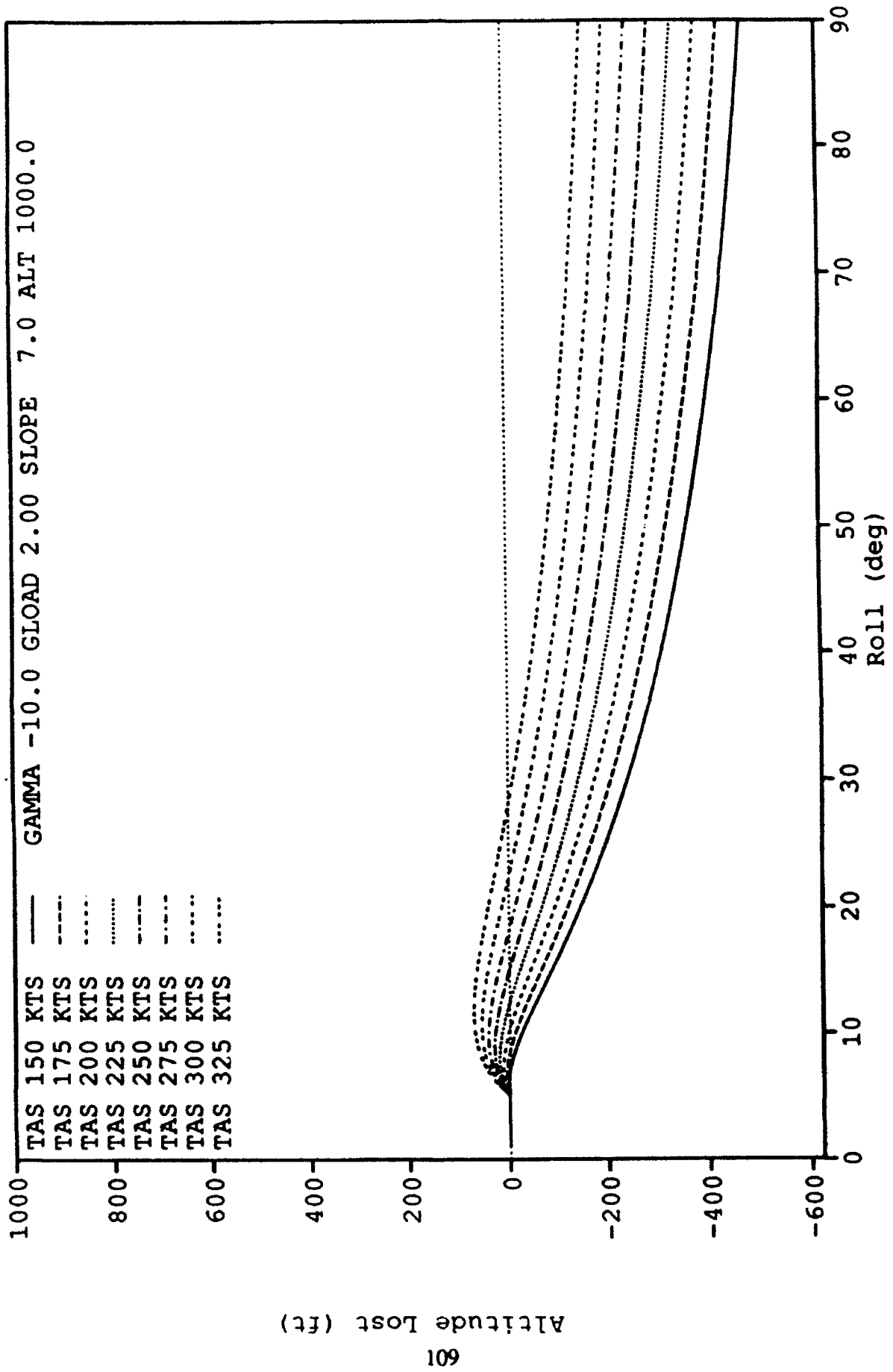


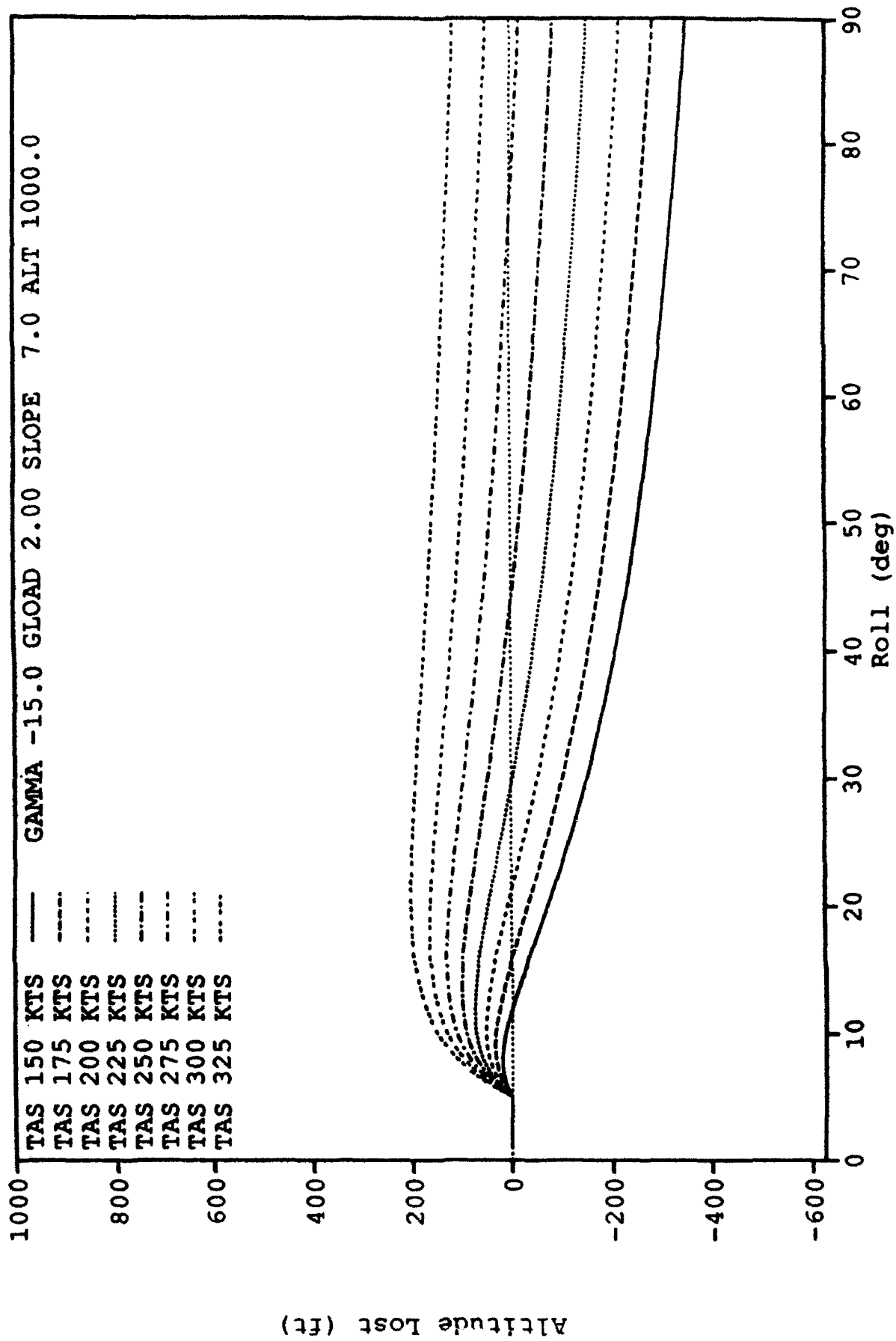


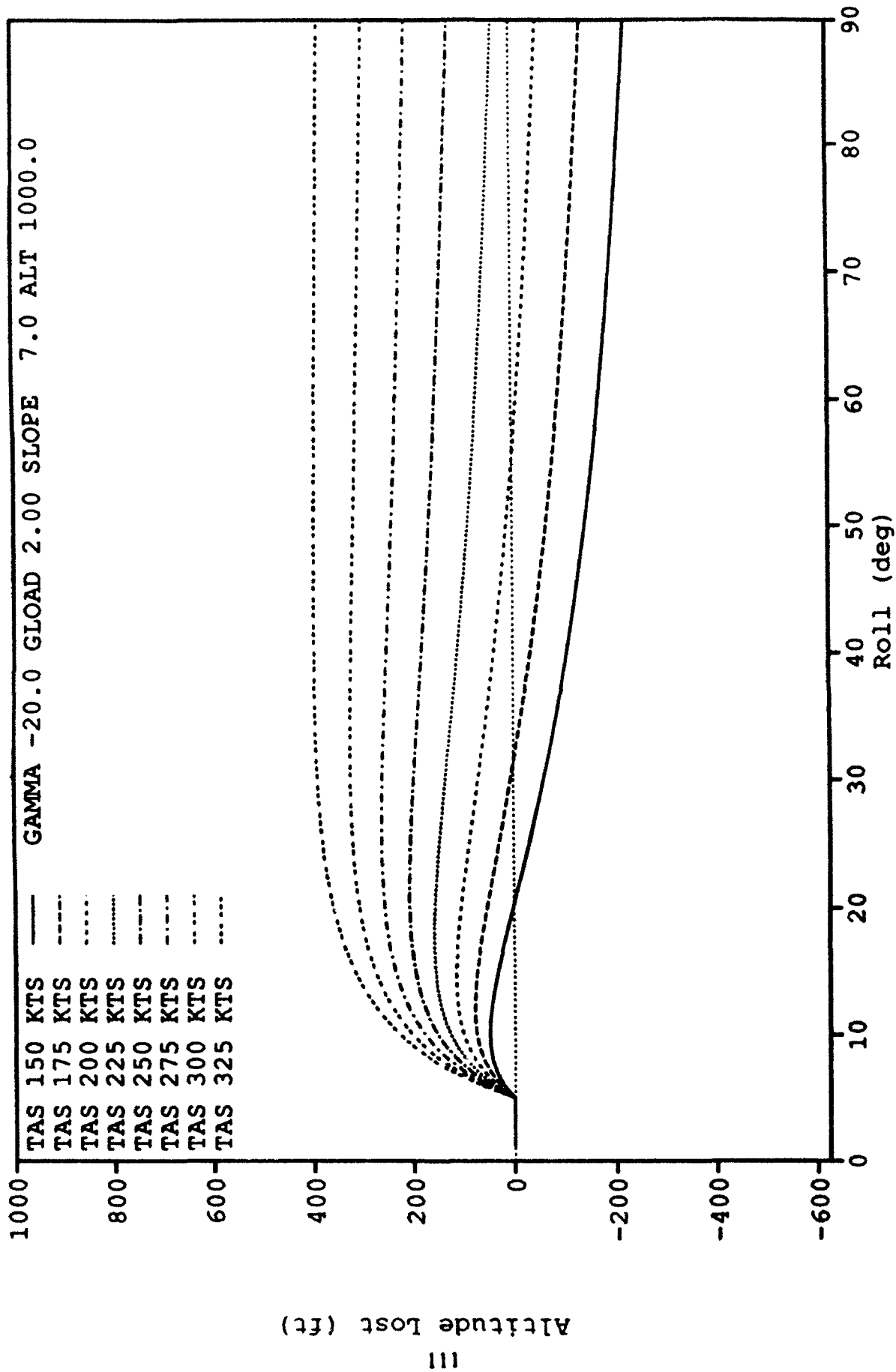


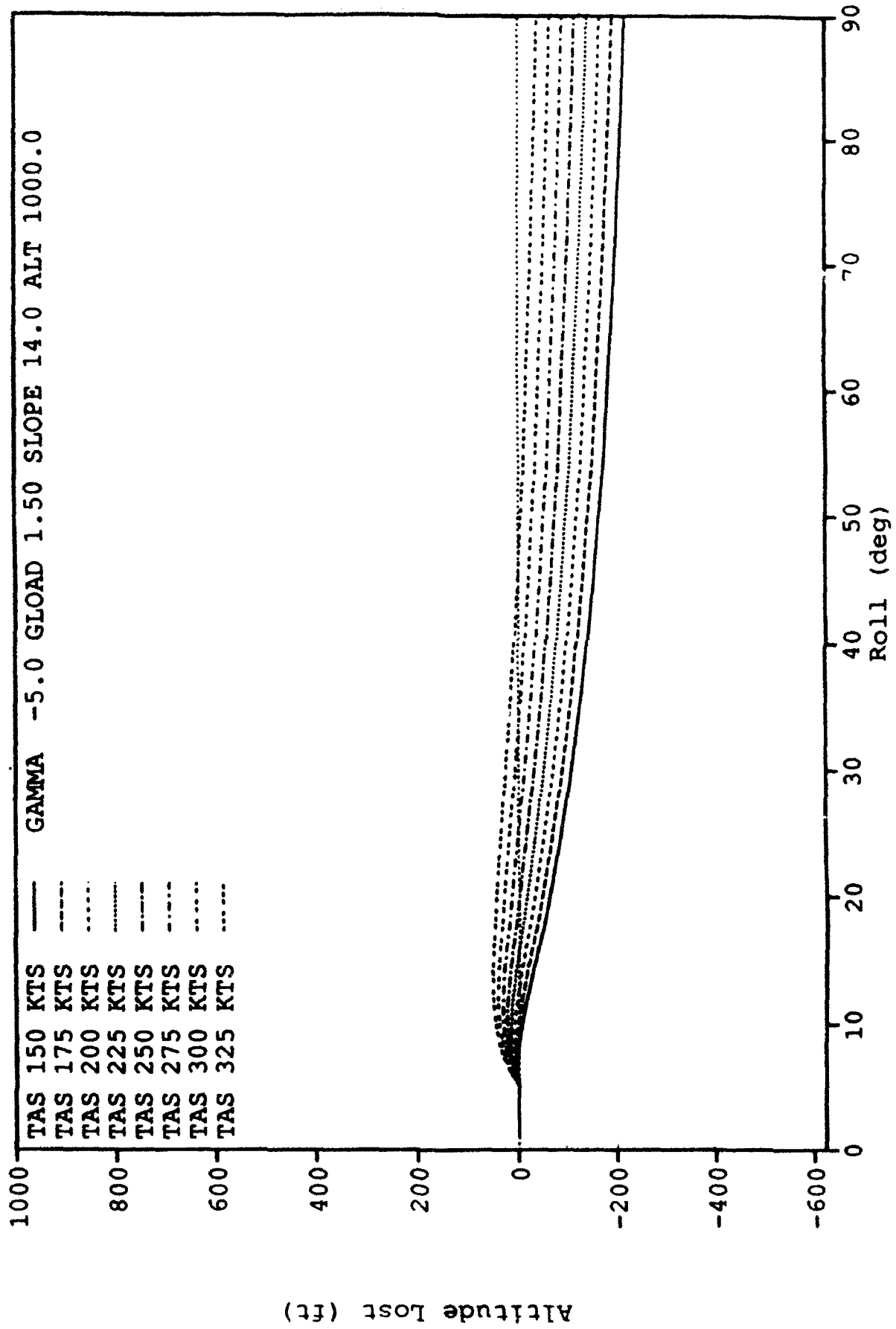


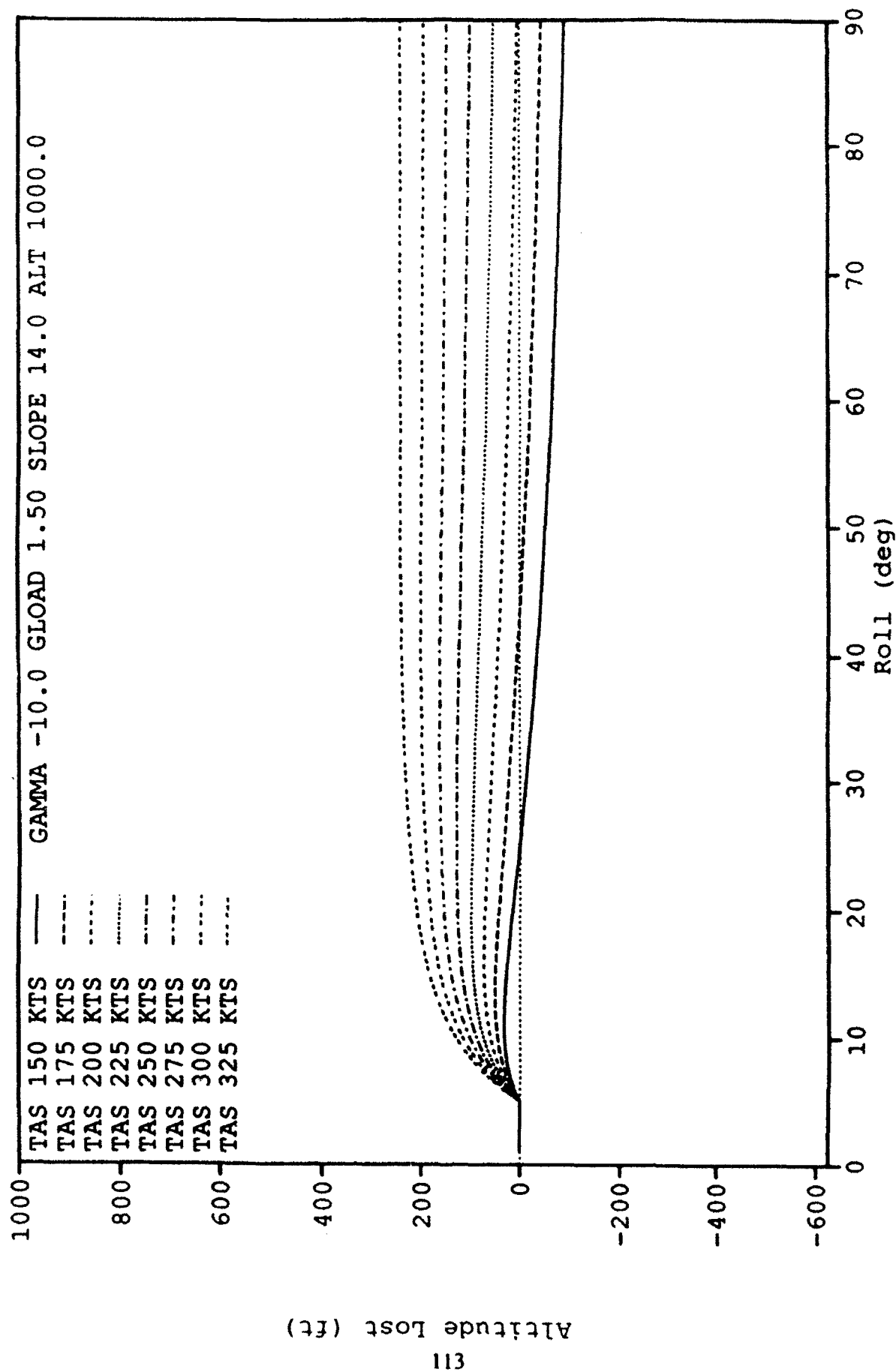


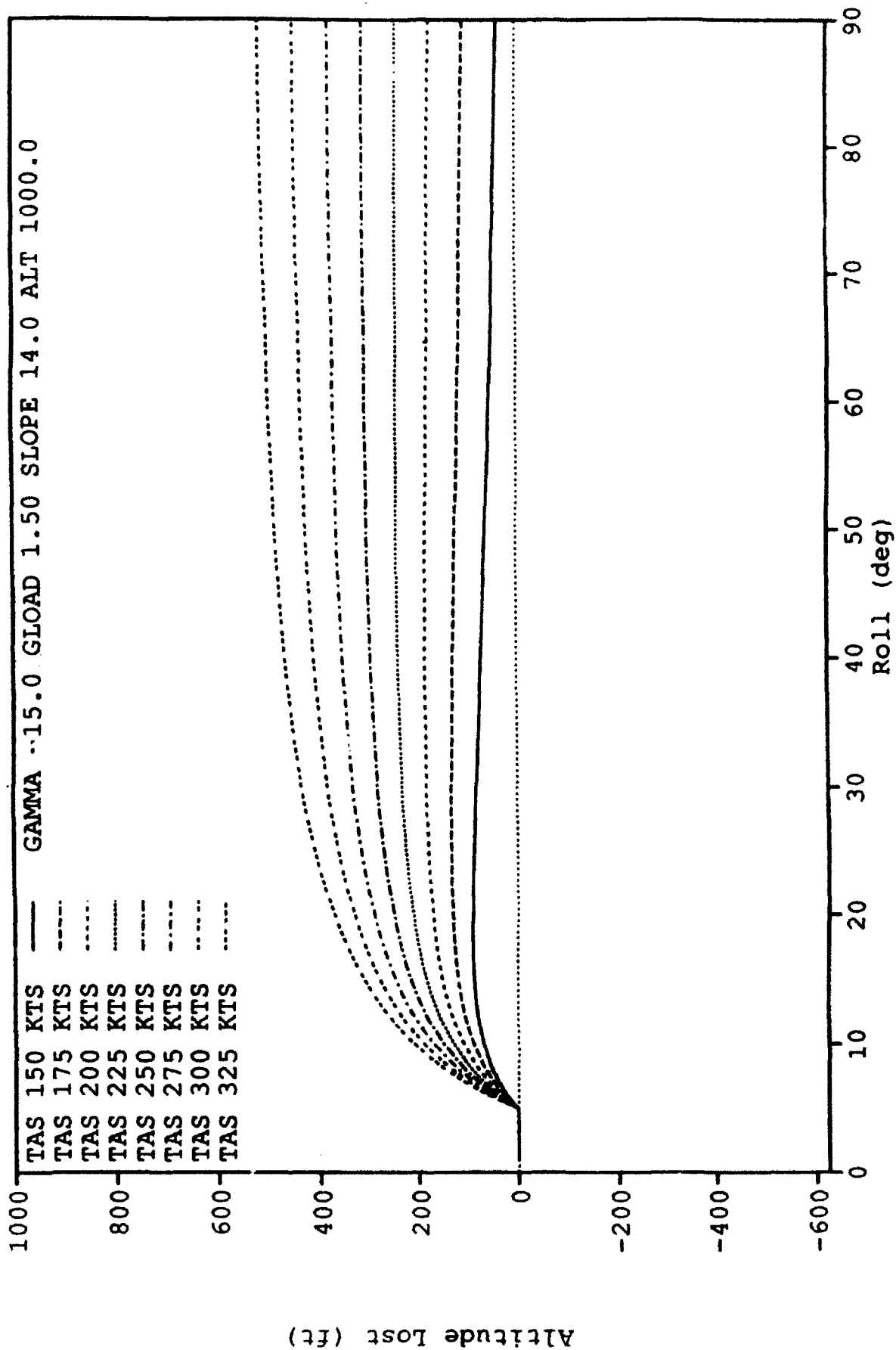


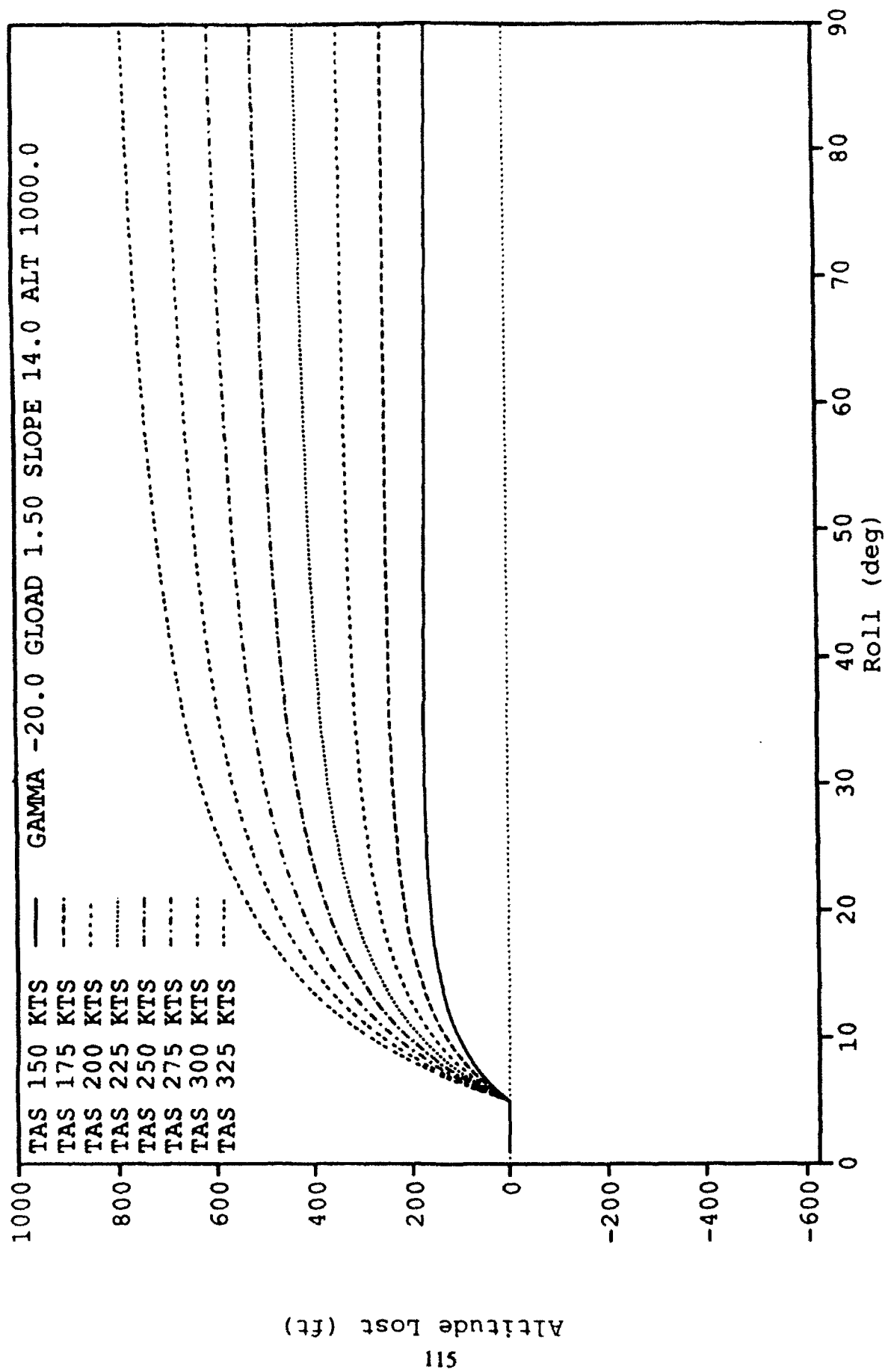


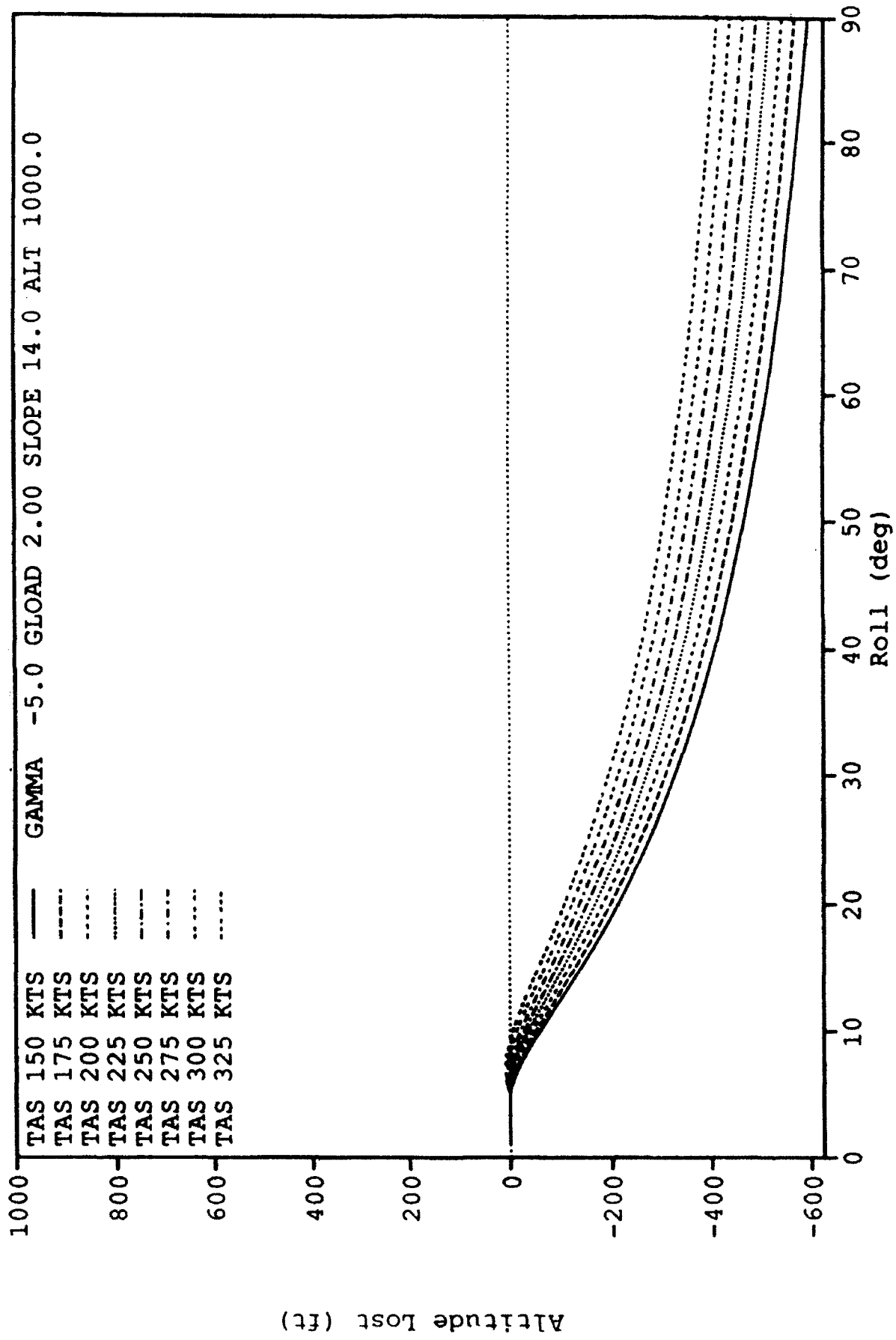


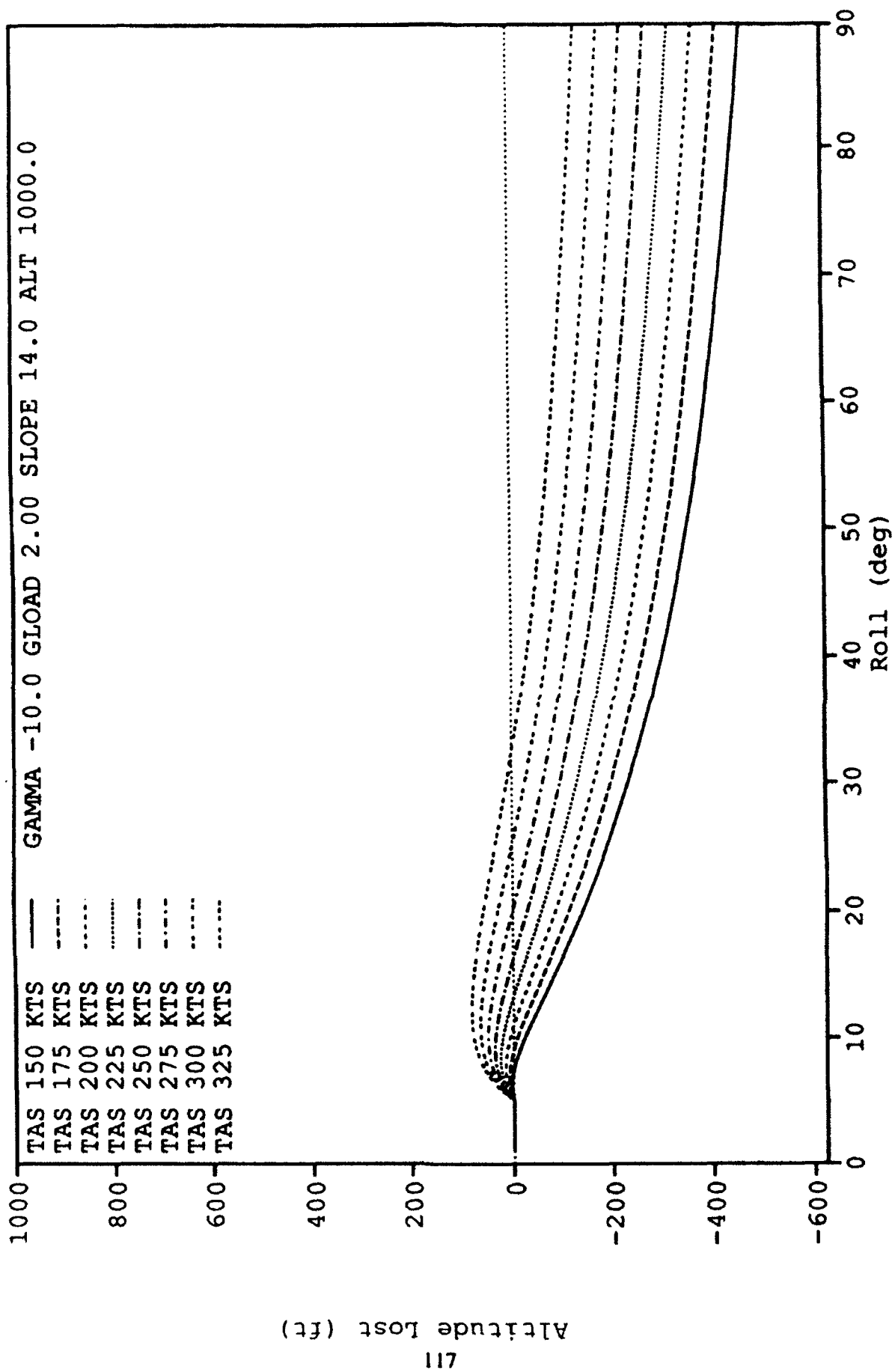


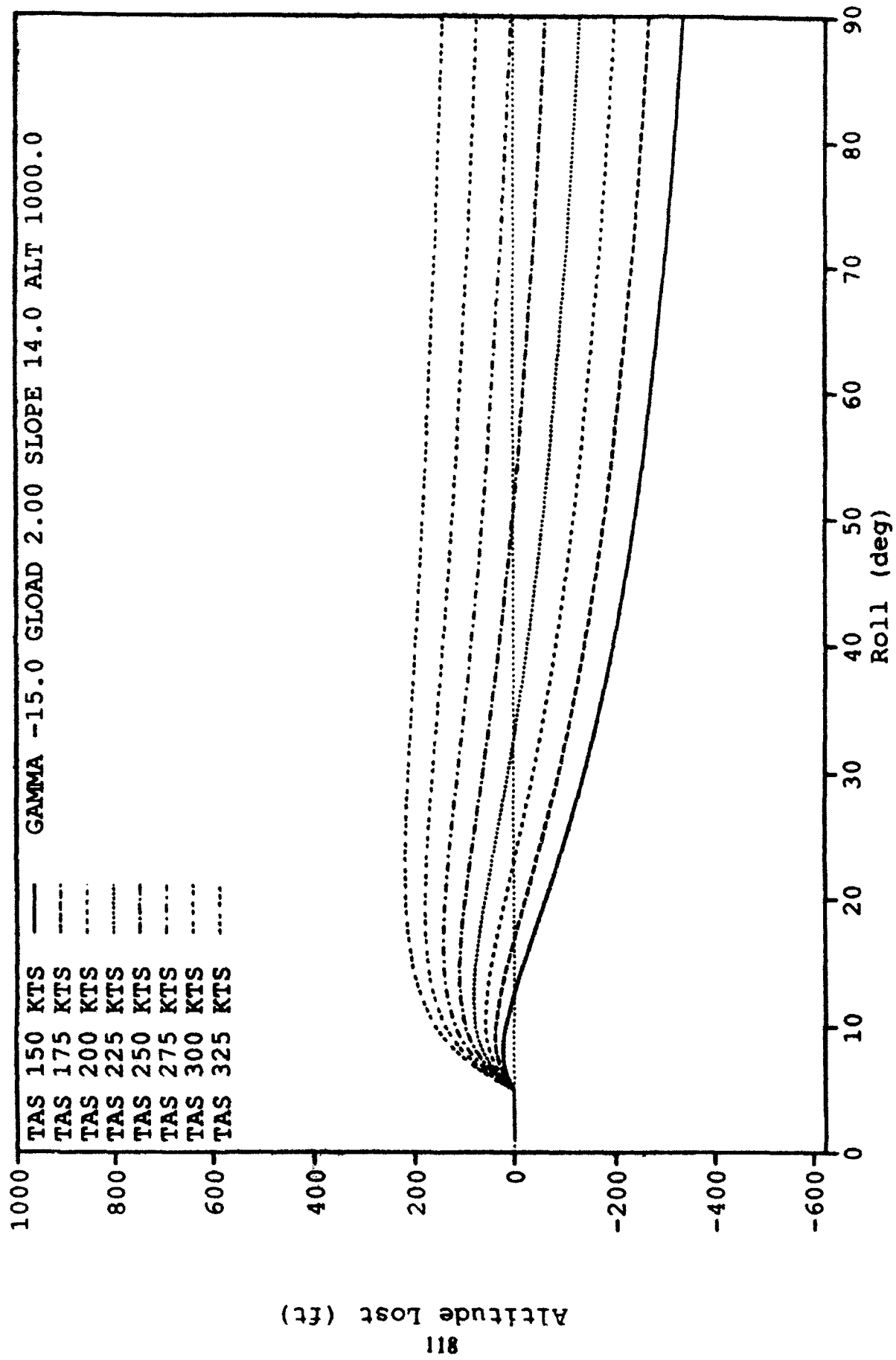


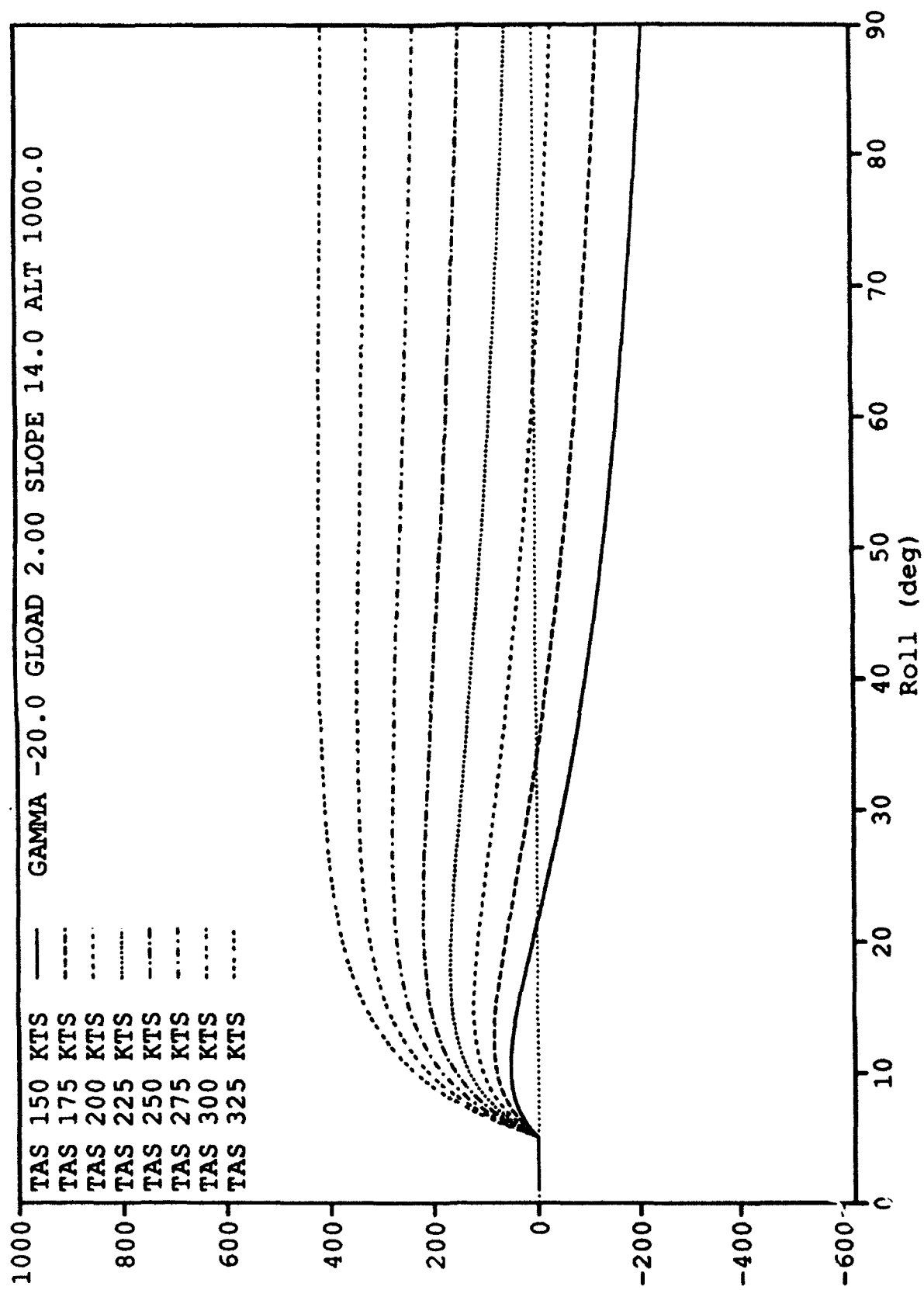


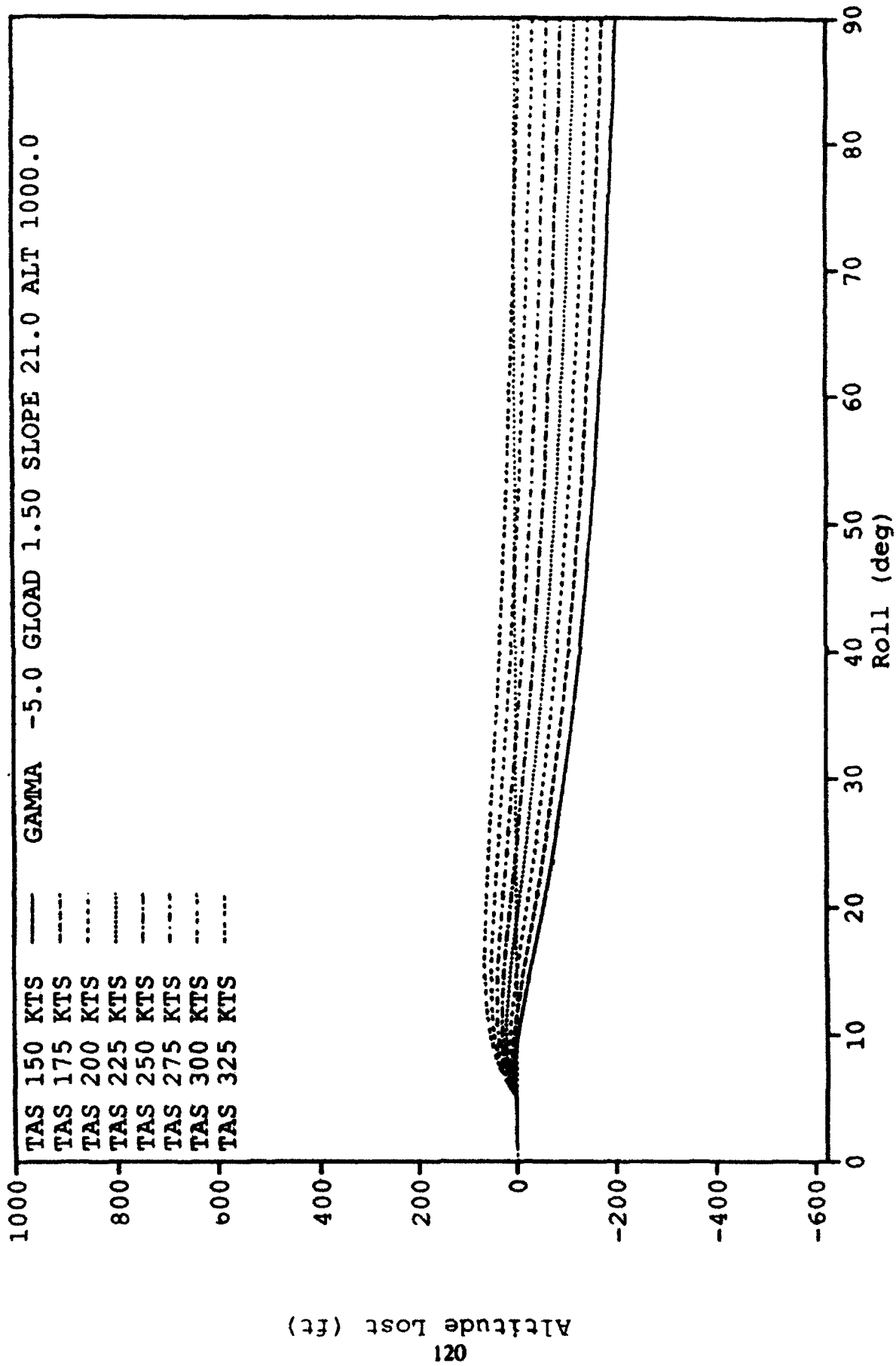


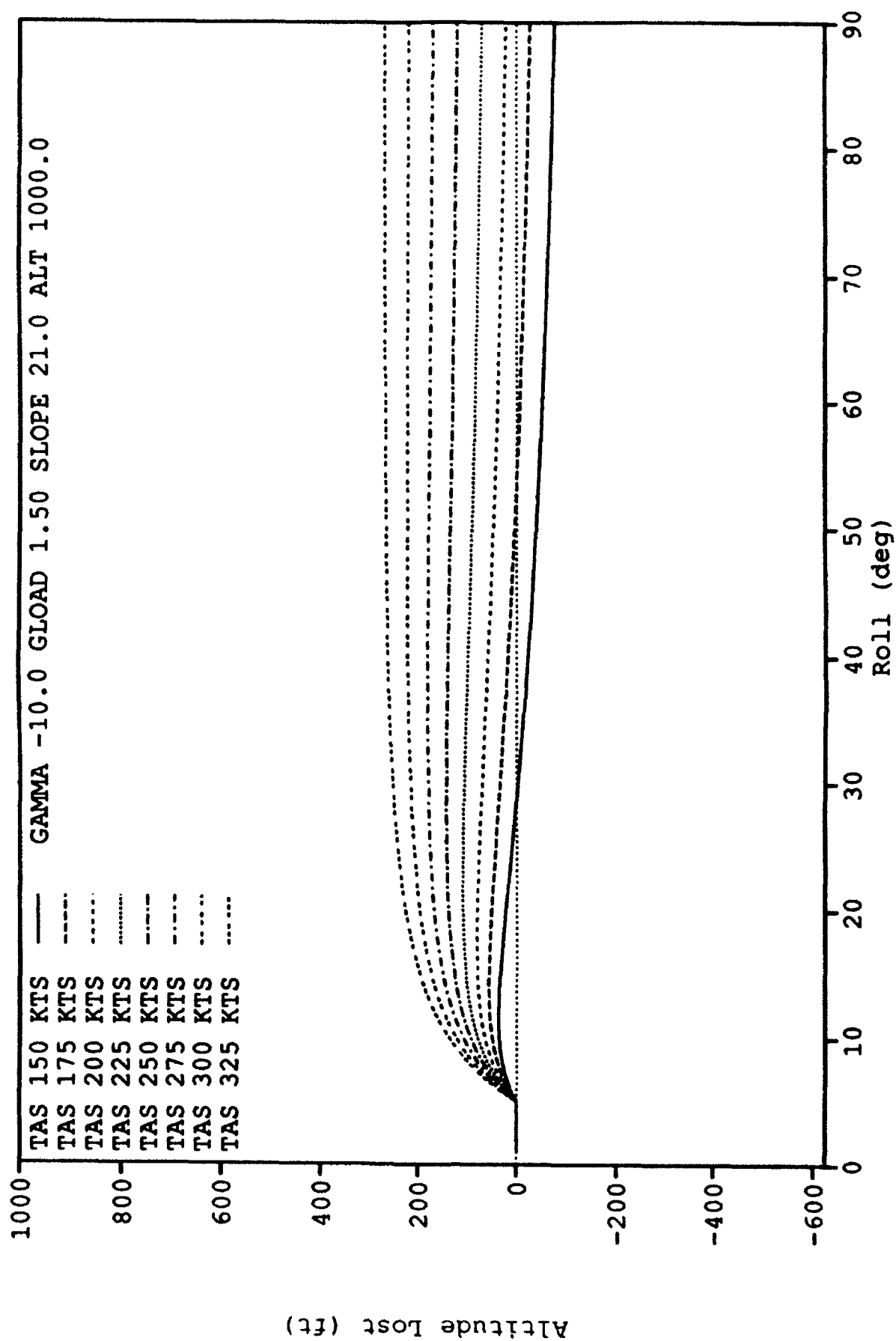


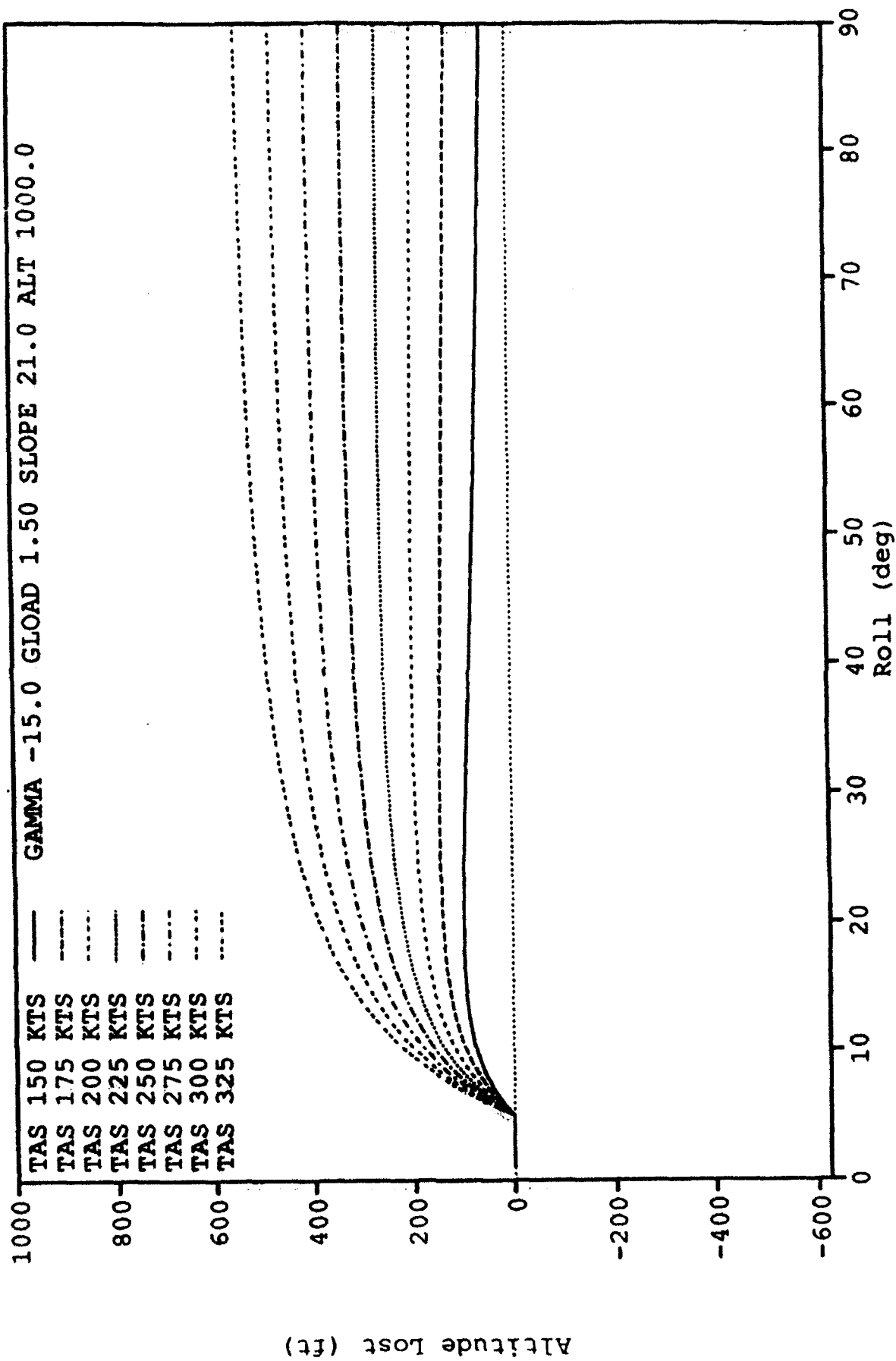


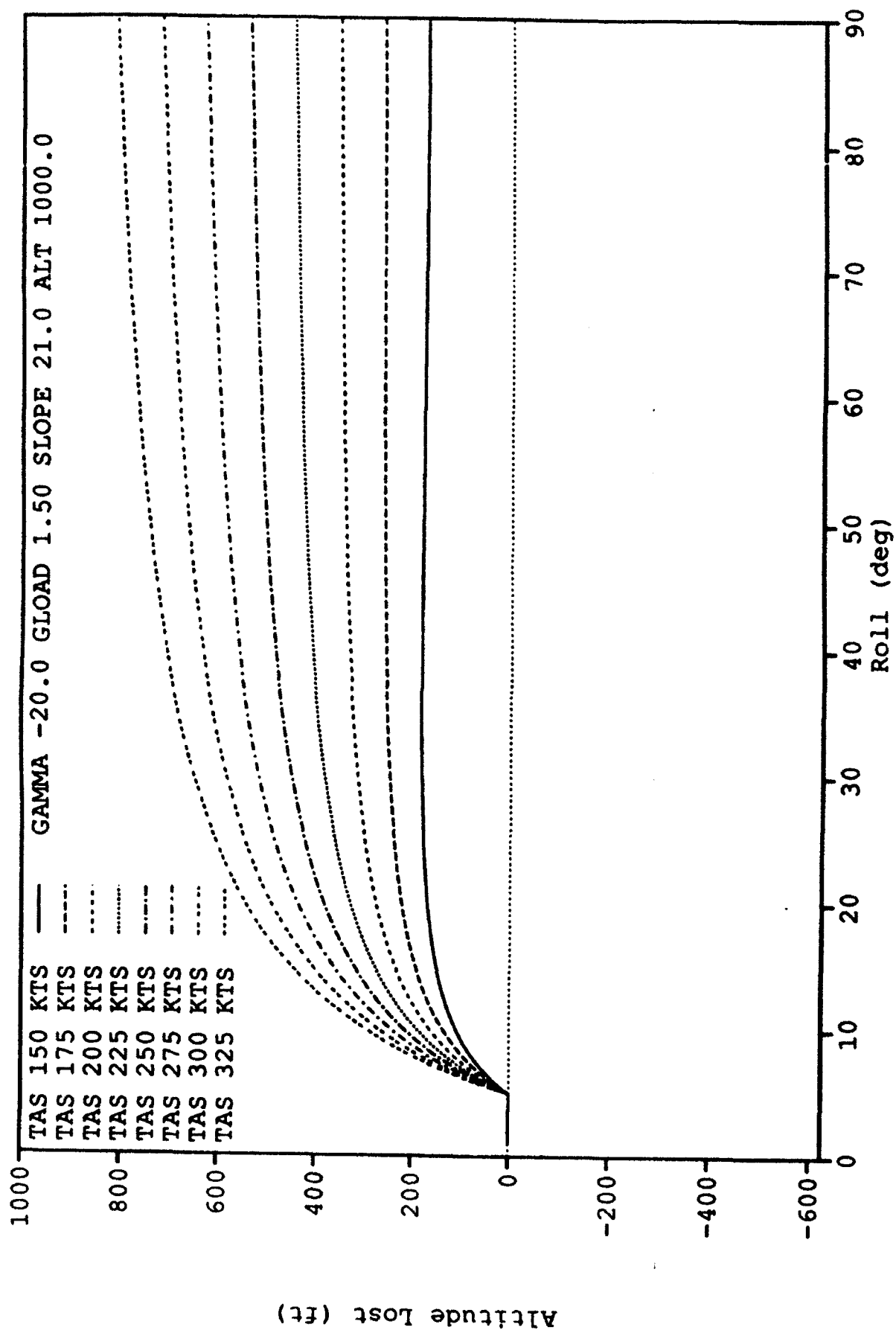


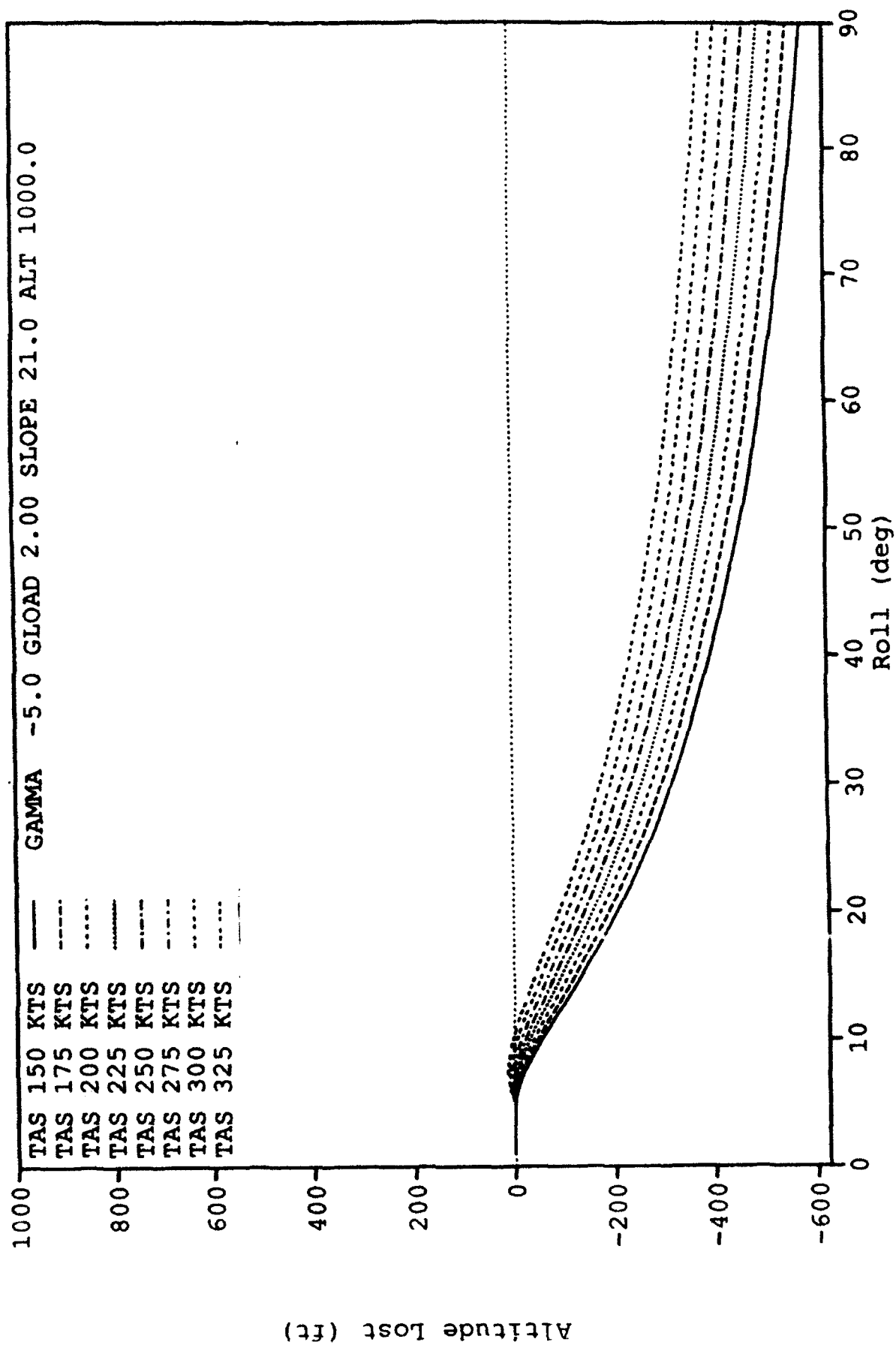


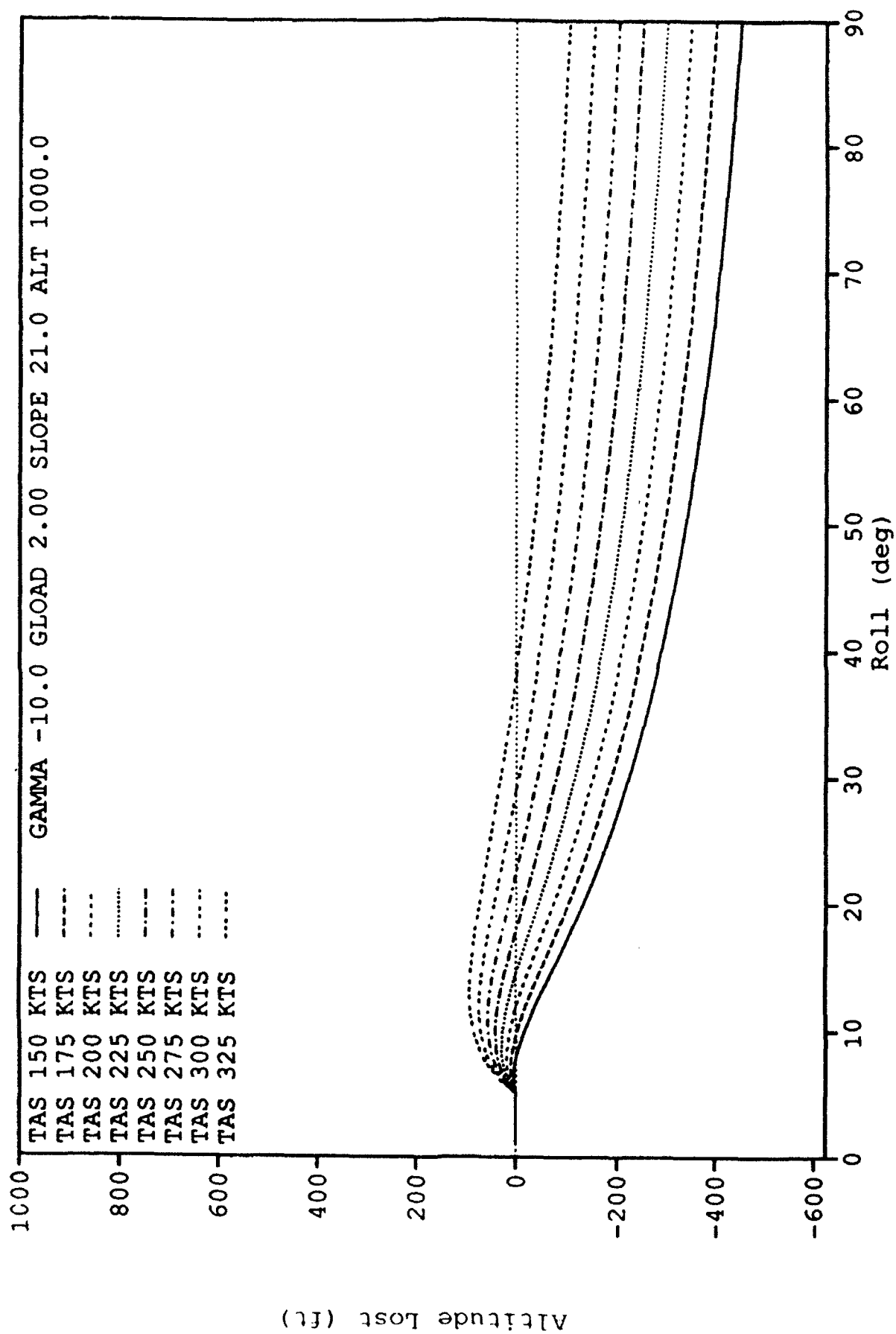


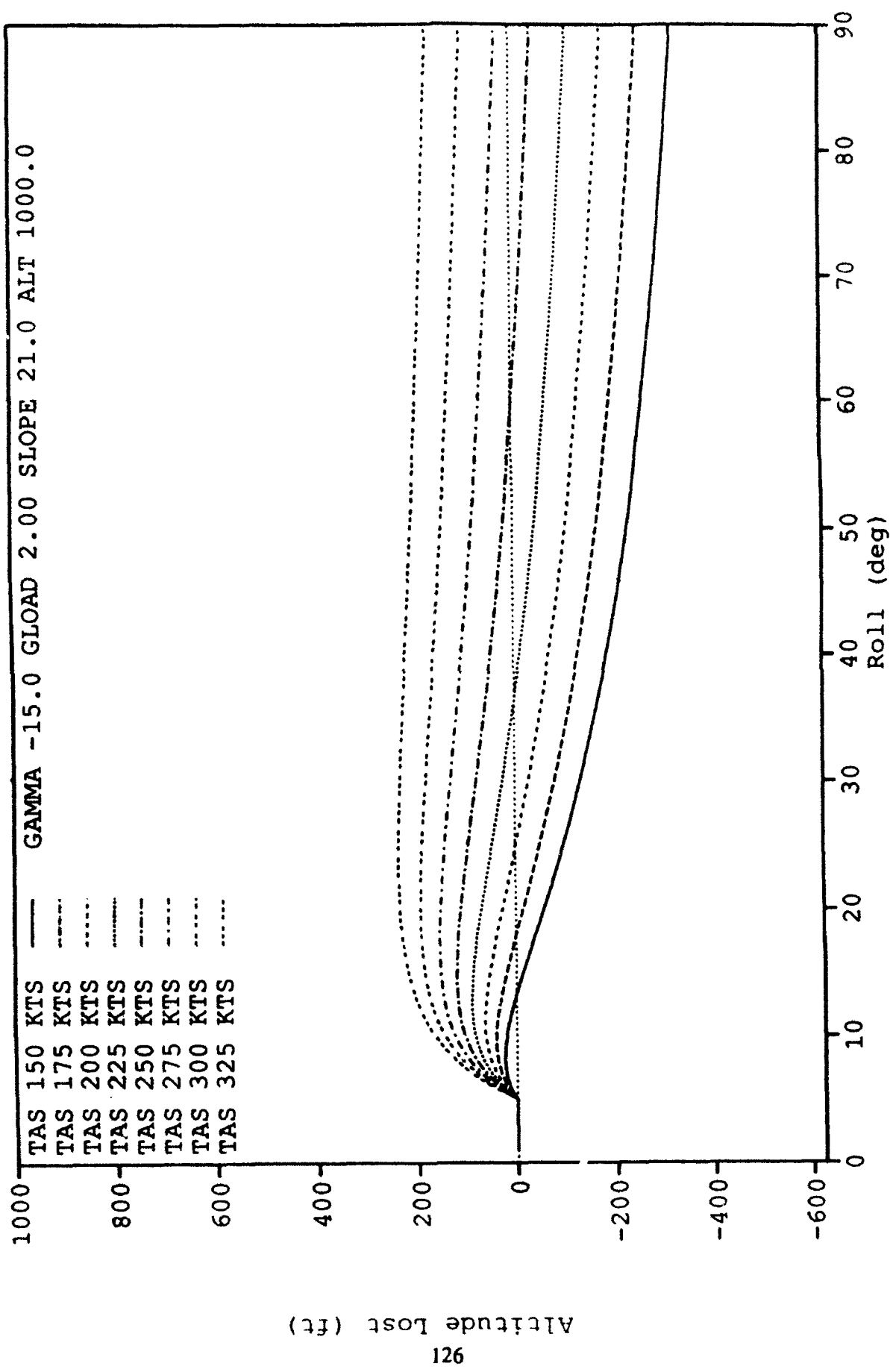


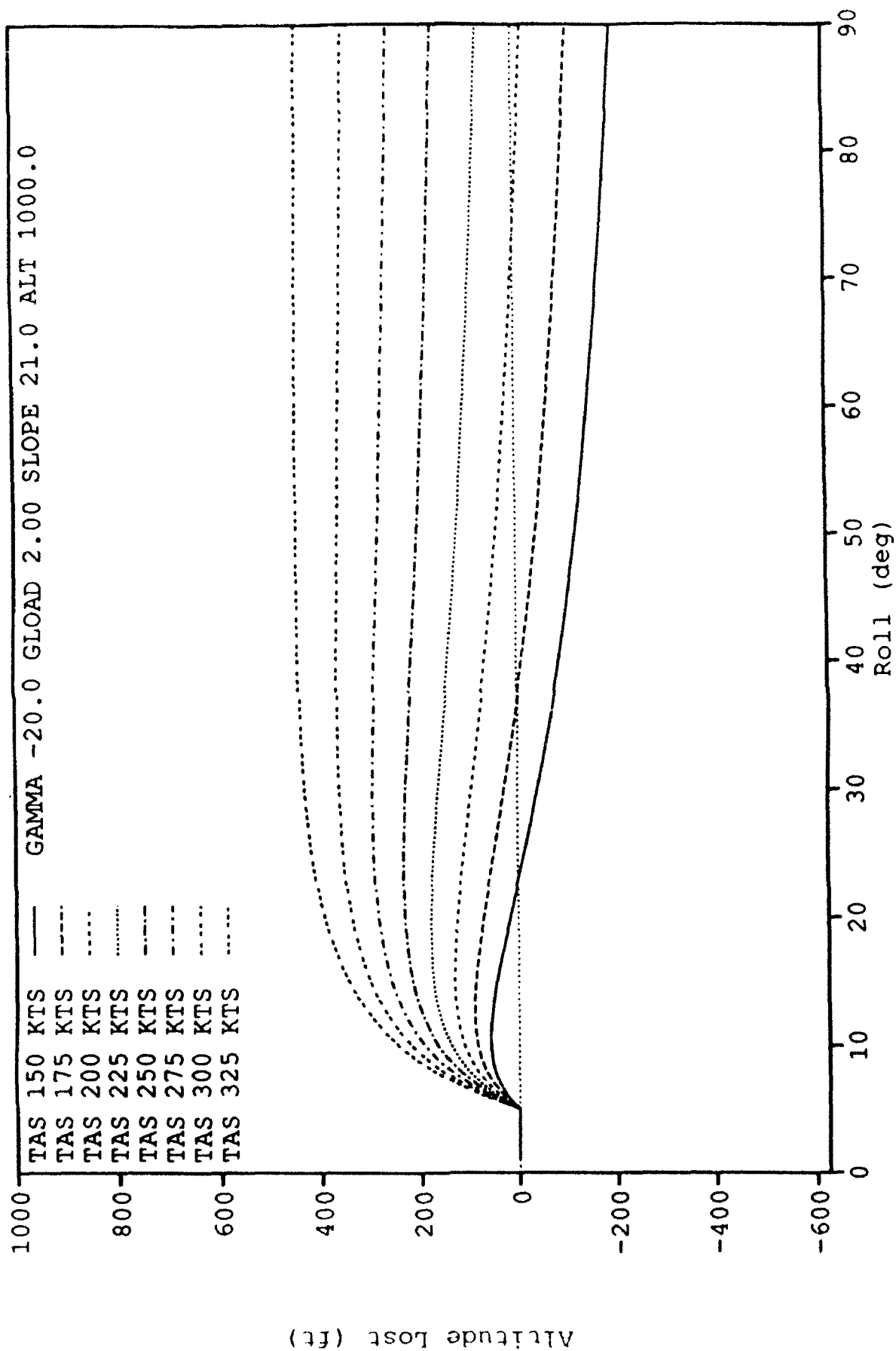








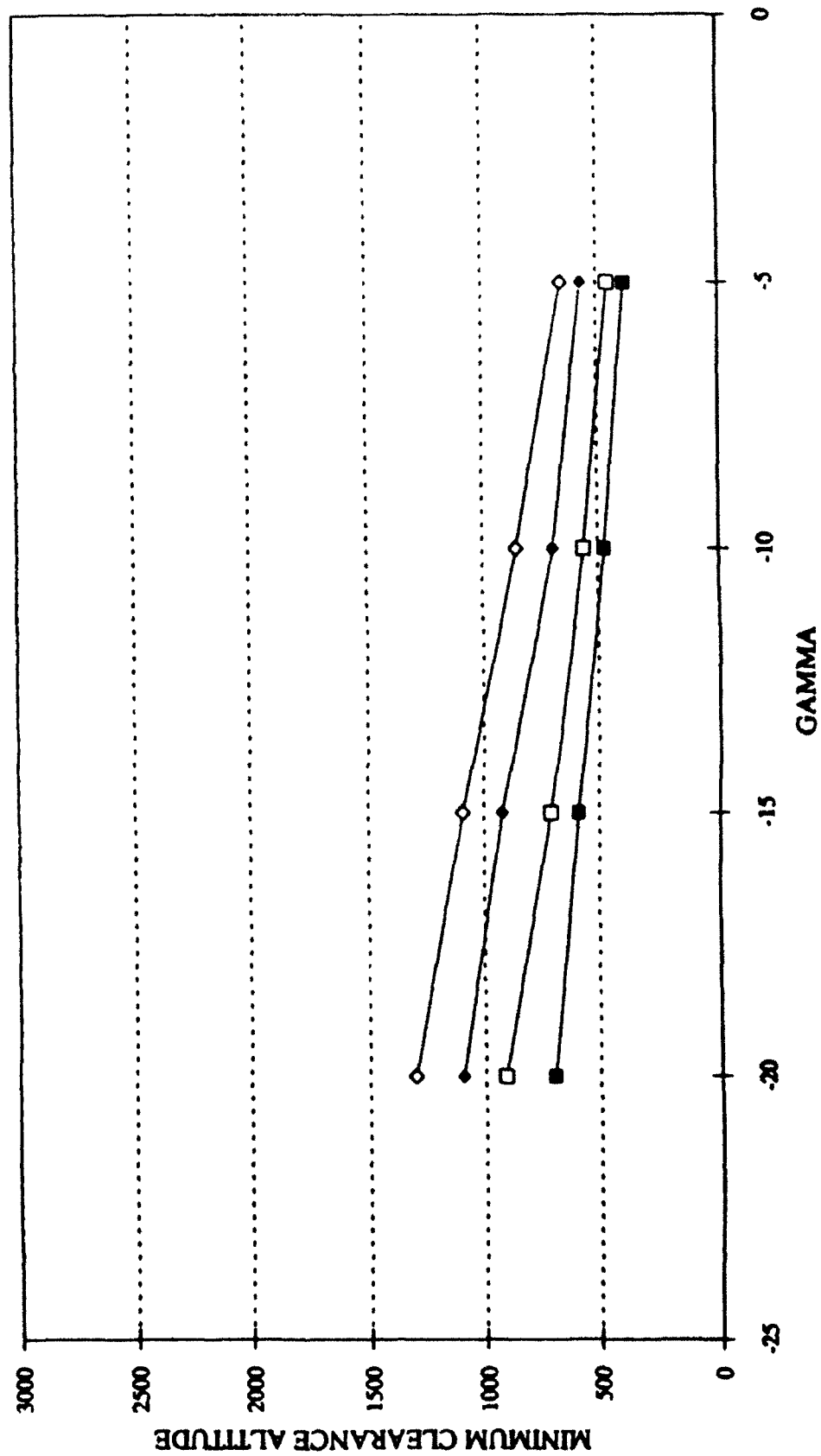




Appendix D
PHASE II
DIVE CONFIGURATION GRAPHS

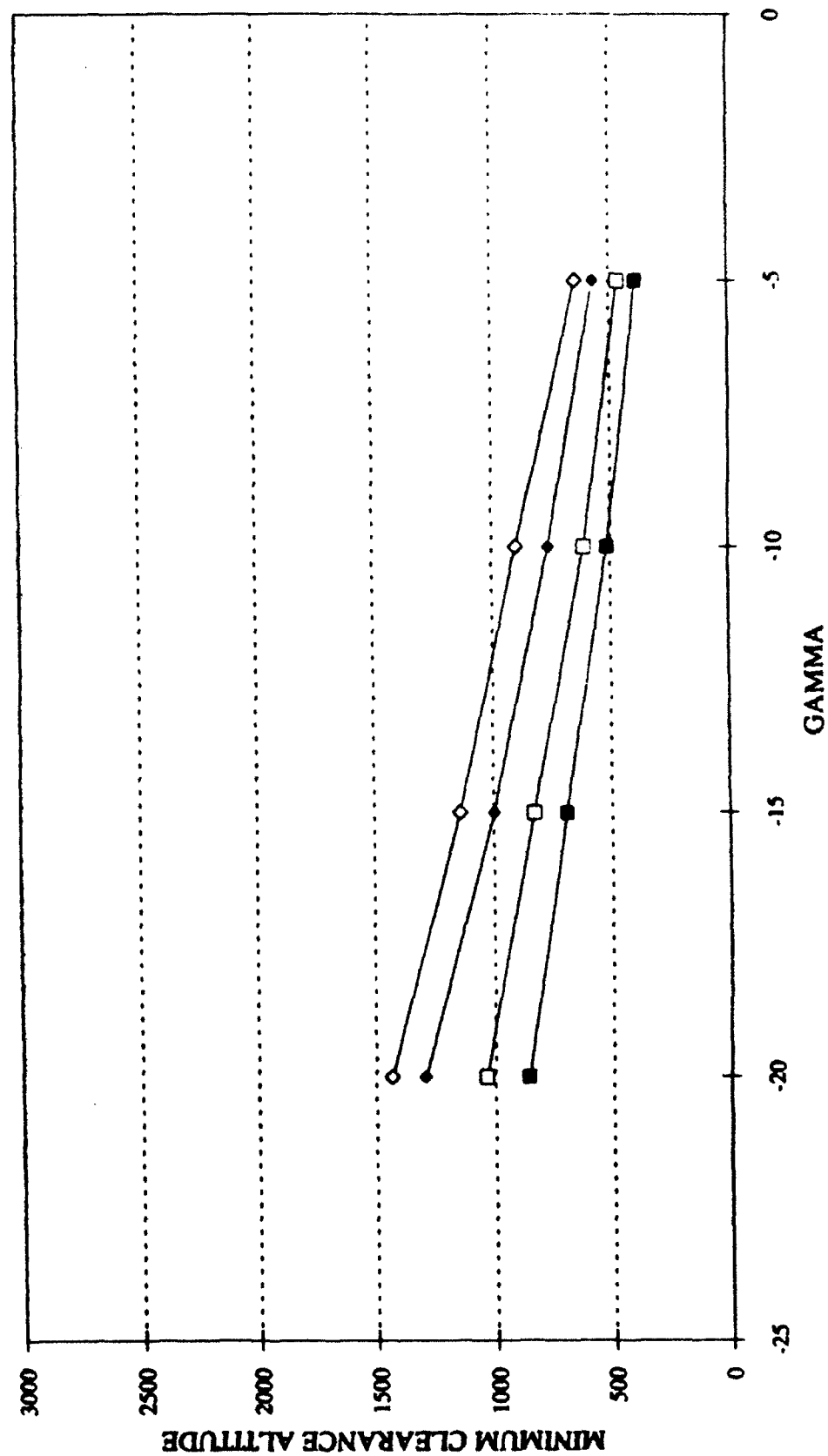
GCAS ROBOT RUNS
IAS=225 SLOPE=0 ELEVATION=1000

—■— ROLL=0 —□— ROLL=15 —◆— ROLL=30 —◇— ROLL=45



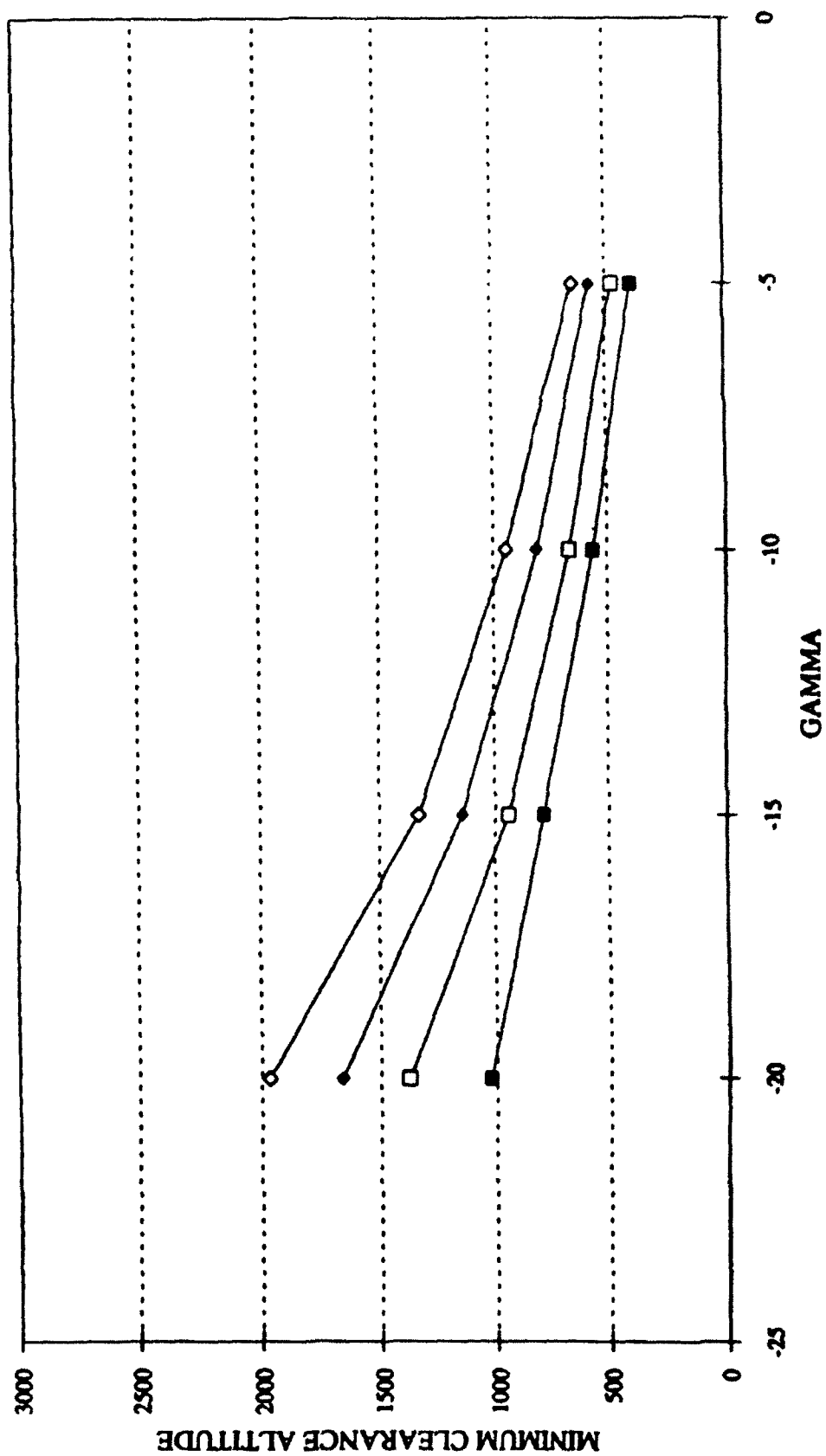
GCAS ROBOT RUNS
IAS=275 SLOPE=0 ELEVATION=1000

—■— ROLL=0 —□— ROLL=15 —◆— ROLL=30 —◇— ROLL=45



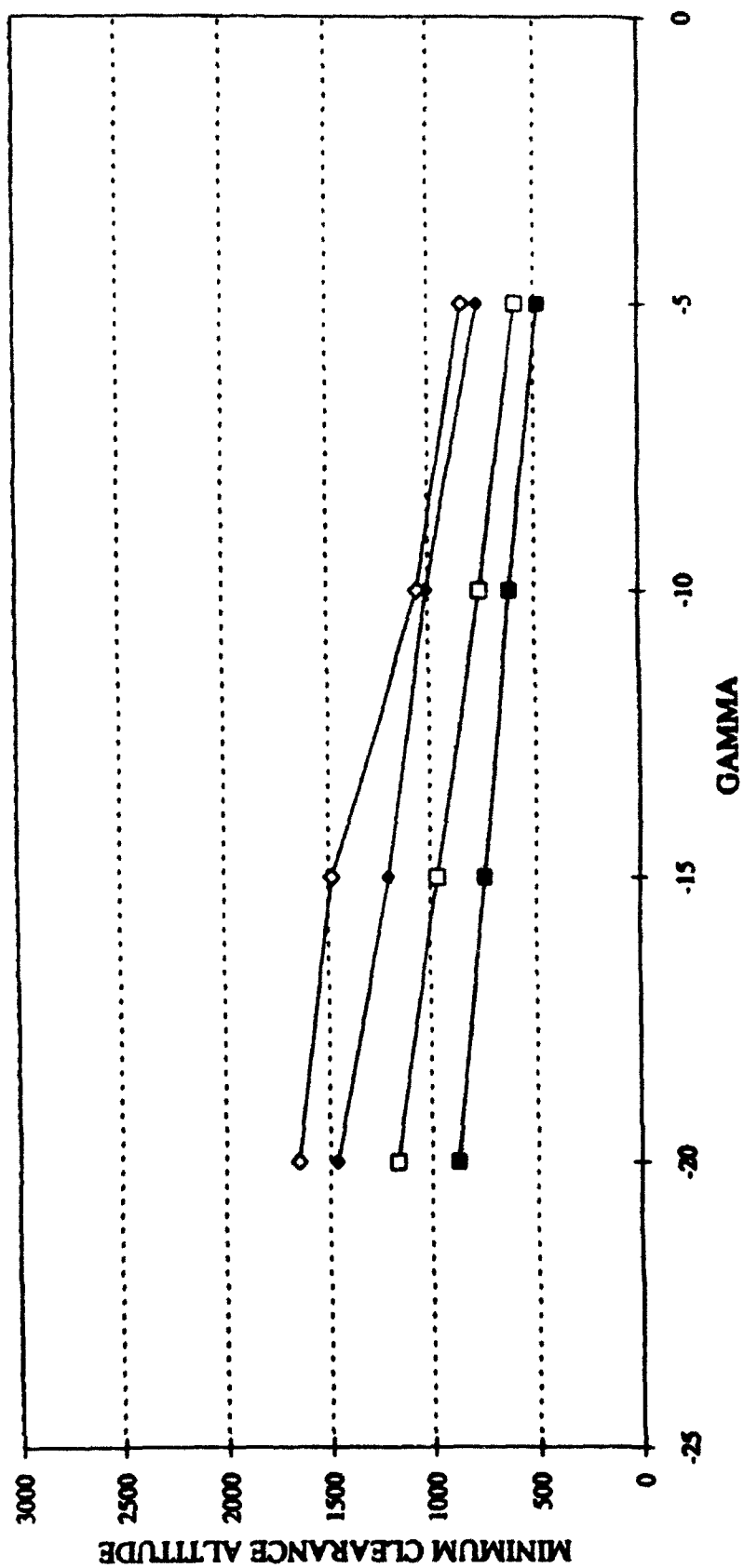
GCAS ROBOT RUNS
IAS=325 SLOPE=0 ELEVATION=1000

—■— ROLL=0 —□— ROLL=15 —◆— ROLL=30 —◇— ROLL=45



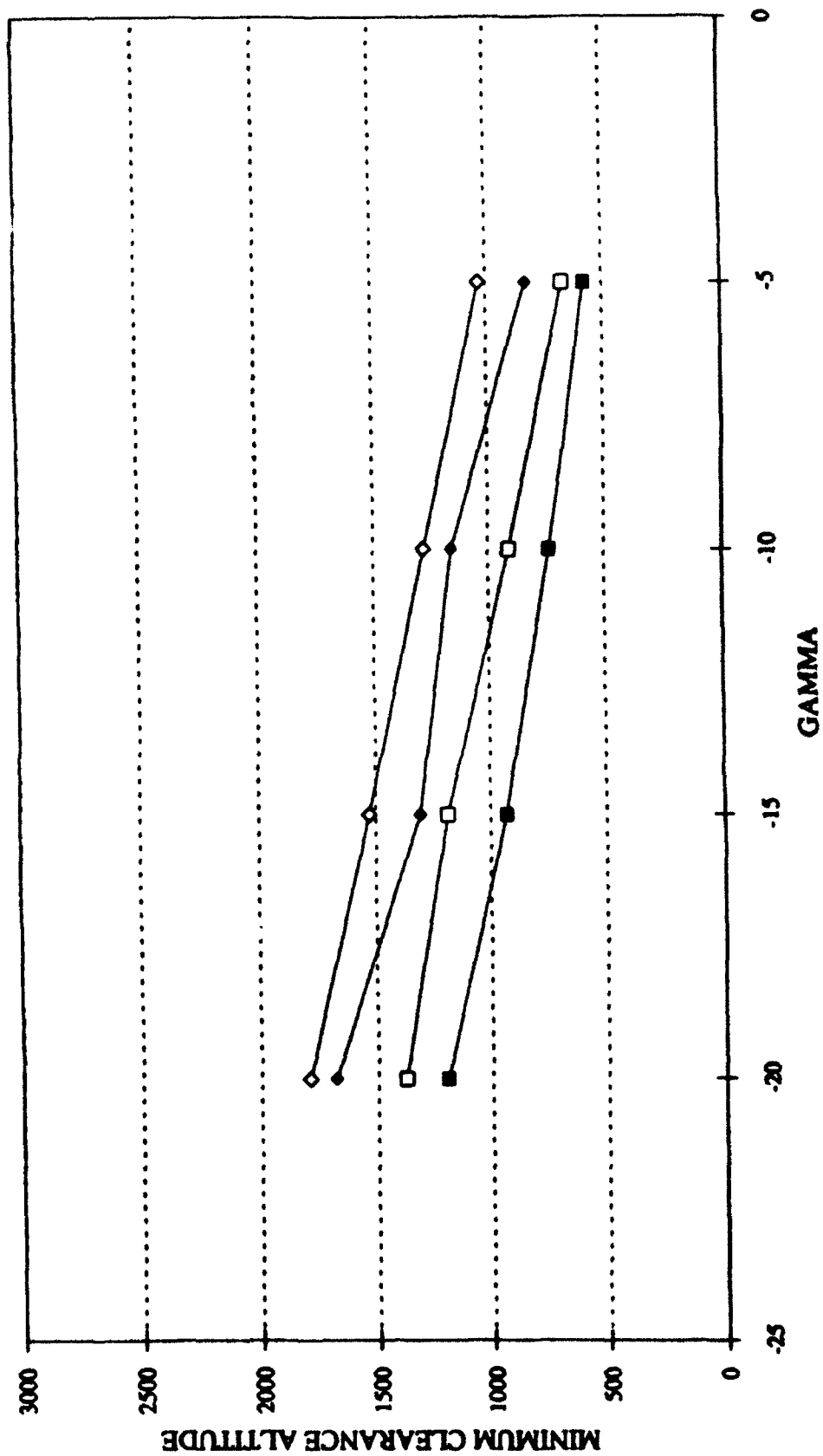
GCAS ROBOT RUNS
IAS=225 SLOPE=7 ELEVATION=1000

—■— ROLL=0 —□— ROLL=15 —●— ROLL=30 —◇— ROLL=45



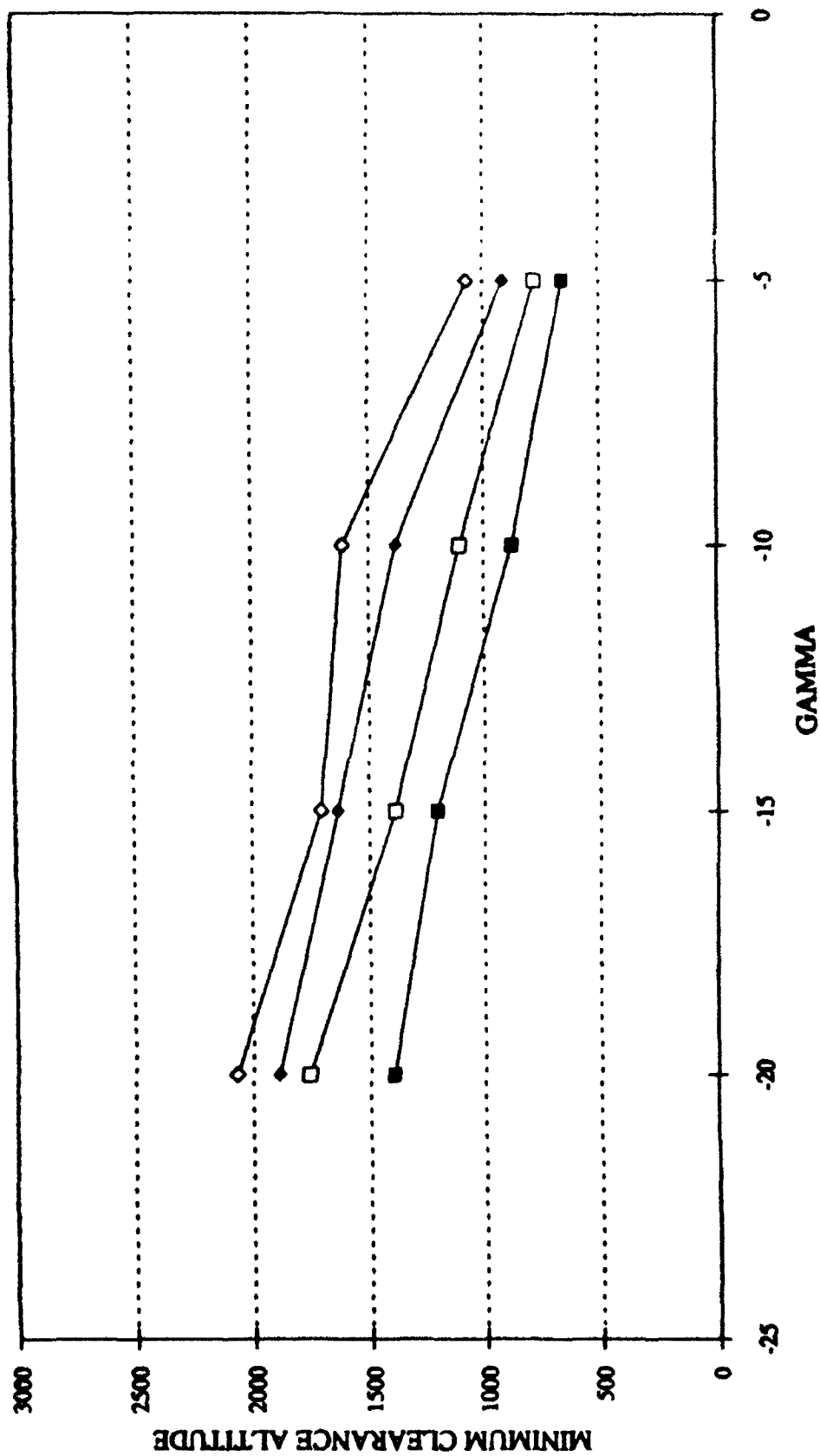
GCAS ROBOT RUNS
IAS=275 SLOPE=7 ELEVATION=1000

—■— ROLL=0 —□— ROLL=15 —◆— ROLL=30 —◇— ROLL=45



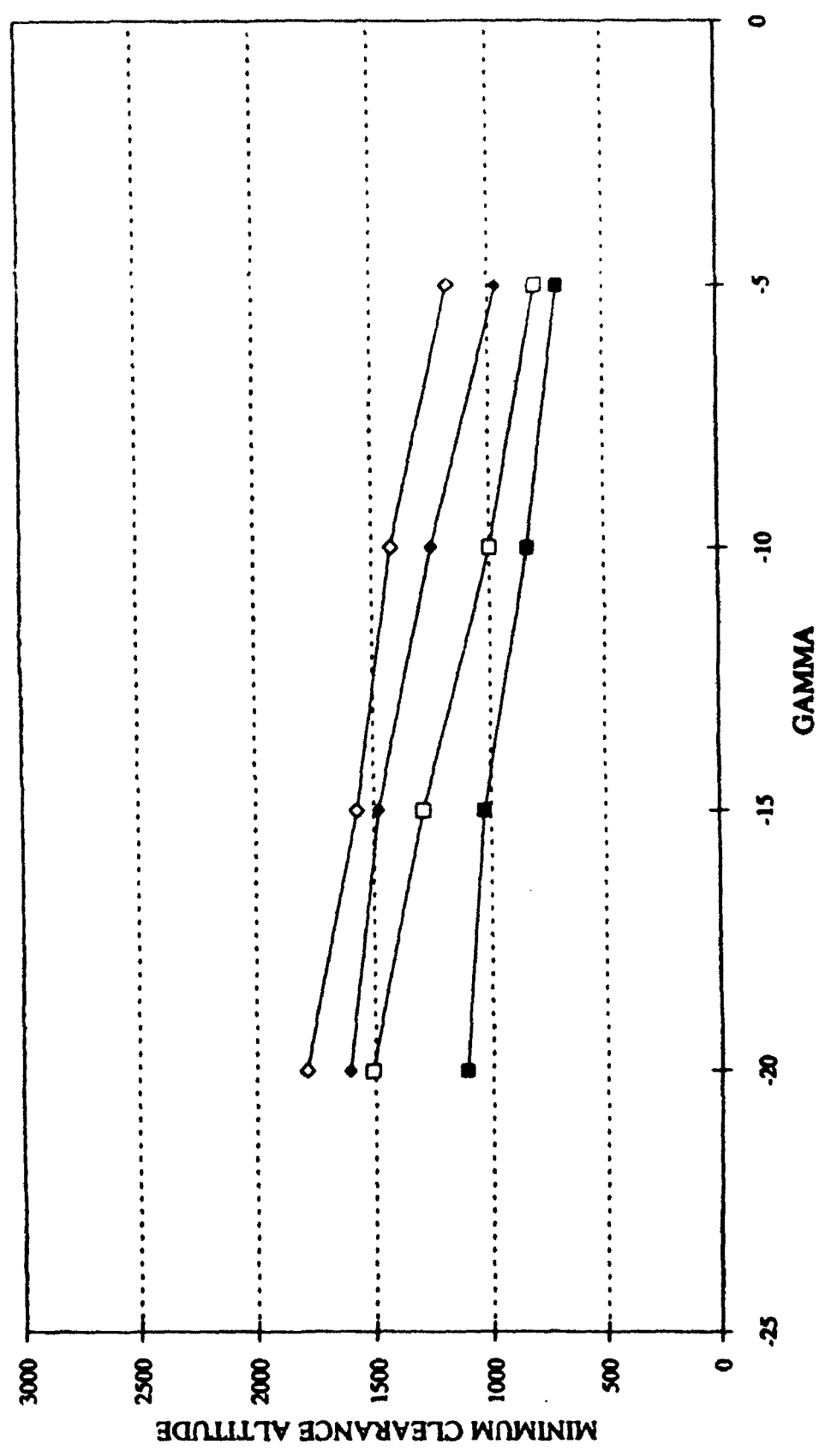
GCAS ROBOT RUNS
IAS=325 SLOPE=7 ELEVATION=1000

—■— ROLL=0 —□— ROLL=15 —◆— ROLL=30 —◇— ROLL=45



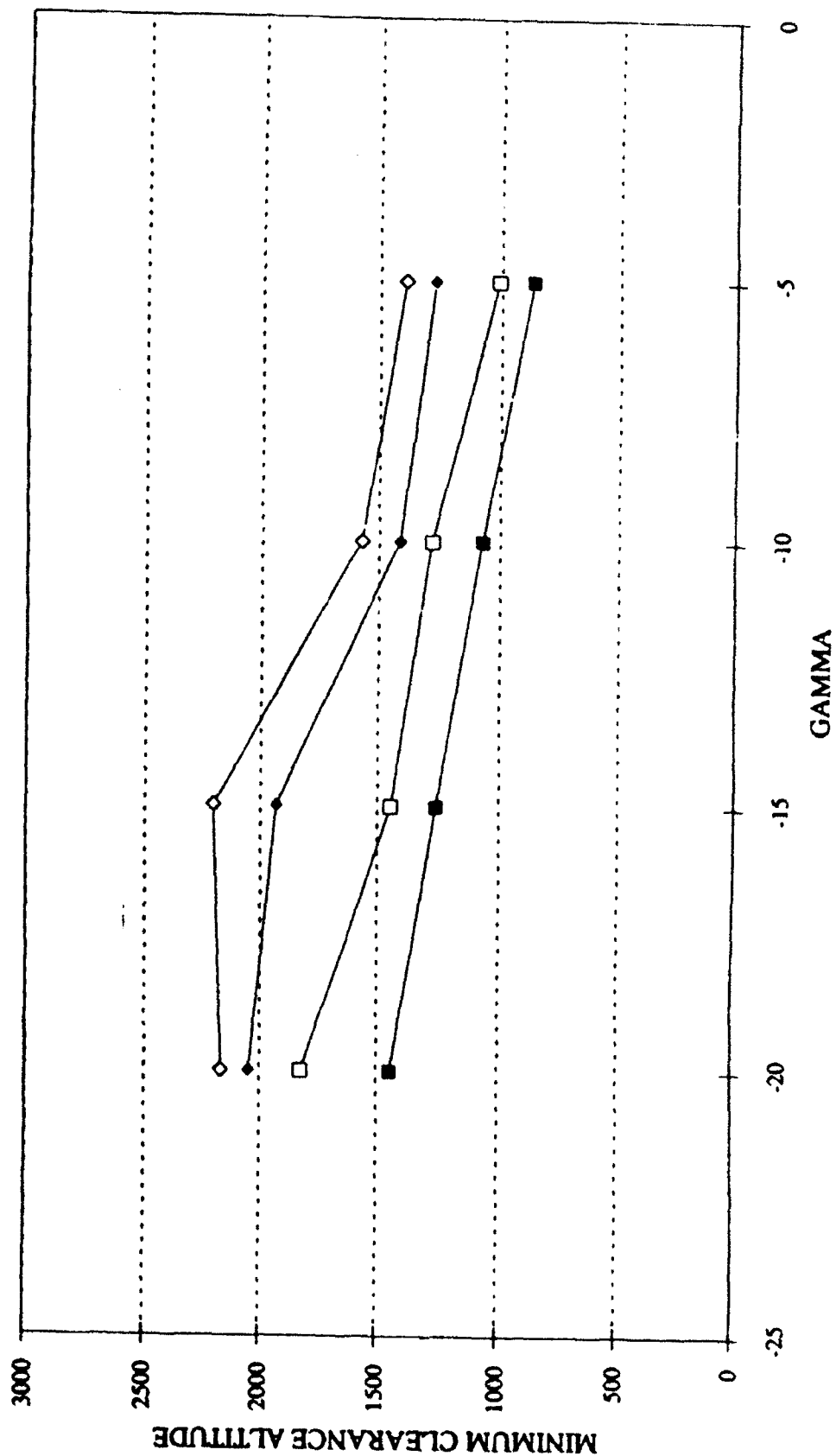
GCAS ROBOT RUNS
IAS=225 SLOPE=14 ELEVATION=1000

—■— ROLL=0 —□— ROLL=15 —◆— ROLL=30 —◇— ROLL=45



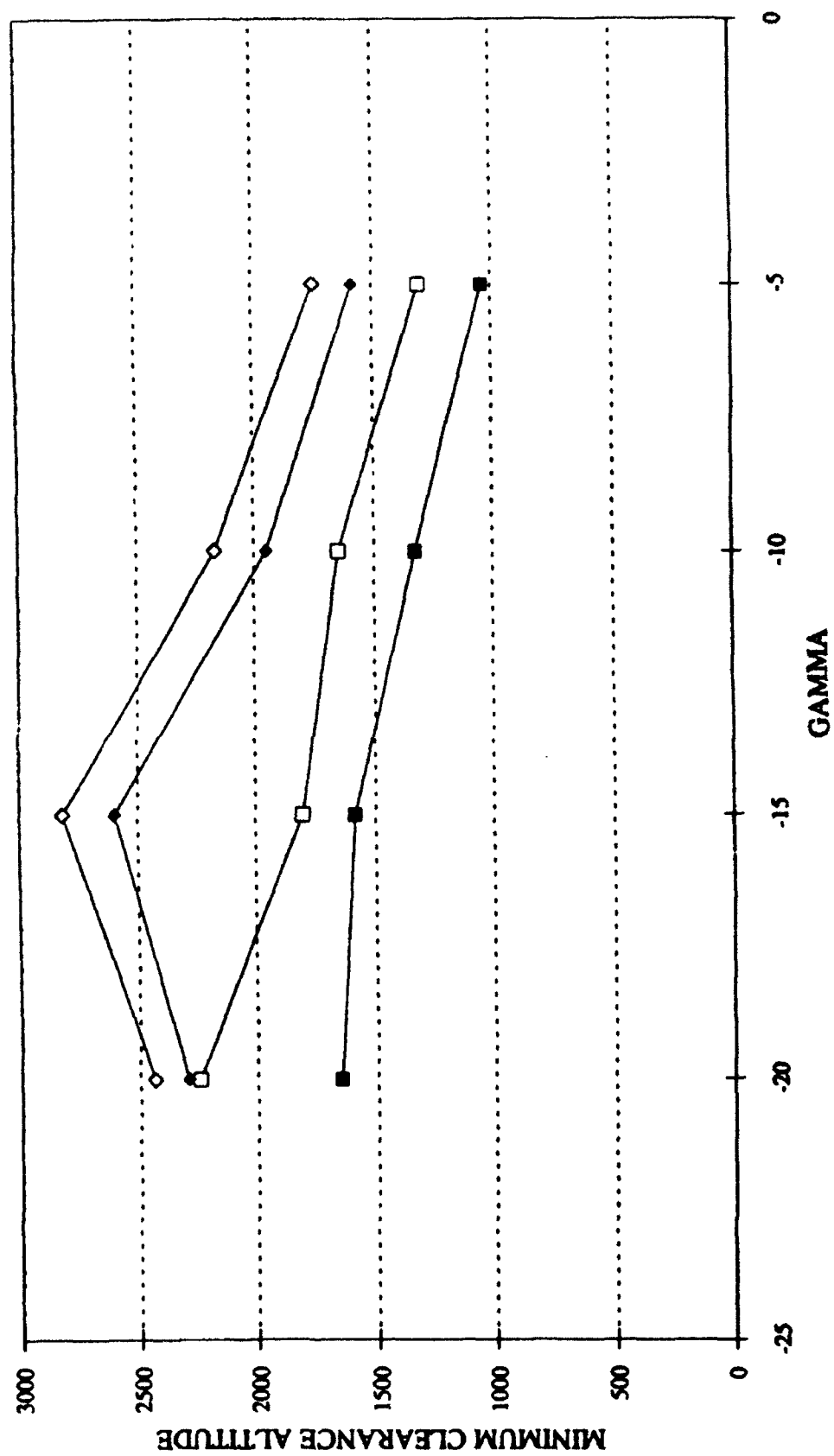
GCAS ROBOT RUNS
IAS=275 SLOPE=14 ELEVATION=1000

■ ROLL=0 □ ROLL=15 ◆ ROLL=30 ◇ ROLL=45



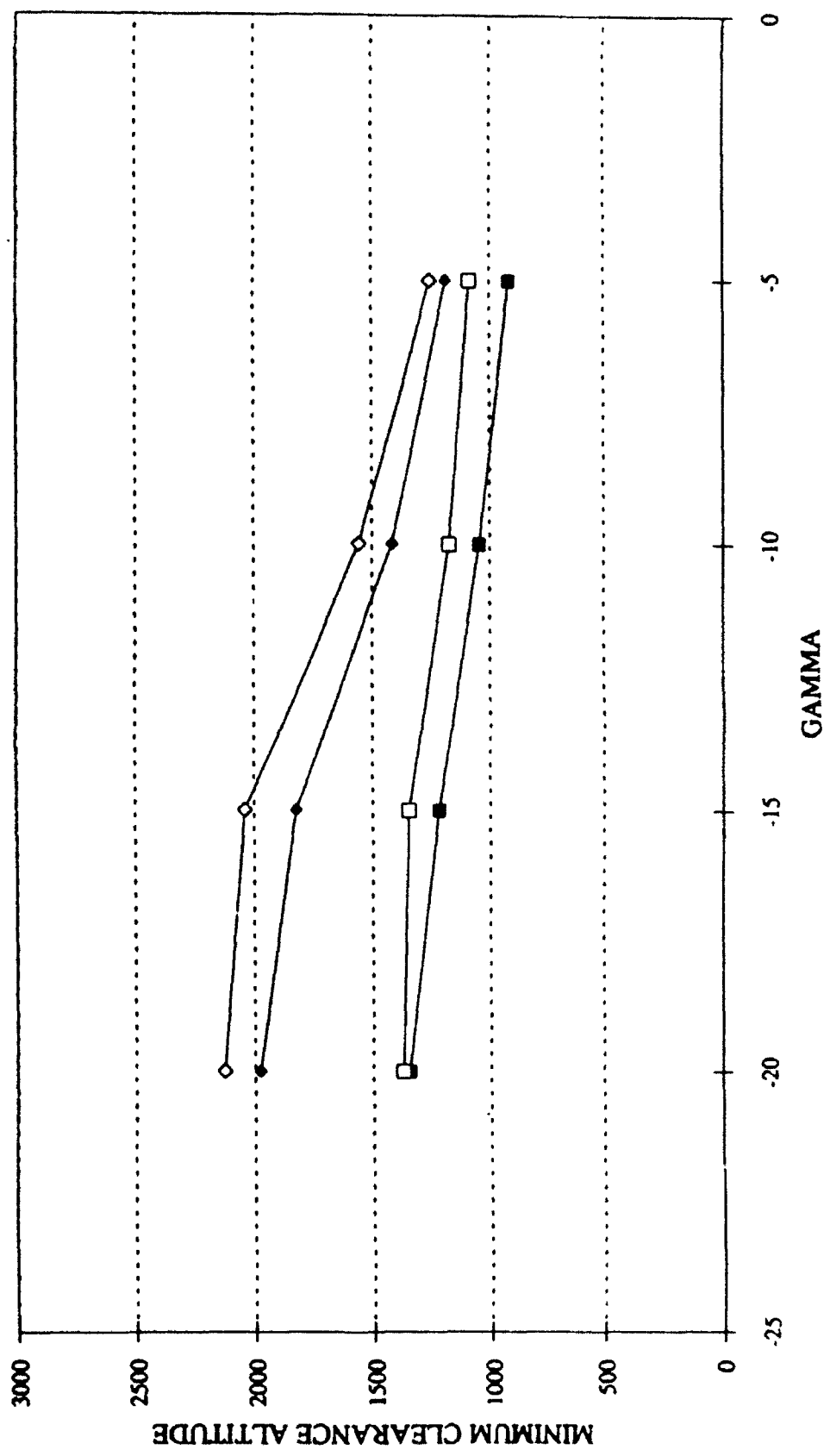
GCAS ROBOT RUNS
IAS=325 SLOPE=14 ELEVATION=1000

—●— ROLL=0 —□— ROLL=15 —◆— ROLL=30 —◇— ROLL=45



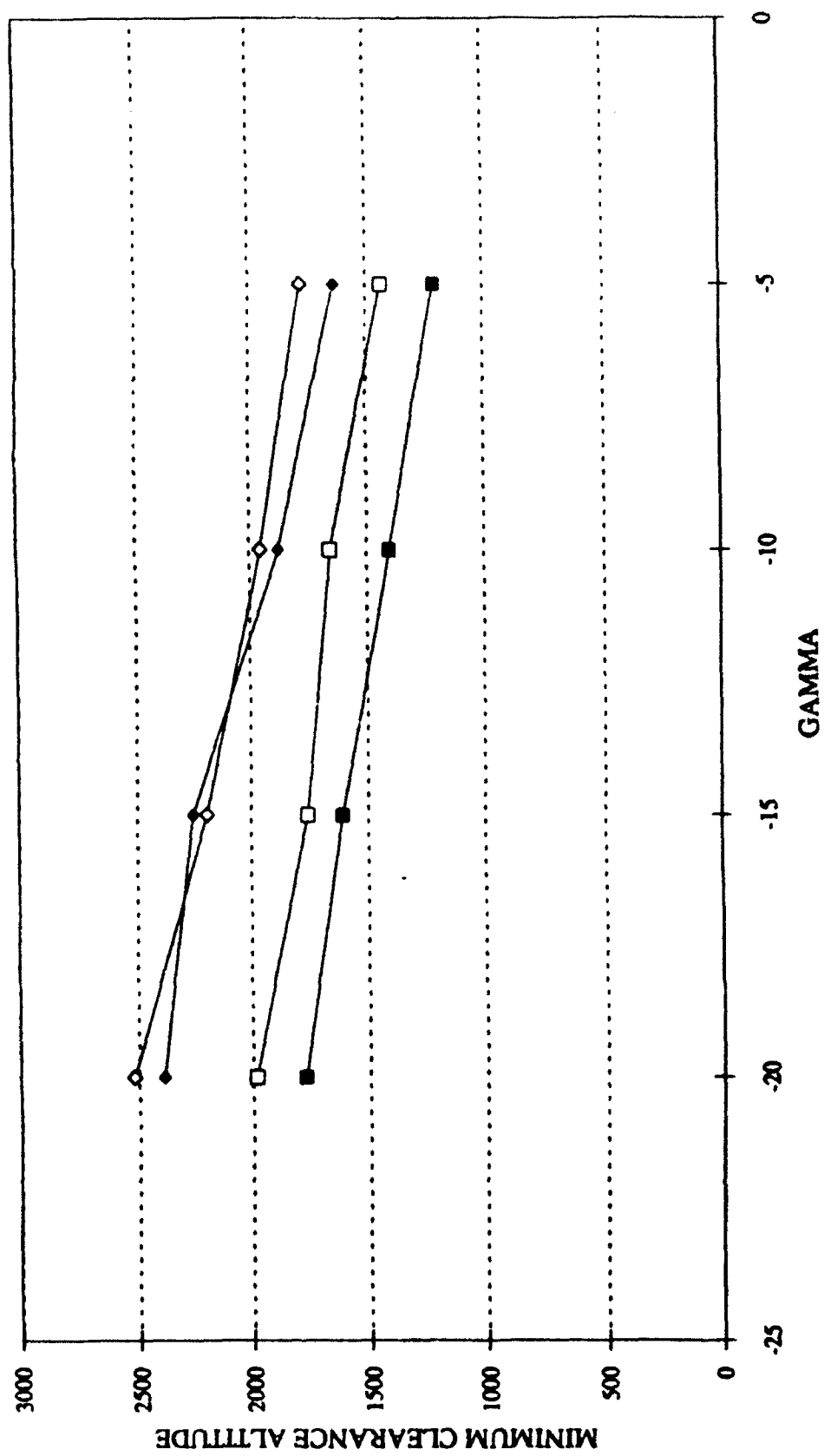
GCAS ROBOT RUNS
IAS=225 SLOPE=21 ELEVATION=1000

—■— ROLL=0 —□— ROLL=15 —●— ROLL=30 —◇— ROLL=45



GCAS ROBOT RUNS
IAS=275 SLOPE=21 ELEVATION=1000

—■— ROLL=0 —□— ROLL=15 —●— ROLL=30 —◇— ROLL=45



GCAS ROBOT RUNS
IAS=325 SLOPE=21 ELEVATION=1000

—■— ROLL=0 —□— ROLL=15 —◆— ROLL=30 —◇— ROLL=45

